Characterisation of LRRK2 – Tubulin Interactions in Parkinson's Disease

Bernard Man Hin Law

Thesis submitted for the degree of Doctor of Philosophy

The School of Pharmacy, University of London

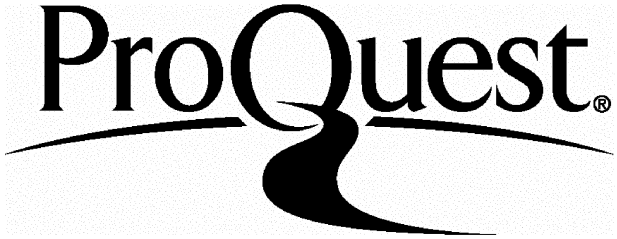

Declaration

This thesis describes research conducted in the School of Pharmacy, University of London between October, 2007 and August, 2010 under the supervision of Dr. Kirsten Harvey. I certify that the research described is original and that any parts of the work that have been conducted by collaboration are clearly indicated. I also certify that I have written all the text herein and have clearly indicated by suitable citation any part of this dissertation that has already appeared in publication.

Bernard Leu

Signature

09.03.2011

Date

Abstract

Mutations in *PARK8* encoding the cytosolic protein leucine-rich repeat kinase 2 (LRRK2) are the most common known cause for Parkinson's disease (PD). LRRK2 belongs to the ROCO family of proteins which are characterised by a Roc (Ras in complex proteins) domain with intrinsic GTPase activity and a COR (C-terminal of Roc) domain. The modification of LRRK2 GTPase and kinase activity by *PARK8* mutations is believed to lead to neuronal cell death but the pathways involved remain elusive. To further our understanding of LRRK2 signalling pathways leading to cell death, several previously identified LRRK2 interacting proteins were characterised. As evidence of an involvement of axonal transport defects in the pathogenesis of PD is accumulating, I decided to focus on the LRRK2 interaction with β-tubulin.

Tubulin is the main component of microtubules, a part of the cytoskeleton. Changes in phosphorylation of tubulin and microtubule-associated proteins lead to changes in the dynamic instability of microtubules with detrimental effects for axonal transport, ultimately leading to synaptic defects and axonal degeneration. Using the yeast two-hybrid (YTH) system I found that the LRRK2 Roc-COR domain interacts specifically with some neuronally expressed β-tubulin isoforms. This interaction was further characterised using the YTH system, biochemical methods and mammalian cellular models. The binding domains on LRRK2 and β-tubulin isoforms mediating the interaction were determined and LRRK2 association with tubulin was shown in a differentiated dopaminergic human neuroblastoma cell model. Importantly, I found that *PARK8* mutations segregating with PD and the phosphorylation state of LRRK2 and β-tubulin might influence the interaction between LRRK2 and microtubules.

Finally, genetic screening for *PARK8* mutations using LightScanner technology of post-mortem samples from the Imperial Parkinson's Disease Society Brain Bank revealed a novel mutation in the LRRK2 GTPase domain.

The modulation of the interaction between β-tubulin isoforms and LRRK2 by *PARK8* mutations and phosphorylation as well as the expression of these proteins in human substantia nigra indicate the patho-physiological relevance of these interactions and

might lead us towards a better understanding of the disruption of signalling pathways resulting in neurodegeneration.

Acknowledgements

Firstly, I would like to sincerely thank my supervisors Dr. Kirsten Harvey and Dr. Brian Pearce for their continual support and unfailing guidance throughout the project, and for providing helpful suggestions and criticisms in all areas for me to improve on my thesis. I would also like to thank Prof. Robert Harvey for providing me with the materials for the generation of the tubulin plasmid constructs in my project.

I would like to thank the Michael J Fox Foundation for providing me with the anti-LRRK2 antibodies as generous gifts for the detection of endogenous LRRK2 in cell lysates.

I would like to thank Prof. Anne Stephenson and Dr. Andreas Kortenkemp for allowing me to use the GeneGNOME instrument and the microplate photometer respectively.

A big thank you must also go to my past and present lab-mates – Caroline Anderson, Daniel Berwick, Marian Blanca-Ramirez, Alex Caley, Eloisa Carta, Celine Fuchs, Jennifer Gill, Victoria James, Sarah Ramsden, Leila Saiepour, Rosa Sancho, Victoria Spain and Philipp Wesche – for being great friends and providing a friendly atmosphere in the laboratory during these three years. Thanks for the humour too!

Special thanks should also go to Daniel Berwick, Alex Caley, Celine Fuchs, Leila Saiepour and Rosa Sancho for teaching me the experimental techniques involved in the project during the first year of my PhD. I would also like to thank Sarah Ramsden for being my thesis reader and providing me valuable advices and suggestions in the use of English in my thesis.

I would like to thank my family for their unending love and concern, and all my friends, especially those from my mother school, who continuously provide me with spiritual support for me to complete my PhD.

Last but not least, I would like to thank the School of Pharmacy for providing the stipend and financial support for me to complete the PhD project.

Table of Contents

List of Figures

List of Tables

Abbreviations

3-AT	3-amino-1,2,4-triazole
4E-BP	Eukaryotic Initiation Factor 4E Binding Protein
AD	Alzheimer's disease
ApoE	apolipoprotein E
BSA	bovine serum albumin
cDNA	complementary DNA
CL	cell lysate
CNS	central nervous system
co-IP	co-immunoprecipitation
COR	C-terminal of Roc
CP	caudate putamen
CPRG	chlorophenol-red-β-galactopyranoside
C_t	cycle threshold
DMEM	Dulbecco's Modified Eagle Medium
DMF	N,N-dimethylformadine
DMSO	dimethylsulphoxide
DO	dropout
DVL	dishevelled
eIF-4E	eukaryotic initiation factor 4E
E.coli	*Escherichia coli*
ER	endoplasmic reticulum
Erk	extracellular signal-related kinase
FADD	Fas-associated Death Domain
FBS	foetal bovine serum
FBXO7	F box protein 7
GAP	GTPase-activating protein
GAPDH	glyceraldehyde-3-phosphate dehydrogenase
GDP	guanosine diphosphate
GEF	guanosine exchange factor
GIGYF2	Grb10-Interacting GYF Protein 2
GSK3β	glycogen synthase kinase 3 beta
GST	glutathione-S-transferase

GTP	guanosine triphosphate
GTP-γS	guanosine triphosphate - gamma sulphate
GWAS	genome-wide association studies
HBSS	Hank's balanced salt solution
HEK293	human embryonic kidney 293
HRP	horse radish peroxidase
HTRA2	High Temperature Requirement A2
IGF	insulin growth factor
JIP	JNK-interacting protein
JNK	c-jun N-terminal kinase
kDa	kilo Daltons
KESTREL	kinase substrate tracking and elucidation
LB	Luria-Bertani
LDS	lithium dodecyl sulphate
LiAc	lithium acetate
LRR	leucine-rich repeat
LRRK2	leucine-rich repeat kinase 2
MAP	microtubule-associated proteins
MAPKKK	mitogen-activated protein kinase kinase kinase
MJFF	Michael J Fox Foundation
MLK	mixed lineage kinase
MOPS	3-(N-morpholino) propanesulphonic acid
MPPP	1-methyl-4-phenyl-4-propionoxy-piperidine
MPTP	1-methyl-4-phenyl-1,2,5,6-tetrahydropyridine
MTOC	microtubule organising centre
MW	molecular weight
NS	nutritional selection
PBS	phosphate buffered saline
PBS-T	phosphate buffered saline containing 0.1% Tween-20
PCR	polymerase chain reaction
PD	Parkinson's Disease
PDL	poly-D-lysine
pen-strep	penicillin-streptomycin
PEG	polyethylene glycol

PINK1	Phosphatase and Tensin-homolog-induced Putative Kinase 1
PLA2G6	phospholipase A2-G6
PMSF	phenylmethyl sulphonyl fluoride
PVDF	polyvinyldiene fluoride
Q-YTH	quantitative yeast two hybrid
RA	retinoic acid
Roc	Ras of complex proteins
ROS	reactive oxygen species
RQ-PCR	relative quantification polymerase chain reaction
RTN3	reticulon 3
SDS-PAGE	sodium dodecyl sulphate – polyacrylamide gel electrophoresis
siRNA	small interfering RNA
SN	substantia nigra
SNP	single nucleotide polymorphism
SNpc	substantia nigra pars compacta
SOD1	superoxide dismutase 1
TAE	tris-acetate ethylenediaminetetra-acetic acid
TC	transformation control
UAS	upstream activation sequences
UCHL1	ubiquitin C-terminal hydrolase-L1
UPS	ubiquitin-proteasome system
UTR	untranslated region
UV	ultraviolet
WT	wild type
X-gal	5-bromo-4-chloro-3-indolyl-β-D-galactopyranoside
YPD	yeast extract/peptone/dextrose
YTH	yeast two hybrid

1. Introduction

1.1 General Introduction to Parkinson's Disease

Parkinson's disease (PD) is a neurodegenerative disease characterised by the death of dopaminergic neurons in a brain region named the substantia nigra pars compacta (SNpc). It is the second most common neurodegenerative disease after Alzheimer's disease (AD). The death of these neurons results in a decreased availability of the neurotransmitter dopamine for neurotransmission to the striatal area in the brain, and subsequently affects the neuronal output to the cortex (figure 1.1). This leads to typical PD symptoms including resting tremor, rigidity, postural instability and bradykinesia. Furthermore, the formation of proteinaceous inclusions termed Lewy bodies also occurs in the surviving dopaminergic neurons. These are spherical eosinophilic intra-cytoplasmic inclusions. They have a dense core surrounded by a halo, with the core stained positively for α-synuclein (Gomez-Tortosa *et al*, 2000), ubiquitin (Kuzuhara *et al*, 1988) and other proteins. However, the mechanisms leading to neuronal death and the formation of Lewy bodies remain elusive.

PD was first described in 1817 by James Parkinson in the 'Essay of Shaking Palsy'. Since the subsequent speculation made by Brissaud in 1895 that PD is caused by the damage of the SNpc (Savitt *et al*, 2006), efforts have been made in the search for mechanisms leading to neuronal death in PD, in the hope of finding an effective way to cure the disease. Currently PD is incurable, and the treatment of this disease is primarily limited to the treatment of symptoms. For example, since typical PD symptoms are caused by the loss of dopamine in the SNpc, drugs like levodopa, an intermediate in dopamine synthesis, are routinely used to relieve PD symptoms. However, levodopa administration cannot eliminate PD progression. The research into the molecular mechanisms of neuronal death is inspired by the idea of finding an effective cure for PD.

In the past decade, research revealed a strong association of oxidative stress with PD. For instance, the injection of a neurotoxin named 1-methyl-4-phenyl-1,2,5,6-tetrahydropyridine (MPTP) with trace amounts of 1-methyl-4-phenyl-4-propionoxy-piperidine (MPPP) into humans led to the development of Parkinsonian symptoms with neuronal degeneration due to mitochondrial dysfunction in the substantia nigra (SN)

(Langston *et al*, 1983). This dysfunction was also accompanied by the depletion of glutathione (Chinta and Andersen, 2006), indicative of oxidative stress. Furthermore, a link between abnormal protein folding, aggregation and phosphorylation with PD was suggested, as the contents of the Lewy bodies include aggregated hyperphosphorylated α-synuclein (Hasegawa *et al*, 2002). However, to date, our knowledge on the molecular mechanisms triggering these events is still limited.

The majority of PD cases are still considered sporadic. However, there are about 10% of PD cases which appear to be inherited (Thomas and Beal, 2007), and are generally termed 'familial PD'. This indicates that there is a genetic component, and in fact mutations in certain genes were found in some patients with PD. Hence, studying the function of these genes and the dysfunction caused by the identified mutations might provide clues about the molecular pathways involved in PD pathogenesis. Results of these studies might present targets for effective therapies preventing the progression of PD in the future.

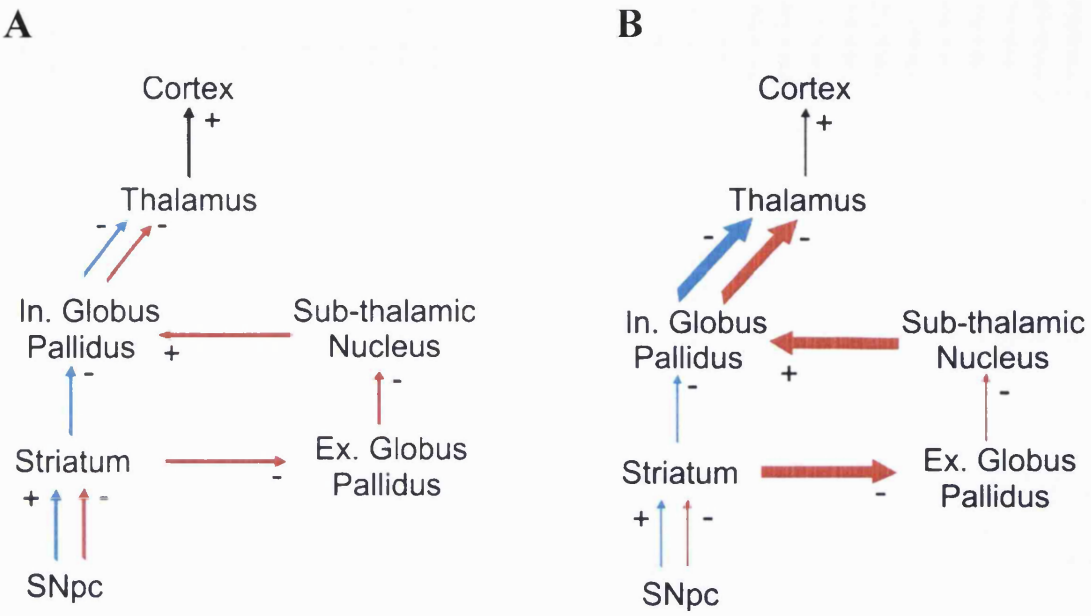

Figure 1.1: The neuronal circuit of the Nigrostriatal Pathway in a healthy individual (A) and a PD patient (B). (A) Two neuronal circuits exist in the nigrostriatal pathway. In the direct pathway, which is shown by blue arrows, projections from the excitatory dopaminergic neurons in the SNpc form synapses with inhibitory GABAergic neurons in the striatum, which innervates the internal globus pallidus (In. Globus Pallidus). These neurons in turn project to inhibitory GABAergic neurons of the thalamus. The inhibitory signals from the internal globus pallidus serve as a negative regulator of the excitatory signal from the thalamus to the cortex which controls movement. The indirect pathway, shown by the red arrows, involves inhibitory dopaminergic neurons from the SNpc to the striatum. The neuronal circuits pass the signal to the internal globus pallidus indirectly through several brain regions such as the external globus pallidus (Ex. Globus Pallidus) and the subthalamic nucleus. (B) The nigrostriatal pathway in the diseased state. Death of dopaminergic neurons in the SNpc causes dopamine depletion in the striatum, resulting in an altered level of signals through the circuitry. Increased activity of the neurons is shown by thick block arrows, and decreased activity is shown by thin arrows. (+ indicates excitatory neurons, - indicates inhibitory neurons)

1.2 PD Genetics

To date, 16 different loci in the human genome have been identified that harbour genes involved in PD pathogenesis. Mutation and/or multiplication of these genes were found to be associated with PD, and are collectively known as '*PARK* genes'. This section aims to provide an introduction to the known physiological roles and dysfunctions caused by mutations of the *PARK* genes.

1.2.1 *PARK1* – α-synuclein

PARK1 is a gene located on chromosome 4 that codes for the protein α-synuclein. The physiological function of α-synuclein was proposed to include recycling and storage of synaptic dopaminergic vesicles at presynaptic sites (Yavich *et al*, 2004), ensuring enough dopamine is available for neurotransmission.

Three rare missense mutations associated with autosomal dominant PD were found in *PARK1*; A53T, A30P and E46K (Polymeropoulos *et al,* 1997). They were shown to lead to a higher tendency of α-synuclein self-aggregation (El-Agnaf *et al*, 1998), providing a rationale for the occurrence of a fibrillar form of hyperphosphorylated α-synuclein in Lewy bodies (Spillantini *et al,* 1998; Anderson *et al,* 2006), and for the impairment of the α-synuclein function in dopamine storage (Lotharius and Brundin, 2002). Leakage of dopaminergic vesicles might contribute to PD pathogenesis as dopamine can be oxidised, generating reactive oxygen species (ROS) that causes oxidative stress. Furthermore, the expression of the A30P α-synuclein mutant in transgenic mice was found to increase sensitivity to MPTP (Nieto *et al,* 2006), which was shown to increase free radical production. In conclusion, α-synuclein was suggested to play a role in synaptic functioning of dopaminergic neurons, and mutations in *PARK1* leading to dysfunction is likely to be caused partially through an increase of oxidative stress.

1.2.2 *PARK2* – Parkin

PARK2 is located on chromosome 6. It codes for the E3 ubiquitin ligase parkin. Parkin attaches a polymer of ubiquitin to a lysine residue of misfolded proteins, tagging them for degradation in the proteasome. Therefore, it plays a part in protein degradation

involving the ubiquitin-proteasome system (UPS). Parkin was suggested to be a pro-survival protein displaying neuroprotective properties (Feany and Pallanck, 2003), as it was shown to activate the IκB/NFκB signalling pathway in neurons which regulates gene expression controlling cellular proliferation and survival (Henn *et al,* 2007). Furthermore, parkin might also play a role in preventing oxidative stress and apoptosis, as it was found to prevent cytochrome c release (Darios *et al,* 2003), triggering apoptosis. Mutations in *PARK2* were found in patients with early-onset recessive parkinsonism (Abbas *et al,* 1999). Mutations were suggested to abolish both the E3 ubiquitin ligase activity (Kitada *et al,* 1998) and the ability to activate the IκB/NFκB pathway (Henn *et al,* 2007). The former effect of *PARK2* mutations indicates that protein misfolding and subsequent aggregation could be one of the causes of PD. More recent work also proposed an ability of parkin to interact with and stabilise microtubules by preventing microtubule associated protein (MAP) kinase activation (Ren *et al,* 2003; Ren *et al,* 2009). Deletion of one of the *PARK2* exons was further shown to abrogate the ability of parkin to attenuate microtubule depolymerisation caused by toxins such as colchicine (Ren *et al,* 2009). These data suggest a function of parkin in mediating microtubule stabilisation and a role of the microtubule cytoskeleton in PD pathogenesis.

1.2.3 *PARK3*

The *PARK3* locus, mapped to chromosome 2, was found to show linkage to early-onset PD with symptoms similar to idiopathic PD (Gasser, 1998; Pankratz *et al,* 2004). The gene involved in causing PD present at this locus awaits identification.

1.2.4 *PARK4*

Families with PD originally linked to the *PARK4* locus were shown to possess duplications or triplications of the *PARK1* gene encoding α-synuclein (Singleton *et al,* 2003). Even though this is a rare cause of familial PD (Johnson *et al,* 2004), these observations showed the importance of gene dosage for the development of PD and further indicated α-synuclein in the development of idiopathic PD. These suggestions were strengthened by more recent genome-wide association studies (GWAS) linking the *PARK1* gene to idiopathic PD (Gonzalez-Perez *et al,* 2009).

1.2.5 *PARK5* - Ubiquitin C-terminal Hydrolase-L1 (UCHL1)

PARK5 codes for the neuronal enzyme UCHL1. It is a neuron-specific deubiquitinating enzyme that removes ubiquitin attached to a protein by E3 ubiquitin ligases (Harada *et al,* 2004). A missense mutation I93M was found to increase the susceptibility of an individual to develop PD with typical symptoms. The *PARK5* mutation was suggested to cause protein accumulation (Leroy *et al,* 1998). In conclusion, *PARK5* is a *PARK* gene implicating the importance of proteasomal protein degradation pathways in the pathogenesis of PD.

1.2.6 *PARK6* - Phosphatase and Tensin-homolog-induced Putative Kinase 1 (PINK1)

PARK6, located on chromosome 1, codes for the mitochondrial serine/threonine kinase PINK1. Mutations in *PARK6* were found to cause early-onset, autosomal recessive PD. As PINK1 was shown to prevent cytochrome c release in mitochondria (Petit *et al,* 2005), and to protect cells from oxidative stress, it was suggested to possess neuroprotective properties. Downregulation of PINK1 through small interfering RNAs (siRNA) was further found to decrease viability of SH-SY5Y cells (Deng *et al,* 2005), and cultured fibroblasts from patients with *PARK6* mutations were shown to exhibit an increase in lipid peroxidation and defects in mitochondrial complex I (Hoepken *et al,* 2007). These defects, however, could be rescued by the over-expression of the anti-oxidant enzyme superoxide dismutase 1 (SOD1) (Wang *et al*, 2006). More recently, PINK1 was found to play a role in mitochondrial quality control. It was suggested to function in concert with parkin in mitochondrial autophagy, and PINK1 appeared to be involved in the recruitment of parkin to the damaged mitochondria (Chu, 2010). This suggests parkin could be acting downstream of PINK1 in mitochondrial autophagy. This is in agreement with the previous observation that expression of parkin could abolish the effect of the loss of function of PINK1 (Yang *et al,* 2006). In summary, PINK1 is considered as a neuroprotective protein. Research provides evidence for an action together with parkin in mitochondrial autophagy and a role in the attenuation of oxidative stress.

1.2.7 *PARK7* – DJ-1

PARK7, located on chromosome 1, codes for the mitochondrial protein DJ-1. Mutations in *PARK7* cause early-onset, autosomal recessive PD. DJ-1 appears to exhibit anti-oxidative properties, as it was shown to reduce hydrogen peroxide by oxidising itself (Taira *et al,* 2004). Furthermore, DJ-1 was shown to facilitate the translocation of the transcription factor Nrf2 to the nucleus, inducing the expression of anti-oxidative genes (Clements *et al,* 2006). It could also activate glutathione ligase to increase the level of the antioxidant glutathione (Zhou and Freed, 2005). Mice deficient in DJ-1 were found to be more susceptible to intoxication by MPTP (Kim *et al,* 2005). Moreover, downregulation of DJ-1 through siRNA interference in SH-SY5Y cells was found to increase cell death by oxidative stress (Yokota *et al,* 2003). DJ-1 was also shown to act as a chaperone of α-synuclein, preventing α-synuclein aggregation (Shendelman *et al,* 2004). In summary, DJ-1 is assumed to be a neuroprotective protein that attenuates oxidative stress and might prevent protein aggregation.

1.2.8 *PARK8* – Leucine-rich Repeat Kinase 2 (LRRK2)

PARK8 encodes leucine-rich repeat kinase 2. LRRK2 plays an important role in PD pathogenesis, as mutations in *PARK8* are the most frequent cause of PD. This protein will be described in detail in the next section.

1.2.9 *PARK9* – ATP13A2

PARK9 codes for a neuronal ATPase called ATP13A2. Mutations in this gene were linked to the development of a form of early-onset recessive parkinsonism known as Kufor-Rakeb Syndrome (Williams *et al,* 2005). The physiological function of this protein is still unclear. However, the protein appears to be associated with lysosomes (Ramirez *et al*, 2006), raising the possibility that this protein is involved in cellular endocytic pathways. A missense mutation in ATP13A2, G504R, was also identified in a Brazilian PD patient with an early age of onset. The patient was reported to suffer from symptoms resembling those of sporadic PD, including levodopa responsiveness and motor deficits (Di Fonzo *et al,* 2007). A missense mutation (A746T) was also found to increase the risk of PD development in the ethnic Chinese population (Lin *et al,* 2008).

1.2.10 *PARK10*

Hicks *et al* (2002) had found that a locus on chromosome 1 is linked to late-onset PD in Icelandic PD patients. The gene present at this locus awaits identification, but the gene coding for Ring-Finger Protein 11 was suggested as one possible candidate. Ring-Finger Protein 11, like parkin, functions as an E3 ubiquitin ligase and was shown to be expressed in neurons (Anderson *et al,* 2007). It appears to play a role in growth factor signalling as well (Azmi and Seth, 2005).

1.2.11 *PARK11* – Grb10-Interacting GYF Protein 2 (GIGYF2)

PARK11, located on chromosome 2, encodes a protein called GIGYF2. Several missense mutations, N56S, T112A and D606E, were found in *PARK11* in Italian and French PD patients, with symptoms similar to idiopathic PD. GIGYF2 is likely to participate in signalling pathways through interaction with Grb10, an adaptor protein that binds tyrosine kinase receptors like insulin receptors (Giovannone *et al,* 2003). Recent evidence also showed the participation of GIGYF2 in signalling pathways involving the insulin growth factor (IGF). GIGYF2 was shown to enhance the phosphorylation of extracellular signal-related kinase 1/2 (Erk1/2) via IGF signalling (Higashi *et al,* 2010). GIGYF2 null mice were reported to exhibit motor dysfunction caused by motor neuron degeneration, decreased IGF receptor phosphorylation and increased Erk1/2 phosphorylation (Giovannone *et al,* 2009). This indicates that loss of function in GIGYF2 might play a role in neurodegeneration through the alteration of IGF signalling.

1.2.12 *PARK12*

PARK12 is located on the X-chromosome (Pankratz *et al,* 2003). The gene involved in causing PD present at this locus is yet to be identified.

1.2.13 *PARK13* – High Temperature Requirement A2 (HTRA2)

PARK13 is located on chromosome 2. This locus encodes a mitochondrial serine protease called HTRA2 (Bogaerts *et al,* 2008). This protein appears to be involved in apoptosis, as it was reported to bind an inhibitor of apoptosis protein and causes the release of caspase (Hegde *et al,* 2002). It was found to be an interactor of PINK1, and

the proteolytic activity of HTRA2 was shown to be regulated by the interaction with PINK1 (Plun-Favreau *et al,* 2007). This suggests that HTRA2 might regulate cell viability through the parkin/PINK1 pathway. A missense mutation, G399S, was suggested to be associated with PD as it was found in four German PD patients with typical PD symptoms and good response to levodopa treatment (Strauss *et al,* 2005). Strauss *et al* also discovered that this mutation could lead to mitochondrial dysfunction and cell death. More recently though, it was suggested that this protein is unlikely to be linked to PD (Yun *et al,* 2008), as the G399S amino acid change was also found in normal individuals (Simón-Sánchez and Singleton, 2008). Nevertheless, an involvement of HTRA2 mutations in PD could provide a link between apoptosis, mitochondrial dysfunction and PD.

1.2.14 *PARK14* – Phospholipase A2-G6 (PLA2G6)

PARK14 is located on chromosome 22. It codes for PLA2G6. Phospholipases are responsible for the breakdown of phospholipids, thereby releasing arachidonic acid. It was shown that *PARK14* mutations could lead to infantile neuroaxonal dystrophy, which is a neurodegenerative disease associated with iron accumulation in the brain. Yoshino *et al* (2010) reported that two mutations, F72L and R635Q, in *PARK14* were present in patients with early-onset, levodopa-responsive parkinsonism, although it is unclear how these mutations contribute to PD pathogenesis.

1.2.15 *PARK15* – F box Protein 7 (FBXO7)

PARK15, located on chromosome 22, encodes the E3 ligase FBXO7. It was shown to ubiquitinate proteins such as inhibitor of apoptosis protein (Chang *et al,* 2006), targeting it for proteasomal degradation. FBXO7 mutations were shown to be associated with autosomal recessive, early-onset PD. Di Fonzo *et al* (2009) had reported the presence of a nonsense mutation (R498stop) and a missense mutation (T22M) in two separate Caucasian families with early-onset PD. However, pathogenic mutations were not found in *PARK15* in PD patients of the ethnic Chinese origin (Luo *et al,* 2010).

1.2.16 *PARK16* – Rab7-L1

PARK16 is located on chromosome 1. It codes for a small GTP binding protein called Rab7-L1, which is an oncogene belonging to the Ras superfamily (Shimizu *et al,* 1997).

The physiological functions of Rab7-L1 are currently unclear. Interestingly, it was recently shown that single nucleotide polymorphisms (SNPs) in *PARK16* are associated with a decrease in the risk of PD pathogenesis in the Chinese population (Tan *et al,* 2010).

In conclusion, genes found to be mutated in PD patients were suggested to play a role in protein aggregation, mitochondrial dysfunction, oxidative stress and apoptosis.

1.3 LRRK2 – The Gene Product of *PARK8*

In 2002, a new locus was identified that showed linkage to PD in a Japanese family (Funayama *et al,* 2002). This locus was assigned as *PARK8*. In 2004, the gene that codes for the protein LRRK2 was identified as the disease-causing gene (Paisán-Ruíz *et al*, 2004). Intriguingly, mutations in *PARK8* are the most common known cause of PD, making LRRK2 an attractive therapeutic target for PD treatment. Understanding the functions of LRRK2 and how *PARK8* mutations lead to PD would therefore be useful in developing our understanding in PD pathogenesis, and ultimately in the search for new strategies for PD treatment. The following section provides a detailed overview of our knowledge on LRRK2, including domain structure, enzymatic functions, and proposed mechanisms leading to neurodegeneration.

1.3.1 The Structure of LRRK2

LRRK2 is a large protein with 2527 amino acids, and it has a molecular weight of over 280 kilo Daltons (kDa). It was suggested to exist as a dimeric protein under native conditions (Greggio *et al,* 2008). This large protein containing multiple domains might have various functions. In the N-terminus of the protein, there is a leucine-rich repeat (LRR) domain. It was suggested that a set of ankyrin repeats also exist towards the N-terminus of the LRR domain (Mata *et al,* 2006). The LRR domain is followed by the Ras of complex proteins (Roc) domain, which possesses intrinsic GTPase activity. Immediately after the Roc domain lies the C-terminal of Roc (COR) domain. The tandem nature of the existence of the Roc and COR domains, or generally Roc-COR domain, is a characteristic of a protein family called ROCO. In fact, the Roc domain

never occurs without being followed by the COR domain (Bosgraaf and Van Haastert, 2003; Gotthardt *et al,* 2008). The Roc-COR tandem domain of LRRK2 is followed by the kinase domain and the WD40 domain which contains seven WD40 repeats. A description of the functions of and the notable pathogenic, disease-segregating mutations in these domains are shown below.

1.3.1.1 The LRR Domain

The LRR domain contains 13 leucine-rich repeats (Mata *et al,* 2006). LRR domains are usually involved in protein-protein interactions (Kobe and Deisenhofer, 1995). To date, little is known about a possible link of the LRR domain to PD pathogenesis, although SNPs without clear segregation with PD within this domain were found in PD patients (section 1.3.5.1).

1.3.1.2 The Roc Domain

The Roc domain of LRRK2 is an important functional domain which possesses intrinsic GTPase activity. It shows sequence homology with the Ras GTPases, which is one of the components of cellular signalling pathways which regulate gene expression for cellular growth and survival. One of such pathways is the Erk/MAPK pathway (Avruch *et al,* 2001). In general, the Ras molecule acts as a molecular switch. The binding of guanosine triphosphate (GTP) to Ras, with the help from a guanosine exchange factor (GEF), results in Ras being activated (Cherfils and Chardin, 1999). In this 'on' state, Ras would be able to interact with an effector in a signalling pathway, including a mitogen-activated protein kinase kinase kinase (MAPKKK) called Raf-1 (Williams *et al,* 1992), for downstream signalling. Ras has intrinsic GTPase activity, albeit low, that hydrolyses the bound GTP to GDP. This event results in Ras being turned off and the termination of signalling. However, the termination of Ras activity is usually facilitated by a GTPase-activating protein (GAP) due to the low intrinsic GTPase activity of Ras (Ahmadian *et al,* 2003).

The Roc domain of LRRK2 was suggested to function in a similar way to the Ras GTPase. The LRRK2 Roc domain was shown to bind GTP (Smith *et al*, 2006; Guo *et al,* 2007; Ito *et al*, 2007), although the GEF for the Roc domain is yet to be identified. Evidence has suggested that the LRRK2 Roc domain has the ability to control the LRRK2 kinase activity (section 1.3.1.4). A GTP binding deficient mutant containing a

T1348N amino acid change was shown to completely abolish LRRK2 kinase activity (Ito *et al,* 2007), suggesting that GTP binding to the LRRK2 Roc domain is essential for the activation of kinase activity. The Roc domain was shown to hydrolyse GTP without the action of GAP *in vitro* (Guo *et al,* 2007). Guo *et al* (2007) also showed that the GTPase activity resulted in Roc being switched to the GDP-bound 'off' state. In conclusion, the Roc domain might play an important role in the activation of LRRK2, and this activation appears to be achieved through intra-molecular communication.

Interestingly, multiple sites of autophosphorylation in LRRK2 were reported recently. LRRK2 activation, like the activation of most kinases, was proposed to require the autophosphorylation of the kinase domain (Pike *et al,* 2008; Li *et al,* 2010). However, the autophosphorylation of the Roc domain was also described. The sites of Roc autophosphorylation include T1343, S1403, T1410 and T1491 (Greggio *et al,* 2009; Kamikawaji *et al,* 2009; Gloeckner *et al,* 2010). The functional significance of Roc autophosphorylation will be discussed in section 1.3.2.

Several SNPs were reported in the Roc domain, but only two mutations at R1441 clearly segregate with PD, R1441C and R1441G, while the R1441H mutation is also likely to be causal in the pathogenesis of PD (Healy *et al,* 2008). Additional SNPs in this domain, such as R1514Q, have also been found in PD patients, although they are not proven to be pathogenic (section 1.3.5). The multiple missense mutations present at R1441 suggests that this arginine might play an important role for LRRK2 function. It was suggested by Mata *et al* (2006) that R1441 is located on the surface of the protein, and might be important for LRRK2 interaction with substrates. Therefore, mutations of this residue might impact on such interactions. Several studies also showed the effect of these mutations on LRRK2 activity. The R1441C and R1441G mutations were found to decrease the ability of the Roc domain to hydrolyse GTP, although they were not found to affect GTP binding (Lewis *et al,* 2007; Li *et al,* 2007; Deng *et al,* 2008; Gotthardt *et al,* 2008; Xiong *et al,* 2010). A study suggested that the decreased GTP hydrolysis caused by the R1441C mutation could possibly be linked to alterations in protein folding, resulting in decreased stability of the LRRK2 dimer (Li *et al,* 2009a). A study also reported that the R1441C mutation affects LRRK2 kinase activity (West *et al,* 2005), although other groups reported that this mutation has no effect on kinase activity (Jaleel *et al,* 2007; Lewis *et al,* 2007). This discrepancy could possibly be due to the use

of different substrates, different experimental conditions and the relatively low activity of LRRK2 *in vitro* kinase assays. Furthermore, a novel pathogenic mutation, N1437H, was discovered recently in PD patients of the Norwegian population. This mutation was reported to lead to an increase in both the GTP binding and kinase activities of LRRK2 (Aasly *et al*, 2010). Taken together, PD-associated mutations in the Roc domain could possibly lead to PD pathogenesis through alterations of the catalytic activities of LRRK2.

1.3.1.3 The COR domain

The COR domain is situated immediately C-terminal to the Roc domain. One group suggested a role for the Roc-COR tandem domain in the dimerisation of LRRK2, as a Roc-COR fragment with a truncated COR domain failed to dimerise (Gotthardt *et al,* 2008). Hence, the COR domain could be involved in mediating LRRK2 dimerisation. The COR domain was also reported to mediate the interaction between LRRK2 and parkin (Smith *et al,* 2005). Interestingly, both LRRK2 and parkin were found in Lewy bodies, although only a small proportion of LRRK2 appears to be localised in these structures (Schlossmacher *et al,* 2002; Vitte *et al,* 2010). Hence, an interaction between these two proteins might be associated with the protein aggregation in Lewy bodies.

One missense mutation, Y1699C, identified in the COR domain clearly segregates with PD (Khan *et al,* 2005). This mutation was found to lower the LRRK2 GTPase activity (Gotthardt *et al*, 2008; Daniëls *et al,* 2010; Xiong *et al*, 2010). A recent study reported that this mutation could lead to the abolition of an interaction between LRRK2 and DVL1, a protein involved in the canonical Wnt signalling pathway (Sancho *et al,* 2009). This observation raises the possibility that this mutation might lead to alterations in Wnt signalling through glycogen synthase kinase 3 beta (GSK3β). GSK3β has previously been implicated in neuronal apoptosis (Wang *et al,* 2009).

1.3.1.4 The Kinase Domain

The kinase domain is the most extensively studied domain in LRRK2 due to the requirement of kinase activity for LRRK2 cytotoxicity. Kinase dead mutants of LRRK2 were reported to have no increased detrimental effect on cell viability in comparison to over-expressed wild type (WT) LRRK2 (Smith *et al,* 2006). The LRRK2 kinase domain shows homology to mixed lineage kinase (MLK) (West *et al*, 2007), but was reported to

show a preference for threonine phosphorylation over serine phosphorylation (Nichols *et al,* 2009). LRRK2 was shown to interact with MKK3/6 and MKK 4/7, which are linked to the JNK signalling pathway involved in cellular stress response and the modulation of cytoskeletal dynamics (Gloeckner *et al,* 2009). Similar to kinases in the Erk/MAPK pathway (Johnson *et al,* 1996), LRRK2 was consistently reported to exhibit autophosphorylation (Luzón-Toro *et al,* 2007; Greggio *et al,* 2008; Li *et al,* 2010). Within the kinase domain, there is a section named the activation loop. The phosphorylation of the activation loop is an essential event for kinase activation, as this causes a conformational change in the active site that positions the essential magnesium ion optimally to achieve catalysis (Nolen *et al,* 2004). LRRK2 was reported to have three putative autophosphorylation sites within the activation loop. They were identified as T2031, S2032 and T2035 (Li *et al,* 2010). The phosphorylation of at least one of these residues appeared to be the pre-requisite for kinase activation. In addition, the kinase domain was also shown to autophosphorylate several sites in the Roc domain (section 1.3.1.2) which might be involved in the regulation of signal output of LRRK2 (section 1.3.2)

One controversy over LRRK2 activation is whether the autophosphorylation event occurs in *trans* or in *cis*. Luzón-Toro *et al* (2007) suggested that the kinase domain of both monomer units in the LRRK2 dimer phosphorylate one another, resembling an inter-molecular phosphorylation. However, Greggio *et al* (2008) suggested that the autophosphorylation is an intra-molecular event. The discrepancy in the conclusions drawn is unclear, but it could be caused by the different experimental conditions used.

The kinase domain of LRRK2 is also interesting for the fact that the mutation G2019S, the most common known mutation among PD patients, is located in this domain. The G2019S and I2020T mutations both clearly segregate with PD. However, only G2019S was consistently shown to cause an increase in LRRK2 kinase activity (West *et al,* 2005; Jaleel *et al,* 2007). I2020T was reported to cause an increase in autophosphorylation (Gloeckner *et al,* 2006), yet a decrease in phosphorylation of a previously suggested LRRK2 substrate called moesin (Jaleel *et al,* 2007). Both of these PD-associated mutations in the kinase domain are located within the activation loop. G2019S is located within the DYG motif, the binding site of the magnesium ion and the N-terminal end of the activation loop (Nolen *et al,* 2004). I2020T is located just

adjacent to this motif (Greggio *et al,* 2006). It is unclear, however, why these mutations can lead to alterations in kinase activity. Greggio *et al* (2006) suggested the possibility that an alteration in protein conformation caused by a substitution for a larger amino acid at these sites might lead to an alteration of the kinase activity of LRRK2. West *et al* (2007) also tried to rationalise this observation and pointed out that the mutations introduce a further potential phosphorylation site within the activation loop.

Another important report on the G2019S and I2020T mutations was an observed shortening of the neurite length and reduced branching in neurons (MacLeod *et al,* 2006). Previously, it was suggested that the shortening of neurites in G2019S-LRRK2-transfected cells might be due to an increase in autophagy, as the knockdown of proteins involved in autophagy was shown to reverse the effect of this LRRK2 mutant on neurite shortening (Plowey *et al,* 2008). In addition, LRRK2 was reported to be present at autophagic vacuoles (Alegre-Abarrategui *et al,* 2009). These observations have suggested a mechanism of LRRK2 mutants in causing PD through deregulated autophagy.

1.3.1.5 The WD40 Domain

The WD40 domain is located at the C-terminus of LRRK2. Like the LRR domain, this domain is present in a wide variety of proteins and plays a role in protein-protein interactions (Li and Roberts, 2001). WD40 domain proteins show a preference to bind to proteins phosphorylated at serines and threonines (Yaffe and Smerdon, 2004). It was recently found that this domain could play a role in LRRK2 dimerisation, autophosphorylation and neurotoxicity, as the removal of this domain led to a failure in dimer formation and autophosphorylation of LRRK2, as well as the abolition of mutant LRRK2 to exhibit cellular toxicity (Jorgensen *et al,* 2009). In other words, LRRK2 dimerisation might not only require the COR domain, but also the WD40 domain. The role of the WD40 in neurotoxicity is controversial, but interestingly, the deletion of the WD40 domain of LRRK2 in zebrafish was reported to lead to locomotive defects and the loss of dopaminergic neurons (Sheng *et al,* 2010).

1.3.2 The Inter-relationship between LRRK2 Roc and Kinase Domains

The Roc and kinase domains are the only two domains in LRRK2 that possess enzymatic activities. The phenomenon of 'one protein, two enzymes' (Mata *et al,* 2006) in LRRK2 suggests that the activity of one of the domains could be regulated by the activity of the other. It is widely accepted that the GTP binding activity of the Roc domain might trigger the activation of the kinase domain through some yet poorly understood mechanisms of intra-molecular communication, leading to autophosphorylation of the residues within the activation loop (section 1.3.1.4) and possibly the phosphorylation of downstream substrates of LRRK2. Increased phosphorylation of LRRK2 substrates may cause modulation of some signalling pathways. Taken together, the Roc domain could be seen as a regulator of the kinase domain. This idea is supported by the observation that the kinase activity was dependent on the intact Roc domain in *in vitro* kinase assays (Smith *et al*, 2006; Guo *et al*, 2007; West *et al*, 2007), whereas the isolated Roc domain exhibited intrinsic GTPase activity (Li *et al,* 2007). The importance of GTP binding in LRRK2 function and cellular viability was also indicated by the report of the prevention of cellular toxicity in *C. elegans* upon over-expression of a GTP binding mutant LRRK2, in comparison to the over-expression of WT LRRK2 which reportedly caused a moderate decrease in cellular viability (Yao *et al,* 2010). The model of this Roc-kinase relationship is depicted in figure 1.2.

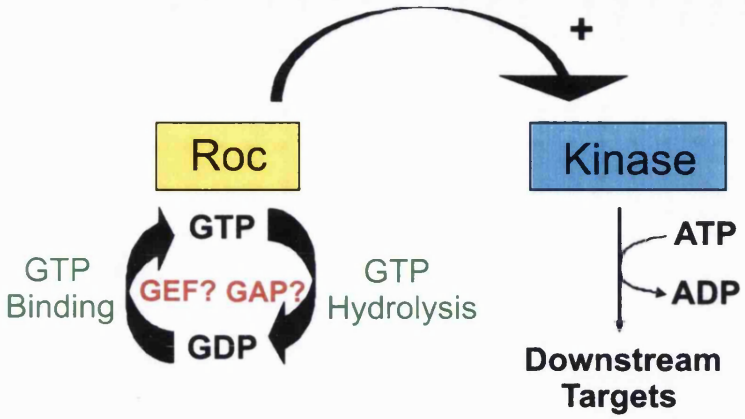

Figure 1.2: Model of LRRK2 kinase activation by GTP binding to the Roc domain. GTP binding to the Roc domain, possibly facilitated by an unidentified GEF, triggers an activation of the kinase domain in an intra-molecular fashion. This activation results in the phosphorylation of LRRK2 substrates and further downstream signalling. The LRRK2 Roc domain possesses intrinsic GTPase activity, and perhaps with the help of a GAP, it hydrolyses the GTP to return LRRK2 into the inactive, GDP-bound state, thereby switching off LRRK2 kinase activity. (+ indicates an activation)

Recently, with the discovery of autophosphorylation sites within the Roc domain, a question was raised whether the kinase domain could also have a regulatory effect on the Roc domain. Kamikawaji *et al* (2009) performed GTP binding assays and kinase assays using LRRK2 phosphomimetic mutants generated by the introduction of aspartate at some Roc autophosphorylation sites, aiming to mimic the phosphorylated state of these residues. They showed that the T1491D mutant, mimicking T1491 autophosphorylation, could cause a significant decrease in both the GTP binding and kinase activities of LRRK2, although they did not observe the effect of T1343 or T1410 autophosphorylation on LRRK2 GTP binding and kinase activities. These data raise the possibility that GTP-bound LRRK2 autophosphorylates not only the activation loop of the kinase domain, but also the Roc domain. Roc autophosphorylation could then serve as a negative feedback mechanism, decreasing LRRK2 kinase activity, via a decrease in GTP binding. However, the effect of Roc autophosphorylation on GTPase activity still requires further investigation. In the diagram below, a second possible model of the inter-relationship of the Roc and kinase domains is depicted (figure 1.3).

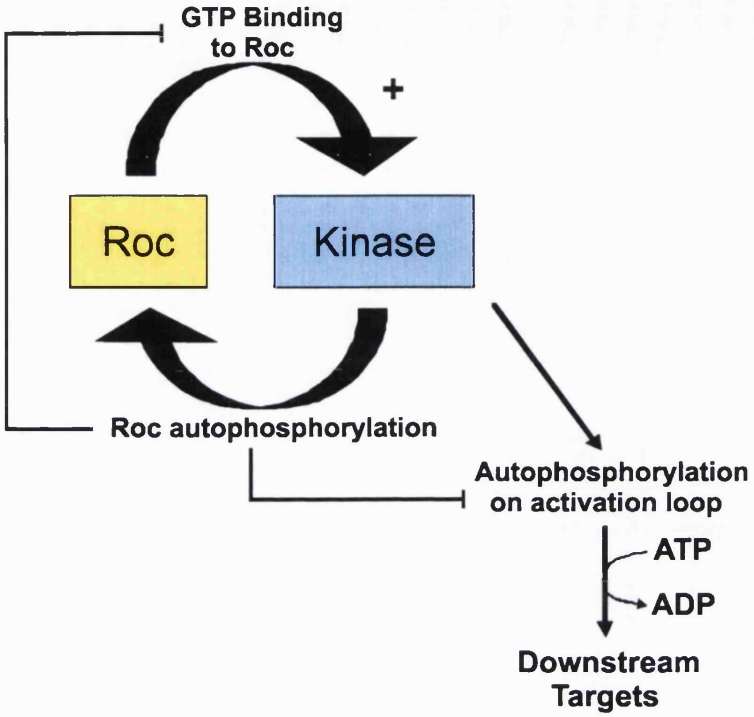

Figure 1.3: Model of the auto-regulation of LRRK2 kinase activity through Roc autophosphorylation. GTP binding to the Roc domain results in the autophosphorylation of the activation loop in the kinase domain and kinase activation, as depicted in figure 1.2. This might result in the phosphorylation of downstream targets. At the same time, the kinase domain autophosphorylates Roc domain residues, resulting in decreased GTP binding to the Roc domain. This in turn leads to a decrease in kinase activation. The autophosphorylation of the Roc domain hence might serve as a feedback mechanism of the LRRK2 kinase activation (+ indicates activation).

1.3.3 LRRK2 Dimerisation in the Functioning of LRRK2

Much experimental evidence has pointed towards a dimeric nature of LRRK2 (Deng *et al,* 2008; Gotthardt *et al,* 2008; Greggio *et al,* 2008; Jorgensen *et al,* 2009; Klein *et al,* 2009). Models proposed a role for the Roc-COR tandem domain in LRRK2 dimerisation events. Deng *et al* (2008) proposed a domain swapping model, in which the tandem domain interacts through protein-protein interactions via the Roc domain. In fact, domain swapping is a well-characterised mechanism in which proteins form dimers or oligomers (Bennett *et al,* 1995). This model also proposed that the COR

domain might act as a messenger, relaying signals of conformational change from the Roc domain, following cycles of GTP binding and hydrolysis, to the kinase domain, thereby leading to kinase activation. Gotthardt *et al* (2008) proposed a different model, whereby the COR domain plays a direct role in Roc-COR dimerisation of LRRK2. However, it is important to note that LRRK2 constructs without the Roc-COR domain still retained dimeric properties (Klein *et al,* 2009). Furthermore, one group also reported the existence of homomultimeric LRRK2 (Sen *et al,* 2009), suggesting that LRRK2 might not only have the ability to form dimers, but also oligomeric species. The role of oligomeric LRRK2 in cells still requires further investigation, although Sen *et al* (2009) proposed that oligomeric LRRK2 is likely to be an inactive form of LRRK2.

In fact, LRRK2 dimerisation seems to be a pre-requisite of the enzymatic activities exhibited by the Roc and kinase domains. Gotthardt *et al* (2008) found that a dimerisation-defective Roc-COR fragment, which lacked the C-terminal region of the COR domain, exhibited no GTPase activity. They also suggested that, unlike small GTPases, GTP hydrolysis might be executed through LRRK2 dimerisation without the need of GAPs. Sen *et al* (2009) presented evidence for the importance of LRRK2 dimerisation for kinase activity. The pharmacological inhibition of LRRK2 autophosphorylation by staurosporine led to a decrease in the amount of LRRK2 dimers in HEK293 cells. As dimerisation of kinases is a well-documented event in the regulation of the activity of serine/threonine kinases (Pelech *et al,* 2006), it is reasonable to speculate that LRRK2 kinase activity might also be regulated by dimerisation.

1.3.4 Expression and Distribution of LRRK2

LRRK2 is a ubiquitously expressed protein which was shown to be present not only in the brain, but also in the kidneys, liver and heart (Miklossy *et al,* 2006; Higashi *et al,* 2007a). Within the central nervous system (CNS), LRRK2 expression was found to be present not only in neurons, but also in astrocytes and microglial cells (Miklossy *et al,* 2006). Furthermore, LRRK2 expression was reported in various regions, including the cerebellum, cerebral cortex and hippocampus (Simón-Sánchez *et al*, 2006; Higashi *et al,* 2007b). Importantly for PD, LRRK2 was also detected in dopamine-innervated areas such as the striatum (Simón-Sánchez *et al*, 2006; Higashi *et al,* 2007a). Interestingly, LRRK2 expression levels were observed to be higher in the striatum than in the SNpc,

the brain region primarily affected in PD (Galter *et al,* 2006; Melrose *et al,* 2006; Schapira *et al,* 2006). However, LRRK2 mRNA was almost undetectable in the SNpc although a low level of LRRK2 protein was reported to be present (Higashi *et al,* 2007b). This discrepancy was suggested to be due to the short half life of some mRNAs (Gandhi *et al,* 2009). Another study observed LRRK2 protein level in the SNpc to be higher than that in the ventral tegmental area, another brain region enriched in dopaminergic neurons but not affected in PD (Han *et al,* 2008). This indicates the possibility of an involvement of LRRK2 in the death of dopaminergic neurons in PD. Interestingly, LRRK2 expression was shown not to be restricted to neurons, but was also detected in astrocytes and oligodendrocytes which play a role in supporting neuronal functions and survival (Miklossy *et al,* 2006).

Within a cell, LRRK2 was found to localise largely in the cytoplasm and dendritic processes (West *et al,* 2005). However, a proportion of LRRK2 was also found in association with membranous structures including the mitochondrial outer membrane, the Golgi apparatus, endoplasmic reticulum, transport vesicles and lipid rafts on the cell membrane (West *et al,* 2005; Biskup *et al,* 2006; Hatano *et al,* 2007). The association of LRRK2 with these membranous structures suggests a function of LRRK2 in synaptic vesicle recycling and cellular transport. Interestingly, LRRK2 was also found to be present in Lewy bodies, and even in neurofibrillary tangles, a hallmark of AD (Miklossy *et al,* 2006).

LRRK2 expression was reported to be prominent during the course of embryonic development. Zechel *et al* (2010) investigated the expression of LRRK2 during mouse embryonic development. LRRK2 expression was found to be the most prominent during embryonic day 11 to day 17, the period when neurogenesis occurs. Furthermore, LRRK2 expression was also detected in migrating cerebellar granule neurons. Although more evidence is required, the presence of LRRK2 expression in developing neurons suggests a role of LRRK2 in neuronal development.

1.3.5 *PARK8* mutations in LRRK2

Since 2004, studies revealed the presence of dominant mutations in *PARK8* in PD patients from many parts of the world. The dominant mode of inheritance of *PARK8*

mutations suggests a gain of function of the mutant protein, meaning that mutations could lead to increased or an additional function of LRRK2.

1.3.5.1 Mutations Segregating with PD are Found in LRRK2 Catalytic Domains

In section 1.3.1, the pathogenic mutations in the Roc-COR tandem domain and kinase domain clearly segregating with PD were introduced. However, SNPs were also found in all the other domains in LRRK2. For example, the R1067Q, S1096C, I1122V and S1228T amino acid changes in the LRR domain were found to be present in PD patients. These four amino acid changes are likely to be located on the surface of the protein (Mata *et al,* 2006), and therefore could play a role in PD pathogenesis through alterations in LRRK2 interactions with substrates. Nonetheless, none of these SNPs has been shown to segregate clearly with PD, and the pathogenicity of these SNPs awaits further investigation. In the WD40 domain, the G2385R mutation, which is only present in PD patients of ethnic Chinese origin, was reported to confer an increased risk for the development of PD (Funayama *et al,* 2007). Figure 1.4 shows the position of the previously found PD-associated mutations and SNPs in relation to the LRRK2 domains.

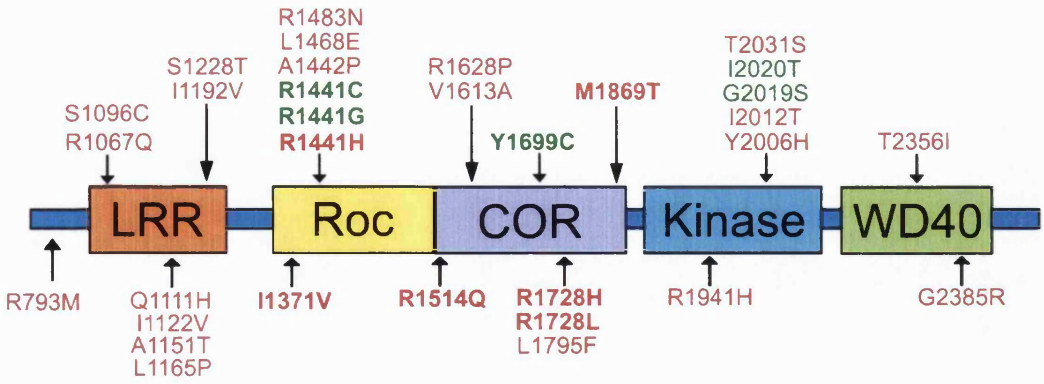

Figure 1.4: SNPs are found in exons encoding all domains of LRRK2. The domain layout of LRRK2 and the reported amino acid changes in each of the domains are shown. Highlighted in green are mutations that have been proved to be pathogenic. Highlighted in red are amino acid changes found previously in PD patients, yet there is no evidence for their pathogenicity to date. Mutations shown in bold are the *PARK8* mutations in the Roc-COR tandem domain that are examined in this thesis.

1.3.5.2 Epidemiological Features of PARK8 Mutations

PARK8 is the only gene with mutations that can cause both late-onset, apparently sporadic and familial PD (Guo *et al,* 2006). *PARK8* mutations account for up to 8% of familial PD cases and 1.6% of sporadic ones (Schapira, 2006). Among the pathogenic *PARK8* mutations, G2019S is the most widely studied of all, owing to its high prevalence in PD. 40% of the familial PD patients in the North African Arabic population (Lesage *et al,* 2005; Lesage *et al,* 2006), 30% of the Ashkenazi Jews (Ozelius *et al,* 2006) and 6% of European Caucasians (Kachergus *et al,* 2005) bear this mutation, whereas the G2019S mutation is not present in PD patients with ethnic Chinese origins (Fung *et al,* 2006). The clinical features of PD patients bearing the G2019S mutation were reported to be almost always indistinguishable from those of idiopathic PD patients (Mata *et al,* 2006). This fact contributes to the extent of the research effort into LRRK2, as this research can potentially reveal molecular events and/or signalling pathways that are involved in the pathogenesis of idiopathic PD.

Incomplete penetrance in PD is also an important feature of *PARK8* mutations. Incomplete penetrance of *PARK8* mutations refers to the phenomenon that the occurrence of mutations at the *PARK8* locus does not always result in PD. The penetrance of *PARK8* mutations was shown to increase with age. For example, in the Caucasian population, the pathogenic G2019S mutation has a penetrance of 17% at the age of 50, increasing to 85% at the age of 70 (Kachergus *et al,* 2005). Incomplete penetrance of *PARK8* mutations suggests that LRRK2-induced neurodegeneration in PD could require additional insults affecting the survival of neurons.

1.3.5.3 PARK8 Mutations Results in Pleomorphic Pathology

An interesting feature of *PARK8* mutations is that they exhibit pleomorphic pathology. Pleomorphism refers to the ability of different mutations in a gene to cause various clinical features or symptoms. As discussed, the G2019S mutation was reported to cause PD symptoms indistinguishable from those observed in idiopathic PD, including nigral cell loss, the presence of Lewy bodies and good response to levodopa, although some G2019S carriers may exhibit AD-like features such as the presence of phospho-tau-abundant neurofibrillary tangles (Rajput *et al,* 2006). Other *PARK8* mutations may cause slightly different Parkinsonian symptoms in several cases. For example, R1441C mutation carriers generally exhibit nigral cell loss, but in one patient the formation of

ubiquitin-positive inclusions in neurons was observed. Carriers of the Y1699C mutation showed ubiquitin-positive inclusions (Zimprich *et al,* 2004). In an additional two cases, amyotrophy was observed. Furthermore, I2020T carriers display nigral cell loss, without the formation of Lewy bodies (Funayama *et al,* 2005). The pleomorphic nature of *PARK8* mutations indicates that LRRK2 may lead to neurodegeneration in different ways through the participation and modulation in various signalling pathways.

1.3.6 Identified Interactors of LRRK2

The search for the proteins that can interact with LRRK2 might help to unravel the neurodegenerative signalling pathways that LRRK2 participates in and further our understanding of the pathological role of mutant LRRK2.

To date, a number of proteins were reported to interact with LRRK2. Table 1.1 summarises the discovered LRRK2 interactors, and the reported effects of *PARK8* mutations on the strength of interaction. A brief introduction to the functions and roles of these proteins is also provided below.

1.3.6.1 Moesin

Moesin was discovered as a LRRK2 interactor using the kinase substrate tracking and elucidation (KESTREL) screen in rat brain lysates (Jaleel *et al,* 2007), and the PD-associated G2019S mutation was found to enhance moesin phosphorylation (Parisiadou *et al*, 2009), although it was reported that LRRK2 may not phosphorylate moesin directly (Nichols *et al*, 2009). Physiologically, moesin acts as a bridge between plasma membrane and actin, thereby attaching the actin cytoskeleton to the cell membrane. Therefore, it possibly plays a role in the regulation of cellular morphology. Furthermore, this protein appears to play a role in the regulation of neurite growth, as knockdown of moesin by RNA interference in primary neurons was shown to lead to an abrogation in neurite development (Paglini *et al,* 1998). The effect of various *PARK8* mutations on moesin phosphorylation reported by Jaleel *et al* (2007) is shown in table 1.1. The interaction between LRRK2 and moesin could suggest a role of LRRK2 in the regulation of cytoskeletal rearrangement.

LRRK2 interactors	Cellular processes involved	Effect of PD-associated mutations	References
Moesin	Cytoskeletal regulation	Moesin phosphorylation (in *in vitro* kinase assays) - G2019S: increased I2012T: decreased I2020T: decreased G2385R: decreased R1441C: no effect R1441G: no effect Y1699C: no effect	Jaleel *et al,* 2007
Rab5b	Synaptic vesicle endocytosis	Rab5b interaction – R1441C: no effect G2019S: no effect	Shin *et al,* 2008
4E-BP	Initiation of translation/protein synthesis	4E-BP phosphorylation (in *in vitro* kinase assays) – I2020T: increased	Imai *et al,* 2008
Hsp90	Protein stability	Not assessed	Wang *et al,* 2008
CHIP	Protein degradation	CHIP interaction – R1441C: no effect G2019S: no effect	Ko *et al,* 2009
14-3-3	Cellular signalling	14-3-3 interaction – R1441C: decreased R1441G: decreased R1441H: decreased Y1699C: decreased G2019S: increased I2020T: decreased	Nichols *et al,* 2010
Parkin	Protein degradation	Not assessed	Smith *et al,* 2005
Tubulin	Formation of microtubules	Tubulin interaction – R1441C: no effect Tubulin phosphorylation – G2019S: increased	Gandhi *et al,* 2008 Gillardon, 2009
FADD	Apoptosis	FADD interaction – R1441C: increased R1441G: increased Y1699C: increased G2019S: increased I2020T: increased	Ho *et al,* 2009
MKK	Erk/MAPK and JNK signalling pathways	MKK6 phosphorylation (in *in vitro* kinase assays) – R1441C: no effect G2019S: increased I2020T: increased	Gloeckner *et al,* 2009
JIP	JNK signalling pathway	Not assessed	Hsu *et al,* 2010

Table 1.1: Summary of the LRRK2 interactors identified to date and the effect of *PARK8* mutations on these interactions.

1.3.6.2 Rab5b

The interaction between LRRK2 and Rab5b was shown using glutathione-S-transferase (GST) pull down and co-immunoprecipitation experiments. This interaction appeared to be GTP dependent, as only upon co-incubation of GTP-γS, a non-hydrolysable GTP analogue, did an interaction between LRRK2 and Rab5b occur (Shin *et al,* 2008). Rab is a small GTPase that is important in membrane trafficking from the cell membrane to early endosomes (Carney *et al,* 2006). This suggests the LRRK2 – Rab5b interaction could be involved in synaptic vesicle endocytosis (Shin *et al,* 2008). This speculation is also supported by the presence of Rab5 on the membrane of synaptic vesicles in dendrites and axons of hippocampal neurons (de Hoop *et al,* 1994). Mutations such as R1441C and G2019S failed to abolish the LRRK2 – Rab5b interaction.

1.3.6.3 Eukaryotic Initiation Factor 4E Binding Protein (4E-BP)

4E-BP is an inhibitor of the eukaryotic initiation factor 4E (eIF-4E), a protein involved in the initiation of translation. eIF-4E functions in the initiation of translation through binding to the cap at the 5' end of mRNAs (Gingras *et al,* 1999). The binding of 4E-BP to eIF-4E, which occurs constitutively, abrogates the eIF-4E – mRNA binding (Richter *et al,* 2005). The phosphorylation of 4E-BP leads to the dissociation from eIF-4E, resulting in translation initiation. Imai *et al* (2008) reported that 4E-BP is a substrate of LRRK2. LRRK2 could phosphorylate 4E-BP on Thr37 and Thr46, and the *PARK8* mutation I2020T resulted in an increase of 4E-BP phosphorylation (table 1.1). However, it was recently reported that 4E-BP may not be a direct substrate of LRRK2 (Kumar *et al*, 2010). Nonetheless, the interaction between LRRK2 and 4E-BP suggests that LRRK2 could play a part in the regulation of protein synthesis, and LRRK2 pathogenic mutants could be involved in neurodegeneration through the deregulation of translation initiation.

1.3.6.4 Hsp90 and Carboxyl Terminus of Hsp70-interacting Protein (CHIP)

Hsp90 and CHIP are both proteins involved in protein folding and stability. LRRK2 was reported to interact with both proteins (Wang *et al,* 2008; Ko *et al,* 2009), suggesting that the interactions could play a part in the regulation of LRRK2 levels in cells. Hsp90 is a chaperone protein responsible for the stabilisation of proteins that bind to it. The binding of Hsp90 to LRRK2 was also suggested to prevent LRRK2 from

being degraded in the proteasome (Wang *et al,* 2008). Inhibition of Hsp90 caused the dissociation of Hsp90 from LRRK2. It is possible that through LRRK2 interaction with CHIP as described below, LRRK2 might be tagged for degradation in the proteasome. The G2019S mutant of LRRK2 was found to form a stable complex with Hsp90 (Wang *et al,* 2008). This suggests a role of this mutant in the stabilisation of LRRK2, possibly resulting in LRRK2 accumulation.

CHIP is an ubiquitin E3 ligase that tags proteins for degradation in the proteasome. Therefore, like parkin, it plays a role in the quality control of proteins. The observation of a LRRK2 – CHIP interaction led to the proposal that LRRK2 could be targeted for degradation in the proteasome by the E3 ligase activity of CHIP. LRRK2 – CHIP interaction was reportedly mediated by the Roc domain, and the LRRK2 mutants R1441C and G2019S showed no influence on this interaction (Ko *et al,* 2009).

1.3.6.5 14-3-3

LRRK2 was recently reported to be an interactor of 14-3-3 protein. The primary role of 14-3-3 as a cellular signalling protein is in controlling the cell cycle (Conklin *et al,* 1995; Shinoda *et al,* 2003). 14-3-3 was also found to be implicated in PD due to its ability to interact with proteins like α-synuclein (Ostrerova *et al,* 1999) and parkin (Sato *et al,* 2006), and the presence of 14-3-3 in Lewy bodies (Ubl *et al,* 2002). 14-3-3 binding to LRRK2 appeared to be mediated by phosphorylation of Ser910 and Ser935 close to the N-terminal of the LRRK2 LRR domain. Disruption of 14-3-3 binding by substituting the serine at both sites for an alanine resulted in LRRK2 aggregation and inclusion body formation (Dzamko *et al,* 2010). Interestingly, R1441C, R1441G, R1441H, Y1699C and I2020T mutations all led to a decrease in the interaction between LRRK2 and 14-3-3 through the decreased phosphorylation of Ser910 and Ser935, resulting in LRRK2 accumulation (Nichols *et al,* 2010). In contrast, the pathogenic G2019S mutation increased autophosphorylation of Ser910 and Ser935 (Nichols *et al,* 2010). The discovery that LRRK2 interacts with 14-3-3, and that this interaction is dependent on LRRK2 phosphorylation, have provided evidence on the role of LRRK2 kinase activity in protein accumulation, which is a hallmark of PD.

1.3.6.6 Parkin

The reported LRRK2 interaction with parkin (Smith *et al*, 2005) might provide further evidence for a role of LRRK2 in the regulation of protein levels in cells. The physiological functions of parkin and the nature of the LRRK2 – parkin interaction are discussed in section 1.2.2 and section 1.3.1.3 respectively.

1.3.6.7 Tubulin

An interaction between LRRK2 and tubulin was first reported by Gandhi *et al* (2008). They showed the interaction of α/β tubulin heterodimers with the LRRK2 Roc domain, and that the R1441C-Roc mutant can retain this interaction. Gillardon (2009) also showed LRRK2 to phosphorylate tubulin, and that the G2019S mutation in LRRK2 leads to an increase in tubulin phosphorylation. The LRRK2 – tubulin interaction is the focus of this thesis, and will be discussed in more detail in chapter 4.

1.3.6.8 Fas-associated Death Domain (FADD)

FADD is one of the components of the extrinsic pathway of apoptosis. Association with Fas molecule following Fas ligand binding leads to the activation of caspase 8 through the cleavage of the death effector domain, which triggers the apoptotic pathway. Ho *et al* (2009) demonstrated the interaction between LRRK2 and FADD, and PD-associated pathogenic LRRK2 mutants (R1441C, R1441G, Y1699C, G2019S and I2020T) all resulted in an increase of the interaction level. Furthermore, knockdown of caspase 8 in primary neurons transfected with mutant LRRK2 was found to attenuate LRRK2-induced neurodegeneration (Ho *et al,* 2009). All these findings suggest a possible role of LRRK2 in triggering apoptosis via FADD and caspase 8. In line with this, Fas and FADD are both expressed in neurons within the SNpc in PD patients (de la Monte *et al,* 1998). Furthermore, caspase 8 activation was found to occur in the SNpc neurons in autopsied PD patients (Hartmann *et al,* 2001). Taken together, the data suggest that mutant LRRK2 could lead to neurodegeneration by the activation of pathways leading to apoptosis.

1.3.6.9 MKK

MKKs are kinases involved in the c-jun N-terminal kinase (JNK) and p38 MAPK signalling pathways. LRRK2 was shown to bind and exhibit kinase activity on MKK3, MKK4, MKK6 and MKK7 (Gloeckner *et al,* 2009). MKK4 and MKK7 are JNK

activators (Ho *et al,* 2006), while MKK3 and MKK6 are activators of p38 (Derijard *et al,* 1995). The discovery of the enzyme-substrate relationship between LRRK2 and MKKs has the potential to place LRRK2 in the JNK and p38 signalling pathways, which are MAPK signalling pathways activated during the cellular stress response. Both JNK and p38 are signalling proteins involved in neuronal apoptosis and the regulation of microtubule dynamics. Furthermore, JNK was found to interact with microtubule-associated protein MAP2 and knockdown of JNK in mice resulted in a decrease in MAP2 phosphorylation and detachment from microtubules (Chang *et al,* 2003). Since MAP2 appears to play a role in the stability of microtubules (Illenberger *et al,* 1996), JNK activation and the subsequent microtubule detachment of MAP2 could affect microtubule stability. Furthermore, LRRK2 was shown to be an interactor of JNK-interacting proteins (JIPs) (Hsu *et al,* 2010). JIPs play a role in the activation of the JNK signalling pathway, as disruption of *JIP1* gene was found to abolish JNK activation in primary neurons in response to stress (Whitmarsh *et al,* 2001). Previously, JIP1 was proposed to act as a linker between the cargo-containing vesicles and kinesin 1 along the microtubules (Horiuchi *et al,* 2007). Activation of JNK by phosphorylation was proposed to lead to dissociation between JIP1 and kinesin 1, as over-expression of MKK7, an activator of JNK, in cultured Drosophila S2 cells abolished the interaction between JIP1 and kinesin 1 in co-immunoprecipitation experiments (Horiuchi *et al,* 2007). p38 activation was shown to enhance tau phosphorylation (Puig *et al,* 2004), a hallmark of AD which causes the dissociation of tau from microtubules, thereby affecting microtubule stability. Taken together, these findings have indicated a possible link between LRRK2 and neuronal viability and microtubule integrity.

1.4 Aims of the Thesis

PARK8 mutations are by far the most common known cause of PD. The clear segregation of some *PARK8* mutations with PD, along with the observation that PD patients bearing *PARK8* mutations show symptoms indistinguishable from those of idiopathic PD, renders LRRK2 an attractive therapeutic target for PD treatment. Despite intense efforts in LRRK2 research, the precise mechanism by which LRRK2 causes PD and neurodegeneration remains elusive. The search for LRRK2 interactors and the

assessment on whether PD-associated *PARK8* mutations can modify LRRK2 interactions could provide clues on the identification of the biological function of LRRK2, and the molecular pathways that LRRK2 could play a role in. This could also potentially help reveal the molecular mechanisms in which mutant LRRK2 contributes to PD pathogenesis.

This thesis focuses on a newly discovered LRRK2 interaction with β-tubulin isoforms. Tubulins are integral components of the microtubule cytoskeleton. Microtubules play an important role in a variety of cellular processes such as axonal transport, which is vital for both synaptic functions and the survival of neurons. The importance of the microtubule cytoskeleton in neuronal function and survival makes the interaction between LRRK2 and microtubules a promising theme of research in the pathobiology of mutant LRRK2. The LRRK2 – tubulin interaction was investigated in detail with the prospect of establishing whether this interaction can provide further evidence for the involvement of the microtubule cytoskeleton in PD. The aims of this thesis include:

- The establishment of the specificity of the LRRK2 interaction with neuronally expressed β-tubulin isoforms, and the identification of the amino acid residues within these isoforms that underlie this specificity;

- Identification of the LRRK2 domains important for the interaction with β-tubulin;

- The investigation of a modulatory effect of PD-associated *PARK8* mutations on the strength of the dimerisation of LRRK2 and the LRRK2 – tubulin interaction in order to see if any modulatory effect on the LRRK2 dimerisation correlates with that on the interaction with tubulin;

- The confirmation of the LRRK2 – tubulin interaction in mammalian cell models, including the investigation of an association of endogenous LRRK2 with components of the cytoskeleton in differentiated SH-SY5Y cells;

- The assessment of the effect of GTP binding to and autophosphorylation of the LRRK2 Roc domain on the strength of the dimerisation of LRRK2 and the LRRK2 – tubulin interaction; and

- Establishment of a LightScanner protocol for the screening of DNA samples from the Parkinson's UK brain bank for mutations in *PARK8*.

2. Materials and Methods

2.1 DNA Cloning Methodology

The generation of plasmid constructs involves the following main steps: 1) polymerase chain reaction (PCR) for amplifying the target sequence within a stretch of complementary DNA (cDNA). 2) Restriction enzyme digest of the amplified DNA and vector DNA and their subsequent ligation. 3) Transformation of ligation product into TOP10 *Escherichia coli (E.coli)* and subsequent extraction of the plasmid DNA by miniprep. The minipreps are subjected to DNA sequencing to ensure they contain the correct cDNA fragment cloned in frame. One of such minipreps will be re-transformed into TOP10 *E.coli* and extracted from the bacteria.

2.1.1 Polymerase Chain Reaction (PCR)

PCR is a molecular biology technique for amplifying a stretch of cDNA, with the use of a thermostable DNA polymerase. It involves repeated cycles of three steps. Firstly, DNA denaturation at 95°C for the breaking of hydrogen bonds between the complementary base pairings along the DNA strands. The resulting single-stranded DNA serves as the template for the thermostable DNA polymerase. Secondly, primer annealing step at 60°C involves the primer oligonucleotides being bound to single-stranded DNA. The lower temperature assists the binding of these primers to the template DNA through hydrogen bonding. These oligonucleotides flank the DNA sequence of interest and define the boundaries of the amplified stretch of DNA. Lastly, the temperature is raised to 68°C, the optimum temperature for the thermostable DNA polymerase to add nucleotides to the oligonucleotide primers, using the existing DNA strand as template.

The template DNA for PCR amplifications in this research was either human brain cDNA (Clontech) or 50 ng/µl of previously generated plasmid constructs. 1 µl of this template was mixed with 1 µl of 10 µM forward primer, 1 µl of 10 µM reverse primer and 22 µl Pfx Accuprime Supermix in a 0.2 ml microcentrifuge tube. The primers utilised for PCR amplification are shown in table 2.1. The mixture was subjected to an initial 3 minute denaturation step at 95°C, followed by the required number of cycles of 1 minute denaturation at 95°C, 1 minute primer annealing at 60°C and primer extension at 68°C for 2 minutes per 1 kilo base pair of DNA (Table 2.2), in a Hybaid PCR Express

thermal cycler. For PCR amplification of cDNA, 40 cycles are required to generate ample DNA for further processing. In the case of plasmid amplification, 25 cycles suffice.

2.1.2 Further Processing of PCR Products

The PCR product was run on an agarose (Invitrogen) gel to check for the presence of amplified products. 1% agarose gel was made up by mixing 100 ml of Tris-acetate ethylenediaminetetra-acetic acid (TAE) buffer (40 mM Tris-base, 20 mM acetic acid, 1 mM EDTA, pH 8) with 1 gram of UltraPURE Electrophoresis Grade agarose (Invitrogen). The mixture was heated in a microwave until boiling. 10 µl SYBR Safe DNA gel stain (Invitrogen) was added to the mixture after it was cooled to a hand-hot temperature. The mixture was then poured into a casting tray and a gel comb was placed in the mixture to generate wells in the gel. The comb was removed after the gel was allowed to set for 30 minutes in the casting tray. The tray was then placed in an electrophoresis tank filled with TAE buffer. 1 µg of 1 kb DNA ladder (Invitrogen) was first mixed with 5 µl of bromophenol blue loading buffer (0.25% (w/v) bromophenol blue, 40% (w/v) sucrose in water), and the mixture was loaded into the first well of the gel. The PCR products, also mixed with 10 µl of the loading buffer, were loaded into subsequent adjacent wells. Electrophoresis was run at 100 volts for 45 minutes. The gel was exposed under ultraviolet (UV) light and was photographed using the InGenius gel doc system (Syngene, Cambridge, UK).

Construct	Primer Direction	Primer Sequence	Restriction site
LRRK2 Constructs			
pDS Roc-COR	forward	tccccgggaatggggaaattaagcaaaatatggg	*XmaI*
	reverse	agcgtcgactcattccaactcatcattattc	*SalI*
pDS Roc	forward	tccccgggaatggggaaattaagcaaaatatggg	*XmaI*
	reverse	tcctcgagtcactgatctcggatcttgaaatt	*XhoI*
pDS COR	forward	cctcccgggcaagatccgagatcagcttgttgttg	*XmaI*
	reverse	agcgtcgactcattccaactcatcattattc	*SalI*
pACT2 Roc-COR	forward	aaaggatcctgccttataaccgaatgaaactta	*BamHI*
	reverse	cctctcgagtcatggatttactaagagatctcc	*XhoI*
pRK5 myc LRRK2 FL	forward	agcggatccgccaccatggagcaaaagctcatttct gaggaagatctcatggctagtggcagctgtcag	*BamHI*
	reverse	attctcgagttactcaacagatgttcgtctcatttt	*XhoI*
pRK5 myc Roc-COR	forward	tctggatccgccaccatggagcaaaagctcatttctg aggaagatctcatggggaaattaagcaaaata	*BamHI*
	reverse	agcgtcgactcattccaactcatcattattc	*SalI*
Tubulin Constructs			
pACT2 TUBB2A C-term	forward	ctgagatcttccggggccgcatgtccatga	*BglII*
	reverse	gaactcgagtaaggatgcacgattgatctg	*XhoI*
pACT2 TUBB2B C-term	forward	ctgagatcttccggggccgcatgtccatga	*BglII*
	reverse	tccctcgaggctttccctaacccgtctcgc	*XhoI*
pACT2 TUBB2C C-term	forward	ccgagatcttcaggggccgcatgtccatga	*BglII*
	reverse	tggctcgagataaagagttcacactgcttc	*XhoI*
pACT2 TUBB3 C-term	forward	ccaagatcttccggggccgcatgtccatga	*BglII*
	reverse	cgggtcgaccctgcctctcactccagctgc	*SalI*
pACT2 TUBB C-term	forward	ctgagatcttccgtggtcggatgtccatga	*BglII*
	reverse	gaactcgagagttgagtaagacggctaagg	*XhoI*
pRK5 N-FLAG TUBB4 FL	forward	gctgaattcgccaccatggactacaaggacgatgac gataagatgcgggagatcgtgcacctg	*EcoRI*
	reverse	tcgaagcttcaggtgggaagcgatgggagc	*HindIII*
pRK5 N-FLAG TUBB4 C-term	forward	tgcgaattcgccaccatggactacaaggacgatgac gataagttccggggccgcatgtccatg	*EcoRI*
	reverse	tcgaagcttcaggtgggaagcgatgggagc	*HindIII*

pRK5 N-FLAG TUBB2A FL	forward	accgaattcgccaccatggactacaaggacgatgac gataagatgcgcgagatcgtgcacatc	*EcoRI*
	reverse	ctactcgagcacgattgatctgagaagttt	*XhoI*
pRK5 N-FLAG TUBB2A C-term	forward	tgcgaattcgccaccatggactacaaggacgatgac gataagttccggggccgcatgtccatg	*EcoRI*
	reverse	ctactcgagcacgattgatctgagaagttt	*XhoI*
pRK5 N-FLAG TUBB FL	forward	ccagaattcgccaccatggactacaaggacgatgac gataagatgagggaaatcgtgcacatc	*EcoRI*
	reverse	tgactcgagtgaggtgatgggggctctgcc	*XhoI*
pRK5 N-FLAG TUBB C-term	forward	tgtgaattcgccaccatggactacaaggacgatgac gataagttccgtggtcggatgtccatg	*EcoRI*
	reverse	tgactcgagtgaggtgatgggggctctgcc	*XhoI*
Other Constructs			
pACT2 ApoE3 C-term	forward	gatggatcccaaggtggagcaagcggtg	*BamHI*
	reverse	cttctcgagtcagtgattgtcgctgggcacagg	*XhoI*

Table 2.1: Primer oligonucleotides required for the cloning of required constructs. The underlined bases indicate the restriction site (FL = full length construct, C-term = C-terminus).

Stage	Temperature (°C)	Time (minutes)	Number of cycles
1	95	3	1
2	94	1	40 (cDNA) 25 (plasmid DNA)
	60	1	
	68	2 minutes per kb of DNA	

Table 2.2: Parameters for DNA amplification. The PCR amplification from cDNA requires 40 cycles of denaturation, primer annealing and primer extension, while amplification from plasmid DNA requires 25 cycles only.

The product was then gel-purified using the QIAquick Gel Extraction Kit (Qiagen), removing the agarose and impurities from the PCR products. The PCR product in the gel was first excised using a clean scalpel under the Safe Imager Transluminator (Invitrogen) for visualisation of the DNA in the gel. The weight of the excised gel was

determined, and 300 µl of solubilisation buffer QG per 100 mg gel was added to dissolve the gel. The mixture was incubated at 50°C for 10 minutes with occasional pulse vortexing, ensuring that the gel slice was completely solubilised in the buffer. 100 µl isopropanol (Fisher Scientific) per 100 µl gel was then added. This mixture was applied to the QIAquick columns provided in the kit. These columns contain a membrane that binds DNA. The mixture was centrifuged in these columns at 16000 *g* for 1 minute. The flow-through was discarded. The bound DNA was washed again by applying 500 µl of solubilisation buffer QG to the columns and 1 minute centrifugation at 16000 *g* in order to remove all traces of agarose. Further impurities were removed by applying 750 µl wash buffer PE to the columns, followed by 1 minute centrifugation at 16000 *g*. The columns were subjected to centrifugation at 16000 *g* for 1 minute again to remove all traces of ethanol present in buffer PE. The DNA was then eluted using 50 µl elution buffer EB into a clean microcentrifuge tube.

2.1.3 Restriction Enzyme Digests, Phenol-Chloroform Extraction and Ligation

25 µl of the gel-purified product was mixed with 1 µl of each appropriate restriction enzyme and 3 µl of the appropriate restriction enzyme buffer. For the restriction digestion of the vector, 1 µg of the appropriate vector was mixed with 1 µl of each appropriate restriction enzyme and 2 µl of the appropriate restriction enzyme buffer, and the mixture was made up to 20 µl with water. Table 2.1 shows the restriction enzymes required for the generation of the required plasmid constructs. Restriction digests were performed at 37°C for 2 hours.

The digested vector and the gel-purified product were then subjected to phenol-chloroform extraction for the removal of the restriction enzymes and impurities. Both were first made up to 100 µl by the addition of water. 100 µl phenol-chloroform isoamyl alcohol (Invitrogen) was then mixed with the aqueous layer containing the DNA. The two phases were separated by centrifugation at 16000 *g* for 10 minutes, and the upper aqueous phase containing the DNA was subjected to ethanol precipitation in order to remove protein impurities and concentrate the DNA. DNA pellets generated from ethanol precipitation were diluted in 10 µl and 50 µl of EB buffer for the insert and vector respectively.

Ligation was then performed by mixing 7 µl of the PCR products and 1 µl of the vector, together with 1 µl of 10x ligation buffer and 1 µl of 1U/µl T4 DNA ligase (Roche Diagnostics). The mixture was incubated at 4°C overnight.

2.1.4 Generation of Chemically Competent TOP10 *E.coli*

Commercial TOP10 *E.coli* cells were obtained from Invitrogen. They were subjected to treatment of divalent cations in order to make them chemically competent. TOP10 *E.coli* cells were streaked onto plates containing Luria-Bertani (LB) agar (Invitrogen) and were allowed to grow overnight. When colonies appeared, a single colony was picked and cultured in 2.5 ml of LB broth (Invitrogen) for 12-16 hours. The culture was further grown in 200 ml fresh LB broth for up to 4 hours so that the OD_{600} of the bacterial cells reached 0.95.

The bacterial pellet was recovered by centrifugation at 3000 *g* for 5 minutes at 4°C. The resulting pellet was resuspended in 10 ml of an ice-cold mixture of 80 mM $CaCl_2$ (Sigma) and 50 mM $MgCl_2$ (Sigma) solution. The pellets were combined together in one tube. The bacterial suspension was incubated on ice for 10 minutes before the recovery of bacterial pellet by centrifugation at 2000 *g* for 3 minutes at 4°C. These procedures were repeated three times before the resuspension of the bacterial pellet in 5.5 ml ice-cold 0.1 M $CaCl_2$. 5.5 ml of ice-cold 50% glycerol was mixed with the suspension. 550 µl of the suspension was pipetted into sterile 0.2 ml microcentrifuge tubes. These tubes were stored in liquid nitrogen until they are ready to be stored at -80°C for future use.

2.1.5 Plasmid Transformation into Competent TOP10 *E.coli*

5 µl of the ligation product was transformed into TOP10 *E.coli* made competent with divalent cations. The ligation product was first mixed with 100 µl competent *E.coli* cells in a microcentrifuge tube pre-chilled on ice. It was left incubating on ice for 30 minutes. The *E.coli* cells were then subjected to the so called 'heat shock' at 42°C for 45 seconds. This facilitates the DNA uptake into the cells through the bacterial cell wall. After a further 2 minute incubation on ice, 250 µl of LB broth was added to the bacteria and the mixture was shaken vigorously for 1 hour at 37°C. The mixture was then plated onto

100 μg/ml ampicillin-containing or 50 μg/ml kanamycin-containing LB agar plates, and incubated overnight at 37°C for bacterial growth.

2.1.6 Isolation of Plasmid DNA

The small-scale isolation of plasmid DNA from the transformed *E.coli* cells, generally known as miniprep, was performed after transformation, using the QIAprep Spin Miniprep Kit (Qiagen). It involves the extraction of DNA from a relatively small quantity of bacterial cells. Three main steps are involved. First, a bacterial suspension was generated followed by bacterial cell lysis. This step breaks the cells up and releases the plasmid DNA they contain. Second, the suspension of lysed cells was subjected to spin columns with silica membranes. The membranes provide a surface for the preferential adsorption of plasmid DNA, while protein impurities are not able to bind. Third, the bound plasmid DNA was washed with ethanol to remove traces of impurities and then eluted.

The transformed bacterial colonies on the selective agar plates were picked and cultured in 2 ml of 100 μg/ml ampicillin- or 50 μg/ml kanamycin-containing LB broth at 37°C overnight. The cells were then harvested by centrifugation at 10000 *g* for 3 minutes. The bacterial pellet was resuspended in 250 μl resuspension buffer P1 (50 mM Tris-HCl, pH 8.0, 10 mM EDTA, 100 μg/ml RNase A) to generate a suspension. Then 250 μl lysis buffer P2 (200 mM NaOH, 1% (w/v) sodium dodecyl sulphate (SDS)) was added and mixed with the suspension in order to lyse the cells. The suspension was left incubated with buffer P2 for no more than 5 minutes. 350 μl neutralisation buffer N3 was then added to terminate bacterial lysis. The contents were subjected to a 10 minute centrifugation at 16000 *g* so that the lysed cell debris stays at the bottom of the tube. The supernatant was transferred to spin columns for plasmid DNA binding. Following centrifugation at 16000 *g* for 1 minute, 500 μl binding buffer PB was added to the columns. Buffer PB can diminish the nuclease activity of the proteins that are not removed by the previous centrifugation, as some bacterial strains have high nuclease activity which destroys DNA. Centrifugation was performed again and 750 μl wash buffer PE was added to remove trace impurities. After the removal of buffer PE by centrifugation, the DNA was eluted from the column into a microcentrifuge tube with 50 μl elution buffer EB. The DNA yield was then determined by measuring the DNA

concentration of the samples using the nanodrop instrument (Thermo Scientific). 1 μg of these miniprep samples were subjected to digestion by the respective restriction enzymes and then run on an agarose gel to check for the presence of insert. Miniprep samples that contain an insert of the expected size were sent for DNA sequencing (Sequencing Service, School of Life Science, University of Dundee, Scotland). 30 μl of the miniprep DNA was supplied at a concentration of 16-20 ng/μl in water. Sequencing primer (Table 2.3) was also supplied, at a concentration of 3.2 μM in water. The sequencing results were analysed using the Sequencher 4.8 software by comparing these sequences with the publicly available consensus sequences (Table 2.4), and to check if the constructs were cloned in frame.

Primer Name	Template	Direction	Sequence
GAL4AD Seq	pACT2 constructs	forward	aataccactacaatggatgat
pACT Rev Seq		reverse	gaggttacatggccaagat
SP6 Seq	pRK5 constructs	forward	acacatacgatttaggtgacac
pRK5 Rev Seq		reverse	ggacaaaccacaactagaatgc
pLexA Seq	pDS constructs	forward	gtcagcagagcttcaccattg
LRRK2 Seq 11	LRRK2 Roc-COR tandem domain	forward	ttcagtacctaccaggt
LRRK2 Seq 12		forward	ggctgtgccttataacc
LRRK2 Seq 13		forward	ccctgtgattctcgttg
LRRK2 Seq 14		forward	agcttcctcacgcagtt
LRRK2 Seq 15		forward	accacaggcctgtgata
LRRK2 Seq 16		forward	tggtttcctgggttgct

Table 2.3: Primer oligonucleotides required for DNA sequencing.

cDNA	Consensus Sequence Number
LRRK2	NM_198578
ApoE	NM_000041.2
TUBB	NM_178014
TUBB2A	NM_001069
TUBB2B	NM_178012
TUBB2C	NM_006088
TUBB3	NM_006086
TUBB4	NM_006087

Table 2.4: Consensus sequences used for sequence alignment of the cloned constructs. These consensus sequences are available on the NCBI website.

2.1.7 Large-scale Isolation of Plasmid DNA (Maxiprep)

The miniprep sample with the constructs containing the correct DNA cloned in frame with the vector was subjected to a large-scale DNA isolation in order to generate a high-concentration DNA stock, using the HiSpeed Plasmid Maxi Kit (Qiagen). This procedure also comprises the three main steps as described in section 2.1.6 – bacterial cell lysis, DNA binding to membrane, and subsequent washes and DNA elution.

20 ng of DNA in the miniprep sample was re-transformed into competent TOP10 *E.coli* cells and plated onto the LB agar plates containing the appropriate antibiotic. When bacterial colonies appeared, one single colony was picked and inoculated into 2 ml LB broth with the appropriate antibiotic. It was incubated at 37°C with agitation for 7-8 hours before being inoculated into 200 ml antibiotic-containing LB broth. The culture was then incubated at 37°C with agitation for 12-16 hours.

Bacterial pellet was first recovered by centrifugation at 3000 *g* for 15 minutes at 4°C, followed by resuspension in pre-chilled resuspension buffer P1 (50 mM Tris-HCl, pH 8.0, 10 mM EDTA, 100 μg/ml RNase A). Lysis of bacterial cells was then carried out by thoroughly mixing the suspension with lysis buffer P2 (200 mM NaOH, 1% SDS (w/v)). The mixture was incubated at room temperature for 5 minutes to ensure

complete lysis of the cells without destroying the DNA. The lysis buffer P2 was then neutralised by mixing with pre-chilled neutralisation buffer P3 to stop the cell lysis process. The lysate was poured into a QIAfilter cartridge and it was left to stand at room temperature for 10 minutes. During this time, the bacterial debris float on the top of the lysate, thereby separating the debris from the lysate containing the DNA. The bacterial lysate was then filtered into a maxi tip previously equilibrated with 10 ml equilibration buffer QBT (750 mM NaCl, 50 mM 3-(N-morpholino) propanesulphonic acid (MOPS), pH 7.0, 15% isopropanol (v/v), 0.15% Triton X-100 (v/v)) by inserting a plunger into the cartridge, and ejecting the lysate into the tip. The maxi tip contains a resin that binds DNA. Whilst the lysate was flowing through the resin by gravity, DNA would have attached to the resin and separated from the other impurities which flow through the resin. The bound DNA was washed with 60 ml of wash buffer QC (1 M NaCl, 50 mM MOPS, pH 7.0, 15% isopropanol (v/v)) to remove any proteins present. The washed DNA was then eluted from the resin by the addition of 15 ml elution buffer QF (1.25 M NaCl, 50 mM Tris-HCl, pH 8.5, 15% isopropanol (v/v)) and was collected in a Falcon tube. The eluted DNA was then subjected to precipitation by the addition of 10.5 ml isopropanol. The mixture was shaken vigorously in order to ensure thorough mixing. A precipitator module was attached to a 30 ml syringe, and the mixture was then poured into the syringe. The precipitator module contains a membrane that binds DNA, and as the mixture flows through the module by gravity, DNA would be separated by the isopropanol from any trace impurities. The DNA was then washed with 2 ml 70% ethanol. The membrane was dried by passing air through the module forcefully several times so that all trace ethanol is removed from the module. The nozzle of the module was also dried by tapping it on a piece of absorbent paper to remove any trace ethanol left behind. The DNA was then eluted from the precipitator module by attaching it to a 5 ml syringe and adding 500 µl EB buffer into the syringe. The DNA was filtered through the membrane into a clean microcentrifuge tube. To ensure that the maximum DNA yield was obtained, the eluate was transferred back into the 5 ml syringe and filtered through the precipitator module once more. The concentration of DNA was then determined using the nanodrop instrument, prior to its storage at -20°C for future use.

2.1.8 Site-directed Mutagenesis

Site-directed mutagenesis is a molecular biology technique to introduce a mutation in a cloned plasmid. The methodology requires a pair of oligonucleotide primers that anneal to the same DNA sequence and cover the mutation site in a stretch of DNA. In order to introduce a mutation, the primer pairs need to contain a triplet base pair that codes for the desired amino acid at the mutation site. PCR would be performed in order to amplify the mutated DNA. Table 2.5 shows the primers required for mutations introduced in the constructs containing the RocCOR domain of LRRK2 and tubulin used in the project.

For site-directed mutagenesis of plasmid DNA, Pfu Ultra DNA polymerase was used in the PCR reactions. It is one of the thermostable DNA polymerases that display the highest fidelity, with an extremely low error rate. Typically 50 ng of the plasmid DNA was used as a template for these PCR reactions. In a microcentrifuge tube, the PCR mixture was made up consisting of the following: 25 µl 2x Pfu Ultra master mix, 1 µl of 10 µM forward primer, 1 µl of 10 µM reverse primer and 1 µl of 50 ng/µl plasmid DNA. The volume of the mixture was adjusted to 50 µl by the addition of 22 µl water. The PCR conditions used were an initial 3 minute denaturation step at 95°C, followed by 20 cycles of 1 minute denaturation at 95°C, 1 minute primer annealing at 60°C and primer extension at 72°C (2 minutes per kb of the size of the plasmid construct). The primer annealing temperature for the M1869T mutagenesis of the LRRK2 RocCOR domain was altered to 45°C as a result of the large ratio of A-T to G-C bases in the primers used for this mutagenesis.

After the PCR, the product was subjected to restriction digestion by *DpnI*. *DpnI* is a restriction enzyme that digests methylated DNA. Since DNA is methylated *in vivo*, any DNA that was methylated in the PCR mixture was the non-mutated template DNA that was cloned in bacteria beforehand. Hence this digestion step serves to remove such non-mutated template DNA. 1 µl of *DpnI* was added directly into the PCR product. The contents were mixed thoroughly and incubated at 37°C for 90 minutes. The digested PCR product was loaded into a 1% agarose gel alongside the DNA ladder (Section 2.1.2), and was subjected to electrophoresis at 100 volts for 45 minutes. Under UV exposure, a thin linear band should appear at a molecular weight similar to the size of

the plasmid and insert. This indicates that the PCR mixture contains the mutated DNA, as any non-mutated, methylated DNA was removed by the *DpnI* digestion. 5 µl of this mixture was used for TOP10 *E.coli* transformation (section 2.1.5). Minipreps were then prepared and subjected to DNA sequencing (section 2.1.6). The miniprep confirmed to contain the mutated sequence was subjected to a large-scale generation of DNA stock (section 2.1.7), and it was stored at -20°C for future use.

Primer name	Primer Direction	Sequence	Resultant Mutant
LRRK2 Constructs (PD-associated mutants)			
LRRK2-I1371V-1	Forward	gccacagttggcgtagatgtgaaagac	Roc-COR bearing **I1371V** mutation
LRRK2-I1371V-2	Reverse	gtctttcacatctacgccaactgtggc	
LRRK2-R1441C-1	Forward	caatataaaggcttgcgcttcttcttc	Roc-COR bearing **R1441C** mutation
LRRK2-R1441C-2	Reverse	gaagaagaagcgcaagcctttatattg	
LRRK2-R1441G-1	Forward	caatataaaggctggcgcttcttcttc	Roc-COR bearing **R1441G** mutation
LRRK2-R1441G-2	Reverse	gaagaagaagcgccagcctttatattg	
LRRK2-R1441H-1	Forward	caatataaaggctcacgcttcttcttc	Roc-COR bearing **R1441H** mutation
LRRK2-R1441H-2	Reverse	gaagaagaagcgtgagcctttatattg	
LRRK2-R1514Q-1	Forward	aatttcaagatccaagatcagcttgtt	Roc-COR bearing **R1514Q** mutation
LRRK2-R1514Q-2	Reverse	aacaagctgatcttggatcttgaaatt	
LRRK2-Y1699C-1	Forward	tatgaaatgccttgttttccaatggga	Roc-COR bearing **Y1699C** mutation
LRRK2-Y1699C-2	Reverse	tcccattggaaaacaaggcatttcata	
LRRK2-R1728H-1	Forward	gaacgagcacttcacccaaacagaatg	Roc-COR bearing **R1728H** mutation
LRRK2-R1728H-2	Reverse	cattctgtttgggtgaagtgctcgttc	
LRRK2-R1728L-1	Forward	gaacgagcacttctcccaaacagaatg	Roc-COR bearing **R1728L** mutation
LRRK2-R1728L-2	Reverse	cattctgtttgggagaagtgctcgttc	

LRRK2-M1869T-1	Forward	cctagaaatattacgttgaataatgat	Roc-COR bearing **M1869T** mutation
LRRK2-M1869T-2	Reverse	atcattattcaacgtaatatttctagg	
LRRK2 Constructs (Mutants of Nucleotide Binding and Autophosphorylation Sites)			
K1347A_F	Forward	actgggagtggtgcaaccaccttattgca	Roc-COR bearing **K1347A** mutation `
K1347A_R	Reverse	tgcaataaggtggttgcaccactcccagt	
T1348N_F	Forward	gggagtggtaaaaacaccttattgcag	Roc-COR bearing **T1348N** mutation
T1348N_R	Reverse	ctgcaataaggtgtttttaccactccc	
T1343A_F	Forward	tgattgtgggaaatgctgggagtggtaaaacc	Roc-COR bearing **T1343A** mutation
T1343A_R	Reverse	ggttttaccactcccagcatttcccacaatca	
T1343D_F	Forward	tgattgtgggaaatgatgggagtggtaaaacc	Roc-COR bearing **T1343D** mutation
T1343D_R	Reverse	ggttttaccactcccatcatttcccacaatca	
T1491A_F	Forward	cactttgtgaatgccgccgaggaatcggatg	Roc-COR bearing **T1491A** mutation
T1491A_R	Reverse	catccgattcctcggcggcattcacaaagtg	
T1491D_F	Forward	cactttgtgaatgccgacgaggaatcggatg	Roc-COR bearing **T1491D** mutation
T1491D_R	Reverse	catccgattcctcgtcggcattcacaaagtg	
ApoE Constructs			
APOE-C112R-1	Forward	acatggaggacgtgcgcggccgcctggtg	ApoE4
APOE-C112R-2	Reverse	caccaggcggccgcgcacgtcctccatgt	
APOE-R158C-1	Forward	atgacctgcagaagtgcctggcagtgtac	ApoE2
APOE-R158C-2	Reverse	gtacactgccaggcacttctgcaggtcat	
Tubulin Constructs			
TUBB A364S_F	Forward	ggcctcaagatgtcagtcaccttcatt	TUBB bearing **A364S** mutation
TUBB_A364S_R	Reverse	aatgaaggtgactgacatcttgaggcc	
TUBB4_A364S_F	Forward	ggcctgaagatgtccgcgaccttcatc	TUBB4 bearing **A364S** mutation
TUBB4_A364S-R	Reverse	gatgaaggtcgcggacatcttcaggcc	

TUBB2AB_S364A-F	Forward	ggcctgaagatggcggccaccttcatc	TUBB2A/ TUBB2B bearing **S364A** mutation
TUBB2AB_S364A-R	Reverse	gatgaaggtggccgccatcttcaggcc	
TUBB2C_S364A-F	Forward	gggctaaaaatggccgccaccttcatt	TUBB2C bearing **S364A** mutation
TUBB2C_S364A-R	Reverse	caatgaaggtggcggccatttttagccc	
TUBB3_S364A-F	Forward	ggcctcaagatggcctccaccttcatc	TUBB3 bearing **S364A** mutation
TUBB3_S364A-R	Reverse	gatgaaggtggaggccatcttgaggcc	

Table 2.5: Primer oligonucleotides required for mutagenesis. The underlined bases indicate those necessary for the mutagenesis to the desired amino acids.

2.2 The Yeast Two Hybrid (YTH) System

The YTH system has been used for years as a means to study protein-protein interactions *in vivo*. Its working principle is based on the fact that eukaryotic transcription factors have a separate DNA binding domain (DNA-BD) and transcriptional activation domain (AD), and that transcription of genes can occur when they come together, or in close proximity to each other. To test if two proteins (protein A and B) can interact with each other using the YTH approach, we first need to generate plasmids that make fusion proteins – the DNA-BD is fused with protein A and the AD with protein B. These plasmids are called bait plasmid and prey plasmid respectively. After these plasmids are co-transformed into yeast cells, fusion proteins encoded by the transformed bait and prey plasmids would be made during protein synthesis. If proteins A and B interact and enter the nucleus of the yeast cells facilitated by the presence of a nuclear localisation signal harboured in the bait fusion protein, the DNA-BD and AD in close proximity form a transcription factor that allows for the transcription of a reporter gene in the yeast cells. The detection of the transcription of reporter genes is assayed to determine whether two proteins can interact with each other. A schematic diagram illustrating the YTH system is shown in figure 2.1.

2.2.1 YTH Vectors

Two YTH vectors were in use for the YTH experiments. The bait vector, pDS vector, contains a gene that codes for the DNA-BD of a transcription factor named LexA, and a gene needed in tryptophan synthesis called *TRP1*. The prey vector, pACT2 vector, contains a gene coding for the AD of another transcription factor called GAL4, and the *LEU2* gene for leucine synthesis. Hence, if the yeast cells are co-transformed with these vectors, they should be able to grow on selective agar plates that lack both leucine and tryptophan.

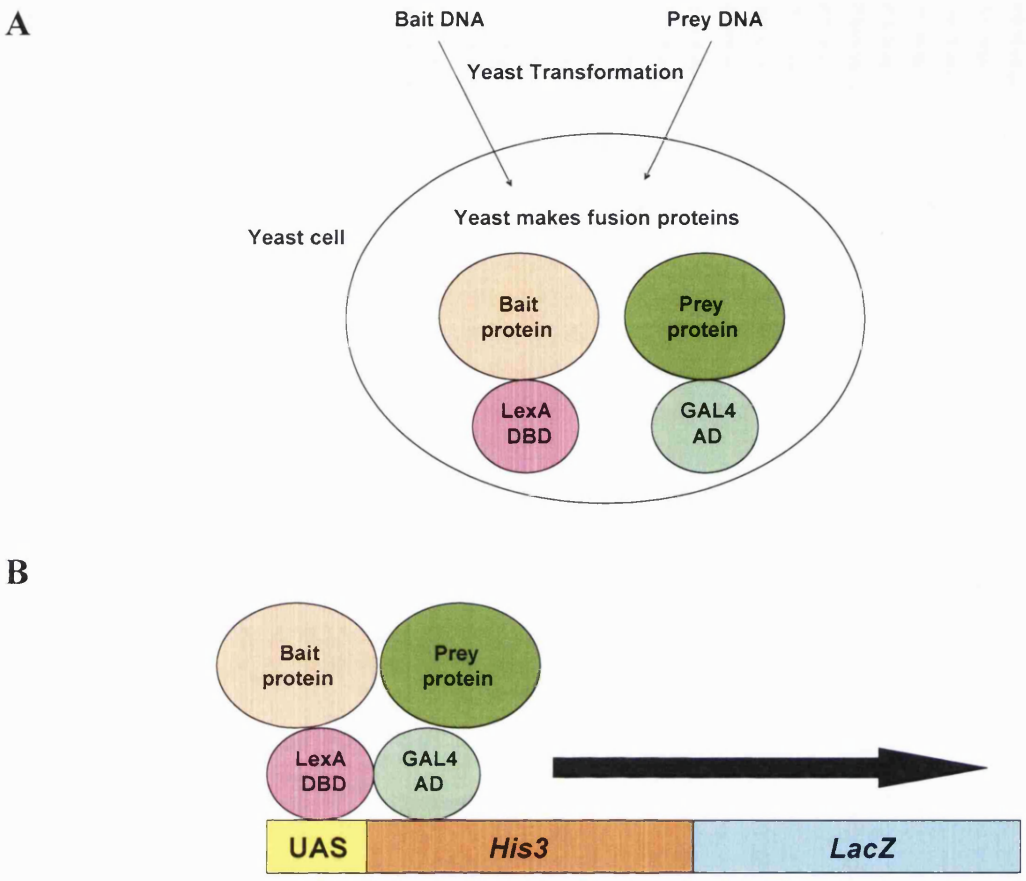

Figure 2.1: A schematic diagram showing the major two steps in an YTH experiment. (A) The DNA coding for the bait and prey fusion proteins was introduced into yeast cells by yeast transformation, using the protocol adapted from Gietz *et al* (1995). Using their own protein expression machinery, yeast cells make the fusion proteins, including the bait protein fused with the DNA binding domain (indicated as DBD in the above figure) of the LexA transcription factor, and the prey protein fused with the activation domain of the GAL4 transcription factor. (B) When the bait and prey proteins can interact with each other, the two transcription factors would come close together. The DNA binding domain of LexA binds the upstream activation sequence (UAS) of the two reporter genes, *HIS3* and *LacZ*. The close proximity of the activation domain of GAL4 to the DNA binding domain of LexA enables the former to activate transcription of both reporter genes. The detection of *HIS3* expression can be assessed by the presence of yeast growth on the agar plates that lack histidine, leucine and tryptophan (Section 2.2.4). The detection of the expression of *LacZ* can be performed by the β-galactosidase freeze-fracture assay (Section 2.2.5).

2.2.2 The Use of L40 Yeast Strain in YTH and its Rationale

In the YTH system, reporter genes such as *LacZ* and *HIS3* are commonly used in the identification of yeast phenotypes. These genes are integrated into the yeast chromosomal DNA in certain yeast strains, and they are preceded by the UAS in the chromosomal DNA. These activation sequences are the binding site for the transcription factors. In a yeast strain called L40, *LacZ* and *HIS3* reporter genes are present in the chromosomal DNA, and the UAS for both reporter genes can be recognised by a transcription factor called LexA, through a DNA-BD. The YTH vectors used contain the LexA-DNA-BD and GAL4-AD, so L40 yeast would be suitable for the purpose of the YTH experiment. The DNA-BD of LexA, fused with protein A, would bind to the UAS of the *LacZ* and *HIS3* reporter genes in the L40 yeast strain. If protein B fused with the AD of GAL4 can interact with protein A, this brings the DNA-BD of LexA at the UAS in close proximity to the AD of GAL4. This allows for the transcription of the reporter genes. In the YTH experiment, we detect the transcription of reporter genes to determine whether two proteins can interact.

2.2.3 Generation and Maintenance of L40 Yeast Strain

YPD agar medium (Clontech - 2% (w/v) agar, 1% (w/v) yeast extract, 2% (w/v) peptone and 2% (w/v) dextrose), supplemented with 0.4 mM adenine (Sigma-Aldrich), were used to make the agar plates. A frozen stock of L40 yeast cells that was stored at -80°C was thawed and streaked onto the YPD agar plates using a sterile spreading loop. The plates were incubated at 30°C until the yeast colonies grew to a diameter of 2 mm. The plates were wrapped in parafilm and stored at 4°C for up to one month. The cells were maintained by streaking a single colony of yeast onto a fresh YPD agar plate every month.

2.2.4 Transformation of L40 yeast Cells

The optimised protocol of the lithium acetate/single-stranded DNA/polyethylene glycol (LiAc/ssDNA/PEG) method, described by Gietz *et al* (1995), was utilised in the transformation of plasmid DNA into L40 yeast cells. A single L40 yeast colony was picked from a YPD agar plate using a sterile spreading loop, and was inoculated into 100 ml YPD medium (Clontech - 1% (w/v) yeast extract, 2% (w/v) peptone and 2% (w/v) dextrose) with 0.4 mM adenine (This medium is referred to as YPDA hereafter).

The culture was allowed to grow by an overnight incubation at 30°C with vigorous shaking. Thereafter, the OD_{600} was determined, and the appropriate volume of the overnight culture was added to fresh pre-warmed YPDA such that the OD_{600} was about 0.3. The volume of this fresh YPDA depends on the number of transformations required (10 ml per transformation). The culture was grown for 2.5 hours, until the OD_{600} reaches approximately 0.6. The cells were harvested by centrifugation at 2000 *g* for 3 minutes at 20°C. The resulting pellet was washed once with 25 ml sterile water and centrifuged again at 2000 *g* for 3 minutes at 20°C to remove traces of YPDA. The pellet was then washed twice with 1x lithium acetate/Tris-EDTA (Sigma-Aldrich – LiAc/TE; 10 mM Tris-HCl, 1 mM EDTA, 100 mM LiAc). This step makes the yeast cells competent. After centrifugation for the second LiAc/TE wash, the pellet was resuspended in an appropriate volume of 1x LiAc/TE (100 µl per transformation) so that the cell density was about 1×10^9 cells/ml. Gietz *et al* (1995) suggested that DNA transformation of 1×10^8 yeast cells would yield high transformation efficiency. Hence 100 µl of this yeast suspension was transferred into microcentrifuge tubes containing 50 µg herring sperm DNA (Sigma-Aldrich) which was denatured by boiling at 100°C for 5 minutes twice, 1 µg bait DNA and 1 µg prey DNA. 600 µl of polyethylene glycol (PEG)/LiAc/TE mixture (40% (w/v) PEG, 1x LiAc, 1x TE) was then added to the mixture in the tubes. PEG has the ability to bring the plasmid DNA and the ssDNA from herring sperm in close proximity to the yeast cells. The contents were mixed thoroughly and were incubated at 30°C for 30 minutes with vigorous shaking. The contents were subjected to a heat shock at 42°C for 20 minutes, and a pulse spin for 10 seconds. The PEG was removed and the yeast pellet was resuspended in 100 µl sterile water. 60 µl of the suspension was plated onto nutritional selection (NS) agar plates comprising 46.7 g/L minimal selective dropout (SD) agar base (Clontech), 0.62 g/L -histidine/-leucine/-tryptophan dropout (DO) supplement (Clontech), 0.4 mM adenine and 0.5 M 3-amino-1,2,4-triazole (3-AT). The remaining 40 µl was plated onto transformation control (TC) agar plates comprising 46.7 g/L minimal SD agar base, 0.64 g/L -leucine/-tryptophan DO supplement (Clontech) and 0.4 mM adenine. The plates were incubated at 30°C until sufficient yeast growth.

When the bait and prey proteins interact with each other, the DNA-BD of LexA and AD of GAL4 would be in close proximity to each other, resulting in transcription of reporter genes such as *LacZ* and *HIS3*. Transcription of the *LacZ* gene results in the expression

of β-galactosidase assayed in the freeze-fracture assay described in section 2.2.5. The synthesis of the *HIS3* gene product, required for histidine synthesis, allows only yeast cells expressing interacting bait and prey proteins to grow on the NS agar plates lacking histidine. This phenotypic determination of the yeast cells allows us to identify interacting partners of the bait protein. The 3-AT added to the NS plates is a competitive inhibitor of the *HIS3* gene product, thereby inhibiting endogenous histidine synthesis in yeast cells. The growth of yeast colonies in the TC agar plates allows us to confirm whether both bait and prey plasmids are successfully transformed into the cells, as the bait and prey plasmids contain the *TRP1* and *LEU2* genes respectively and only yeast cells transformed with both plasmids can grow on the tryptophan- and leucine-deficient TC plates.

2.2.5 β-galactosidase Freeze-fracture Assay

One of the reporter genes in L40 yeast cells, *LacZ*, codes for the enzyme β-galactosidase. It is a bacterial hydrolase that cleaves a compound called 5-bromo-4-chloro-3-indolyl-β-D-galactopyranoside (X-gal) into galactose and blue-coloured indolyl-blue. Hence yeast transformed with DNA coding for bait and prey proteins that interact with each other will turn blue after the treatment with X-gal in this β-galactosidase freeze-fracture assay. This assay allows us to detect the expression of β-galactosidase in yeast cells and screen for the interactors of the bait protein.

2.4 mM X-gal solution, comprising 2 mg X-gal (BDH Laboratory Supplies), 20 µl N,N-dimethylformadine (DMF), 2 ml LacZ buffer (60 mM $Na_2HPO_4.2H_2O$, 40 mM $NaH_2PO_4.2H_2O$, 10 mM KCl, 1 mM $MgSO_4.7H_2O$) and 5.4 µl β-mercaptoethanol (final concentration of 40 mM) per yeast agar plate, was made up. The solution was thoroughly mixed and protected from light exposure in the fume hood. 2 ml of this mixture was dispensed into the lid of Petri dishes. Using a replica block, the yeast colonies grown on the TC and NS plates were transferred onto 54-Whatman filter paper (90 mm circle). The filter papers were then plunged twice into liquid nitrogen for 5 seconds to freeze-fracture the yeast cells and release the expressed β-galactosidase. The filter papers were incubated in the X-gal solution dispensed onto the lid. Air bubbles were removed from beneath the filter papers, and they were covered with the base of the Petri dishes and incubated at 37°C until the yeast cells turn blue. The reaction was

quenched by placing the filter papers in the fume hood to air-dry. This assay allows a semi-quantitative assessment of the interaction strength of the expressed proteins.

2.2.6 Quantitative Yeast two hybrid (Q-YTH) Assay

The Q-YTH assay was used to quantify the level of interaction among the interactors in yeast cells. This assay utilises a compound called chlorophenol-red-β-galactopyranoside (CPRG), which is also a substrate of β-galactosidase. The enzyme hydrolyses CPRG, turning the yellow-coloured CPRG solution into red. The rate of the red colour development is roughly proportional to the interaction strength between the bait and prey proteins, as this indicates the expression level of the reporter gene *LacZ*. Hence the intensity of the developed red colour at specific time points was used to compare interaction levels.

The protocol used was adapted from that described by Ramamoorthy *et al* (1997). Plasmid DNA coding for the bait and prey proteins were transformed into L40 yeast cells and plated onto leucine- and tryptophan-deficient TC agar plates as shown in section 2.2.4. The plates were incubated at 30°C for approximately 3 days. A yeast colony was picked and transferred into 10 ml of a selective liquid medium composed of 26.7 g/L minimal SD base, 0.64 g/L -leucine/-tryptophan DO supplement and 0.4 mM adenine. The cultures were incubated at 30°C with vigorous shaking overnight. The OD_{600} of each culture was measured on the next day. The yeast cultures were diluted to an OD_{600} of 0.3 with fresh selective liquid medium and the cultures were incubated for a further 3-4 hours. The cultures were centrifuged at 2000 *g* for 3 minutes at 20°C. The supernatant was removed and the yeast pellet was resuspended in 1 ml of resuspension buffer (50 ml LacZ buffer, 40 mM β-mercaptoethanol, 1x complete mini protease inhibitor cocktail). The yeast suspensions were then diluted in a microcentrifuge tube and they were normalised in the resuspension buffer to a desirable OD_{600} depending on the strength of the interaction. Yeast transformed with DNA coding for strong interactors had the suspension normalised to a lower OD_{600}. The samples were treated with 12 µl 0.1% SDS, followed by 15 µl chloroform. This chemically breaks up the yeast cell wall and permeabilises the cells. The samples were then vortexed for 2-3 seconds and incubated at 30°C for 15 minutes with gentle shaking. 10 µl of 17 µM CPRG solution was then added to each sample and mixed. 200 µl of this mixture was

dispensed in triplicate into a 96-well flat bottom plate. The plate was left protected from light during the red colour development. The OD_{540} of each sample was first read using the microplate photometer Multiskan MULTISOFT 220V (Labsystems). The OD_{540} measures the intensity of the red colour developed and is an indication of the interaction strength of the bait and prey proteins. The OD_{620} was then measured in the microplate photometer, and this indicates the optical density proportional to the number of yeast cells in each sample. The OD_{540} values of each sample were divided by OD_{620} values of the corresponding sample in order to determine the OD_{540} of each sample per unit of yeast cells present. The quotient (OD_{540}/OD_{620}) value of each interactor was first subtracted by the quotient value of the corresponding negative control (yeast transformed with bait and empty prey). Since all quantifications compared WT LRRK2 and LRRK2 mutants, the strength of each LRRK2 mutant-prey protein interaction was expressed as the percentage of the strength between WT LRRK2 – prey protein interaction. The following formula was hence used:

$$\text{Interaction strength (\%)} = (OD_{540}/OD_{620\ \text{mutant LRRK2 + prey}} - OD_{540}/OD_{620\ \text{mutant LRRK2 + pACT2}}) / (OD_{540}/OD_{620\ \text{WT LRRK2 + prey}} - OD_{540}/OD_{620\ \text{WT LRRK2 + pACT2}}) \times 100\%$$

Two-tailed, two-sample equal variance student's t-test was carried out to assess for the significance of the difference between WT LRRK2-prey and mutant LRRK2-prey interaction.

2.2.7 Extraction of Proteins from Yeast

Negative results were sometimes obtained from YTH experiments and they can be explained by either of the following two possibilities. First, the bait and prey proteins do not interact with each other, yielding no *LacZ* and *HIS3* expression. Second, the construct is not expressed, meaning that the protein cannot be made from the plasmid DNA construct for some reasons. In order to eliminate the latter possibility as the cause of the negative results obtained, detection of the expression of these proteins was performed in these yeast cells.

Plasmids encoding the protein of interest were transformed into L40 yeast cells as described in section 2.4 and plated onto agar plates deficient in tryptophan only (for

pDS plasmid constructs) or in leucine only (for pACT2 plasmid constructs). After sufficient yeast growth, a single colony was inoculated into 5 ml of selective liquid medium detailed in section 2.2.6 and incubated overnight at 30°C with vigorous shaking. The entire overnight culture was transferred into 50 ml fresh YPDA medium on the next day, and was incubated for about 6 hours at 30°C with shaking, until the OD_{600} reached 0.4-0.6. The OD unit of each culture was determined by multiplying the OD_{600} by the culture volume. The OD units were used to determine the optimum volume of buffer to be used for yeast cell lysis as shown later. The culture was poured into two 50 ml Falcon tubes, each filled with 25 ml of ice. They were immediately centrifuged at 2000 *g* for 5 minutes at 4°C. The supernatant was removed together with the unmelted ice. The pellet in the two tubes was pooled together by resuspending in 50 ml ice-cold sterile water. After another centrifugation at 2000 *g* for 5 minutes at 4°C was performed and the supernatant was removed, the pellet was immediately frozen on dry ice. The yeast cells were then lysed by the addition of the appropriate volume of cracking buffer (8 M urea, 5% (w/v) SDS, 40 mM Tris-HCl, pH 6.8, 0.1 mM EDTA, 0.4 mg/ml bromophenol blue, 0.13 M β-mercaptoethanol, 1x complete mini protease inhibitor cocktail, 20x phenylmethyl sulphonyl fluoride (PMSF) – 100 µl of cracking buffer per 7.5 OD units) pre-warmed to 60°C. The sample was added to a clean microcentrifuge tube containing 80 µl glass beads (Sigma-Aldrich) per 7.5 OD units. The sample was incubated at 70°C for 10 minutes, and vortexed for 1 minute. This mechanically disrupts the yeast cell wall, which complements the chemical cell wall disruption by the cracking buffer. The released proteins were then separated from the cell debris by centrifugation at 16000 *g* for 5 minutes at 4°C. The supernatant, containing the proteins, was kept in a clean, pre-chilled microcentrifuge tube. The remaining pellet with the residual cracking buffer was boiled at 100°C for 4 minutes and vortexed for 1 minute. The sample was spun down again at 16000 *g* for 5 minutes at 4°C. The resulting supernatant was transferred to the previous supernatant in the microcentrifuge tube, increasing the protein yield. The supernatant was boiled at 100°C for protein denaturation and was stored at -80°C. An SDS – polyacrylamide gel electrophoresis (SDS-PAGE) and western blot (section 2.4) were performed to test for the presence of the protein expressed in yeast. Mouse anti-HA antibody was used for the detection of the product of pACT2 constructs. The details of the use of the antibody are shown in section 2.4.4.

2.3 Mammalian Cell Culture

2.3.1 Cell Culture

All cell handling was performed with sterile techniques in a class II laminar flow hood. All incubation of cells was performed in a CO_2 incubator (Sanyo) kept at 37°C with a supply of 5% CO_2 in air. An inverted Zeiss light microscope was used to observe cells in culture. A Denley BS400 centrifuge was used to spin down the cells for cell seeding. Cells were cultured in culture flasks with a 75 cm^2 base. Cell transfection was performed on cells seeded onto 10 cm diameter culture dishes or 6-well culture plates.

2.3.2 Cell lines

Human embryonic kidney 293 (HEK293) cells and human neuroblastoma SH-SY5Y cells were purchased from the European Collection of Cell Cultures (Dorset, UK). HEK293 cells were primarily used for co-immunoprecipitation (co-IP) experiments while SH-SY5Y cells were mainly used for immunocytochemical staining.

2.3.3 Cell Culture Media

HEK293 cells were cultured in Dulbecco's Modified Eagle Medium (DMEM – 4500 mg/L glucose, L-glutamine, pyruvate; Invitrogen), with the addition of 10% (v/v) foetal bovine serum (FBS – PAA Laboratories) and 1% (v/v) penicillin-streptomycin (pen-strep – 10000 U/ml penicillin, 10 mg/ml streptomycin; Invitrogen). SH-SY5Y cells were cultured in DMEM-F12 (15 mM 4-(2-hydroxyethyl)-1-piperazineethanesulphonic acid, L-glutamine and pyridoxine HCl; Thermo Fisher Scientific) with the addition of 10% (v/v) FBS and 1% (v/v) pen-strep. Induction of SH-SY5Y differentiation was performed with neurobasal medium (Invitrogen) supplemented with 2 mM L-glutamine (Invitrogen), 1% (v/v) pen-strep and 10 ml B27 supplement (50x; Invitrogen). This medium mixture was changed every day for 5 days until the cells were fully differentiated and developing cellular processes. All culture media were kept at 4°C and pre-warmed to 37°C before use. In the subsequent text, DMEM, DMEM-F12 and neurobasal medium that were supplemented with the aforementioned sera and antibiotics are referred to as DMEM, DMEM-F12 and neurobasal medium respectively.

2.3.4 Thawing of Cryopreserved Mammalian Cells

Upon receipt of the cells, they were stored at -150°C for cryo-preservation. Before starting the culturing of the cells, they were quickly thawed by holding the tube of cells in the palm. The cells were resuspended in a tissue culture flask (Nunc) containing 20 ml of the appropriate medium. The flask was gently swirled and incubated in the 37°C incubator until sufficient cell growth had occurred.

2.3.5 Maintenance of Mammalian Cell Cultures

Cell growth is indicated by the confluency of the cells in culture. Cellular confluency is observed and estimated under the Zeiss microscope. Normally the cells need to be passaged when the confluency reaches over 90%. The medium was first removed from the culture flask. The residual medium that contains FBS was washed away by adding 10 ml Hank's balanced salt solution (HBSS; Invitrogen). The flask was gently rocked to ensure every part of the flask base was washed. 1 ml of trypsin-EDTA solution (0.25% (w/v) trypsin, 0.02% (w/v) EDTA; Invitrogen) was added after discarding the HBSS. Trypsin digests the cell adhesion proteins that enable the cells to attach to the plastic at the base of the flask, while EDTA chelates calcium ions that are required for the activity of such proteins like cadherins. Incubation with trypsin-EDTA was performed for 2 minutes at room temperature. The flask was gently agitated so that the trypsin can work on all the cells in the flask. The trypsin was then inhibited by the addition of the appropriate medium, which contains FBS. The cells were resuspended by pipetting up and down. The appropriate volume of suspension was added to a fresh culture flask containing the appropriate fresh medium so as to achieve the desired cell density. The final volume of the culture should be 20 ml. The cells were generally passaged every 72 hours. Table 2.6 shows the details of passaging the HEK293 and SH-SY5Y cells.

Cell type	Passage ratio	Culture medium required	Volume of cell suspension (ml)	Volume of medium (ml)
HEK293	1:10	DMEM	1	19
SH-SY5Y	1:3	DMEM-F12	3	17

Table 2.6: Culture media and their volume required for passaging the HEK293 and SH-SY5Y cells.

2.3.6 Cryopreservation of Cells

Cells were harvested for cryopreservation when they are 80% confluent. The cells were washed with HBSS, trypsinised and resuspended in 10 ml of the appropriate medium as described in section 2.3.5. The cells were pelleted by centrifugation at 500 *g* for 2.5 minutes. The supernatant was removed and the pellet was resuspended in 1 ml of 10% (v/v) dimethylsulphoxide (DMSO) in FBS. The suspension was pipetted into a 2 ml cryogenic polypropylene vial. DMSO is a cryoprotectant so that freeze-damage due to ice formation on the cells is kept to a minimum. The vial was kept in a quick-freeze container and stored at -80°C overnight. The vial of cells was then transferred to -150°C for long-term storage. This provides the cells a more gradual change in temperature in order to minimise cellular damage due to a sudden temperature change.

2.3.7 Preparation of Coverslips for Immunocytochemistry

A batch of glass coverslips (BDH Laboratory Supplies) were first sterilised by heating in an oven at 200°C for 1-2 hours. They were left in the laminar flow hood for future use. One coverslip was placed in each well in a tissue culture plate, and was coated with 0.1 μg/μl poly-D-lysine (PDL) for cell attachment on glass. The coverslips were incubated with PDL for 45 minutes at room temperature. They were then washed with sterile water three times and allowed to dry before use.

2.3.8 Seeding Cells into Culture Dishes and Plates

The cells were first detached from the bottom of the flask as described in section 2.3.5. The cells were pelleted by centrifugation at 500 *g* for 2.5 minutes. The pellet was

resuspended with 1 ml of the appropriate medium and 10 µl of this suspension was transferred into 90 µl of the appropriate fresh medium to achieve a 10-fold dilution. A coverslip was placed over the counting chamber of a hematocytometer. 10 µl of the diluted suspension was pipetted into the space between the hematocytometer and the coverslip. The hematocytometer was inverted and the chamber was placed under the Zeiss microscope. The cells situated in 1 mm^2 area in the chamber were counted. The counted number was multiplied by 10 to take account of the 10-fold dilution performed beforehand, and then by 10^4. The appropriate number of cells was seeded into the culture dishes. For HEK293 cells, 2×10^6 cells were seeded with 10 ml DMEM into each 10 cm culture dish for co-IP experiments. For SH-SY5Y cells, 2×10^5 cells were seeded with 2 ml DMEM-F12 into each 3 cm well in culture plates for immunocytochemistry experiments. The cultures were then incubated in the CO_2 incubator at 37°C overnight.

2.3.9 HEK293 Transfection with Plasmid DNA

Transfection is a technique that introduces the hydrophilic DNA into mammalian cells through the hydrophobic cell membrane. DNA is first surrounded by lipid molecules and the whole DNA-lipid complex crosses the cell membrane and is taken up by the cell. This foreign DNA is then expressed using the host machinery through transcription and subsequent translation. Before transfection was performed, the cells were seeded into 10 cm culture dishes as described in section 2.3.8. Transfection can be performed when the cell confluency is 50-80%. A total of 8 µg of plasmid DNA was generally used for transfection. For co-transfections, 4 µg of each plasmid DNA was used. Since LRRK2 constructs are big and more difficult to transfect, 5 µg of LRRK2 construct was normally used for transfection together with 3 µg of a second construct. The plasmid DNA was diluted in 800 µl Opti-MEM I reduced serum medium (Invitrogen). This was followed by the addition of 16 µl lipofectamine LTX (Invitrogen). Lipofectamine LTX forms a lipid-soluble complex with plasmid DNA and can transport the DNA across the cell membrane. The DNA-Opti-MEM-LTX mixture was thoroughly mixed and incubated at room temperature for 30 minutes. The DMEM in the culture dishes was replaced by pre-warmed Opti-MEM I. This serum-starves the cells and improves the efficiency of the cells to take up DNA. The DNA-Opti-MEM-LTX mixture was added dropwise onto the cells in the dishes. The dishes were gently swirled to ensure even

distribution of the mixture. The cells were then incubated in the CO_2 incubator for 5 hours before the Opti-MEM I was replaced with pre-warmed DMEM again. The cells were returned to the incubator for a further incubation of 24-48 hours.

2.3.10 Co-immunoprecipitation (co-IP)

2.3.10.1 Extraction of Proteins from Transfected HEK293 Cells

HEK293 cells were harvested when the cells in the culture dishes were almost 100% confluent. The DMEM was removed, and the cells were washed with 2 ml ice-cold phosphate buffered saline (PBS) twice to completely remove the residual medium. They were then lysed using the NP-40 lysis buffer (150 mM NaCl, 50 mM Tris, pH 7.5, 5 mM EDTA, pH 8.0, 0.25% (v/v) NP-40, 1x complete mini protease inhibitor cocktail in water). NP-40 is a detergent that can break cell membrane, and release the contents of the cytoplasm into solution. 1 ml of NP-40 lysis buffer was added in a dropwise manner around the dish, and the cells were detached from the dish by a pre-chilled cell scraper. The cell lysate was transferred to a clean, pre-chilled microcentrifuge tube and incubated on ice for 20 minutes. The cells were then pelleted by centrifugation at 16000 *g* for 10 minutes at 4°C. The lysate, appearing as supernatant, was transferred to a new pre-chilled microcentrifuge tube and stored on ice until further processed.

2.3.10.2 Bradford Assay

Bradford assay is a technique to determine the concentration of proteins in a sample, developed by Bradford in 1976 (Bradford, 1976). A standard curve of OD_{600} against protein concentration was first generated. Various dilutions of bovine serum albumin (BSA; New England Biolabs) in water, ranging from 0.1 mg/ml to 1 mg/ml, were made up. 1 µl of the cell lysate sample was transferred to 9 µl lysis buffer to achieve a 10-fold dilution. 990 µl Quickstart Bradford Dye Reagent (Biorad) was added to each of these BSA dilutions and diluted cell lysate (CL) samples. They were incubated at room temperature for 15 minutes, protected from light. The Dye Reagent contains a brown Coomassie dye that turns blue upon binding to proteins. The OD_{600} of all the BSA dilutions were first determined to generate the standard curve. This was followed by measuring the OD_{600} of the CL samples. The values obtained were used to determine the protein concentration of these samples from the standard curve. The determined

concentration was multiplied by 10 to take account of the 10-fold dilution performed beforehand.

2.3.10.3 Preparation of Anti-FLAG Beads for co-IP

The co-IP experiment utilised anti-FLAG beads to retain the FLAG-tagged fusion protein in the IP column, and to pull down the interacting myc-tagged fusion protein. 40 µl of monoclonal anti-FLAG M2 affinity gel was first washed with 1 ml NP-40 wash buffer (150 mM NaCl, 50 mM Tris, pH 7.5, 5 mM EDTA, pH 8.0, 0.05% (v/v) NP-40, 1x complete mini protease inhibitor cocktail in water) three times. The monoclonal anti-FLAG M2 affinity gel contains mouse monoclonal IgG covalently attached to the beads in the gel. These IgGs bind specifically to the FLAG peptide. The FLAG-tagged fusion proteins would hence be attached to the affinity gel until the elution step. The bead washing step was performed by mixing the affinity gel and the 1 ml wash buffer thoroughly, followed by centrifugation at 100 *g* for 3 minutes at 4°C and the removal of the supernatant. After the beads were washed thrice, the lysate was added to the washed IgG beads and the samples were placed on a turning disk at 4°C overnight, allowing for the thorough mixing of the beads and the lysate.

2.3.10.4 Washing the Beads

The samples were centrifuged at 100 *g* for 3 minutes at 4°C to recover the anti-FLAG beads. The supernatant was discarded and 1 ml ice-cold NP40 wash buffer was added. The beads were thoroughly washed by returning them to the turning disk for 5 minutes. The beads were washed three times by following these procedures. After the final wash, the FLAG fusion protein was eluted from the anti-FLAG beads by incubation with 100 µl 3x FLAG peptide (Sigma-Aldrich) at room temperature for 30 minutes. The samples were mixed well every 5 minutes during the incubation. They were then centrifuged at room temperature at 16000 *g* for 1 minute in order to pellet the beads. The supernatant, containing the fusion proteins, was transferred to a pre-chilled microcentrifuge tube. The samples were either immediately subjected to electrophoresis (section 2.4) or stored at -80°C until further processing.

2.3.10.5 Co-IP in the Presence of GTP-γS and GDP

In order to assess the effect of GTP binding on protein-protein interaction, the following co-IP protocol was employed. The cells were lysed and processed as shown in section

2.3.10.1. The anti-FLAG beads were equilibrated by subjecting them to three washes with the NP-40 wash buffer. The cell lysate containing the expressed proteins were mixed with the beads. The mixture was incubated on a turning disk at 4°C overnight (Section 2.3.10.3). The anti-FLAG beads were then washed three times with the NP-40 wash buffer as shown in section 2.3.10.4. As the assessment of the effect of guanosine nucleotide binding on the strength of protein-protein interaction performed was based on the amount of the myc-tagged proteins pulled down during co-IP, and that the amount of anti-FLAG beads present could affect the amount of the myc-tagged protein being pulled down, the amount of the beads for each co-IP reaction should ideally be the same. Hence, after the bead washing step, the beads were first pooled together and then split equally afterwards. The beads were first pooled together in 250 µl reaction buffer (2 mM $MgCl_2$ in PBS). They were then subjected to centrifugation at 100 *g* for 3 minutes at 4°C. The supernatant was removed and 350 µl fresh reaction buffer was added to the settled beads. The beads were resuspended gently, and 110 µl of the suspension was dispensed into three clean pre-chilled microcentrifuge tubes. The tubes were centrifuged at 100 *g* for 3 minutes at 4°C. After the removal of the supernatant, 495 µl of the reaction buffer was added to the tubes. This was followed by the addition of 5 µl of 500 µM GTP-γS or GDP in water to a final concentration of 5 µM. A control was included by the addition of 5 µl of water to the third tube of the equally divided beads. The beads were incubated at 37°C for 30 minutes with occasional shaking. The beads were then subjected to two washes with the ice-cold NP-40 wash buffer before elution as shown in 2.3.10.4.

2.3.11 Differentiation of SH-SY5Y Cells into Neurons

Retinoic acid (RA) was utilised for the differentiation of SH-SY5Y cells. It has the ability to regulate transcription of genes that results in SH-SY5Y cell differentiation into neurons (López-Carballo *et al*, 2002). The cells were first seeded into 3 cm wells in the culture plate as described in section 2.3.8. The medium required for the seeding process is neurobasal medium supplemented with 10 µM RA. 2×10^5 cells were seeded into each well with this medium. The culture plate was gently swirled and placed in the 37°C CO_2 incubator for 5 days. The medium (neurobasal medium + RA) was replaced daily.

2.3.12 Transfection of Differentiated SH-SY5Y Cells

Transfection of differentiated SH-SY5Y cells was achieved by a technique called magnetofection – the use of magnetism to transfer DNA across cell membranes. The Neuromag reagent (Oz Biosciences), composed of magnetic particles that can associate with DNA, was used in magnetofection. In general, 4 μg of plasmid DNA was used for transfection of SH-SY5Y cells in 3 cm wells. The Neuromag reagent was vortexed and briefly centrifuged. 3.5 μl Neuromag reagent per μg of DNA was added to a microcentrifuge tube. In another clean microcentrifuge tube, 4 μg of plasmid DNA was diluted with 200 μl serum-free DMEM-F12. The mixture was mixed thoroughly and was added to the Neuromag reagent in the other microcentrifuge tube. This mixture was pipetted up and down to ensure the DNA was mixed well with the Neuromag reagent. The mixture was left at room temperature for 20 minutes. The mixture was then added dropwise onto the differentiated cells and the culture plate was swirled. It was then placed on a magnetic platform for 15 minutes. This platform generates a magnetic field. The magnetic properties of the Neuromag particles are able to transfer the DNA complexed with them through the cell membrane once the magnetic field is applied. The medium in each well of the culture plate was aspirated. The pre-warmed, RA-supplemented neurobasal medium was then added. The plate was returned to the CO_2 incubator for 48 hours.

2.3.13 Immunocytochemistry

2.3.13.1 Fixation

Fixation is the first process performed in the protocol of immunocytochemical staining. It can generally maintain the morphology of the cells on the coverslip. Furthermore, the fixation reagents, or fixatives, can prevent the growth of bacteria on the coverslips, thereby preserving the specimen for subsequent staining. There are a number of fixation protocols. The protocol used in this study is called cytoskeletal protein fixation.

This protocol was adapted from Ciani and Salinas (2007), and was used when association of proteins to the microtubule cytoskeleton was investigated. The culture medium was aspirated, followed by two brief washes with pre-warmed 1x PBS to remove traces of media. The cells were then fixed with the fixation buffer (3% (v/v)

formaldehyde, 0.2% (v/v) glutaraldehyde, 0.2% (v/v) Triton-X100 and 10 mM EGTA, pH 7.2) for 10 minutes at 37°C. The cells were then washed three times with 1x PBS, and were further permeabilised with 0.02% Triton X-100/PBS. The cells were washed once with 1x PBS to remove traces of Triton X-100 prior to blocking with 2% (w/v) BSA in PBS for 40 minutes.

2.3.13.2 Immunocytochemical Staining

Primary antibodies against LRRK2 (Michael J Fox (MJFF) Foundation), acetylated tubulin (Sigma-Aldrich), tyrosinated tubulin (Sigma-Aldrich) and myc (Sigma-Aldrich) were used for immunocytochemical staining in differentiated SH-SY5Y cells. 75 µl of the primary antibodies diluted with the blocking solution were pipetted on a piece of parafilm and the coverslip was placed onto the bubble of antibody solution on the parafilm facing down. The incubation of primary antibodies was performed for 2 hours at room temperature. The coverslips were then placed back into the culture plate facing up and washed for 5 minutes in 1x PBS three times with constant, gentle swirling. Secondary antibody incubation utilised antibodies conjugated with fluorophores such as Alexa 488 or Alexa 546 (Invitrogen). These antibodies were diluted 600-fold in blocking solution, and the coverslips were incubated in the diluted secondary antibodies for 1 hour at room temperature, on a piece of parafilm protected from light. The coverslips were washed for 5 minutes in 1x PBS three times again, and were mounted onto microscope slides with 7 µl glycerol jelly pre-heated at 55°C. Slides were left overnight in the dark at room temperature before long-term storage at 4°C.

2.3.13.3 Confocal Microscopy

Microscope slides were viewed under a Zeiss LSM 710 META Confocal Microscope. The microscope contains several lasers that cause excitation of the fluorophore conjugated to the secondary antibodies. The argon laser emits light with wavelength 458, 477, 488 and 514 nm, and it excites the Alexa 488 fluorophore. The Alexa 546 fluorophore is excited by the HeNe 1 mW laser, which emits light with the wavelength of 543 nm. The Alexa 633 fluorophore is excited by the HeNe 5 mW laser, emitting blue fluorescent light of 633 nm. The DAPI stain was visualised by exciting the fluorophore with the diode laser emitting light of 405 nm. The objective lens used for specimen viewing was Plan-Apochromat 63x/1.4 with immersion oil. The images were

scanned at 1024 × 1024 pixels for the optimal resolution. The detector gain and amplifier offset were adjusted to obtain the best quality images.

2.4 Protein Methodology

2.4.1 SDS-PAGE

SDS-PAGE is a widely used technique that separates proteins in a sample by their molecular weight. Pre-cast 4-12% gradient Bis-Tris (Bis-(2-hydroxyethyl)-imino-tris-(hydroxymethyl) methane-HCl) gels available from Invitrogen were used. These gels provide a physiological pH (pH 7.0), which helps stabilise the mammalian cell-derived proteins during SDS-PAGE.

2.4.1.1 Setting up the Bis-Tris Gel

Two types of gel tank are available for SDS-PAGE depending on the number of samples run. The XCell Surelock^{TM} Mini-Cell (Invitrogen) can accommodate two 10-well Bis-Tris gels, while The XCell Surelock^{TM} Midi-Cell (Invitrogen) can accommodate four 20-well gradient Bis-Tris gels. The gels were placed on the buffer core so that the wells of the gels are facing each other. The entire core was then placed in a buffer chamber, and was secured by the gel tension wedge. 600 ml 1x MOPS (Invitrogen) buffer was poured into the lower buffer chamber, the chamber outside the buffer core. For a mini-cell, 0.5 ml of NuPAGE antioxidant (Invitrogen) was added to a fresh 200 ml 1x MOPS buffer and it was poured into the upper buffer chamber, the chamber in between the two gels. For a midi-cell, 1 ml of NuPAGE antioxidant was added to 400 ml fresh 1x MOPS buffer instead. The antioxidant prevents the re-formation of disulphide bridges in proteins so that it is kept at a denatured state during electrophoresis.

2.4.1.2 Sample Preparation and Electrophoresis

Determination of the protein concentration of each sample was first performed using the Bradford assay. Approximately 20 μg of protein was normally loaded into the gel for electrophoresis. The protein samples were first denatured before being loaded into the gel. The appropriate volume of 4x lithium dodecyl sulphate (LDS) sample loading buffer (106 mM Tris-HCl, 141 mM Tris base, 2% LDS, 10% glycerol, 0.51 mM EDTA, 0.22 mM Coomassie Blue G-250, 0.175 mM Phenol red, pH 8; Invitrogen) and 10x NuPAGE reducing agent (500 mM dithiothreitol; Invitrogen) were added and mixed. A brief centrifugation was performed and the samples were boiled at 95°C for 5 minutes.

10 µl of Rainbow molecular weight (MW) marker (Amersham Biosciences) was loaded into the first lane of each gel, and 15-30 µl of the denatured samples were run in subsequent lanes, depending on the size of the wells. Electrophoresis was run at a constant voltage of 150 volts for 90 minutes, until the dye present in the LDS sample loading buffer had reached the bottom of the gel.

2.4.2 Western Blotting

The proteins in the gel were transferred onto a hydrophobic polyvinyldiene fluoride (PVDF) membrane (Amersham Biosciences) by western blotting. 8 pieces of Whatman 3MM paper, cut to the size of the gel, were soaked in transfer buffer (25 mM Trizma Base, 192 mM glycine, 20% (v/v) methanol). 4 pieces were placed on the anode platform of the trans-Blot semi-dry transfer cell (Biorad). A 50 ml Falcon tube was used to roll across the stack of buffer-soaked paper to remove any air bubbles. A piece of PVDF membrane, also cut to the size of the gel, was first soaked in methanol, followed by the incubation in water for 1 minute to elute the methanol. The membrane was soaked again in transfer buffer and placed on top of the stack of soaked Whatman 3MM paper. The gel was then removed from the gel cassette. The bits of wells and the bottom of the gel filled with the tracking dye were removed. The gel was then soaked in transfer buffer and placed on top of the PVDF membrane. 4 more pieces of Whatman 3MM paper, soaked in transfer buffer, were placed on top of the gel to complete the stack. The stack was rolled across again to remove air bubbles. The blotting was run for 1 hour, under a constant voltage of 20 volts.

2.4.3 Membrane Blocking

The PVDF membrane was first blocked with the antibody diluent required (Table 2.7) after blotting. The membrane was incubated at room temperature with gentle agitation in the antibody diluent for 1 hour. The most common antibody diluent used is non-fat dry milk (Marvel; 5% (w/v)) in PBS, horse serum (PAA Laboratories) and 5% BSA in PBS. The proteins present in the milk, horse serum and BSA can attach to areas on the hydrophobic membrane that are not occupied by the proteins from the samples. This can prevent non-specific binding of the antibodies to the membrane.

2.4.4 Antibody Incubation

Primary antibody incubation was performed after membrane blocking. The appropriate primary antibody was diluted to the desired concentration by the antibody diluent as shown in table 2.7. The antibody diluent used for membrane blocking was discarded, and 10 ml of the diluted primary antibody was added. The membrane was placed on a gently shaking platform and incubated in the solution overnight at 4°C. The antibody solution was discarded afterwards, and was followed by three washes of the membrane with PBS containing 0.1% Tween-20 (PBS-T) with gentle agitation on a gyro rocker, each for 10 minutes. Secondary antibody solution was prepared for the subsequent secondary antibody incubation step. Donkey anti-goat, goat anti-mouse or goat anti-rabbit immunoglobulin G conjugated with horse radish peroxidase (HRP; Santa Cruz Biotechnology) were used as secondary antibody, depending on the host species where the primary antibody used was raised from. A 10 ml solution of 2000-fold diluted secondary antibody was prepared in PBS-T. The membrane was incubated in this solution at room temperature with gentle agitation for 1 hour. Three 10-minute washes with PBS-T were performed following the secondary antibody incubation.

Antibody	Supplier	Host	Dilution used	Antibody diluent used
Anti-c-myc	Sigma-Aldrich	Rabbit	1:2000	5% milk/PBS
Anti-FLAG polyclonal	Sigma-Aldrich	Rabbit	1:2500	Horse serum
Anti-HA	Covance	Mouse	1:1000	5% milk/PBS
Anti-β-actin	Sigma-Aldrich	Mouse	1:6000	5% milk/PBS
Anti-LRRK2	MJFF	Mouse	1:100	5% milk/PBS
Anti-LRRK2	Everest	Goat	1:2500	5% milk/PBS

Table 2.7: The details of the use of the antibodies utilised in Western blots.

2.4.5 Chemiluminescence Detection

The HRP conjugated to the secondary antibody allows us to detect the presence of proteins indirectly bound to the secondary antibody, via the primary antibody, by chemiluminescence. SuperSignal West Pico chemiluminescence substrate solutions (Pierce) were utilised for this purpose. The solutions include Luminol Enhancer

Solution containing luminol (3-aminophthalhydrazide) and Stable Peroxide Solution containing hydrogen peroxide. The HRP can oxidise the luminol in the presence of hydrogen peroxide, which generates light. The amount of light emitted reflects the amount of secondary antibody, and hence the protein of interest, that is present on the membrane. 500 µl of each solution was mixed on a piece of cling film. The membrane was removed from the PBS-T and excess PBS-T was removed by blotting the membrane gently on a piece of absorbent paper. The membrane was inverted and placed on the solution mixture, so the proteins on the membrane can access the solutions. The membrane was incubated in the solution for 1-3 minutes. Excess solution was removed by blotting the membrane gently on the absorbent paper. The membrane was wrapped with a clean piece of cling film. A strip of tracker tape was positioned along the MW lane of the membrane for the visualisation of the bands in the MW lane. The membrane was exposed in the GeneGnome chemiluminescence bio-imaging system (Syngene). The exposure duration is dependent on the antibody used, and can vary from 30 seconds to 1 hour. Quantification of the amount of light emitted was performed using the Genetools software (Syngene).

2.5 Assessment of Gene Expression at the Transcriptional and Translational Level

2.5.1 RNA Extraction

A flask of HEK293 and SH-SY5Y cells were incubated in a 37°C CO_2 incubator until the confluency of cells reached over 90%. A flask of differentiated SH-SY5Y cells was also prepared for RNA extraction using the RNeasy kit (Qiagen). The cell culture medium was first aspirated, and the cells were trypsinised (section 2.3.5). The cells were suspended in fresh medium and subjected to centrifugation at 500 *g* for 5 minutes at room temperature. The supernatant was completely removed, and 600 µl of lysis buffer RLT was added to achieve cell lysis. The contents were vortexed briefly and the cell pellet was loosened from the wall of the tube by flicking the suspension. The lysate was homogenised for 30 seconds with a rotor-stator homogeniser. This was followed by mixing the lysate with 600 µl 70% ethanol. The mixture was then loaded into an RNeasy spin column provided in the kit. The column was centrifuged for 15 seconds at 12000 *g*. RNA binds to the silica membrane in the spin column while the other impurities flow through. 700 µl of wash buffer RW1 was applied to the column for washing the RNA. The column was centrifuged again to remove the buffer. A concentrated wash buffer containing ethanol (Buffer RPE) was used to further wash the membrane-bound RNA in the column. The RNA was washed twice with 500 µl buffer RPE. Following the second wash, the column was centrifuged for 2 minutes to ensure no carry-over of ethanol in the column. The RNA was then eluted into a fresh microcentrifuge tube with 50 µl RNase-free water.

2.5.2 Reverse Transcription and PCR Amplification

The conversion of the extracted total RNA to cDNA by reverse transcription was performed using the High-Capacity cDNA Reverse Transcription Kit (Applied Biosystems), which is the recommended kit for subsequent relative quantification PCR (RQ-PCR) experiments. Random primer was first allowed to anneal to the extracted RNA. 2 µl of 10x RT random primer was first mixed with 0.8 µl dNTP mix containing 100 mM of each dNTP, 2 µl 10x RT buffer and 1 µl reverse transcriptase. The mixture was made up to 10 µl with RNase-free water. 10 µl of this mixture was mixed with 50 ng of the extracted RNA which was made up to 10 µl with water. The mixture was

incubated at 25°C for 10 minutes, then 37°C for 120 minutes, and finally 85°C for 5 seconds in a Hybaid PCR Express thermal cycler.

The resultant cDNA was then subjected to PCR amplification using Pfx Accuprime and the PCR conditions detailed in section 2.1.1. The primers for amplification of the untranslated region of LRRK2 are shown in table 2.8. The PCR products were run on a 2% agarose gel to check for the presence of amplified products.

Primer name	Direction	Sequence	Amplicon
LRRK2 5' UTR F	forward	agcagcggacgttcatgctggga	5'-UTR
LRRK2 5' UTR R	reverse	tcccaatcatttccaacatcctg	
LRRK2 3' UTR F	forward	cctgttgtggaagtgtgggataag	3'-UTR
LRRK2 3' UTR R	reverse	ttttcctatccaaagacaattcc	

Table 2.8: Primers used for PCR amplification of the untranslated regions of LRRK2 for the endogenous LRRK2 detection in HEK293 and SH-SY5Y cells. (UTR = untranslated region)

2.5.3 RQ-PCR

RQ-PCR is a quantitative way to assess the expression level of a gene in the genome in comparison to the expression of a housekeeping gene, a gene expressed at a constitutively high, and presumably constant, level in cells. For example, glyceraldehyde-3-phosphate dehydrogenase (GAPDH), which catalyses the sixth step of the glycolytic pathway in cellular respiration, is considered a housekeeping gene, and was used as an endogenous control for RQ-PCR experiments. This technique utilises the Taq DNA polymerase for PCR amplification of the target cDNA generated from reverse transcription (section 2.5.2), and a short DNA probe that can bind to the cDNA. This probe has a fluorescent reporter attached to the 5' end, and a non-fluorescent quencher at the 3' end. The probe was allowed to bind to the cDNA, and the close proximity of the reporter and quencher hampers the fluorescence properties of the reporter. As the Taq DNA polymerase starts amplifying the cDNA during PCR, the 5'-3' polymerase activity exhibited by Taq DNA polymerase results in the probe being pried apart, separating the reporter and quencher. The quencher can no longer inhibit the

fluorescence properties of the reporter, and the reporter emits fluorescence. The level of fluorescence signal increases proportionally after each PCR cycle as more and more reporter molecules are freed from the quencher. The level of fluorescence emitted is an indication of the starting amount of cDNA. By comparing with the amount of signal given off from the endogenous control, we can compare the relative level of expression of the different genes of interest in various samples, which is expressed as the percentage of the expression of the endogenous control.

A mixture of the cDNA sample and the Taqman Universal PCR Mastermix was first made up, comprising 1 µl of cDNA sample, 25 µl of the mastermix and 21.5 µl water. A 'no DNA control' was also prepared as a negative control. In this control sample, the 1 µl cDNA was substituted by 1 µl water. 2.5 µl of the DNA probe (Applied Biosystems), or Taqman Gene Expression Assay primer for the gene of interest, was loaded into the wells of an optical 96-well plate (MicroAmp), followed by the 47.5 µl cDNA + Taqman mastermix mixture. Experiments were performed in triplicate. 2.5 µl of DNA probe of the housekeeping gene GAPDH was also loaded onto a separate set of wells in the plate, followed by the cDNA + Taqman mastermix mixture. The plate was subjected to a brief spin and loaded into an ABI 7500 RT-PCR machine. The real-time PCR was performed using the conditions shown in table 2.9. The quantification of the amount of the amplified cDNA started when the increase in fluorescence signal became exponential. The fluorescence level at which the signal started to increase exponentially was known as the threshold level, and the number of PCR cycles required for the cDNA amplification to cross this threshold is called the cycle threshold (C_t). This follows that the lower the C_t value, the more copies of cDNA the sample originally has, which is an indication of a higher level of gene expression. To take account of the endogenous control GAPDH, the ΔC_t value was calculated by subtracting the C_t value of the gene of interest by the C_t value of the endogenous control. This value allows us to compare relatively the original amount of cDNA present before PCR in each sample, using the GAPDH as a standard. For example, if the ΔC_t value is 3, that means the gene of interest took 3 more cycles to reach threshold than the GAPDH control, or 3 times less cDNA is present compared to GAPDH. The data were expressed in terms of the percentage of GAPDH expression for relative comparison of the gene expression level.

Stage	Temperature (°C)	Time	Number of cycles
1	50	2 mins	1
2	95	10 mins	1
3	95	15 sec	40
	60	1 min	

Table 2.9: The parameters utilised in the amplification step in RQ-PCR.

2.5.4 Total Protein Extraction and Western Blotting

In order to assess LRRK2 protein expression in human cell lines, a western blot on lysates from HEK293 cells and SH-SY5Y cells at different time points of differentiation (section 6.2) was carried out and the membrane was probed with an anti-LRRK2 antibody (Michael J Fox Foundation). HEK293 and SH-SY5Y cells were grown in 10 cm diameter cell culture dishes until they were more than 90% confluent. The cells were then lysed using 1 ml of lysis buffer (50 mM NaCl, 1x protease inhibitor) and scraped after being washed with ice-cold PBS twice. The lysate was homogenised in a glass pestle and mortar by plunging the lysate with the pestle 10 times. The lysate was then transferred to a clean microcentrifuge tube and centrifuged at 16000 *g* for 10 minutes at 4°C. The supernatant was transferred to and kept in a clean microcentrifuge tube. The samples were either loaded into an SDS-PAGE gel immediately afterwards or stored at -80°C until further processing.

2.6 Mutation Scanning

Mutation scanning is a technique used to determine whether there are nucleotide sequence variations within a given stretch of DNA, and it is often used to scan genomic DNA extracted from humans for any mutations in an exon of a certain gene. This technique utilises the LightScanner instrument (Idaho Technology) and a duplex DNA binding dye called LCGreen. The principle relies on the fact that the duplex DNA melting profile obtained from a mutated DNA sample is different from that in a WT counterpart, due to the difference in nucleotide sequences. Duplex DNA would generally denature or 'melt' when a critical temperature is reached. When the DNA is in the duplex form, LCGreen can bind to the DNA and emit fluorescence. However, when DNA melts, LCGreen becomes dissociated from the DNA and the fluorescence emission stops. The LightScanner instrument contains a camera that can capture the level of fluorescence as the temperature inside the instrument increases. A graph of fluorescence emission level versus temperature is generated, which constitutes the melting curve of the sample.

2.6.1 Mutation Scanning using the LightScanner

Genomic DNA samples of PD patients obtained from the Imperial Parkinson's Disease Society Brain Bank were diluted to 20 ng/μl for use in mutation scanning. The genomic DNA was first subjected to PCR, generating multiple copies of the DNA. To each well in a black-body 96-well plate (Klent), 4 μl of LightScanner Mastermix (Idaho Technology), which contains the LCGreen, was mixed with 1 μl of the genomic DNA and 0.25 μl of the 10 μM forward and reverse primers for exon amplification, achieving a final primer concentration of 0.25 μM. The PCR reaction was topped up to 10 μl with water. To prevent sample evaporation, 15 μl of mineral oil was added to each well before the addition of the PCR mix described above. Each genomic DNA sample was tested in duplicate in order to ensure reproducibility of results.

Prior to the PCR amplification of the genomic DNA samples, the PCR conditions were first optimised using a temperature gradient ranging from 58°C to 70°C in the Hybaid PCR Express thermal cycler. This allows us to determine the best primer annealing temperature for the amplification of LRRK2 exon 31 and 35. The PCR products

obtained for each temperature across the temperature gradient were run in a 2% agarose gel. The temperature that gave one single DNA band which appeared the most prominent was chosen as the optimal primer annealing temperature for PCR. The PCR optimisation revealed that the best primer annealing temperature for exon 31 amplification was 64.6°C, and that for exon 35 amplification was 63.1°C.

The 96-well plate was covered with a piece of adhesive film, and was subjected to centrifugation at 100 *g* for 2 minutes at room temperature. The PCR reactions were subjected to an initial denaturation step for 2 minutes, followed by 45 cycles of duplex denaturation for 30 seconds and primer annealing and extension for 30 seconds, using the primer annealing temperature as detailed above. A final denaturation step was carried out at 94°C for 30 seconds, followed by a rapid cooling to 25°C. The plate was spun at 100 *g* for 2 minutes to remove any air bubbles before being loaded into the LightScanner instrument.

The LightScanner instrument was set to start detecting the level of fluorescence when the temperature reached 77°C. The detection was performed until the temperature reached 95°C. The analysis of the melting profiles was performed by following the manufacturer's protocol. First, it involves the identification of the negative controls and failed PCR reactions. These reactions were filtered out in the analysis. The data were then normalised due to the fact that minute differences in the amount of template DNA would cause a large difference in fluorescence level. Normalisation was done by selecting one region before and after the fluorescence level transition, and these were defined as 100% fluorescence baseline and 0% fluorescence baseline respectively. This allows the definition of the starting and end-point fluorescence levels of all the samples. The samples which showed a different melting profile from the WT control, as well as those which gave different melting profiles in the duplicates, were first directly sequenced, and then for sequence confirmation, TOPO-cloned and sequenced (Section 2.6.2).

2.6.2 TOPO cloning

TOPO cloning was performed using the TOPO TA Cloning Kit for Sequencing (Invitrogen). 20 ng/μl genomic DNA was first amplified by PCR using the parameters

shown in section 2.1.1, except that Taq polymerase was utilised as the DNA polymerase in the primer extension step, which was carried out at 72°C. Taq polymerase has the ability to add a single adenine to the ends of the PCR amplicon through its terminal transferase activity, thereby generating an overhang of an adenine. The PCR product was gel-purified using the QIAquick Gel Extraction Kit (QIAGEN, 28706). 4.5 µl of the cleaned PCR product was mixed with 1 µl of the provided salt solution (200 mM NaCl, 10 mM $MgCl_2$) and 0.5 µl TOPO vector. The mixture was incubated at 22 °C for 20 minutes.

The TOPO vector supplied is a linearised vector that contains a thymine overhang. It is bound to topoisomerase I that specifically cleaves the phosphodiester backbone after 5'-CCCTT. A tyrosine residue in the topoisomerase forms a phospho-tyrosyl bond by a nucleophilic attack using the hydroxyl group. The phosphoryl group of thymine thereby becomes attached to the enzyme. In the presence of the PCR product containing an adenine overhang, the adenine in the PCR product binds to the thymine overhang in the linearised vector through complementary base pairing. The hydroxyl group on the cleaved strand of the PCR product undergoes a nucleophilic attack on the phospho-tyrosyl bond, releasing the topoisomerase I from the vector. The PCR product then forms a phosphodiester bond with the vector backbone. The rationale of TOPO cloning is depicted in figure 2.2.

After the 20-minute incubation, 2 µl of the mixture was transformed into competent TOP10 *E.coli* as shown in section 2.1.5, and plated onto ampicillin-containing agar plates. An overnight culture was set up and four minipreps for each sample were prepared (section 2.1.6). The miniprep samples were sent for DNA sequencing using the M13 sequencing primers (section 2.1.6). The sequences obtained were compared with the sequences of the appropriate exons of LRRK2 that are available on the NCBI website (http://www.ncbi.nlm.nih.gov/nuccore/NM_198578.3, NM_198578).

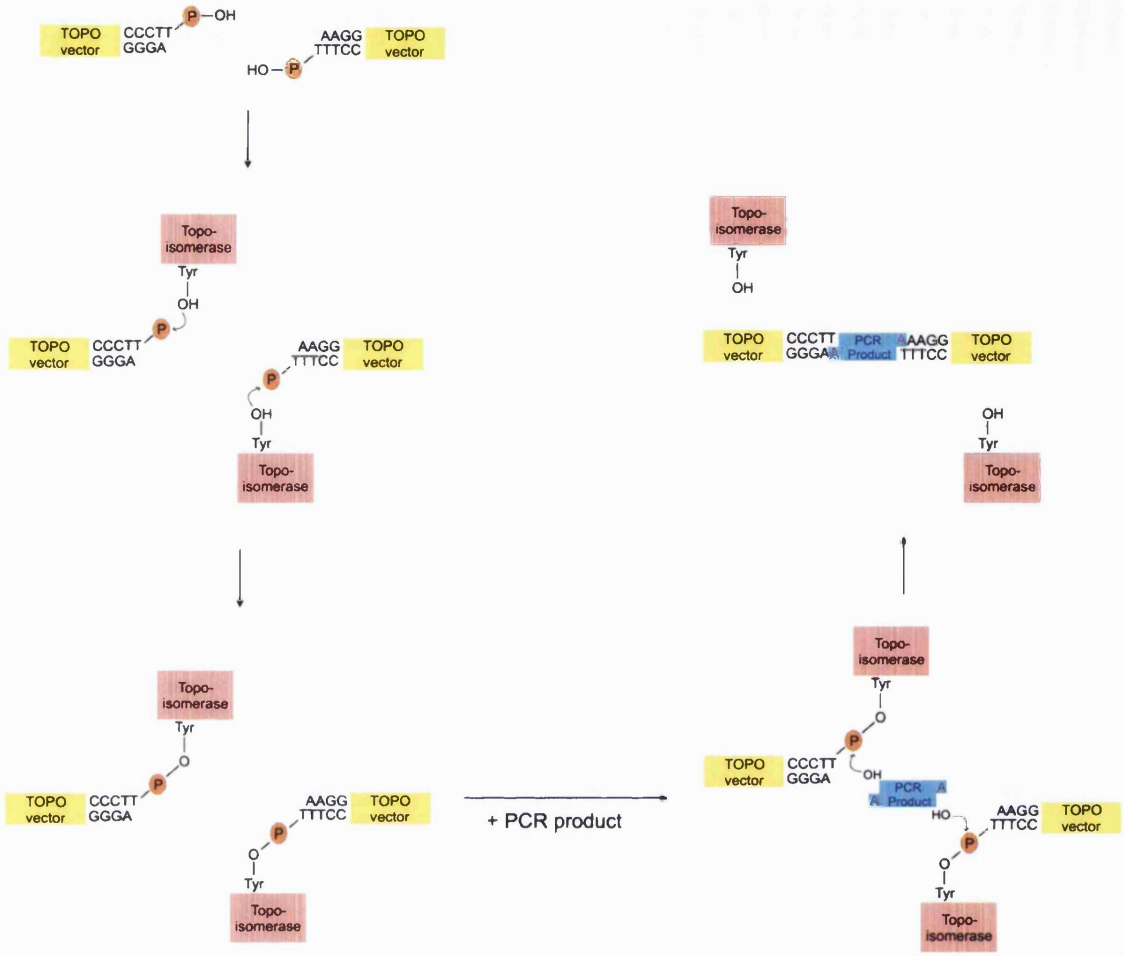

Figure 2.2: The Rationale of TOPO Cloning. The TOPO vector supplied in the TOPO TA Cloning kit is attached to topoisomerase I. The hydroxyl group of the tyrosine nucleophilically attacks the 3' phosphate of the thymine overhang, resulting in the phospho-tyrosyl bond between the TOPO vector and the tyrosine residue of the topoisomerase. PCR product resulting from the amplification of genomic DNA by Taq polymerase has an adenine overhang at its 3' end. This can bind to the thymine overhang of the TOPO vector through complementary base pairing. Meanwhile, the 5'-OH group nucleophilically attacks the phosphate group of the thymine overhang in the TOPO vector, thereby forming a covalent bond between the TOPO vector and the PCR product, which causes the release of topoisomerase. The PCR product cloned into the TOPO vector can then be transformed into chemically competent *E.coli*.

3. The Effect of *PARK8* Mutations on LRRK2 Interactions

Mutations in *PARK8* have been widely accepted as being the most common known cause for PD (Schapira, 2006). However, the mechanisms in which *PARK8* mutations lead to PD remain elusive. Ongoing research on LRRK2 has investigated the physiological functions with one focus being on possible roles in cellular signalling pathways. It is of crucial importance to uncover the molecular events that LRRK2 participates in, in order to understand the role of LRRK2 in PD pathogenesis. This project serves to investigate the effect of *PARK8* mutations on the strength of interaction between LRRK2 and proteins that were found to interact with it. Such investigation is important, as a change in the protein-protein interaction caused by a PD-associated mutation may suggest a role of such interaction in the pathogenesis of PD.

Most research work on LRRK2 has focussed on the effect of the kinase activity on cellular viability, and it was shown that the PD-associated mutation G2019S in the kinase domain caused cell death in cellular assays (West *et al,* 2005). However, the GTPase activity of LRRK2 was also recently reported to play a pathological role of LRRK2. Ras-like mutants in LRRK2, which increase GTPase activity, were found to increase yeast viability, while GTP binding deficient mutants which display no GTPase activity significantly lowered yeast viability (Xiong *et al,* 2010). Furthermore, as discussed in chapter 1, the GTPase activity and kinase activity in LRRK2 might have an auto-regulatory relationship. The GTPase activity might control the kinase activity (Guo *et al,* 2007; West *et al,* 2007). The kinase activity might in turn affect the Roc domain by lowering the ability of LRRK2 to bind GTP (Kamikawaji *et al,* 2009). My research focus is on LRRK2 interactors of the Roc-COR tandem domain and the influence of *PARK8* mutations on interactions with protein interactors. This may also open a path of research to the possibility that these interactors might alter LRRK2 GTPase activity.

3.1 Potential LRRK2 Interactors

A human whole brain cDNA library screen was performed previously in our lab to reveal interactors of the Roc-COR domain of LRRK2. The Roc-COR domain cloned into the pDS vector was used as bait, and the human embryonic whole brain cDNA library (Clontech) cloned into the pACT2 vector was used as prey in the library screen.

The screen was performed using competent L40 yeast cells. Four interactors potentially important for neurodegeneration, reticulon 3 (RTN3), S100A10, apolipoprotein E3 (ApoE3) and β-tubulin 4 (TUBB4), were prioritised for analysis and briefly described below.

3.1.1 RTN3

RTN3 is a protein that was reported to be upregulated during endoplasmic reticulum (ER) stress (Wan *et al*, 2007). ER stress is characterised by an accumulation of misfolded proteins at the ER, resulting in a disruption of ER function in producing properly folded tertiary and/or quaternary protein structures. Under such conditions, RTN3 is thought to exhibit anti-apoptotic activity through initiating the accumulation of Bcl-2 in mitochondria (Wan *et al*, 2007). Even though previous reports found that RTN3 over-expression in the immortalised HeLa cell line could lead to apoptosis due to the depletion of calcium stores in the ER (Qu *et al,* 2002), more recently it was found that if the HeLa cells were co-transfected with RTN3 and Bcl-2, RTN3 exhibited an anti-apoptotic effect by interacting with Bcl-2 and lead to Bcl-2 accumulation in mitochondria (Zhu *et al,* 2007). In line with this, ER-stress-induced RTN3 upregulation was shown to encourage the translocation of Bcl-2 from the ER to mitochondria, while RTN3 downregulation induced apoptosis in HeLa cells (Wan *et al,* 2007). Furthermore, the relevance of RTN3 in neurodegenerative diseases was implicated by the presence of aggregated RTN3 deposits in neurofibrillary tangles and Lewy bodies (Heath *et al*, 2010). In conclusion, RTN3 might have a role in regulating cellular viability that could play a role in the pathogenesis of neurodegenerative diseases such as AD and PD.

3.1.2 S100A10

S100A10, also called p11, is a calcium-binding protein. It was found to have anti-apoptotic activity through binding to a protein called BAD, resulting in the inhibition of the pro-apoptotic function of BAD (Hsu *et al,* 1997). S100A10 has previously been implicated in certain neurological conditions such as depression. S100A10 was shown to interact with the serotonin receptors $5HT_{1B}$ and induced recruitment of these receptors to synapses (Svenningsson *et al,* 2006). Reduced expression of $5HT_{1B}$ receptors at synapses might lead to the development of depression. Furthermore, S100A10 was reported to interact with and inhibit the activity of phospholipase A2 (Wu

et al, 1997), which plays a role in inflammation as it releases arachidonic acid in an inflammatory response. This observation also suggests an anti-inflammatory role of S100A10.

Since S100A10 was also implicated in apoptosis and neurological diseases, it would be of interest to see if it plays a role in the pathogenesis of PD through the interaction found with LRRK2.

3.1.3 Apolipoprotein E (ApoE)

The physiological function of ApoE is the mediation of cholesterol transport in the body, and the redistribution of lipids in the CNS (Strittmatter and Bova Hill, 2002). The ApoE gene has three different variants: *ApoE2*, *ApoE3* and *ApoE4*. The variants differ only at two amino acid residues in the amino acid sequence. However, these ApoE variants have different effects on neurons. For example, ApoE2 and ApoE3 were both suggested to be neuroprotective. They were found to bind to tau, a microtubule-associated protein responsible for microtubule stabilisation, and prevent tau phosphorylation, thereby stabilising microtubules (Strittmatter *et al,* 1994). However, the third variant, ApoE4, had almost the opposite effect to ApoE2 and ApoE3. It encouraged tau hyperphosphorylation and caused microtubule destabilisation (Tesseur *et al*, 2000). ApoE4 is well known as a risk factor for AD. 40-80% of patients with idiopathic AD were found to have at least one *ApoE4* allele (Farrer *et al,* 1997). The inheritance of an *ApoE4* allele was also reported to be associated with an increased risk of parkinsonism with dementia, and the age of onset of dementia in individuals carrying an *ApoE4* allele might be earlier than those carrying *ApoE2* or the more common *ApoE3* allele. (Pankratz *et al,* 2006a). However, conflicting data were published. Harhangi *et al* (2000) reported an increased risk of PD with dementia in individuals bearing an *ApoE4* allele, while Oliveri *et al* (1999) reported no difference in the allelic frequency of ApoE among PD patients and controls.

It was also found that ApoE4 can inhibit Wnt signalling in PC12 cells (Caruso *et al,* 2006). The inhibition of the Wnt pathway could result in GSK3β being active (Dale, 1998). GSK3β was shown to cause tau phosphorylation and microtubule destabilisation (Wagner *et al,* 1996), which has a detrimental effect on neurons. Since LRRK2 was

shown to interact with the Wnt signalling component dishevelled (DVL) (Sancho *et al,* 2009), it would be interesting to see whether ApoE variants display different interactions with the LRRK2 Roc-COR domain, and whether *PARK8* mutations in these domains can affect such interaction.

3.1.4 TUBB4

β-tubulin is a component of the microtubule cytoskeleton in cells. In microtubules, α-tubulin and β-tubulin alternate with each other in polymers called protofilaments. These protofilaments form a bundle with a hollow centre to form cylindrical filaments. Microtubules are important in neuronal functions. One of such functions is axonal transport, transporting proteins such as ion channels made in the ER and neurotransmitter-containing vesicles from the soma to the synapses (anterograde transport), thereby playing a role in synaptic functions. Furthermore, the microtubule cytoskeleton is also important for the retrograde transport of neurotrophic factors, which are vital for neuronal survival, from the dendrites to the cell body. It is believed that microtubules may play a role in neurodegeneration as well. For example, in dopaminergic neurons where dopamine is used as a neurotransmitter, microtubule destabilisation can disrupt the transport of dopamine vesicles along axons, causing vesicle accumulation. However, vesicles containing catecholamine neurotransmitters like dopamine were shown to be 'leaky' (Eisenhofer *et al,* 2004). Such leakage might result in elevated concentrations of dopamine in the cytosol of axons. As dopamine auto-oxidation can yield ROS (Chiueh *et al,* 2000), this elevated level of dopamine caused by vesicular leakage could exacerbate oxidative stress in neurons, causing neurodegeneration (Feng, 2006). Microtubule destabilisation was also found to be implicated in PD (Ren *et al,* 2005).

3.2 Modulation of Interaction Strength between LRRK2 and Interactors by *PARK8* Mutations

As discussed previously, LRRK2 possesses both kinase and GTPase activities, indicating a role of LRRK2 in cellular signalling. Since proteins involved in a signalling cascade are required to interact with each other for signal transduction, the strength of

interaction between these proteins could affect the 'signalling strength'. I looked at the possible alteration in interaction strength between the Roc-COR domain of LRRK2 and the aforementioned potential interactors by PD-associated *PARK8* mutations. YTH assays were carried out to assess the presence of interaction between the Roc-COR domain and interactors, and the relative level of interaction among the different Roc-COR proteins was assessed based on the intensity of the colour development (section 2.2.5). An alteration in the interaction level with the interactors caused by the *PARK8* mutations could indicate an importance of the interactions in PD pathogenesis.

The Roc-COR domain cloned into the pDS bait vector and the identified Roc-COR interactor cloned into the pACT2 prey vector were generated previously in our lab. Site-directed mutagenesis was employed to generate the various mutants of the Roc-COR domain. The procedures and the primers required for these mutagenesis reactions are shown in section 2.1.8 and table 2.5 respectively. The bait was co-transformed with the prey into the L40 yeast strain. The yeast colonies on the TC plates were lifted after 3-4 days of incubation, whilst the colonies on the NS plates were lifted after 6-7 days of incubation.

3.2.1 The Roc-COR – RTN3 Interaction

The effect of PD-associated mutations in the LRRK2 Roc-COR domain on the strength of interaction with full length RTN3 was investigated. Figure 3.1 shows the results of this experiment. Additional transformations were performed using the empty bait and empty prey vectors, in order to ensure that the blue colour developed in the transformants was not due to autoactivation.

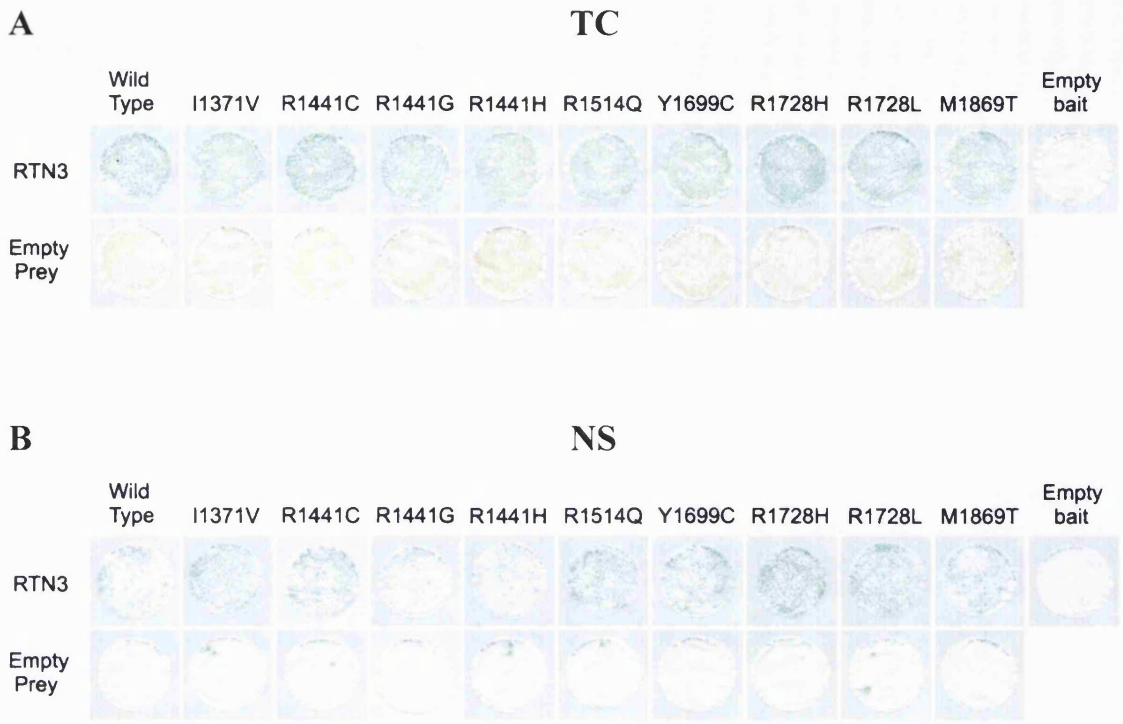

Figure 3.1: WT LRRK2 Roc-COR domain constructs expressed in yeast can interact with RTN3, and some mutations in the Roc-COR domain are able to modify the interaction strength. Interactions between a full length RTN3 construct and the WT and mutant Roc-COR domain construct expressed in yeast are indicated by the blue colonies on the TC filters (A) and the NS filters (B). All negative controls with the empty prey and bait vectors did not show an interaction. The I1371V, R1441G, R1441H, Y1699C and M1869T mutations appeared to decrease the strength of the Roc-COR – RTN3 interaction, while the R1728H mutation appeared to increase the strength of the interaction in comparison to the WT LRRK2 Roc-COR protein.

Figure 3.1A shows the filters lifted from the TC plates while figure 3.1B shows those lifted from the NS plates. They will be referred to as the TC filters and NS filters, respectively, hereafter. The blue colour developed in all these filters indicates the presence of an interaction between RTN3 and the Roc-COR domain. All the tested Roc-COR mutants were still able to retain an interaction. However, certain mutations appeared to influence the strength of the interaction between the Roc-COR domain and RTN3. In the LacZ freeze-fracture assay, the filters were incubated in the LacZ reaction buffer for the same duration, allowing for a semi-quantitative assessment of the blue

colour development. This rate gives an indication on the strength of the interaction between the two proteins. Figure 3.1A shows that the I1371V, R1441G/H, Y1699C and M1869T mutations resulted in a weakening of the Roc-COR – RTN3 interaction, as shown by the decreased intensity of the colour developed compared to the WT Roc-COR domain. The colonies on the NS filters also showed that Roc-COR mutants failed to abolish the Roc-COR – RTN3 interaction. The fewer colonies formed on the NS filters for these mutants might be a result of a decreased strength of interaction with RTN3, as less histidine was made in the yeast cells due to the lowered interaction strength between the bait and the prey. In contrast, the R1728H mutation appeared to increase the strength of the Roc-COR – RTN3 interaction. In summary, mutations within the Roc-COR domain of LRRK2 failed to abolish the LRRK2 – RTN3 interaction completely. However, some mutations resulted in a modification of the interaction strength.

3.2.2 The Roc-COR – S100A10 Interaction

Figure 3.2 shows the results of the YTH assay between the LRRK2 Roc-COR domain and S100A10. Similar to the Roc-COR – RTN3 interaction, the Roc-COR – S100A10 interaction was not abolished by any of the Roc-COR mutants tested. Nevertheless, the Roc-COR domain mutants R1441G, Y1699C and M1869T, when co-expressed with S100A10, showed a clear decrease in colour development compared to the WT Roc-COR domain. Furthermore, mutations at R1728 resulted in an increase in the intensity of the colour development (figure 3.2A). The NS filters in figure 3.2B provide further evidence for this altered interaction strength, as the filters for R1441G, Y1699C and M1869T had fewer colonies while those for R1728H/L had more, compared to the filter for the WT Roc-COR domain. This indicates that some PD-associated mutations can also affect the interaction between the Roc-COR domain and S100A10 in yeast.

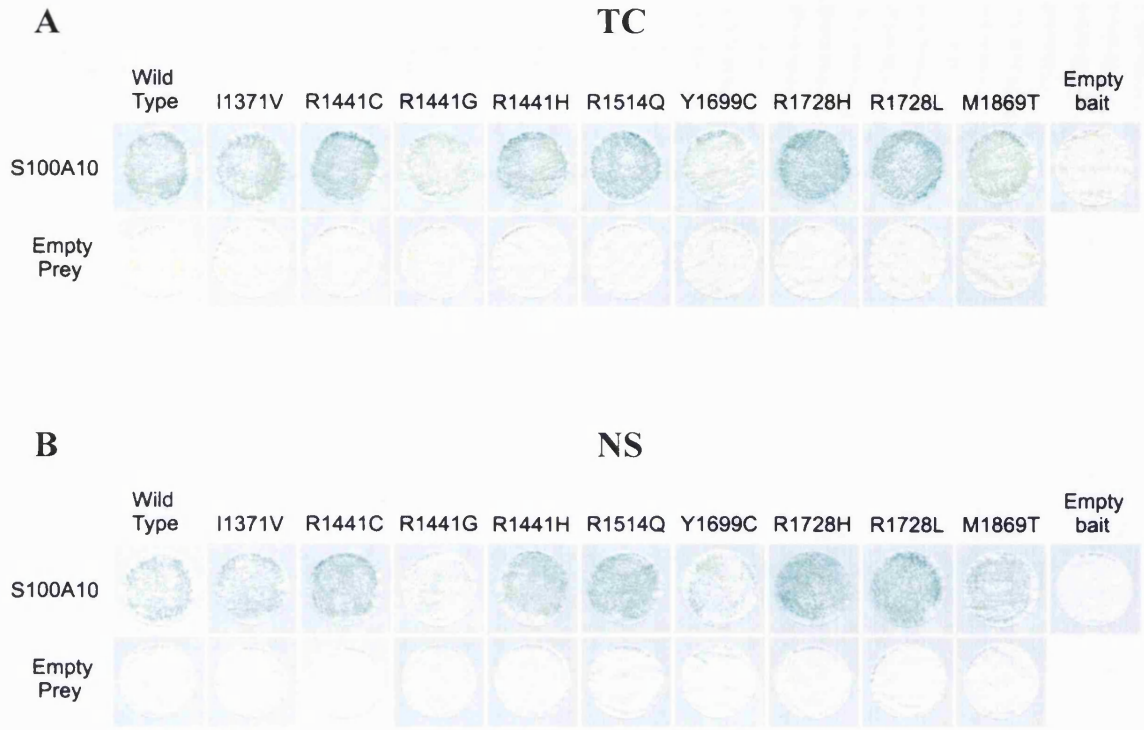

Figure 3.2: WT LRRK2 Roc-COR domain constructs expressed in yeast can interact with S100A10, and some mutations in the Roc-COR domain are able to modify the interaction strength. Interactions between a full length S100A10 construct and the WT and mutant Roc-COR domain construct expressed in yeast are indicated by the blue colonies on the TC filters (A) and the NS filters (B). All negative controls with the empty prey and bait vectors did not show an interaction. The R1441G, Y1699C and M1869T mutations appeared to decrease the strength of the Roc-COR – S100A10 interaction, whilst the R1728H and R1728L mutations appeared to increase the strength of the interaction.

3.2.3 The Roc-COR – ApoE Interaction

The interaction between the Roc-COR domain and the three variants of ApoE was investigated to see whether Roc-COR mutations can affect the interaction strength. Results showed that the Roc-COR – ApoE interaction was not abolished by Roc-COR mutations, and the R1441G mutation appeared to weaken the strength of the interaction (figure 3.3A and 3.3B). One observation to note was that the pattern of interaction strength of these Roc-COR variants with ApoE was strikingly similar among the three ApoE variants. For example, R1441G showed a clear decrease in interaction strength

with all the three ApoE variants to a similar degree. All other mutants and WT Roc-COR also showed a similar level of interaction with the ApoE variants. In summary, the Roc-COR – ApoE interaction was decreased by the R1441G mutation, but ApoE variants did not seem to play a part in the modification of the level of interaction.

3.2.4 The Roc-COR – TUBB4 Interaction

Finally, the effect of Roc-COR mutations on the strength of the interaction between the Roc-COR domain and TUBB4 was determined. As figure 3.4 shows, all of the Roc-COR variants were able to interact with the C-terminus of TUBB4. However, similar to the other interactors, some of the Roc-COR mutations showed different interaction strength compared to the WT Roc-COR domain (figure 3.4A). For example, the R1441G and R1441H mutations seemed to show a decreased level of interaction with TUBB4. Interestingly, mutations at the residue R1728 resulted in an increased interaction strength with TUBB4. The NS filters also confirmed this observation (figure 3.4B). In summary, all Roc-COR variants had the ability to interact with TUBB4, but several mutations in the Roc-COR domain could modify the level of interaction with TUBB4.

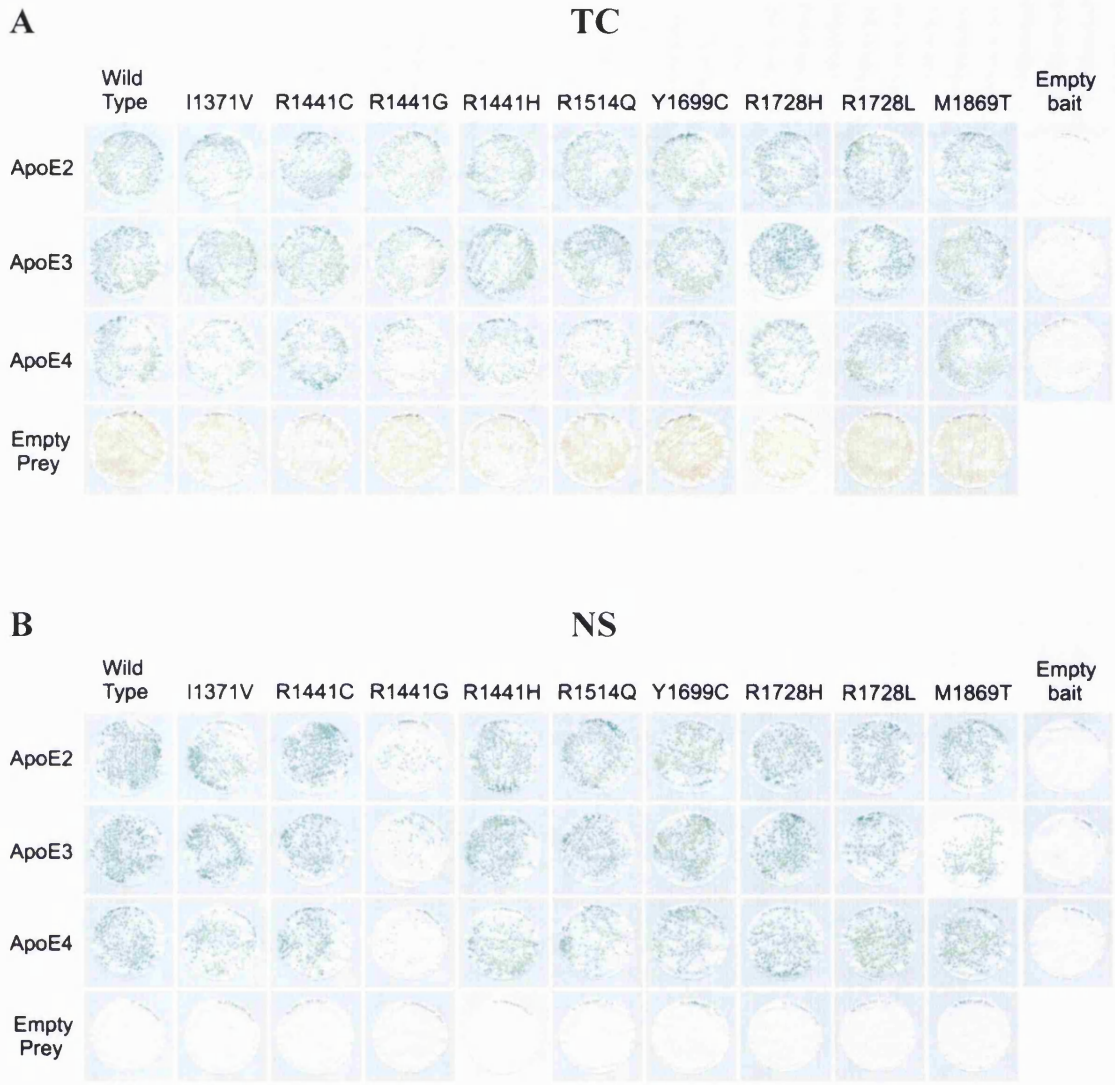

Figure 3.3: The pattern of the alteration in the interaction strength of mutant LRRK2 Roc-COR domain proteins with ApoE appears similar among the three ApoE variants. Interactions between all the full length ApoE constructs and the WT and mutant Roc-COR domain constructs expressed in yeast are indicated by the blue colonies on the TC filters (A) and the NS filters (B). All negative controls with the empty prey and bait vectors did not show an interaction. The pattern of alterations in the interaction strength between the Roc-COR mutants and ApoE appeared to be similar among the three ApoE variants. The R1441G mutation in the Roc-COR domain showed a clear decrease of the interaction strength with all the three ApoE variants.

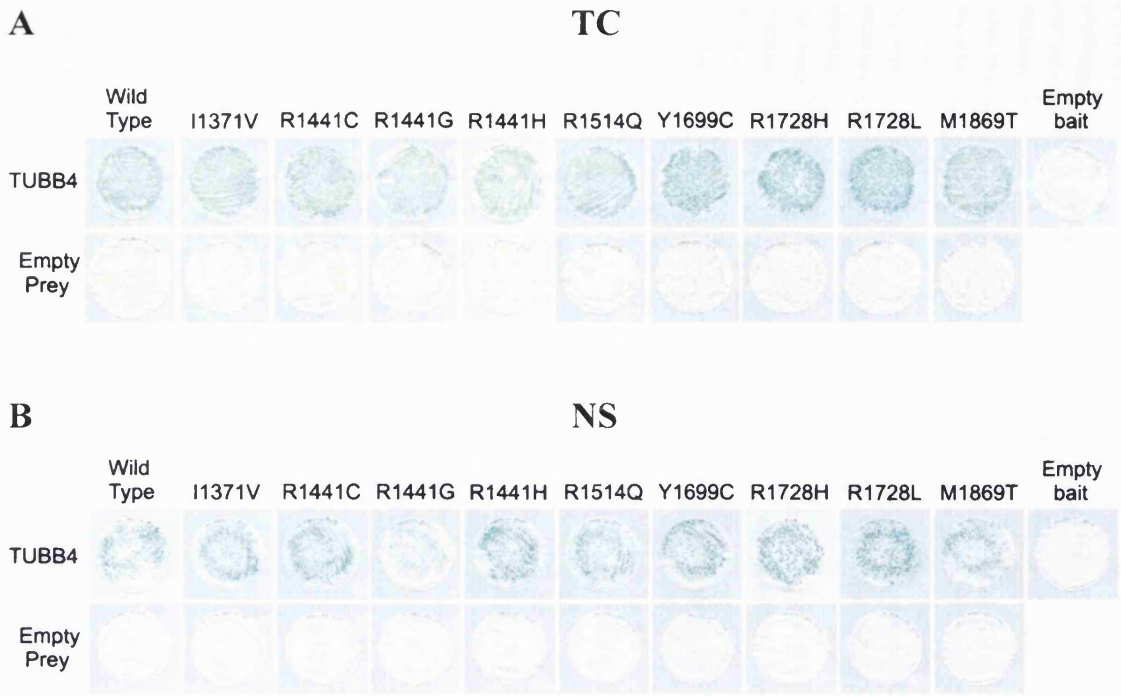

Figure 3.4: WT and mutated LRRK2 Roc-COR domain constructs expressed in yeast can interact with the C-terminus of the β-tubulin isoform TUBB4, and Roc-COR mutations appear to modify the strength of the interaction. Interactions between the C-terminus of TUBB4 and the WT and mutant Roc-COR domain proteins expressed in yeast are indicated by the blue colonies on the TC filters (A) and the NS filters (B). All negative controls with the empty prey and bait vectors did not show an interaction. The R1441G and R1441H mutations appeared to decrease the strength of the Roc-COR – TUBB4 interaction, whilst the R1728H and R1728L mutations appeared to strengthen this interaction.

3.2.5 The Expression of the Roc-COR Protein Variants in Yeast

From the above semi-quantitative YTH experiments, we can observe a clear decrease in the interaction strength between the R1441G – Roc-COR protein and the interactors, including RTN3, S100A10, ApoE and TUBB4. However, this observed decrease could be caused by the lowered expression level of this Roc-COR variant in yeast. In order to eliminate this possibility, I transformed yeast cells with WT Roc-COR, R1441G – Roc-COR and some selected Roc-COR variants. Proteins were extracted as shown in section 2.2.7. A western blot was performed and it is shown in figure 3.5. The WT and various mutant Roc-COR proteins appear to be expressed at a similar level to each other in

yeast cells, making it unlikely that the lowered expression of the R1441G Roc-COR mutant is the cause of the observed decreased interaction with that mutant. In conclusion, the observed decrease in the interaction level between R1441G – Roc-COR and the aforementioned interactors is unlikely to be due to the decreased protein expression in yeast cells.

Figure 3.5: The WT and various mutant Roc-COR proteins were expressed at similar levels in yeast. Constructs encoding the WT and mutant Roc-COR protein were over-expressed in L40 yeast cells and extracted as shown in section 2.2.7. The extracted proteins were run on an SDS-PAGE gel and a western blotting was performed. The upper panel shows the membrane probed with the anti-LexA antibody for the detection of the Roc-COR proteins cloned into the pDS vector. The lower panel shows the membrane probed with the anti-pan-tubulin antibody to show even loading of the proteins. The numbers on the left of the panels indicate the molecular weight in kDa.

3.3 Conclusions

In conclusion, the Roc-COR domain of LRRK2 was shown to have the ability to interact with RTN3, S100A10, ApoE and TUBB4 in yeast. All of these proteins were previously suggested to be important for neurodegeneration. For all of these interactors, differences between the interaction strength of WT and mutant Roc-COR domain were observed. The WT and various mutant Roc-COR proteins also appear to be expressed at a similar level to each other in yeast (figure 3.5), making it unlikely that the lowered expression of the R1441G Roc-COR mutant as the cause of the decreased interaction of

the interactors with that mutant. Table 3.1 provides a summary on the effect of the PD-associated mutations in the Roc-COR domain on the strength of these interactions. The PD-associated mutation R1441G is particularly interesting, as it caused a decrease in interaction strength with all of the interactors tested. Although more evidence is required, the modification of interaction strength caused by PD-associated mutations suggests that Roc-COR interactions with at least some of the above interactors may play a role in the mechanisms leading to neurodegeneration.

	RTN3	S100A10	ApoE2	ApoE3	ApoE4	TUBB4
I1371V	↓↓	↓	no change	no change	no change	no change
R1441C	no change	↑	no change	no change	no change	no change
R1441G	↓↓	↓↓↓	↓↓	↓↓	↓↓	↓↓
R1441H	↓↓	no change	no change	no change	no change	↓
R1514Q	↓	↑	no change	no change	no change	no change
Y1699C	↓↓	↓↓↓	no change	no change	no change	↑
R1728H	↑	↑↑	no change	no change	no change	↑↑
R1728L	no change	↑↑	no change	no change	no change	↑↑
M1869T	↓↓	↓↓	no change	no change	no change	↓

Table 3.1: An overview of the alterations in the interaction strength between the LRRK2 Roc-COR domain mutants and the interactors, compared to WT Roc-COR domain. No change means the mutation apparently does not alter the interaction strength. '↑' and '↓'means a slight increase or decrease in the interaction strength occurred respectively due to the mutation. Clearer alterations in the interaction strength are indicated by double or triple arrows.

3.4 Discussion

3.4.1 The Effect of Roc-COR Mutations on Protein Interactions

This study focuses efforts on the characterisation of protein-protein interactions of the LRRK2 Roc-COR domain. Very little is known about this unique tandem domain, which is a characteristic of ROCO proteins. As neither the Roc nor COR domain was ever found to occur in nature separately, these domains seem to function together (Bosgraaf and Van Haastert, 2003; Gotthardt *et al,* 2008) and should be investigated as

a whole. Protein interactors of the Roc-COR tandem domain might give insight into upstream activators or downstream targets of the GTPase domain or modulators of LRRK2 GTPase activity. This study examined the modulation of LRRK2 interactions with interactors previously found in an YTH screen. The first step in my project hence involved the investigation whether *PARK8* mutations in the Roc-COR domain could affect the interaction with the identified interactors implicated in neurodegeneration, RTN3, S100A10, ApoE and β-tubulin.

In the YTH assays, a decreased colour development in the colonies on the TC filters may correlate with a decrease in the number of colonies formed on the NS filters. However, it is important to note that the number of colonies on the NS filters may also be influenced by other factors including transformation efficiency, amount of DNA used for transformation and whether the expression of the proteins can contribute to cellular toxicity. The rate of colour development is a more reliable indication of interaction strength, and hence colour intensity of the colonies on the TC and NS filters would be a better indication on the strength of protein-protein interaction.

The data revealed that some pathogenic *PARK8* mutations, particularly R1441G, appeared to decrease the strength of the interactions between the Roc-COR domain and all the tested interactors. This consistency triggers a question: Since R1441G is known to clearly segregate with PD (Mata *et al*, 2005), could the pathogenesis of PD somehow relate to the decreased level of interaction between LRRK2 and protein interactors? It is difficult to draw a definite conclusion at this stage. However, since there is a significant difference in the size between the arginine in WT LRRK2 and the glycine introduced by this mutation, a conformational change that might influence the ability of the Roc-COR domain to interact with other proteins is likely. As the R1441 was suggested to be situated at the interface between the Roc-COR dimer (Deng *et al,* 2008), it might also affect the stability of the Roc-COR dimer. This speculation is further supported by the recent finding that the R1441C mutation altered the protein folding of the Roc domain (Li *et al,* 2009a). The positive charge of the arginine in position 1441 is likely to play a role in the dimer formation through electrostatic interactions. The nitrogen in the side chain of the arginine may further contribute to the stability of the dimer by being a hydrogen bond donor, thereby providing further interaction through hydrogen bonding. The R1441G mutation not only could destroy these stabilising interactions in the Roc-

COR dimer, but could also induce a considerable conformational change that could disrupt interactions with heterogenous protein interactors. However, whether PD pathogenesis triggered by *PARK8* mutations could be a direct result of decreased Roc-COR dimer stability and/or decreased interaction with interactors remains to be determined.

3.4.2 Roc-COR – Tubulin Interaction as the Candidate for Further Characterisation

The experiments in this chapter not only aimed to find an effect of *PARK8* mutations on Roc-COR interaction with the interactors identified in the previous library screen. One candidate should also be selected for further characterisation. I observed differences in the interaction strength among some Roc-COR mutants with all the tested interactors, some of which were mutants segregating with PD. Hence it seems that those interactions could play a role in the pathogenesis of PD. In the case of S100A10, both R1441G and Y1699C led to a decline in the strength of interaction with the Roc-COR domain. This observation implies a specific influence of the LRRK2 R1441G or Y1699C mutations on apoptotic pathways through the anti-apoptotic, calcium-binding protein S100A10. For RTN3, a number of the PD-associated mutations in the Roc-COR domain also appeared to decrease protein interaction. Both S100A10 and RTN3 are involved in cellular apoptosis, although their mechanism in apoptosis is not yet well defined (Hsu *et al,* 1997; Xiang *et al,* 2006; Zhu *et al,* 2007; Lee *et al,* 2009). To date, there is no evidence that the activity of either protein is regulated by phosphorylation. As mentioned, LRRK2 is a kinase, and the kinase activity is responsible for conferring toxicity to cells (Smith *et al,* 2006). Although it is unlikely that the activities of RTN3 and S100A10 are regulated by phosphorylation, the interaction between the LRRK2 Roc-COR GTPase domain and these two proteins may still be of interest for further investigation due to their relevance in apoptotic cell death, which is a hallmark of PD.

Previous library screen data in my lab revealed that ApoE3, an ApoE variant, can interact with the Roc-COR domain of LRRK2. An interesting fact about ApoE is that another ApoE variant – ApoE4 – is well-known for conferring an increased risk in the development of AD. It has a detrimental effect to the CNS, which is possibly linked to lowered glucose utilisation and metabolism in the brain (Reiman *et al,* 2004). On the

other hand, ApoE2 and ApoE3 were suggested to have neuroprotective effects (Strittmatter *et al*, 1994), and their effects on neurons appear to be strikingly different from that of ApoE4. Following this line of argument, if the PD pathogenesis of LRRK2 is via ApoE, it would be expected that ApoE2 and ApoE3 would have different interaction strength with LRRK2 compared to ApoE4, owing to their opposite effects on neurons. However, my data suggest that the Roc-COR domain of LRRK2 interacts with a similar strength among the ApoE variants. No obvious strengthening or weakening in their interaction was observed. A similar degree of decrease in interaction strength was observed for the interaction between the R1441G Roc-COR mutant and all ApoE variants. This suggests that mutations in LRRK2 are unlikely to exert their detrimental effects via ApoE. However, the relevance of ApoE variants on the viability of neurons may justify further investigations into the LRRK2 – ApoE interaction in the future.

Despite the potential importance of the interactions evaluated above, I decided to focus on the LRRK2 interaction with tubulin for reasons explained below. As an integral part of microtubules, tubulin plays a crucial role in the function and viability of neurons, as microtubule stability is essential for both. Several lines of evidence indicate that the phosphorylation events taking place at microtubules can affect the stability of microtubules. The phosphorylation of MAPs including MAP2 and tau was shown to promote the stabilisation of microtubules (Brugg and Matus, 1991; Cho and Johnson, 2004). It was also found that the phosphorylation of tubulin itself decreases microtubule stability due to the inability of MAP2 to bind to phosphorylated tubulin (Wandosell *et al,* 1986). Furthermore, LIM kinase, a kinase that was found to be normally associated with microtubules, could be activated by phosphorylation, which subsequently detached from microtubules. This event would be followed by microtubule destabilisation (Gorovoy *et al,* 2005). All these data implicate a connection between the phosphorylation state of microtubules and MAPs and microtubule stability. Since LRRK2 is a kinase, it is possible that LRRK2 could play a role in the phosphorylation events taking place at the microtubules. It would then be interesting to see if LRRK2 can interact with tubulin and microtubules. Multiple lines of evidence showed that mutant LRRK2 could induce increased phosphorylation of tau (Li *et al,* 2009b; Lin *et al,* 2010; Melrose *et al,* 2010). This event was also shown to impair dopaminergic neurotransmission in transgenic mice (Melrose *et al,* 2010). Furthermore, over-expression of mutant LRRK2 resulted in an accumulation of phospho-tau in spheroidal

inclusions in neuronal processes (MacLeod *et al,* 2006). These data indicate the ability of mutant LRRK2 to affect dopaminergic neurons possibly through an increased phosphorylation of tau and subsequent microtubule destabilisation. Microtubule destabilisation was also suggested to be involved in PD pathogenesis (section 3.1.4). Rotenone, a pesticide that can lead to microtubule depolymerisation (Marshall and Himes, 1978), was found to be toxic to dopaminergic neurons, and this toxicity is linked to the alteration in microtubule dynamics (Ren *et al,* 2005). Furthermore, Yang *et al* (2005) revealed that parkin can interact with tubulin, and this interaction may serve to stabilise microtubules by preventing tubulin depolymerisation. These observations indicated a possibly crucial role of the LRRK2 – tubulin interaction for microtubule stability with relevance in the pathogenesis of PD caused by *PARK8* mutations to me. For these reasons, I decided that the interaction of LRRK2 with β-tubulin is to be investigated in more depth in this project. In the next chapter, the LRRK2 – tubulin interaction will be explored further.

4. Further Characterisation of the LRRK2 – Tubulin Interaction

In the last chapter, I have established that the LRRK2 – tubulin interaction might be of particular interest for investigation, owing to the relevance of microtubule stability in neuronal integrity and functions. In this chapter, we are going to look into this particular interaction more closely. I will introduce the concept of neuronal transport via microtubules before looking into the data for the characterisation of the LRRK2 – β-tubulin interaction.

4.1 Microtubule Transport and Neuronal Function

In general, the microtubule cytoskeleton has two major functions, namely intracellular transport and cellular division. In neurons, microtubules originate from the microtubule organising centre (MTOC) (Sunkel *et al,* 1995), where γ-tubulin is complexed with various proteins to form the γ-tubulin ring complex (Oegema *et al,* 1999). This complex participates in the nucleation of microtubules. Subunits of α- and β-tubulin dimerise, and are added to the nucleated microtubules. Each α- and β-tubulin molecule is bound to a guanosine nucleotide GTP. Tubulin itself has GTPase activity (Carlier and Pantaloni, 1981), and it can hydrolyse the GTP to GDP after its assembly into the growing microtubule. In fact, microtubules have a tendency to display a characteristic dynamic instability in which the tubulin polymer extends and shrinks continuously (Mitchison and Kirschner, 1984). This instability is regulated by a group of proteins including MAPs (Drewes *et al,* 1998).

MAPs have a general function in keeping the microtubules stable, through direct binding to the tubulin subunits (Al-Bassam *et al,* 2002). Microtubule integrity is particularly important in neurons. The chief function of microtubules in neurons is cellular transport, especially the anterograde transport of vesicles containing neurotransmitters from the cell body to the distal end of the long axon, and retrograde transport of neurotrophic factors from the distal end of the axons and dendrites towards the cell body. The anterograde transport is executed by a group of molecules called kinesins (Hirokawa, 1993), while the retrograde transport is performed by dyneins (Schnapp and Reese, 1989). Both molecules possess two head domains which can bind ATP. Cycles of ATP binding and hydrolysis induce conformational changes, allowing

the molecule to 'walk' along the microtubule. One cycle of ATP hydrolysis enables the molecule to advance eight nanometres (Schnitzer and Block, 1997). The movement of these motor proteins along the microtubules, and the efficiency of the entire neuronal transport network, requires the microtubules to be stable and intact. As mentioned in section 3.1.4, microtubule destabilisation causes problems in neuronal transport and, especially in dopaminergic neurons, oxidative stress which damages the neurons.

It was established in the previous chapter that the Roc-COR domain displays an altered level of interaction with β-tubulin, one of the main components of microtubules, upon introduction of some PD-associated mutations. Since microtubules play an important role in neuronal function and viability, it is tempting to speculate that the LRRK2 – tubulin interaction may play a part in the pathomechanism leading to PD in *PARK8* mutation carriers. Could LRRK2 in some way affect the stability or integrity of neuronal microtubules that might reduce the viability of neurons? By looking into the LRRK2 – tubulin interaction, we may find some clues to this critical question. The work presented in this chapter hence aims to characterise this interaction. I will establish the specificity of the LRRK2 – β-tubulin interaction for certain isoforms, confirm the interaction in a mammalian system and investigate the domains/amino acid residues important for this interaction. In addition, I will investigate the influence of several disease-segregating *PARK8* mutations and SNPs in a quantitative assay to establish the significance of the observations made in the previous chapter using a semi-quantitative method.


TUBB MREIVHIQAGQCGNQIGAKFWEVISDEHGIDPTGTYHGDSDLQLDRISVYYNEATGGKYV
TUBB2A MREIVHIQAGQCGNQIGAKFWEVISDEHGIDPTGSYHGDSDLQLERINVYYNEAAGNKYV
TUBB2B MREIVHIQAGQCGNQIGAKFWEVISDEHGIDPTGSYHGDSDLQLERINVYYNEATGNKYV
TUBB2C MREIVHLQAGQCGNQIGAKFWEVISDEHGIDPTGTYHGDSDLQLERINVYYNEATGGKYV
TUBB3 MREIVHIQAGQCGNQIGAKFWEVISDEHGIDPSGNYVGDSDLQLERISVYYNEASSHKYV
TUBB4 MREIVHLQAGQCGNQIGAKFWEVISDEHGIDPTGTYHGDSDLQLERINVYYNEATGGNYV
TUBB PRAILVDLEPGTMDSVRSGPFGQIFRPDNFVFGQSGAGNNWAKGHYTEGAELVDSVLDVV
TUBB2A PRAILVDLEPGTMDSVRSGPFGQIFRPDNFVFGQSGAGNNWAKGHYTEGAELVDSVLDVV
TUBB2B PRAILVDLEPGTMDSVRSGPFGQIFRPDNFVFGQSGANNWAKGHYTEGAELVDSVLDVV
TUBB2C PRAVLVDLEPGTMDSVRSGPFGQIFRPDNFVFGQSGAGNNWAKGHYTEGAELVDSVLDVV
TUBB3 PRAILVDLEPGTMDSVRSGAFGHLFRPDNFIFGQSGAGNNWAKGHYTEGAELVDSVLDVV
TUBB4 PRAVLVDLEPGTMDSVRSGPFGQIFRPDNFVFGQSGAGNNWAKGHYTEGAELVDAVLDVV
TUBB RKEAESCDCLQGFQLTHSLGGGTGSGMGTLLISKIREEYPDRIMNTFSVVPSPKVSDTVV
TUBB2A RKESESCDCLQGFQLTHSLGGGTGSGMGTLLISKIREYPDRIMNTFSVMPSPKVSDTVV
TUBB2B RKESESCDCLQGFQLTHSLGGGTGSGMGTLLISKIREEYPDRIMNTFSVMPSPKVSDTVV
TUBB2C RKEAESCDCLQGFQLTHSLGGGTGSGMGTLLISKIREEYPDRIMNTFSVVPSPKVSDTVV
TUBB3 RKECENCDCLQGFQLTHSLGGGTGSGMGTLLISKVREEYPDRIMNTFSVVPSPKVSDTW
TUBB4 RKEAESCDCLQGFQLTHSLGGGTGSGMGTLLISKIREEFPDRIMNTFSVVPSPKVSDTVV
TUBB EPYNATLSVHQLVENTDETYCIDNEALYDICFRTLKLTTPTYGDLNHLVSATMSGVTTCL
TUBB2A EPYNATLSVHQLVENTDETYSIDNEALYDICFRTLKLTTPTYGDLNHLVSATMSGVTTCL
TUBB2B EPYNATLSVHQLVENTDETYCIDNEALYDICFRTLKLTTPTYGDLNHLVSATMSGVTTCL
TUBB2C EPYNATLSVHQLVENTDETYCIDNEALYDICFRTLKLTTPTYGDLNHLVSATMSGVTTCL
TUBB3 EPYNATLSIHQLVENTDETYCIDNEAYDICFRTLKLATPTYGDLNHLVSATMSGVTTSL
TUBB4 EPYNATLSVHQLVENTDETYCIDNEALYDICFRTLKLTTPTYGDLNHLVSATMSGVTTCL
TUBB RFPGQLNADLRKLAVNMVPFPRLHFFMPGFAPLTSRGSQQYRALTVHETQQVFDAKNMM
TUBB2A RFPGQLNADLRKLAVNMVPFPRLHFFMPGFAPLTSRGSQQYRALTVPELTQQMFDSKNMM
TUBB2B RFPGQLNADLRKLAVNMVPFPRLHFFMPGFAPLTSRGSQQYRALTVPELTQQMFDSKNMM
TUBB2C RFPGQLNADLRKLAVNMVPFPRLHFFMPGFAPLTSRGSQQYRALTVPELTQQMFDAKNMM
TUBB3 RFPGQLNADLRKLAVNMVPFPRLHFFMPGFAPLTARGSQQYRALTVPELTQQMFDAKNMM
TUBB4 RFPGQLNADLRKLAVNMVPFPRLHFFMPGFAPLTSRGSQQYRALTVPELTQQMFDAKNMM
TUBB AACDPRHGRYLTVAAVFRGRMSMKEVDEQMLNVQNKNSSYFVEWIPNNVKTAVCDIPPRG
TUBB2A AACDPRHGRYLTVAAIFRGRMSMKEVDEQMLNVQNKNSSYFVEWIPNNVKTAVCDIPPRG
TUBB2B AACDPRHGRYLTVAAIFRGRMSMKEVDEQMLNVQNKNSSYFVEWIPNNVKTAVCDIPPRG
TUBB2C AACDPRHGRYLTVAAVFRGRMSMKEVDEQMLNVQNKSSYFVEWIPNNVKTAVCDIPPRG
TUBB3 AACDPRHGRYLTVATVFRGRMSMKEVDEQMLAIQSKNSSYFVEWIPNNVKVAVCDIPPRG
TUBB4 AACDPRHGRYLTVAAVFRGRMSMKEVDEQMLSVQSKNSSYFVEWIPNNVKTAVCDIPPRG
TUBB LKMAVTFIGNSTAIQELFKRISEQFTAMFRRKAFLHWYTGEGMDEMEFTEAESNMNDLVS
TUBB2A LKMSATFIGNSTAIQELFKRISEQFTAMFRRKAFLHWYTGEGMDEMEFTEAESNMNDLVS
TUBB2B LKMSATFIGNSTAIQELFKRISEQFTAMFRRKAFLHWYTGEGMDEMEFTEAESNMNDLVS
TUBB2C LKMSATFIGNSTAIQELFKRISEQFTAMFRRKAFLHWYTGEGMDEMEFTEAESNMNDLVS
TUBB3 LKMSSTFIGNSTAIQELFKRISEQFTAMFRRKAFLHWYTGEGMDEMEFTEAESNMNDLVS
TUBB4 LKMAATFIGNSTAIQELFKRISEQFTAMFRRKAFLHWYTGEGMDEMEFTEAESNMNDLVS
TUBB EYQQYQDATAEEEEDFGEEAEEEA-----
TUBB2A EYQQYQDATADEQGEFEEEEGEDEA----
TUBB2B EYQQYQDATADEQGEFEEEEGEDEA----
TUBB2C EYQQYQDATAEEEGEFEEEAEEEVA----
TUBB3 EYQQYQDATAEEGEMYEDDEEESEAQGPK
TUBB4 EYQQYQDATAEEGEFEEEAEEEVA-----

Figure 4.1: Amino acid sequence alignment of the neuronally expressed β-tubulin isoforms. The asterisks (*) indicate the same amino acid is present in one position of all the isoforms. Note that the amino acid sequence is very well-conserved with the longest stretch of sequence variation at the C-terminal end of the β-tubulins. The yellow-highlighted residues (residue 364) indicate the only site where the amino acid sequence is different between TUBB/TUBB4 and all other isoforms.

4.2 Various β-tubulin Isoforms

Eight different isoforms of β-tubulin have been identified in the past two decades. They are *TUBB*, *TUBB1*, *TUBB2A*, *TUBB2B*, *TUBB2C*, *TUBB3*, *TUBB4* and *TUBB6*. All of these, except *TUBB1*, are expressed in neurons and other cell types (Ludueña, 1998). *TUBB1* expression was found to be mainly restricted to platelets and megakaryocytes (Lecine *et al,* 2000). *TUBB6* was also very recently identified to be ubiquitously expressed in humans (Leandro-García *et al,* 2010). Intriguingly, the neuronally expressed β-tubulin isoforms show a high sequence homology with each other, although a slightly higher degree of sequence variation exists at the C-terminus (figure 4.1). It is important to note that the C-termini of the tubulins contain the region responsible for interaction with proteins like MAPs (Littauer *et* al, 1986; Nogales *et al,* 1998). Hence, the C-termini of β-tubulins are the regions with a role in the regulation of microtubule stability. Owing to the sequence variation in the β-tubulin C-terminal region and the role in microtubule stability, this project focused on the interaction between the Roc-COR domain of LRRK2 and the C-termini of these neuronally expressed β-tubulins.

4.3 Preparation of Mammalian and Yeast β-Tubulin Expression Constructs

The primer design for the PCR amplification of all the neuronally expressed β-tubulin isoforms from cDNA (Clontech) is shown in table 2.1. The cDNA was amplified as shown in section 2.1. The gel-purified PCR products were cloned into a pACT2 vector.

The pACT2 – tubulin constructs were then used as preys in YTH experiments. Furthermore, mammalian N-terminally FLAG-tagged tubulin was expressed from the pRK5 vector and was used for co-IP experiments.

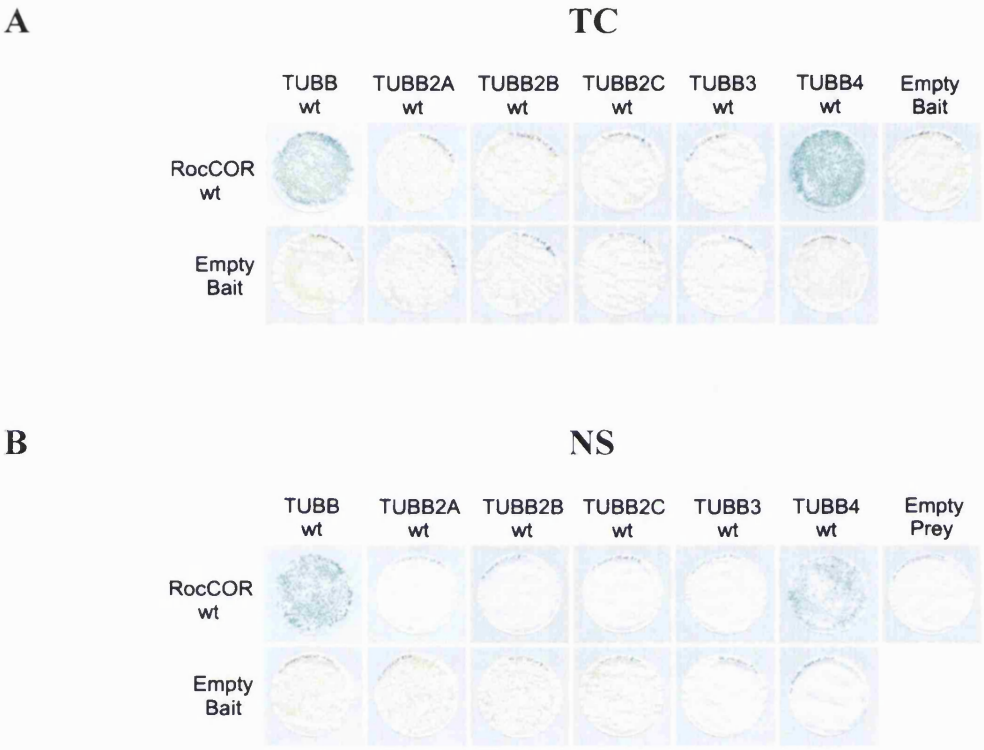

Figure 4.2: A WT LRRK2 Roc-COR domain construct expressed in yeast specifically interacts only with the TUBB and TUBB4 isoforms. The interaction between the WT Roc-COR domain construct and the C-terminus of the TUBB and TUBB4 constructs are indicated by the blue colonies on the TC filters (A) and the NS filters (B). The failure in the interaction between the C-terminus of the other β-tubulin isoforms and the Roc-COR domain construct expressed in yeast are indicated by the white colonies. All negative controls with the empty prey and bait vectors did not show an interaction.

4.4 Roc-COR Interaction with β-Tubulin Isoforms

4.4.1 The Specificity of the Roc-COR – Tubulin Interaction

The first step in the investigation of the Roc-COR – tubulin interaction was to establish if the Roc-COR domain can interact with all the neuronal β-tubulins. A YTH experiment was performed using the WT Roc-COR domain cloned into the pDS vector as the bait and the various β-tubulin isoforms cloned into the pACT2 vector as the preys. As figure 4.2 shows, only yeast colonies expressing TUBB or TUBB4 together with the Roc-COR domain turned blue after the LacZ freeze-fracture assay on both the TC and NS filters, indicating that TUBB and TUBB4 are the only two neuronally-expressed β-tubulin isoforms that can interact with the Roc-COR domain of LRRK2. For the other isoforms, no yeast colonies were present on the NS filters, although white colonies were present on the TC filters. This indicates that both the Roc-COR domain and tubulin constructs were transformed successfully into the yeast cells, and yet due to the lack of interaction between the Roc-COR domain and tubulin proteins and the subsequent lack of reporter gene transcription, no colonies could be formed on NS agar plates. Hence, the yeast data suggest a specific interaction between the LRRK2 Roc-COR domain and some β-tubulin isoforms, TUBB and TUBB4.

4.4.2 Expression of β-Tubulin in Yeast

In the YTH experiment investigating the specificity of the Roc-COR – tubulin interaction, four tubulin isoforms, namely TUBB2A, TUBB2B, TUBB2C and TUBB3, showed negative results. This outcome could be interpreted in two ways. Firstly, there is a lack of interaction between the Roc-COR domain and these tubulin isoforms. Secondly, there is a possibility that the yeast failed to express the tubulin. In order to eliminate the latter possibility, I transformed yeast with all of the pACT2 β-tubulin constructs, and carried out a yeast protein extraction procedure described in section 2.2.7. The yeast lysates were run on an SDS-PAGE gel and a western blot was carried out. The presence of expression of these prey proteins in yeast was detected by the anti-HA antibody. The blot is shown in figure 4.3. All of the β-tubulin isoforms, including those that showed no interaction with LRRK2 in the previous YTH experiment (section 4.4.1), were expressed in yeast. Thus, this confirms that the lack of interaction was not due to the lack of tubulin expression in yeast.

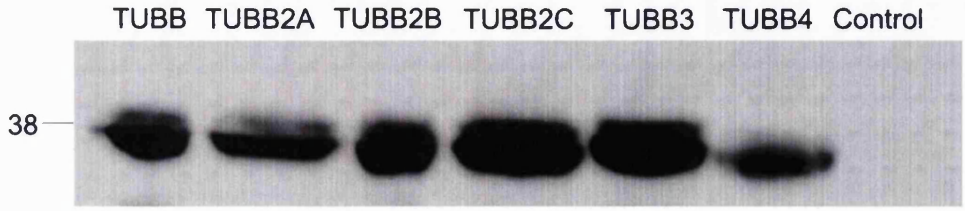

Figure 4.3: All neuronally expressed β-tubulin isoforms are expressed in yeast cells. The expression of all neuronally expressed β-tubulin isoforms in yeast cells is shown by the presence of a protein band at about 38kDa on the western blot after the cell lysates were obtained from yeast transformed with constructs expressing each tubulin isoform. The number on the left shows the molecular weight in kDa.

4.4.3 The Roc Domain is Sufficient for the Roc-COR Domain Interaction with TUBB and TUBB4

After establishing that the Roc-COR domain of LRRK2 can interact with tubulin, the next question was which part of the domain is responsible for this interaction. An YTH experiment was carried out, using Roc-COR tandem domain, Roc domain and COR domain cDNA cloned into the pDS bait vector. These constructs were co-transformed with the pACT2-TUBB and pACT2-TUBB4 prey constructs. The other isoforms were omitted from this experiment as it was established that they are not interactors of the Roc-COR domain. The results shown in figure 4.4 indicate that the Roc domain alone is sufficient for LRRK2 to interact with both TUBB and TUBB4. The isolated COR domain failed to interact with the two tubulin isoforms. A closer inspection of the colour intensity of the blue colonies on the TC filters (figure 4.4A) revealed a stronger interaction between the Roc domain and TUBB/TUBB4 than the Roc-COR tandem domain and TUBB/TUBB4, as shown by the more intense blue colour developed in the colonies expressing the Roc domain and TUBB/TUBB4. This observation might indicate that the COR domain could play a regulatory inhibitory role in the Roc-COR – tubulin interaction.

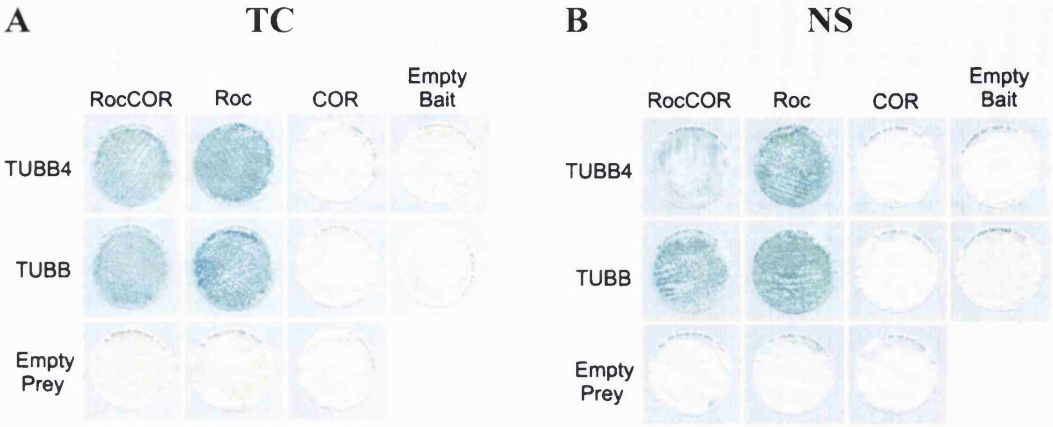

Figure 4.4: The LRRK2 Roc domain is sufficient for the LRRK2 interaction with TUBB and TUBB4. The interaction between the WT Roc and Roc-COR domain construct and the C-terminus of the TUBB and TUBB4 constructs are indicated by the blue colonies on the TC filters (A) and the NS filters (B). The failure in the interaction between the WT COR domain construct and the tubulin constructs are indicated by the white colonies. All negative controls with the empty prey and bait vectors did not show an interaction.

4.4.4 LRRK2 – Tubulin Interaction in a Mammalian Cell Model

After the specific interaction between the Roc-COR domain and TUBB/TUBB4 was established in yeast, I carried out a co-IP experiment to test whether this interaction also occurs in mammalian cells. HEK293 cells were transfected with myc-tagged Roc-COR domain or myc-tagged full length LRRK2, together with TUBB4 with a FLAG tag at the N-terminus. All of these constructs were cloned into the pRK5 vector. The cells were harvested 24 hours post-transfection. The cells were lysed and the lysates obtained were subjected to co-IP with anti-FLAG beads as described in section 2.3.10.1. The eluted sample after co-IP was run in an SDS-PAGE gel together with the cell lysates. After western blotting, the membrane was probed with anti-myc or anti-FLAG antibodies to detect the presence of the myc-tagged and FLAG-tagged fusion proteins respectively. The membrane was then re-incubated with anti-β-actin antibody to show even loading of the samples into the gel.

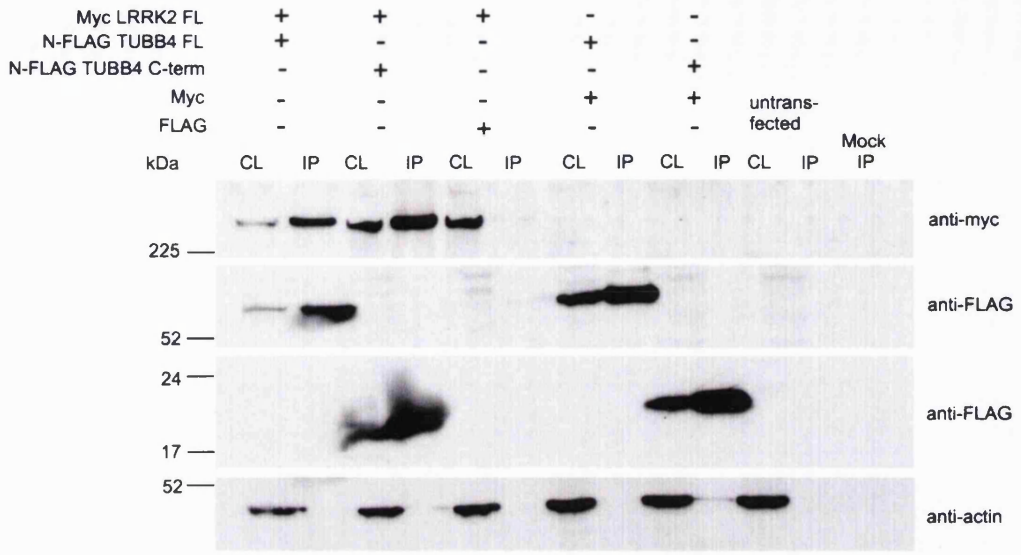

Figure 4.5: The myc-tagged full length LRRK2 protein and FLAG-tagged TUBB4 can interact with each other in HEK293 cells. Both fusion proteins were co-immunoprecipitated and analysed by a western blot. The numbers on the left of the panels show the molecular weight in kDa. The uppermost 'anti-myc' panel shows the membrane probed with rabbit anti-myc antibody for the detection of LRRK2. The upper 'anti-FLAG' panel shows the membrane probed with rabbit anti-FLAG antibody for the detection of the full length FLAG-tagged TUBB4 protein which appears at around 52 kDa. The lower 'anti-FLAG' panel shows the detection of the C-terminus of the FLAG-tagged TUBB4 protein which appears at about 15 kDa. The 'anti-actin' panel shows the membrane probed with mouse anti-actin antibody to show even loading of the lysates. (CL = cell lysate, IP = immunoprecipitation)

The results shown in figure 4.5 – 4.10 indicate that full length myc-LRRK2 and myc-Roc-COR were both pulled down by full length FLAG-tagged TUBB4 and the TUBB4 C-terminus attached to the anti-FLAG column. A negative control, in which the cells were transfected with myc-tagged Roc-COR/LRRK2 and FLAG alone showed no interaction, indicating that the observed LRRK2 – tubulin interactions are not due to an interaction between the myc-tagged protein and the FLAG tag. The results hence indicate that LRRK2 has the ability to interact with TUBB4, and confirms that the LRRK2 Roc-COR domain and the tubulin C-terminus is sufficient for this interaction as previously observed in yeast.

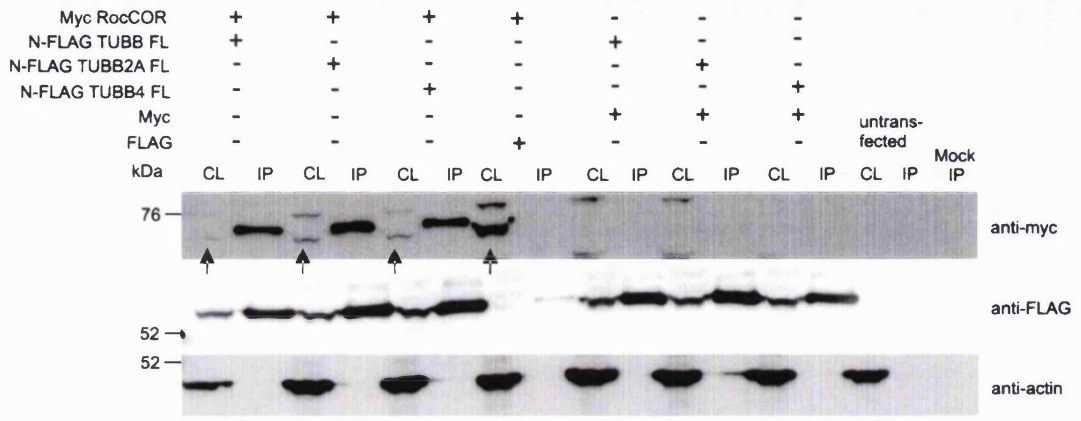

Figure 4.6: The myc-tagged Roc-COR protein can interact with the full length FLAG-tagged TUBB, TUBB2A and TUBB4 in HEK293 cells. The myc-tagged and FLAG-tagged fusion proteins were co-immunoprecipitated and analysed by a western blot. The numbers on the left of the panels show the molecular weight in kDa. The uppermost 'anti-myc' panel shows the membrane probed with rabbit anti-myc antibody for the detection of the Roc-COR protein. The 'anti-FLAG' panel in the middle shows the membrane probed with rabbit anti-FLAG antibody for the detection of the full length FLAG-tagged β-tubulin protein. The 'anti-actin' panel shows the membrane probed with mouse anti-actin antibody to show even loading of the lysates. The arrows in the 'anti-myc' panel indicate the band for the Roc-COR protein. (CL = cell lysate, IP = immunoprecipitation)

With the confirmation that both the Roc-COR domain and full length LRRK2 can interact with TUBB4 in HEK293 cells, I sought to determine whether the specific interaction could also be confirmed in the mammalian cellular system. The cells were transfected with either myc-Roc-COR or myc LRRK2 together with the full length FLAG-TUBB4, TUBB, or TUBB2A constructs. The negative controls were included and the cell lysates were processed and western blotting was performed as described above. The results confirmed an interaction between full length TUBB and TUBB4 and full length LRRK2 and the Roc-COR domain as expected, but full length FLAG-tagged TUBB2A was also able to immunoprecipitate LRRK2 (figure 4.6 and 4.7).

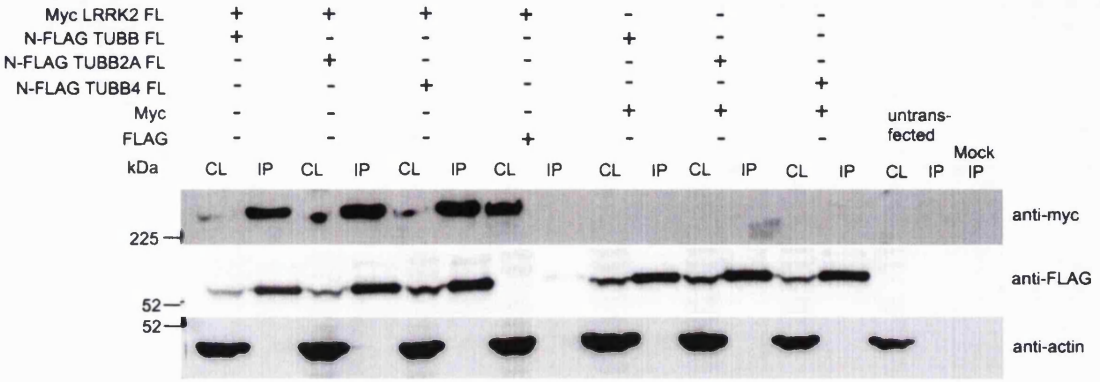

Figure 4.7: The myc-tagged full length LRRK2 protein immunoprecipitates full length FLAG-tagged TUBB, TUBB2A and TUBB4 in HEK293 cells. The myc-tagged and FLAG-tagged fusion proteins were co-immunoprecipitated and analysed by a western blot. The numbers on the left of the panels show the molecular weight in kDa. The uppermost 'anti-myc' panel shows the membrane probed with rabbit anti-myc antibody for the detection of LRRK2. The 'anti-FLAG' panel in the middle shows the membrane probed with rabbit anti-FLAG antibody for the detection of the full length FLAG-tagged β-tubulin protein. The 'anti-actin' panel shows the membrane probed with mouse anti-actin antibody to show even loading of the lysates. (CL = cell lysate, IP = immunoprecipitation)

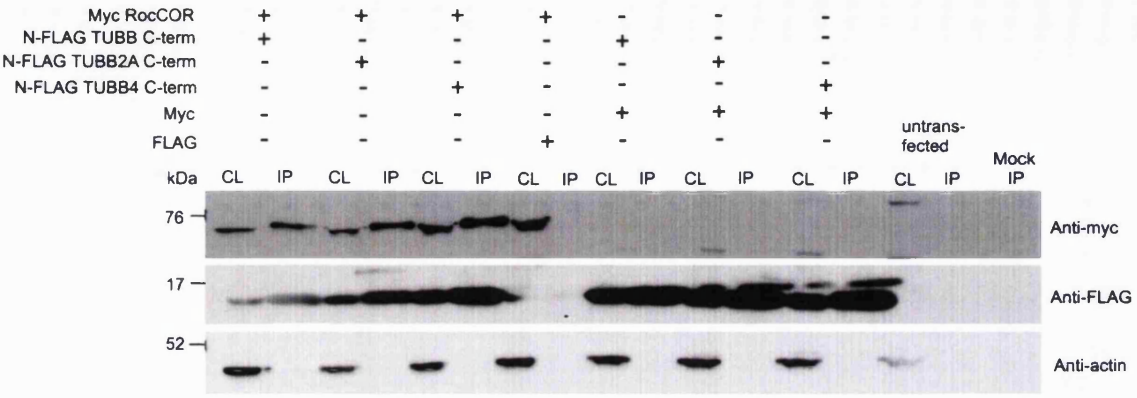

Figure 4.8: The myc-tagged Roc-COR protein immunoprecipitates the C-terminus of FLAG-tagged TUBB, TUBB2A and TUBB4 in HEK293 cells. The myc-tagged and FLAG-tagged fusion proteins were co-immunoprecipitated and analysed by a western blot. The numbers on the left of the panels show the molecular weight in kDa. The uppermost 'anti-myc' panel shows the membrane probed with rabbit anti-myc antibody for the detection of the Roc-COR protein. The 'anti-FLAG' panel in the middle shows the membrane probed with rabbit anti-FLAG antibody for the detection of the C-terminus of the FLAG-tagged β-tubulin protein. The 'anti-actin' panel shows the membrane probed with mouse anti-actin antibody to show even loading of the lysates. (CL = cell lysate, IP = immunoprecipitation)

As it is possible that the full length tubulin construct may have integrated into microtubules in the HEK293 cells, which would affect the outcome of co-IP experiment, the experiment was repeated using the C-termini of the tubulin constructs instead. The C-terminus of TUBB2A still retained the ability to immunoprecipitate both the Roc-COR domain and full length LRRK2 (figure 4.8 and 4.9). In light of this, a trial experiment was performed using a slightly altered protocol to test for the interaction between TUBB4/TUBB2A and LRRK2. Thirty minutes before harvesting the transfected cells, they were placed at 4°C in order to depolymerise the microtubules in the cells. The cells were lysed as usual, but the anti-FLAG beads were washed with a more stringent buffer containing a higher salt concentration (500 mM NaCl) and a higher NP-40 concentration (2% (v/v) NP-40) after the incubation with cell lysates.

However, as shown in figure 4.10, the C-terminus of TUBB2A could still immunoprecipitate LRRK2.

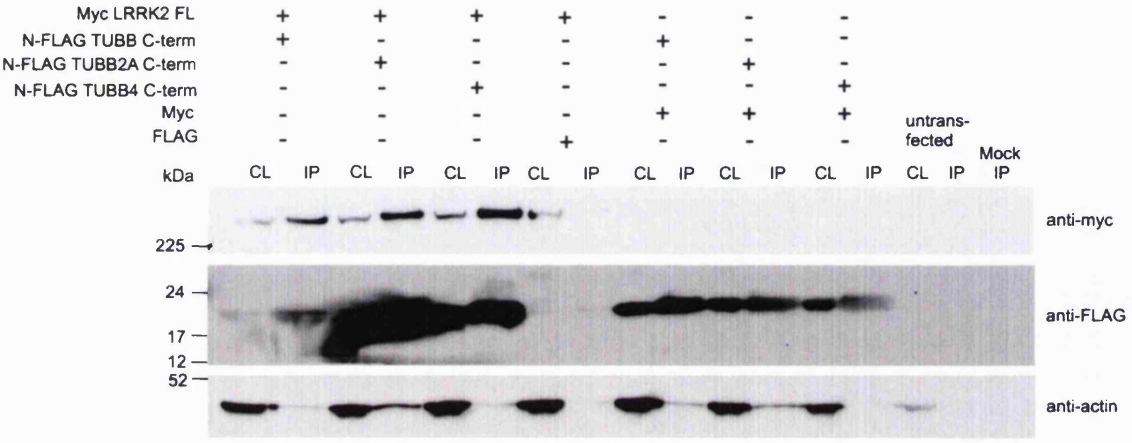

Figure 4.9: The myc-tagged full length LRRK2 protein immunoprecipitates the C-terminus of FLAG-tagged TUBB, TUBB2A and TUBB4 in HEK293 cells. The myc-tagged and FLAG-tagged fusion proteins were co-immunoprecipitated and analysed by a western blot. The numbers on the left of the panels show the molecular weight in kDa. The uppermost 'anti-myc' panel shows the membrane probed with rabbit anti-myc antibody for the detection of LRRK2. The 'anti-FLAG' panel in the middle shows the membrane probed with rabbit anti-FLAG antibody for the detection of the C-terminus of the FLAG-tagged β-tubulin protein. The 'anti-actin' panel shows the membrane probed with mouse anti-actin antibody to show even loading of the lysates. (CL = cell lysate, IP = immunoprecipitation)

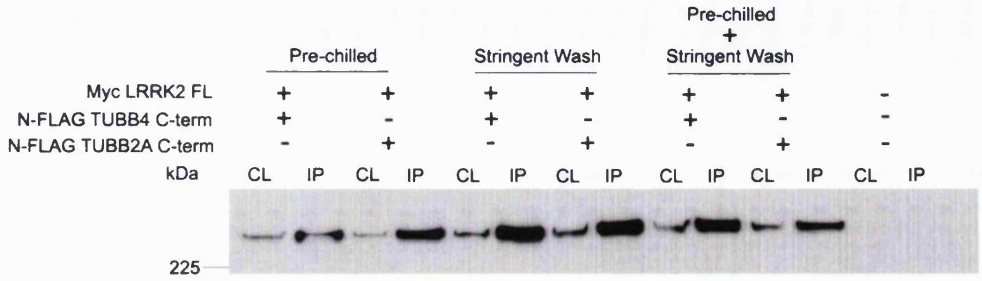

Figure 4.10: The myc-tagged full length LRRK2 protein can still immunoprecipitate the C-terminus of FLAG-tagged TUBB4 and TUBB2A in HEK293 cells after co-IP optimisation. The myc-tagged and FLAG-tagged fusion proteins were co-immunoprecipitated and analysed by a western blot. The number on the left of the panel shows the molecular weight in kDa. The panel shows the membrane probed with rabbit anti-myc antibody for the detection of LRRK2. Pre-chilled means the cells were pre-chilled at 4°C for 30 minutes before cell lysis and protein extraction. Stringent wash means the co-immunoprecipitated proteins were washed with a more stringent wash buffer as detailed in the result section 4.4.4. (CL = cell lysate, IP = immunoprecipitation)

4.5 Further Investigation of the Effect of *PARK8* Mutations on the Roc-COR – Tubulin Interaction

4.5.1 Roc-COR – TUBB Interaction

In the previous chapter, I observed that some *PARK8* mutations can alter the interaction strength between TUBB4 and the Roc-COR domain. Since it was discovered that the Roc-COR domain can also interact with TUBB, I decided to test whether some Roc-COR mutants can also modify the interaction strength between the Roc-COR domain and TUBB using YTH assays. As shown by the colonies on the TC filters in figure 4.11A, all of the Roc-COR mutants were able to interact with TUBB. However, it seemed that yeast colonies expressing the R1441G and R1441H Roc-COR mutants developed a slightly less intense blue colour after the LacZ freeze-fracture assay, while those expressing the R1728H and R1728L Roc-COR mutants developed a more intense

colour. This indicated that the R1441G and R1441H Roc-COR mutants exhibited a weaker interaction with TUBB than the WT Roc-COR domain, while the R1728H and R1728L mutants exhibited a stronger interaction with TUBB. The colour of the colonies on the NS filters of all the Roc-COR variants were of similar intensity (figure 4.11B). This is likely to be due to the saturation of the colour development, as the colonies on the NS filters tend to develop colour faster than those on the TC filters. Hence, it seemed that the Roc-COR – TUBB interaction is also influenced by some Roc-COR mutations.

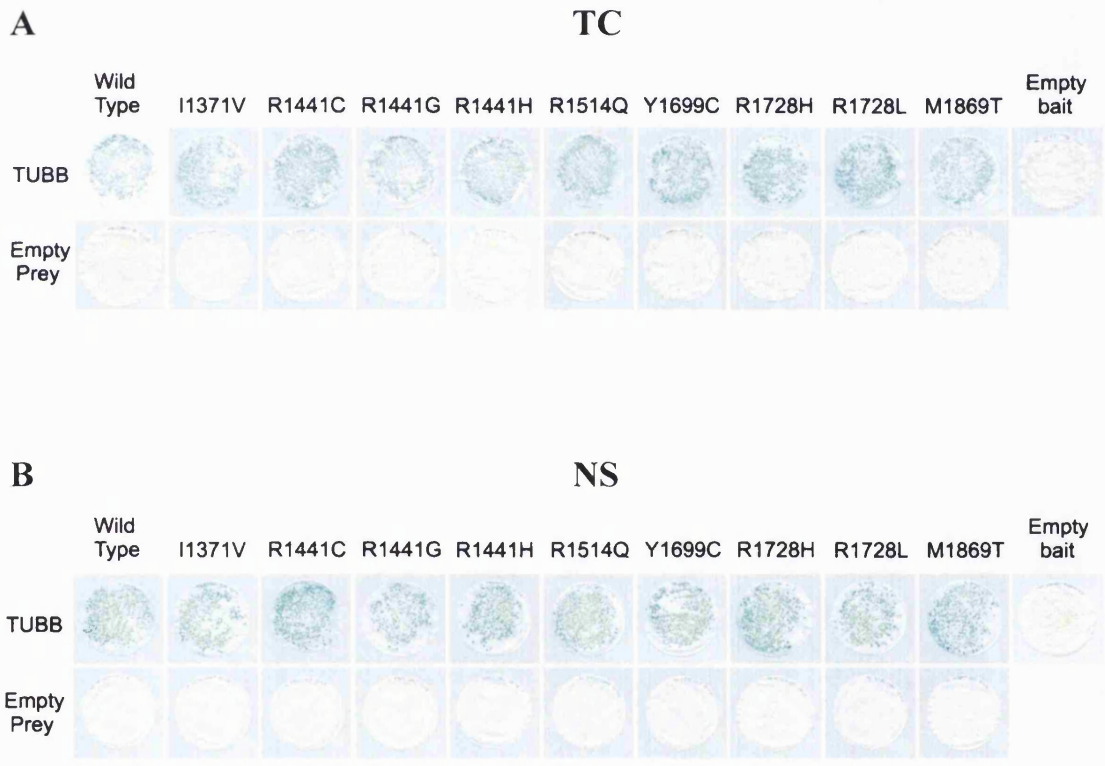

Figure 4.11: WT and mutated LRRK2 Roc-COR domain constructs expressed in yeast can interact with the C-terminus of the β-tubulin isoform TUBB. Interactions between the C-terminus of TUBB and the WT and mutant Roc-COR domain expressed in yeast are indicated by the blue colonies on the TC filters (A) and the NS filters (B). All negative controls with the empty prey and bait vectors did not show an interaction.

4.5.2 Quantification of the Influence of *PARK8* Mutations on the Interaction between the Roc-COR Domain and Tubulin

The main purpose of the YTH assay is to test whether two proteins can interact with each other, although we can assess roughly the strength of interaction by observing the intensity of the colour development in the yeast colonies over a fixed period of time. However, the assessment of interaction strength by this technique is at best semi-quantitative. In light of this, a more reliable and sensitive method known as the quantitative YTH (Q-YTH) assay was employed to assess the effect of *PARK8* mutations on the Roc-COR – tubulin interaction. The experiment was performed as described in section 2.2.6, and the data were analysed using the unpaired, two-tailed Students' T test.

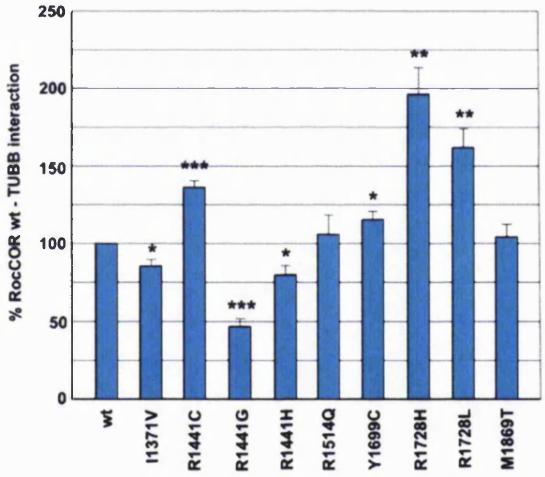

Figure 4.12: Some PD-associated mutations in the LRRK2 Roc-COR domain affect the strength of Roc-COR interaction with TUBB. The relative strength of interaction for each Roc-COR variant and TUBB is expressed as the percentage of interaction level compared to that between WT Roc-COR and TUBB. The I1371V, R1441G and R1441H Roc-COR mutant showed a significantly weaker interaction with TUBB than the WT Roc-COR does, while the R1441C, Y1699C, R1728H and R1728L mutants exhibited a stronger interaction with TUBB. Statistical significance was determined using the unpaired, two-tailed Students' T test. (* $P < 0.05$, ** $P < 0.01$, *** $P < 0.001$, $n = 5$)

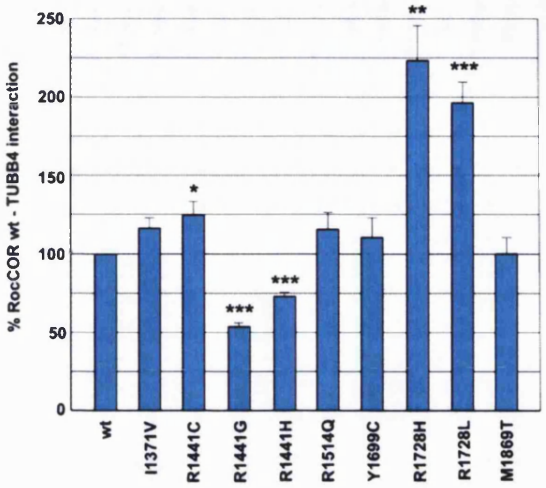

Figure 4.13: Some PD-associated mutations in the LRRK2 Roc-COR domain affect the strength of Roc-COR interaction with TUBB4. The relative strength of interaction for each Roc-COR variant and TUBB4 is expressed as the percentage of interaction level compared to that between WT Roc-COR and TUBB4. The R1441G and R1441H Roc-COR mutants showed a significantly weaker interaction with TUBB4 than the WT Roc-COR did. However, the R1441C, R1728H and R1728L mutants exhibited a significantly stronger interaction with TUBB4. Statistical significance was determined using the unpaired, two-tailed Students' T test. (* $P < 0.05$, ** $P < 0.01$, *** $P < 0.001$, $n = 5$)

The results shown in figure 4.12 and 4.13 revealed that some mutations in the Roc-COR domain could lead to a significant alteration in the interaction strength between the Roc-COR domain and both TUBB and TUBB4. The pattern of the changes among the Roc-COR mutants was similar for TUBB and TUBB4. For example, the R1441C mutation led to a significant increase in the interaction strength between the LRRK2 Roc-COR domain and TUBB and TUBB4. The R1441G mutant, however, resulted in a significant decrease in the interaction strength with TUBB and TUBB4 in comparison to WT Roc-COR domain, confirming the observations made in the semi-quantitative YTH assay. When compared to WT Roc-COR domain, the R1441G mutation conferred a decrease of about 50% in the Roc-COR interaction strength with both tubulin isoforms. Similarly, the R1441H mutation decreased the level of interaction. Mutations at R1728 conferred an increased interaction strength between the LRRK2 Roc-COR domain and

tubulin, compared to WT. R1728H even caused a 2-fold increase in the interaction strength. In conclusion, the YTH and Q-YTH assays confirmed that some Roc-COR mutations do have the ability to modify the strength of interaction between the Roc-COR domain of LRRK2 and both TUBB and TUBB4. As some of these mutations clearly segregate with PD (R1441C, R1441G and R1441H), this raises the question whether this interaction might be playing a role in the pathway leading to PD.

4.6 Residue 364 in β-Tubulin as the Determinant of the Roc-COR - Tubulin Interaction

After examining on the interaction between the Roc-COR domain and TUBB/ TUBB4, I then tried to explain why the Roc-COR domain can only interact with two β-tubulin isoforms but not others. At the beginning of this chapter, an alignment of the amino acid sequences of the tested tubulin isoforms is shown (figure 4.1). We can see that there is only one position in the amino acid sequence that is different between TUBB/TUBB4 and the other isoforms. That position is residue 364 (highlighted in yellow in figure 4.1), an alanine in TUBB and TUBB4 but a serine in TUBB2A, TUBB2B, TUBB2C and TUBB3. This immediately triggers a question. Could the difference in this residue at this position be important for the observed specific interaction between LRRK2 and β-tubulin isoforms as shown in figure 4.2? The difference between serine and alanine is an extra hydroxyl group attached to the side chain. Serine is one of the residues that can be phosphorylated. Proteins expressed in yeast can be phosphorylated by yeast kinases too. Hence it is possible that the specificity of the Roc-COR – tubulin interaction is due to phosphorylation at S364 in the β-tubulin molecule.

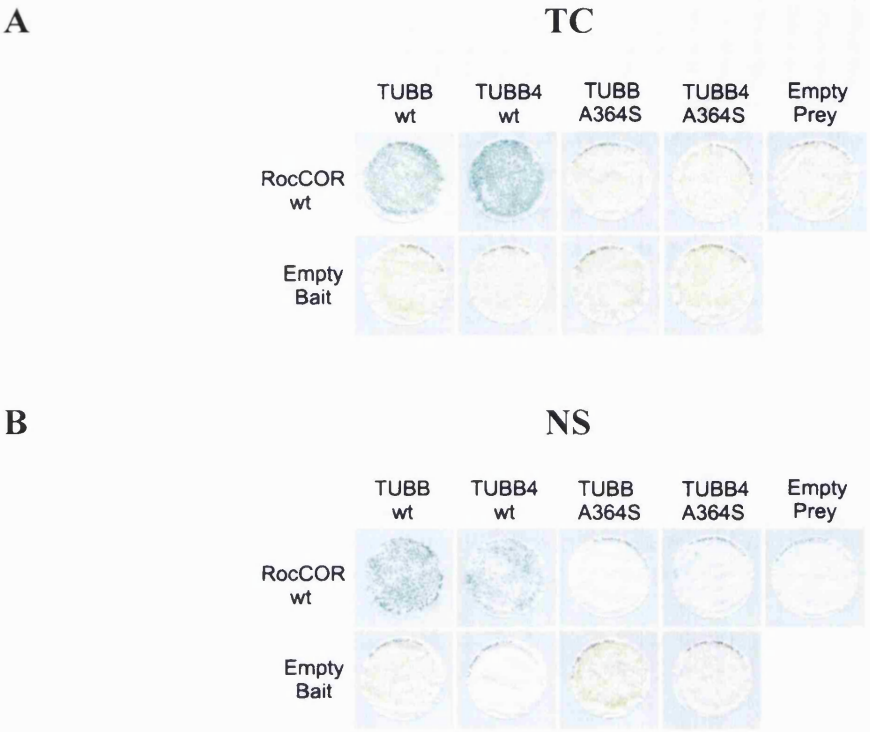

Figure 4.14: Mutation of A364 to serine in TUBB and TUBB4 completely abolishes Roc-COR interaction with tubulin. The interaction between the WT Roc-COR domain and the C-terminus of WT TUBB and TUBB4 are indicated by the blue colonies on the TC filters (A) and the NS filters (B). Tubulin mutants containing the A364S amino acid change failed to interact with the Roc-COR domain expressed in yeast, as indicated by the white colonies. All negative controls with the empty prey and bait vectors did not show an interaction.

To test the hypothesis that the amino acid at position 364 of β-tubulin might be important for the specificity of the Roc-COR – tubulin interaction, primers were designed to mutate this site in the pACT2 – β-tubulin constructs (Table 2.5). Alanine at position 364 in TUBB and TUBB4 was mutated to serine, and serine at position 364 in TUBB2A, TUBB2B, TUBB2C and TUBB3 to alanine. An YTH experiment was carried out with the newly generated mutants to investigate an effect on the Roc-COR – tubulin interaction.

The A364S mutation in TUBB and TUBB4 abolished the interaction with the LRRK2 Roc-COR domain (Figure 4.14), whereas the introduction of a serine at position 364 in

TUBB2A, TUBB2B, TUBB2C and TUBB3 enabled the Roc-COR protein to bind to these β-tubulin isoforms (figure 4.15). These results suggest that this site plays a crucial role in the specific interaction between LRRK2 and tubulin, and that phosphorylation at S364 of β-tubulin might confer a phospho-dependent inhibition of this interaction.

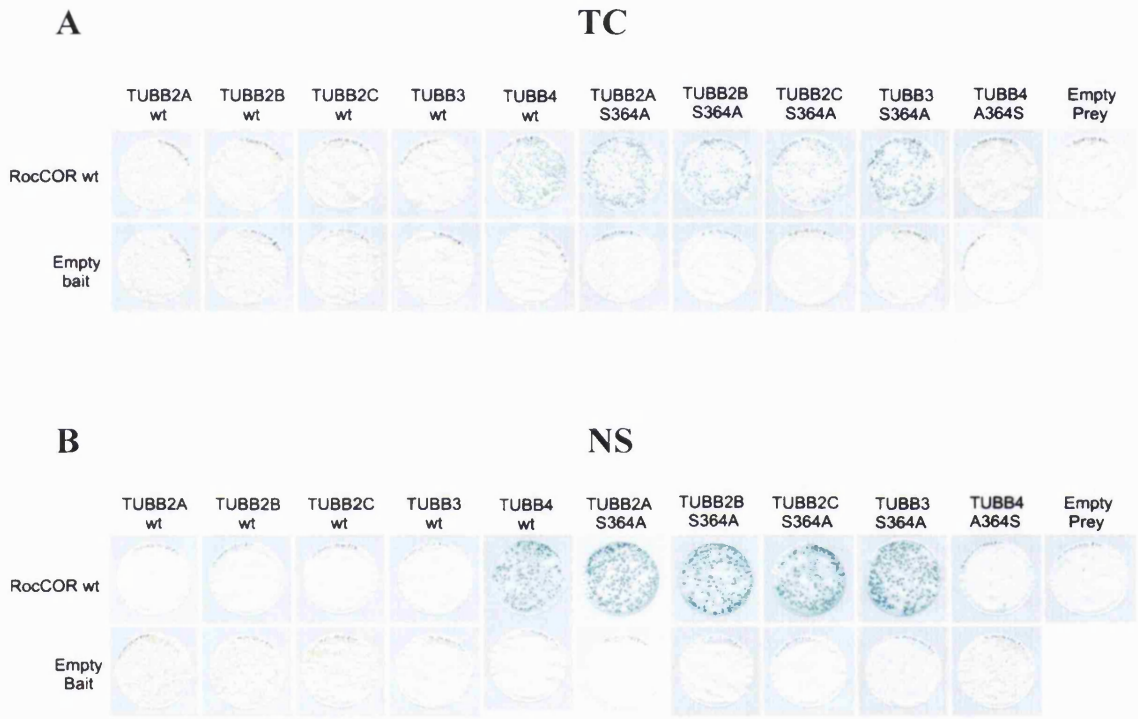

Figure 4.15: Mutation of S364 to alanine in TUBB2A, TUBB2B, TUBB2C and TUBB3 confers Roc-COR interaction with tubulin. The WT Roc-COR domain was not able to interact with the C-terminus of WT TUBB2A, TUBB2B, TUBB2C and TUBB3, indicated by the white colonies on the TC filters (A) and the NS filters (B). By contrast, the S364A tubulin mutants were able to interact with the Roc-COR domain expressed in yeast, indicated by the blue colonies. All negative controls with the empty prey and bait vectors did not show an interaction.

4.7 Expression of β-Tubulin Isoforms in the Human Brain

So far we have established and characterised the Roc-COR – tubulin interactions in yeast and mammalian cells. However, little is known about the expression of these tubulin isoforms in human brain. In order to address this, an RQ-PCR experiment was carried out to assess the expression level of each β-tubulin isoform in adult whole brain, foetal whole brain and the SN at the transcriptional level.

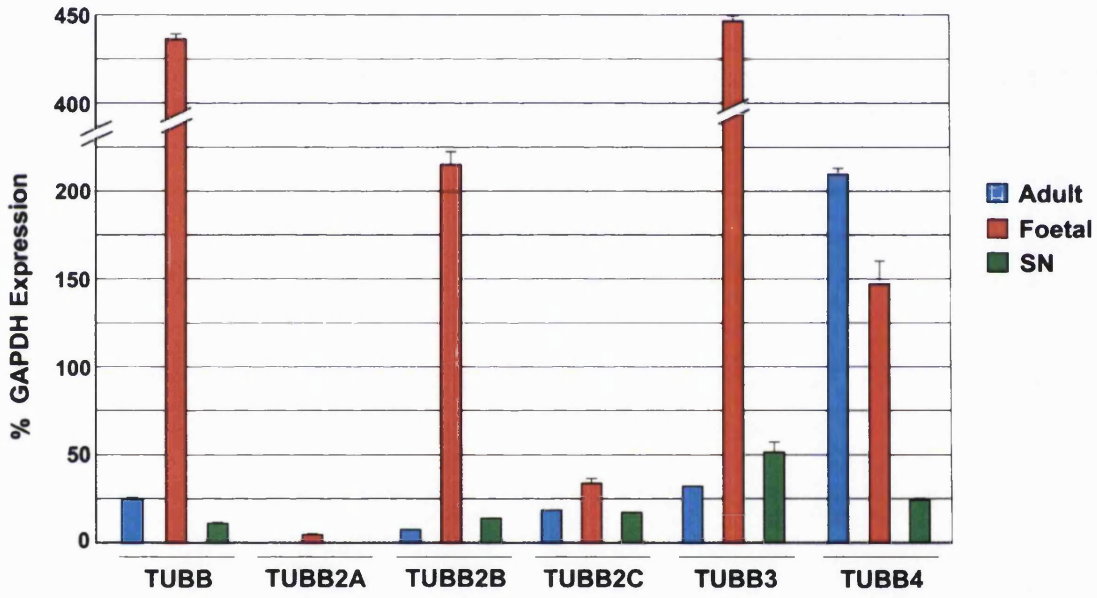

Figure 4.16: The relative expression level of the neuronally expressed β-tubulin isoforms in the adult brain, foetal brain and substantia nigra. RQ-PCR experiment on the commercially available RNA from the human adult and foetal brain and the substantia nigra was performed to assess the expression level of each neuronally expressed β-tubulin isoform. The expression level is expressed as the percentage of that for the housekeeping gene GAPDH. TUBB4 is expressed most abundantly in the adult brain, while TUBB3 and TUBB are the two most abundantly expressed isoforms in the foetal brain. All isoforms, except TUBB2A, are expressed in the substantia nigra. (n = 3)

RNA from human adult and foetal brain, as well as from the substantia nigra, the brain region that is most affected in PD, were bought from Clontech. The RNA was subjected to reverse transcription as shown in section 2.5.2. The resultant cDNA were subjected to RQ-PCR together with the cDNA of the housekeeping gene GAPDH. The quantification of the amount of cDNA formed after PCR is expressed as a percentage of the amount of GAPDH cDNA, and shown in figure 4.16. All β-tubulin isoforms, except TUBB2A, were expressed in human brain. TUBB4 was shown to be the most abundant isoform expressed in the adult brain. In the foetal brain, TUBB3 and TUBB were the dominant isoforms expressed. Since LRRK2 was found to specifically interact with TUBB and TUBB4 only, the RQ-PCR data suggest that the LRRK2 – tubulin interaction might play a role in neuronal maintenance in the adult brain and neuronal development in the foetal brain.

4.8 The Effect of *PARK8* Mutations on Roc-COR Dimerisation

In light of the finding that some *PARK8* mutations could lead to an alteration in the interaction between LRRK2 and TUBB/TUBB4, I next asked how do these mutations lead to the observed alteration in the interaction level. As discussed, LRRK2 normally exists as a dimer. Could the dimerisation of the Roc-COR domain in LRRK2 play a role in this interaction? In other words, is it possible that the mutations in the Roc-COR domain affect the interaction with tubulin via a modulation of the Roc-COR dimer formation? The interaction strength between a Roc-COR WT prey and Roc-COR WT and mutant baits was assessed in a Q-YTH assay as shown in figure 4.17. The data were analysed using a paired two-tailed Students' T test. Interestingly, all of the tested Roc-COR mutants were found to significantly alter the strength of the dimerisation between WT and mutant protein in comparison to a WT Roc-COR dimer. Most mutants decreased the dimer interaction strength. The R1441G and M1869T mutants led to an almost 40% decrease in the dimerisation strength of the Roc-COR domain in comparison to a WT dimer interaction, whereas mutations at R1728 led to an increase in the dimerisation strength. All other tested mutants weakened the Roc-COR dimer interaction strength to between 70% and 90% of the WT Roc-COR dimer interaction

strength. Interestingly, despite the fact that not all mutations affect the LRRK2 – tubulin interaction and the Roc-COR dimer formation in the same way, the pattern of the relative differences between LRRK2 mutants is strikingly similar for all tested interactions. However, since some mutants appeared to show different effects in LRRK2 – tubulin interaction and Roc-COR dimerisation, it is unlikely that the Roc-COR mutations confer an alteration of the LRRK2 – tubulin interaction via the modification of Roc-COR dimerisation.

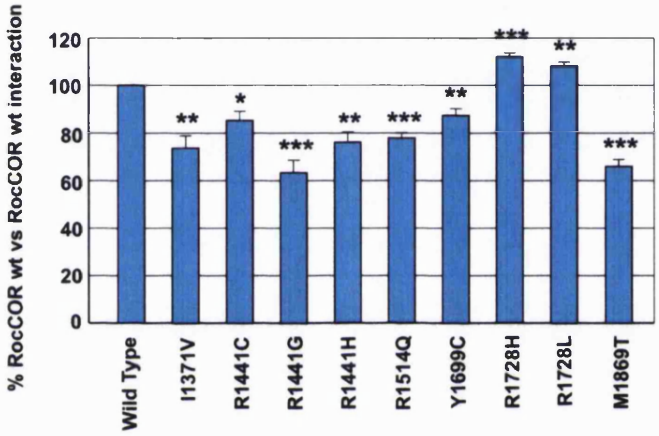

Figure 4.17: PD-associated mutations in the LRRK2 Roc-COR domain affect the strength of Roc-COR dimerisation. The relative strength of interaction for each Roc-COR mutant bait and WT Roc-COR prey is expressed as the percentage of interaction level compared to that between WT Roc-COR bait and WT Roc-COR prey. All of the Roc-COR mutants showed the ability to alter the level of Roc-COR dimerisation. Statistical significance was determined using unpaired two-tailed Students' T test. (* $P < 0.05$, ** $P < 0.01$, *** $P < 0.001$, $n = 5$)

4.9 Discussion

4.9.1 LRRK2 Interaction with β-tubulin is conferred by the Roc Domain

This chapter focused on the interaction between LRRK2 and β-tubulin, owing to the possible relevance of this interaction for PD. An interaction between LRRK2 and

microtubules was previously suggested by Gandhi *et al* (2008), showing that the Roc domain of LRRK2 is sufficient for the interaction between LRRK2 and a heterodimer of α- and β-tubulin using a GST pull down assay in a mammalian cell model. My findings confirmed this observation in a yeast model. I also observed a slight inhibitory effect in the Roc – tubulin interaction in the presence of the COR domain. This suggests that while the COR domain is not necessary for the LRRK2 – tubulin interaction, it might play a role in the regulation of this interaction.

4.9.2 The Specificity of the LRRK2 – Tubulin Interaction

One of the major findings in this project is that the LRRK2 – tubulin interaction is specific for certain β-tubulin isoforms. In this study, six different isoforms of β-tubulin expressed in neurons were tested for interaction with LRRK2. The amino acid sequences of these isoforms are highly conserved, with the clearest difference at the C-terminus. Using the YTH assay, the LRRK2 – tubulin interaction was shown to be specific only to two β-tubulin isoforms – TUBB and TUBB4. The other tested isoforms, TUBB2A, TUBB2B, TUBB2C and TUBB3, were not able to interact with the LRRK2 Roc-COR domain. This result seems to contradict the findings by Gillardon (2009), who observed an interaction between LRRK2 and TUBB2C. This discrepancy could perhaps be explained by the difference in the experimental techniques employed. Gillardon (2009) found TUBB2C to interact with LRRK2 using immunoprecipitation. This result might not reflect a direct interaction between LRRK2 and TUBB2C, but might be conferred by a third protein. The YTH system is a more reliable method to assess a direct interaction between two mammalian proteins, as interactions take place in the yeast nucleus need the close proximity of a bait DNA-BD and a prey AD, and yeast is less likely to express proteins able to interact with the expressed mammalian proteins. Hence, it is likely that the observed LRRK2 – TUBB2C interaction is indirect, most likely conferred by other tubulin isoforms in the same microtubule.

Furthermore, the specificity of the Roc-COR – tubulin interaction could provide clues on the physiological function of this interaction. My RQ-PCR data showed TUBB4 as the major isoform in the adult brain. Hence the specific interaction of LRRK2 with TUBB4 raises the possibility that LRRK2 might play a role at the microtubule cytoskeleton in the developed adult brain. LRRK2 could perhaps be involved in the

regulation of microtubule stability, and microtubule instability conferring toxicity especially to dopaminergic neurons might be caused by *PARK8* mutations. In addition, phosphorylation of tubulin and MAPs could affect microtubule stability (Wandosell *et* al, 1986; Brugg and Matus, 1991; Khan and Ludueña, 1996). Since LRRK2 is a kinase, it could be involved directly or indirectly in the phosphorylation of tubulin and/or MAPs. The possibility that the LRRK2 – tubulin interaction might be important for microtubule stability was also suggested by Gillardon (2009).

TUBB and TUBB3 were found to be the two major isoforms of β-tubulin expressed in the developing foetal brain. The expression level was more than four times higher than that of GAPDH. With the abundant expression of these two isoforms, they are likely to constitute the majority of the neuronal microtubules in the foetal brain. The specific interaction of LRRK2 with TUBB would hence suggest that the LRRK2 – tubulin interaction could play a role in neuronal development. In agreement with this, Zechel *et al* (2010) found that LRRK2 is expressed abundantly in the developing embryonic brain, and it was expressed highly during neurogenesis. In addition, LRRK2 expression was also found to be prominent in migrating cells in the cerebellum (Zechel *et al*, 2010), indicating a role of LRRK2 in brain development. Alterations in the LRRK2 – TUBB interaction in the foetal brain might therefore affect the development of the brain in *PARK8* mutation carriers. An early small developmental defect could then lay the basis for progressive neurodegeneration later in life.

In order to show the specificity of the interaction of LRRK2 and tubulin in mammalian cells, I carried out a co-IP experiment in HEK293 cells, testing the interaction of LRRK2 with TUBB, TUBB4 and TUBB2A in these cells. Results revealed an interaction of LRRK2 with TUBB2A in these experiments. The interaction between LRRK2 and TUBB2A is most likely indirect and conferred by the interaction of TUBB2A with other tubulin isoforms or MAPs present in HEK293 cells. YTH assays are more reliable in detecting direct interactions between two proteins because the assays rely on the close proximity of a DNA-BD and AD fused with the proteins of interest that is necessary for the formation of a transcription factor.

After confirming the LRRK2 – tubulin interaction in mammalian cells, and establishing the specificity of the LRRK2 – TUBB/TUBB4 interaction in a yeast model, the next

question was what is the basis of the specific interaction. When we compare the aligned amino acid sequences shown in figure 4.1, there is only one position at which the amino acid sequence is different between TUBB/TUBB4 and TUBB2A, TUBB2B, TUBB2C, TUBB3, i.e. position 364. At this position, TUBB and TUBB4 have an alanine, while the other isoforms possess a serine. Serine and alanine are similar in size but differ in their ability to be phosphorylated. Phosphorylation leads to a change in the conformation of proteins, due to the bulky phosphoryl group and introduction of a negative charge, impacting on protein folding and contributing to further binding through charge-charge interactions. Indeed, mutation of A364 in TUBB and TUBB4 to serine led to the abolition of interaction between LRRK2 and these two β-tubulin isoforms, whereas mutation of S364 in TUBB2A, TUBB2B, TUBB2C and TUBB3 to alanine enabled the interaction between LRRK2 and these β-tubulin isoforms. This observation confirmed the crucial importance for the amino acid at position 364 for the interaction between LRRK2 and β-tubulin. As mentioned, serine and alanine have a similar size, while they differ just by the presence of an additional hydroxyl group in serine. Although the presence of the hydroxyl group may cause a conformational change by creating an extra hydrogen bond to be formed within the tubulin molecule, a more likely reason for the failure of the β-tubulin isoforms containing a serine at position 364 to interact with LRRK2 might be a phosphorylation-dependent inhibition. Since yeast contains endogenous serine/threonine kinases (Lim *et al,* 1993), it is possible that TUBB2A, TUBB2B, TUBB2C and TUBB3 transformed into yeast could be phosphorylated by the endogenous kinases at S364, rendering them unable to interact with the Roc-COR domain. TUBB and TUBB4 contain an alanine at that site, and are therefore unable to be phosphorylated. Therefore, phosphorylation events on the microtubule cytoskeleton could play a role in the localisation of LRRK2 to microtubules.

4.9.3 The Effect of *PARK8* Mutations on the LRRK2 – Tubulin Interaction

Microtubule stability might play an important role in the process of neurodegeneration, owing to the importance of efficient transport along the axonal microtubules for neuronal functions (Feng, 2006). It is tempting to speculate that a disruption of the interaction between LRRK2 and tubulin in *PARK8* mutation carriers could play a part in

the neurodegenerative process. In light of this, the effect of the PD-associated *PARK8* mutations on the interaction with tubulin was examined.

The PD-associated mutation R1441C was previously shown to retain interaction between the LRRK2 Roc domain and a heterodimer of α- and β-tubulin (Gandhi *et al,* 2008). Using a yeast model, my data confirmed this observation, although in addition a slight, but significant, increase in the Roc-COR – TUBB and Roc-COR – TUBB4 interaction was observed for this mutation in comparison to the TUBB/TUBB4 – WT LRRK2 interaction. My data also show differences in the strength of the Roc-COR – tubulin interaction among the other Roc-COR mutants. A clear decrease in the interaction strength was observed for the R1441G mutation. This mutation showed a clear decrease in the interaction strength with RTN3, S100A10 and the ApoE isoforms too. This raises the question whether this mutation can cause a significant conformational change in the Roc-COR dimer so as to affect the Roc-COR interaction with tubulin and other protein interactors. Indeed, the R1441 residue was suggested to be situated at the Roc-COR dimer interface (Deng *et al,* 2008). It could be involved in the interactions within the Roc-COR dimer. A mutation from the large and charged arginine to the small and neutral glycine might cause an alteration in these interactions. It was thus tempting to speculate that the mutation at R1441 or the residues located at the Roc-COR dimer interface could be involved in the modulation of the interaction strength between the LRRK2 Roc-COR domain and tubulin via a conformational change of the Roc-COR dimer. A problem with this speculation is that I1371 was also shown to be located at the interface of the Roc-COR dimer, playing a role in the stabilisation of the LRRK2 dimer (Deng *et al,* 2008), but the I1371V mutation resulted in a relatively less significant alteration of the interaction strength between the Roc-COR domain and TUBB/TUBB4. This could be due to the relative similarity in the structure of isoleucine and valine, The I1371V mutation would hence have a smaller effect on the LRRK2 protein conformation than the R1441G mutation.

The next question I asked was whether *PARK8* mutations could affect the Roc-COR – tubulin interaction by altering the ability of the LRRK2 Roc-COR domain to dimerise. Although it appeared that the conformation of the Roc-COR dimer can alter the interaction strength between the Roc-COR domain and tubulin, there is no evidence that indicate an effect of the strength of the Roc-COR dimer on this interaction. It would be

interesting to investigate whether the mutations could affect the dimerisation process, which in turn lead to an alteration in the interaction level of the Roc-COR – tubulin interaction.

4.9.4 The Effect of *PARK8* Mutations on Roc-COR Dimerisation

As discussed, LRRK2 was suggested to exist naturally as a dimer. This is especially relevant in the context of LRRK2 functionality, as dimerisation was found to be important to both the GTPase (Gotthardt *et al,* 2008) and kinase activities (Sen *et al,* 2009) of LRRK2. To determine whether Roc-COR dimerisation affects the ability of the Roc-COR domain to interact with tubulin, I determined whether the Roc-COR mutants alter the strength of Roc-COR dimerisation in a similar way they did to the strength of the Roc-COR – tubulin interaction. My data showed that all Roc-COR mutants significantly altered the strength of Roc-COR dimerisation in comparison to the interaction between the WT Roc-COR domains. The R1441G and M1869T mutations resulted in the clearest decrease in the Roc-COR dimerisation strength, while the R1728H and R1728L mutations led to an increase. Although a similarity in the pattern of alterations in the interaction strength was observed in both the Roc-COR dimerisation and the Roc-COR – tubulin interaction, some Roc-COR mutants failed to significantly alter the strength of the Roc-COR – tubulin interaction. Moreover, the R1441C mutation led to opposite effects in Roc-COR dimerisation and Roc-COR – tubulin interaction. These observations render it unlikely that the alteration in the interaction strength between the LRRK2 Roc-COR domain and tubulin is caused by the altered strength of Roc-COR dimerisation.

Another question that could be raised is whether these data could help explain the effect of *PARK8* mutations on the functionality of LRRK2. As discussed, the abolition of Roc-COR dimerisation was found to drastically reduce the level of both the LRRK2 GTPase and kinase activities. Since all of the PD-associated mutants led to a decreased strength of interaction within the Roc-COR dimer, all these mutants could potentially affect LRRK2 enzymatic activities. Indeed, Deng *et al* (2008) found that mutations at R1441 could affect the interaction between the Roc-COR domain and the γ-phosphate of GTP and magnesium ion, as the orientation of the amino acids responsible for such interaction – R1398 and D1394 – could possibly be altered (Deng *et al,* 2008), although

an earlier study reported that mutations at R1441 failed to affect LRRK2 GTP binding (Li *et al,* 2007). It was shown that the I1371V, R1441C/G and Y1699C mutations could disrupt GTP hydrolysis (Lewis *et al,* 2007; Li *et al,* 2007; Deng *et al*, 2008; Gotthardt *et al,* 2008; Daniëls *et al*, 2010; Xiong *et al,* 2010). My data are in agreement with these findings by showing that these mutations led to a decline in Roc-COR dimerisation strength. However, I also found that mutations in the COR domain, especially M1869T, led to a decrease in dimerisation level. Could these mutations also lead to a decreased GTPase activity? Since the M1869T mutation appeared to cause a similar marked decrease in Roc-COR dimerisation level as the R1441G mutation, could the M1869T mutation also cause a decrease in LRRK2 GTPase activity like the mutations that segregate with PD? If so, could M1869T and other mutations which show a decrease in Roc-COR dimerisation be pathogenic too? To date, there is no evidence to show that the M1869T mutation is pathogenic, and the occurrence of these mutations in PD patients was shown to be a rare event (Pankratz *et al,* 2006b). Furthermore, the R1514Q mutation was suggested to be non-pathogenic (Nichols *et al,* 2007). If a decrease in LRRK2 GTPase activity conferred by a weakening of the Roc-COR dimerisation is responsible for PD pathogenesis, at least the R1514Q mutation would not be expected to alter the dimerisation strength of the Roc-COR domain. My data showing the decrease in Roc-COR dimerisation in all tested Roc-COR mutants hence seems to contradict the data in the literature. This discrepancy could be explained by the ability of the WD40 domain at the C-terminus of LRRK2 to dimerise as well, as the truncation of this domain results in the failure of LRRK2 to dimerise (Jorgensen *et al,* 2009). It is possible that the dimerisation of the LRRK2 WD40 domain could rescue the weakening of Roc-COR dimerisation caused by some *PARK8* mutations such as R1514Q. In other words, it seemed that the dimerisation of both the LRRK2 Roc-COR domain and WD40 domain play a role together in the function of LRRK2. It is likely though that the dimerisation of the Roc-COR domain could have a larger role in LRRK2 functions, as more mutations in this domain were shown to be pathogenic (section 1.3.5 and figure 1.4). As Roc-COR dimerisation is so important to LRRK2 function, further studies into this event could be worthwhile.

Previous data indicated the importance of GTP binding to the LRRK2 Roc domain as the pre-requisite of LRRK2 activation (Ito *et al,* 2007), including autophosphorylation of LRRK2. LRRK2 GTP binding and autophosphorylation was also shown to be

interlinked, by the observation that the GTP binding mutant K1347A abolished LRRK2 autophosphorylation (Smith *et al,* 2006; West *et al*, 2007). In light of this, the effect of LRRK2 autophosphorylation and the disruption of GTP binding on Roc-COR dimerisation and the Roc-COR – tubulin interaction were examined in the next chapter.

5. The Role of GTP Binding and Autophosphorylation of LRRK2 on Dimerisation and Protein Interactions

Dimerisation of the Roc-COR domain was shown to be an important event required for enzymatic activities of LRRK2. However, the precise mechanism of the activation of LRRK2 is not clearly understood. Initially, it was believed that the GTPase activity of LRRK2 controls the kinase activity. It was shown that LRRK2 undergoes conformational change upon GTP binding to the Roc domain, resulting in the activation of the kinase domain (Gotthardt *et al,* 2008). This activation could be caused by autophosphorylation of T2031, S2032 and T2035 within the activation loop of the LRRK2 kinase domain (Li *et al,* 2010). The Roc GTPase activity then turns off the kinase activity, terminating LRRK2 activation. Recently, numerous phosphorylation sites within the Roc domain, such as T1343 and T1491, were identified (Greggio *et al,* 2009; Kamikawaji *et al,* 2009; Gloeckner *et al,* 2010). Therefore, LRRK2 autophosphorylation could also serve as a regulatory mechanism of LRRK2 activity by phosphorylation of threonine residues in the Roc domain. The phosphorylation of these sites was shown to alter the kinase activity and the GTP binding activity of the LRRK2 Roc domain (Kamikawaji *et al,* 2009), providing a negative feedback mechanism of LRRK2 kinase activity. Therefore, GTP binding to and autophosphorylation of the LRRK2 Roc domain both seem important for the function of LRRK2.

Previous findings suggested that the GTP binding deficient mutant K1347A failed to trigger LRRK2 autophosphorylation (Smith *et al,* 2006), although it remains uncertain why defects in GTP binding hamper this process. It is possible that defects in GTP binding to the Roc domain affect LRRK2 dimerisation. To test this hypothesis, the effect of the abolition of GTP binding to the LRRK2 Roc domain on Roc-COR dimerisation and interaction with tubulin was investigated. In addition, the G2019S mutation was suggested to increase the autophosphorylation of T1343 and T1491 (Greggio *et al,* 2009). Could this mutation alter LRRK2 interaction with tubulin and microtubules via an increase in Roc autophosphorylation? Hence, the effect of Roc autophosphorylation on both Roc-COR dimerisation and the Roc-COR – tubulin interaction was also examined.

5.1 The Generation of GTP Binding Mutants and Phosphomimetic Mutants

In order to investigate the effect of the abolition of Roc GTP binding on protein interactions of the LRRK2 Roc-COR domain, 2 separate Roc-COR mutants were generated with mutations previously used to abolish GTP binding, K1347A and T1348N (Smith *et al,* 2006; Ito *et al,* 2007; Yao *et al,* 2010). The Roc-COR domain previously cloned into the pDS bait vector was mutated using site-directed mutagenesis (section 2.1.8), generating the pDS Roc-COR K1347A and pDS Roc-COR T1348N constructs. The K1347A mutant construct was used to investigate the effect of GTP binding defects on Roc-COR interaction with LRRK2 interactors and Roc-COR dimerisation. The T1348N mutant construct was also included in further Q-YTH experiments on the Roc-COR – tubulin interaction and Roc-COR dimerisation to show the reproducibility of data with different mutants.

For the experiment investigating the effect of Roc autophosphorylation on Roc-COR dimerisation and interaction with tubulin, phosphomimetic mutants were generated – the T1343 and the T1491 Roc-COR mutants. Both threonine residues were mutated to an aspartate, generating the phosphomimetic T1343D and T1491D Roc-COR mutants. The negatively charged aspartate mimics the negative charge present on phosphoryl groups, hence the autophosphorylated Roc domain. In addition, the threonines at these two sites were mutated to an alanine, generating the T1343A or T1491A mutant constructs. These mutations abolish these two phosphorylation sites in the Roc-COR constructs and served as a control in the YTH experiment described in section 5.2.

5.2 The Effect of the Abolition of GTP Binding to LRRK2 on Roc-COR Interaction with Protein Interactors

In order to establish the effect of the abolition of GTP binding to the Roc domain on the interaction with the identified LRRK2 interactors, I carried out a YTH experiment to assess the interaction between the K1347A Roc-COR mutant and the LRRK2 interactors – RTN3, S100A10, ApoE2, ApoE3, ApoE4, TUBB and TUBB4. Previous data (Sancho *et al,* 2009) revealed the interaction between the LRRK2 Roc-COR domain and members of the DVL protein family DVL1, DVL2 and DVL3. These proteins were also included in this investigation. In addition, the effect of the K1347A mutation on Roc-COR dimerisation was also determined by including a WT Roc-COR prey in this experiment. Constructs harbouring cDNA coding for the protein interactors cloned into the pACT2 vector were used as preys, while the pDS Roc-COR K1347A construct was used as the bait in the YTH experiment. The YTH experiment was carried out as shown in section 2.2.

Figure 5.1 showed that the WT Roc-COR protein was able to interact with all protein interactors. Interestingly, the GTP binding deficient mutant K1347A seemed to abolish all these interactions, although Roc-COR dimerisation was not abolished by this mutation. It is important to note that the blue colour of the colonies for the dimerisation between mutant Roc-COR and WT Roc-COR proteins was considerably less intense than that for the dimerisation of two WT Roc-COR proteins. This could be an indication of a decreased strength of Roc-COR dimerisation upon the abolition of Roc GTP binding activity. Taken together, The GTP binding deficient K1347A mutant abolished the interaction between the LRRK2 Roc-COR domain and LRRK2 interactors, and significantly lowered the strength of Roc-COR dimerisation. The data suggested a possibility that GTP binding to the Roc domain is essential for LRRK2 to interact with other proteins.

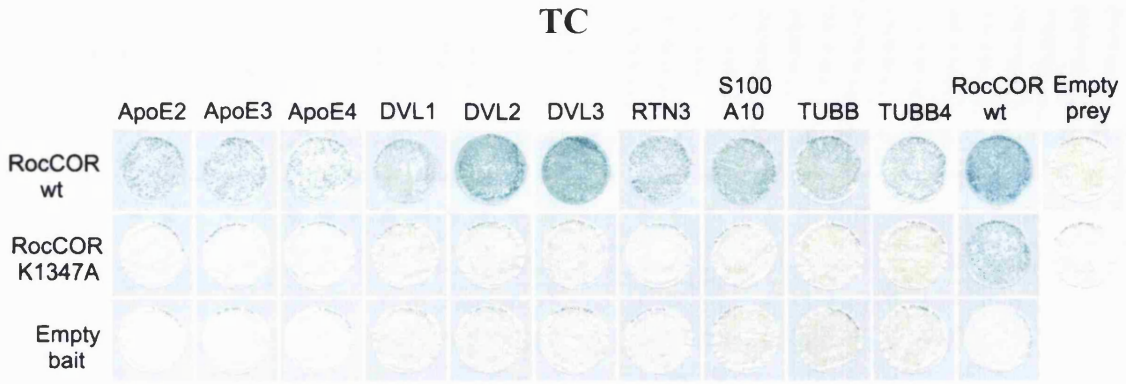

Figure 5.1: The K1347A mutation in the LRRK2 Roc-COR domain abolishes interaction with all protein interactors and decreases the strength of Roc-COR dimerisation. The interaction between the WT Roc-COR domain and the previously identified LRRK2 interactors is indicated by the blue colonies on the TC filters. Failure of interaction between the GTP binding Roc-COR domain mutant and the interactors is indicated by the white colonies. The decreased interaction strength between the mutant Roc-COR and WT Roc-COR proteins is indicated by the lower colour intensity of the blue colonies. All negative controls with the empty prey and bait vectors did not show an interaction.

5.3 The Effect of Abolition of Roc GTP Binding and Roc Autophosphorylation on the Roc-COR – tubulin Interaction

The main focus of the project is on the interaction between the LRRK2 Roc-COR domain and tubulin or microtubules. Hence, the next step of the investigation was to determine to what extent the LRRK2 Roc-COR interaction with tubulin is affected by the abolition of GTP binding. Although the YTH LacZ freeze-fracture assay described in the previous section showed no interaction between the mutant Roc-COR domain of LRRK2 and TUBB or TUBB4, I decided to investigate if some interaction could still be detected using a quantitative YTH assay. In the following experiments, another GTP binding mutant, T1348N, was also used to assess the influence of the abolition of GTP binding on LRRK2 interactions. This allows us to determine, in a quantitative way,

whether these two mutants have similar effects on the Roc-COR – tubulin interaction. In addition, the phosphomimetic mutants and their respective controls were included in the experiment to reveal the effect of autophosphorylation at T1343 and T1491 in the LRRK2 Roc domain on the Roc-COR – tubulin interaction. The effect of the deficiency in Roc GTP binding and Roc autophosphorylation on the ability of the LRRK2 Roc-COR domain to interact with TUBB and TUBB4 was assessed quantitatively using the Q-YTH assay.

Figure 5.2A and 5.2B show that both the K1347A and T1348N mutations resulted in almost a total abolition of interaction between the LRRK2 Roc-COR domain and TUBB/TUBB4. This further confirmed the inhibitory effect of the abolition of Roc GTP binding on the interaction between the LRRK2 Roc-COR domain and tubulin. In other words, GTP binding appeared to be critical for the Roc-COR – tubulin interaction.

The Q-YTH data also showed the inhibitory effect of Roc autophosphorylation on the Roc-COR – tubulin interaction. Both the T1343D and T1491D phosphomimetic mutants led to a significant decrease in the Roc-COR – TUBB and the Roc-COR – TUBB4 interaction. On the other hand, the T1343A and T1491A mutants did not affect the strength of interaction between the Roc-COR domain and tubulin to the same extent as the phosphomimetic mutants. Nonetheless, a slight but significant variation in the strength of the Roc-COR – TUBB4 interaction was observed, leading to a slight increase or decrease in the interaction between TUBB4 with the T1343A and T1491A mutant respectively. In conclusion, the phosphomimetic mutants appeared to cause a significant decrease in the strength of the Roc-COR – tubulin interaction, suggesting that Roc autophosphorylation could weaken the interaction between the LRRK2 Roc-COR domain and tubulin, and possibly lead to LRRK2 detachment from microtubules.

A

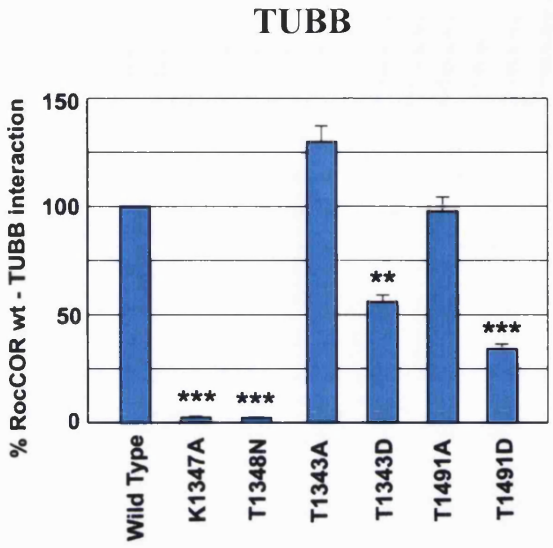

B

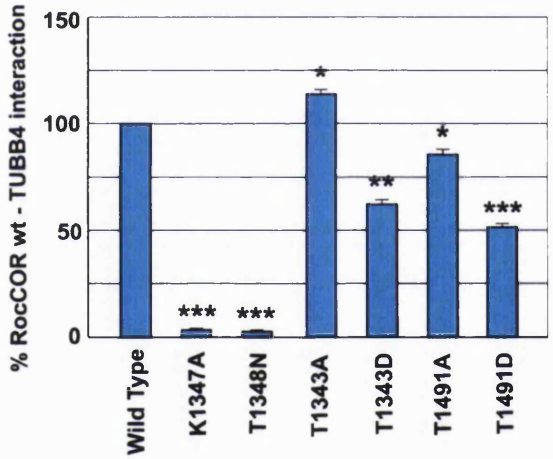

Figure 5.2: The effect of the abolition of Roc GTP binding and Roc autophosphorylation on the Roc-COR – tubulin interaction. The relative strength of interaction between each Roc-COR mutant and TUBB (A) and TUBB4 (B) is expressed as the percentage of interaction level compared to that between WT Roc-COR and tubulin. GTP binding mutants K1347A and T1348N could almost totally abolish the Roc-COR – tubulin interaction. The phosphomimetic mutants T1343D and T1491D could also significantly decrease the interaction strength. The T1343A mutant and the T1491A mutant respectively increased and decreased only the interaction with TUBB4 significantly but the same trends were observed for the interaction of these mutants with TUBB. Statistical significance was determined using the unpaired, two-tailed Students' T test. (* $P < 0.05$, ** $P < 0.01$, *** $P < 0.001$, $n = 4$)

5.4 The Effect of the Abolition of Roc GTP Binding and Roc Autophosphorylation on Roc-COR Dimerisation

The observation that Roc autophosphorylation led to a weakening of the Roc-COR – tubulin interaction has triggered a question: Could this weakening effect be linked to the ability of the Roc-COR domain to dimerise? In chapter 4, it was suggested that the alterations in the Roc-COR – tubulin interaction caused by *PARK8* mutations might not be related to the alteration in the Roc-COR dimerisation strength. Here, I investigate the effect of Roc autophosphorylation on Roc-COR dimerisation using the Q-YTH assay to assess if observed changes in the interactions with tubulin correspond to changes in the Roc-COR dimer upon phosphorylation. In addition, the effect of the abolition of Roc GTP binding on Roc-COR dimerisation was also assessed quantitatively.

The results presented in figure 5.3 show that the GTP binding mutants K1347A and T1348N dramatically reduced the level of Roc-COR dimerisation to only about 5% of the interaction between two WT Roc-COR proteins. This suggested that GTP binding to the Roc domain could also be critical for Roc-COR dimerisation. Furthermore, the effect of T1348N on both the Roc-COR dimerisation and Roc-COR – tubulin interaction appeared to be greater than that of K1347A, suggesting that T1348 could play a larger role in the GTP binding event in the Roc domain. By contrast, the phosphomimetic mutants and their respective alanine mutants did not significantly alter the Roc-COR dimerisation strength, indicating that Roc autophosphorylation has no effect on the dimerisation of LRRK2. Taken together, the data revealed that GTP binding is important for the LRRK2 Roc-COR domain to dimerise and to interact with tubulin. Roc autophosphorylation, however, has no effect on Roc-COR dimerisation, but leads to a decrease in the strength of interaction between the Roc-COR domain and tubulin. This suggests an inhibitory effect of Roc autophosphorylation on the localisation of LRRK2 to microtubules.

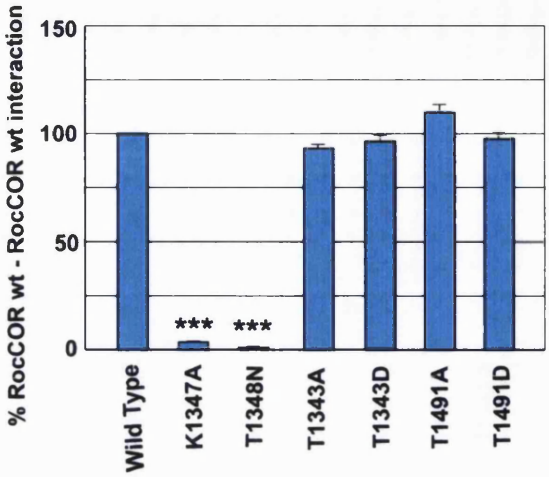

Figure 5.3: The effect of the abolition of Roc GTP binding and Roc autophosphorylation on Roc-COR dimerisation. The relative strength of interaction between each Roc-COR mutant and the WT Roc-COR protein is expressed as the percentage of interaction level compared to that between two WT Roc-COR proteins. Both GTP binding deficient mutants led to almost a total abolition of Roc-COR dimerisation. However, the phosphomimetic mutants failed to affect Roc-COR dimerisation. Statistical significance was determined using the unpaired, two-tailed Students' T test. (*** $P < 0.001$, $n = 4$)

5.5 The Effect of the Presence of Guanosine Nucleotides on the Roc-COR – Tubulin Interaction

The failure of the GTP binding deficient Roc-COR mutants to dimerise and interact with tubulin could be explained by the following two possibilities. Firstly, GTP binding is required for both Roc-COR dimerisation and Roc-COR – tubulin interaction. Secondly, the mutants might have caused a considerable conformational change in the Roc-COR protein that ablates Roc-COR dimerisation and interaction with tubulin. In order to eliminate the latter possibility, the interaction between the Roc-COR domain and tubulin was assessed in the presence of a non-hydrolysable GTP analogue called GTP gamma sulphate (GTP-γS) or guanosine diphosphate (GDP), using co-IP in HEK293 cells.

The co-IP was carried out as described in section 2.3.10.5. After the Roc-COR protein was pulled down by the N-terminally FLAG-tagged TUBB4 or TUBB, 5μM GTP-γS/GDP was added to the beads. The mixture was incubated for 30 minutes for the nucleotides to bind to the Roc-COR protein bound to the beads. This incubation step of GTP-γS/GDP allowed us to determine if the tubulin interaction with the LRRK2 Roc-COR domain is influenced by the presence of guanosine nucleotides. GTP-γS served to keep LRRK2 in a constitutively active state. Hence, assuming that GTP binding is a requirement for the Roc-COR – tubulin interaction, GTP-γS incubation was expected to make the Roc-COR protein show stronger interaction with tubulin than a presumably inactive GDP-bound LRRK2.

The co-IP experiment was repeated four times. The immunoreactivity of the myc-tagged LRRK2 Roc-COR protein on a western blot was quantified, indicating the amount of Roc-COR protein pulled down by the FLAG-tagged tubulin. This provides an indication of the interaction strength between the myc-tagged Roc-COR domain and the FLAG-tagged tubulin. The immunoreactivity of the FLAG-tubulin fusion protein was also quantified to normalise results according to the 'tubulin input'. The strength of the Roc-COR – tubulin interaction was therefore expressed by myc immunoreactivity divided by FLAG immunoreactivity, which is referred to as myc/FLAG hereafter. The results shown in figure 5.4B are expressed as the percentage of myc/FLAG of the control immunoprecipitation conducted in the absence of nucleotides (section 2.3.10.5). The results of the experiments showed wide variations, as indicated by the large error bars in figure 5.4B. It is hence difficult to draw a firm conclusion as to whether nucleotide binding could influence the Roc-COR – tubulin interaction.

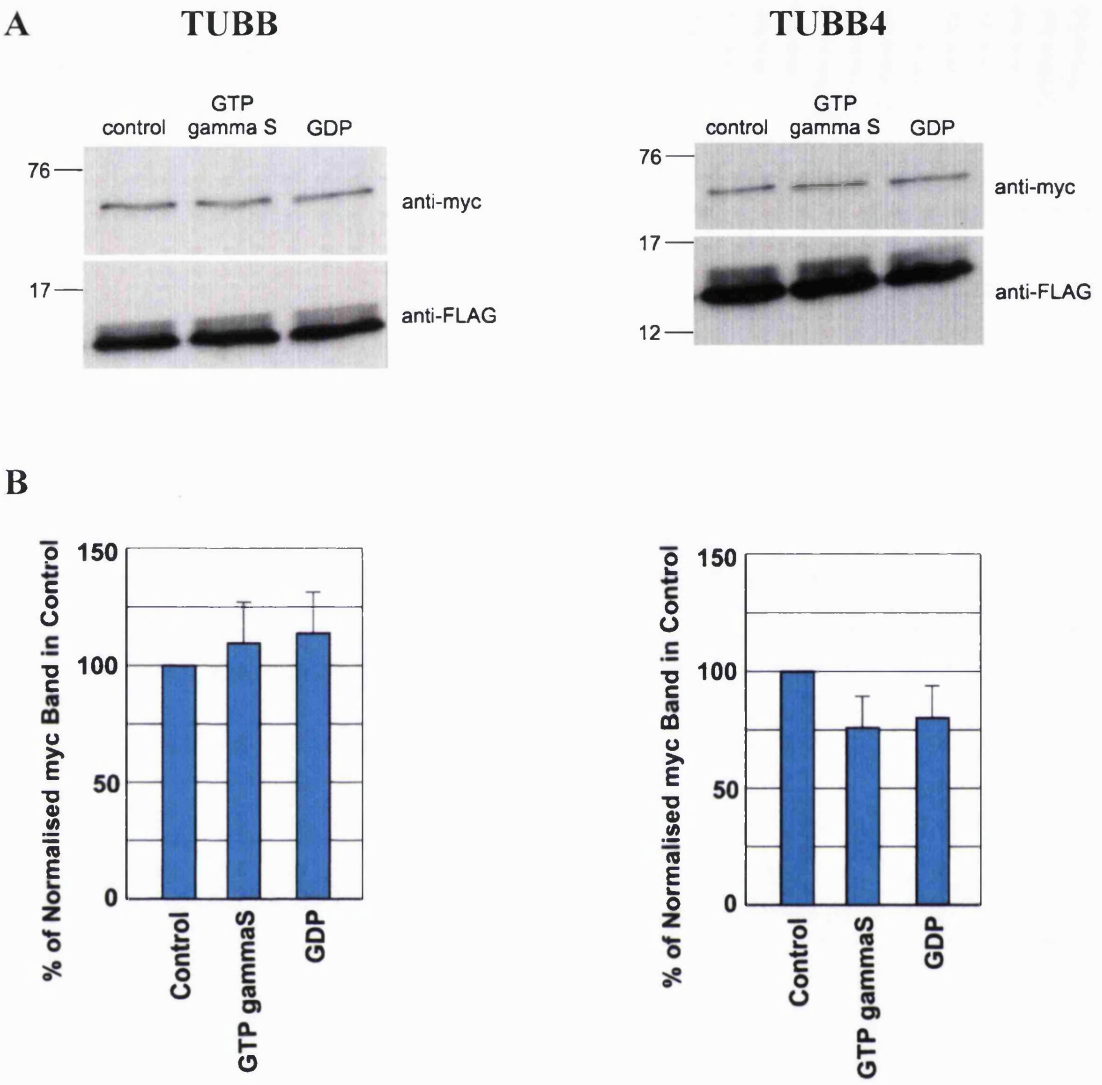

Figure 5.4: The effect of nucleotide binding on the Roc-COR – tubulin interaction. (A) The myc-tagged Roc-COR protein and the FLAG-tagged C-terminus of TUBB/TUBB4 were co-immunoprecipitated and the proteins were analysed on a western blot. The numbers on the left of the panels show the molecular weight in kDa. The upper panel shows the membranes probed with rabbit anti-myc antibody for the detection of the Roc-COR protein. The lower panel shows the membranes probed with rabbit anti-FLAG antibody for the detection of tubulin. Lane 1 shows the immunoprecipitated protein of the control sample, in which no nucleotides were added during the incubation step. Lane 2 shows the immunoprecipitated protein of the sample incubated in the presence of 5 μM GTP-γS. Lane 3 shows the immunoprecipitated protein of the sample incubated in the presence of 5 μM GDP. (B) Quantitative analysis of four independent experiments showed no significant influence of the addition of

nucleotides on the interaction between LRRK2 and tubulin. Statistical significance was determined using the unpaired, two-tailed Students' T test (n = 4).

5.6 Discussion

5.6.1 Influence of GTP Binding to LRRK2 on Protein Interactions

Previous findings showed the regulatory relationship between LRRK2 GTPase and kinase activities, and the importance of LRRK2 kinase activity for cytotoxicity. Recent work was carried out to investigate the effect of *PARK8* mutations on GTP binding activity, although conflicting data were generated. One group reported that the R1441C mutation led to an increase in GTP binding (West *et al,* 2007), while others found that this mutation had no effect (Guo *et al,* 2007; Lewis *et al,* 2007). My YTH results suggested that the abolition of GTP binding to the Roc domain of LRRK2 could completely inhibit the interaction between the Roc-COR domain of LRRK2 and the examined protein interactors. This indicates that GTP binding is not only important for LRRK2 kinase activity, but also the ability of LRRK2 to interact with other proteins. This raises a question: Could the GTP binding activity and the ability of LRRK2 to interact with proteins be linked together in a chain of events that lead to neurodegeneration? Previously, Webber and West (2009) proposed a model of LRRK2 activation. GTP binding might induce a conformational change allowing the Roc domain to be juxtaposed to the kinase domain, which might cause autophosphorylation of the Roc domain. This could stabilise the dimeric, kinase-active form of LRRK2, as well as enabling it to interact with other proteins. If this is true, GTP binding should be important in Roc-COR dimerisation, and abolition should have a significant impact on this event. My data on the effect of the abolition of GTP binding on Roc-COR dimerisation has shed light on this speculation, by showing that the K1347A and T1348N mutations could significantly reduce the strength of Roc-COR dimerisation. Previously, Gotthardt *et al* (2008) showed that the Roc-COR protein extracted from *C. tepidum* was intact, in the presence of a GTP non-hydrolysable analogue, GppNHp, even when it was subjected to tryptic cleavage. This suggests that nucleotide binding results in the stabilisation of the Roc-COR protein. Gotthardt *et al* (2008) speculated that this stabilisation helps keeping the COR domain intact, which was thought to be

crucial for Roc-COR dimerisation. In other words, LRRK2 GTP binding appears to favour Roc-COR dimerisation, possibly by keeping the COR domain intact. My data provided further evidence for the importance of LRRK2 GTP binding in Roc-COR dimerisation using a yeast model.

My Q-YTH data showed that the GTP binding deficient K1347A and T1348N Roc-COR domain mutants caused a reduction in the interaction strength between the Roc-COR domain and tubulin to less than 5% of the strength of the WT Roc-COR – tubulin interaction. However, the significantly lowered interaction strength could perhaps be due to the potential of these mutations to alter the conformation of the Roc-COR protein significantly enough to abolish interaction with other proteins like tubulin. In order to eliminate this possibility as the cause of the abolition of protein interaction, a co-IP experiment was carried out to test for the strength of the Roc-COR – tubulin interaction in the presence of GTP-γS or GDP. The interaction level of the GTP-bound and GDP-bound states of the Roc-COR protein with TUBB and TUBB4 were compared to that of the unbound state of the Roc-COR protein with these β-tubulin isoforms. However, a firm conclusion could not be drawn from the co-IP experiment, as various outcomes were obtained from the repeat trials of the experiment. This could be due to the fact that co-IP is at best a semi-quantitative method and might have therefore not allowed us to see small changes in interaction strength conferred by adding additional nucleotides during co-IP. Quantification of immunoreactivity on western blots is influenced by capillary transfer of proteins from the gel to the membrane, distribution of the primary and secondary antibodies during the antibody incubation steps, and distribution of the substrate of the horse radish peroxidase enzyme on the membrane. Variations in these factors during the repeat experiments might have prevented the observation of small changes. A quantitative method to analyse the effect of nucleotide binding on the Roc-COR – tubulin interaction more reliably in the future would be the use of the BIAcore analysis. The use of this technique can provide information on both the interaction strength and the association and dissociation rates of protein interactions.

In conclusion, my results and published data suggest the importance of guanosine nucleotide binding for LRRK2 activity through effects on LRRK2 protein dimerisation, GTPase activity, kinase activity and possibly interaction with heterogenous proteins.

5.6.2 The Effect of LRRK2 Autophosphorylation on Protein Interactions

Upon the unravelling of autophosphorylation sites in the Roc domain (Greggio *et al,* 2009; Kamikawaji *et al*, 2009; Gloeckner *et al*, 2010), it became increasingly evident that LRRK2 activation could involve autophosphorylation of the Roc domain. As I already showed that the Roc domain is responsible for the interaction of LRRK2 with TUBB and TUBB4 and phosphorylation is likely to change the conformation of proteins significantly enough to alter protein interactions, it is tempting to speculate that the autophosphorylation of the Roc domain of LRRK2 could affect interaction with tubulin. Here, the effect of Roc autophosphorylation on the Roc-COR – tubulin interaction was examined. Since Greggio *et al* (2009) and Kamikawaji *et al* (2009) had identified T1343 and T1491 as potential autophosphorylation sites in the Roc domain, threonine to aspartate mutations were introduced at these two sites to mimic the negative charge of the phosphoryl group. Interestingly, both mutants exhibited a clear decrease in the strength of interaction with both tubulin isoforms. Their respective phosphorylation-deficient mutants T1343A and T1491A had relatively little effect on the strength of Roc-COR interaction with tubulin, in comparison to the WT Roc-COR domain. This indicates that Roc autophosphorylation decreases the ability of LRRK2 to interact with tubulin, and could potentially cause the detachment of LRRK2 from microtubules. This raises an interesting question: Could Roc autophosphorylation and LRRK2 activation play a role in the release of LRRK2 from microtubules to terminate a potential effect of LRRK2 on microtubules? Greggio *et al* (2009) suggested that the G2019S mutation, whilst causing increased Roc autophosphorylation, could perhaps lead to a decrease in the Roc GTPase activity and prolong the activation of LRRK2 kinase activity. This could also potentially cause hyperphosphorylation on LRRK2 substrates. Potential LRRK2 substrates are MAPs, such as tau. Although no direct interaction between LRRK2 and tau has been proven (Smith *et al,* 2005), hyperphosphorylated tau was found upon over-expression of mutant LRRK2 (Lin *et al,* 2010; Melrose *et al,* 2010). These data indicate that the increased kinase activity of mutant LRRK2 could perhaps lead to increased MAP phosphorylation via the activation of certain signalling pathways. Thus, I hypothesise that *PARK8* mutations such as G2019S and I2020T increase Roc autophosphorylation (West *et al,* 2005; Gloeckner *et al,* 2006), and over-ride the negative feedback mechanism of LRRK2 activity described

in section 1.3.2 by some unknown mechanism, causing alterations in LRRK2 activity. Meanwhile, increased autophosphorylation of the Roc domain could also result in a prolonged detachment of LRRK2 from microtubules, rendering it free to interact with proteins involved in MAP phosphorylation. This might affect the phosphorylation state of certain MAPs and hence microtubule stability. Other PD mutations such as the R1441C/G mutants could also lead to neurodegeneration through a decrease in GTPase activity, prolonging GTP binding and autophosphorylation of LRRK2 (Greggio *et al,* 2009). This might cause a prolonged detachment of LRRK2 from microtubules, rendering it free to interact with, as well as prolong the activation of proteins in some signalling pathways that potentially result in microtubule destabilisation. As mentioned, microtubule instability could cause problems in the axonal transport of proteins, and could potentially affect neuronal function and survival. In particular, the transport of dopamine-containing vesicles could be hampered, which might result in the development of oxidative stress and potentially trigger apoptosis (Lennon *et al,* 1991).

Could the decrease in LRRK2 – tubulin interaction be caused by a decreased ability of Roc-COR dimerisation? My Q-YTH data showed that both the phosphorylation-deficient and phosphomimetic mutants had no effect on the strength of Roc-COR dimerisation. This suggests that the decrease in the strength of the Roc-COR – tubulin interaction is not due to an effect of LRRK2 Roc autophosphorylation on the ability of the Roc-COR domain to dimerise.

In conclusion, GTP binding to the Roc domain of LRRK2 is an essential process for LRRK2 to interact with proteins including tubulin. It is likely that GTP binding facilitates the dimerisation of the Roc-COR domain, which in turn enables the dimer to interact with heterogenous protein interactors. On the other hand, autophosphorylation of the Roc domain of LRRK2 affects the ability of LRRK2 to interact with tubulin, by a mechanism independent of Roc-COR dimerisation strength.

In these first three result chapters of the thesis, the characterisation of the LRRK2 – tubulin interaction was mainly performed by the over-expression of proteins in cells. The endogenous expression and the distribution of LRRK2 in cultured cells were subsequently investigated and described in chapter 6.

6. Endogenous Expression and Sub-cellular Localisation of LRRK2

The expression of LRRK2 in human cells had been widely studied in the last few years. LRRK2 was found to be ubiquitously expressed (section 1.3.4). However, it is unclear whether LRRK2 is expressed endogenously in cell models used in PD research, such as the human neuroblastoma cell line SH-SY5Y.

LRRK2 was shown to associate with microtubules and membranous structures like synaptic vesicles (West *et al,* 2005; Biskup *et al,* 2006). After I showed a direct interaction of LRRK2 with tubulin, I proceeded to investigate the association of LRRK2 with microtubules in human cell lines.

This chapter of the thesis focuses on the endogenous expression of LRRK2 in the human cell lines HEK293 and SH-SY5Y, both at the transcriptional and the translational levels. The relative expression level of LRRK2 was also compared between non-differentiated SH-SY5Y and differentiated SH-SY5Y cells, in order to find out whether endogenous LRRK2 expression changes during the course of neuronal differentiation. Furthermore, the association of LRRK2 with microtubules was assessed in differentiated SH-SY5Y cells using immunocytochemical techniques, in order to visualise the direct interaction between LRRK2 and microtubules.

6.1 Expression of LRRK2 in Human Cell Lines at the Transcriptional Level

The first step to show the endogenous expression of LRRK2 in HEK293 and SH-SY5Y cells was to assess LRRK2 expression in these cells at the transcriptional level. The total RNA of HEK293 and non-differentiated and differentiated SH-SY5Y cells was first extracted as described in section 2.5.1, and converted into cDNA. Both the 5'-UTR and 3'-UTR were amplified using the primers shown in table 2.7 and Pfx Accuprime with PCR conditions detailed in section 2.1.1. The PCR products were run in a 2% agarose gel. The results presented in figure 6.1 showed that the HEK293 cells, non-differentiated SH-SY5Y cells and differentiated SH-SY5Y cells all expressed LRRK2 at the transcriptional level, as indicated by the presence of the PCR products of both the 5'-UTR and 3'-UTR of LRRK2. Furthermore, it appeared that the presence of LRRK2

mRNA was more prominent in HEK293 cells than in SH-SY5Y cells. The difference in the intensity of the DNA bands between the HEK293 and SH-SY5Y cells appeared clearer for 3'-UTR LRRK2 amplification. This indicates that embryonic kidney cells might express more LRRK2 than dopaminergic neurons at the transcriptional level.

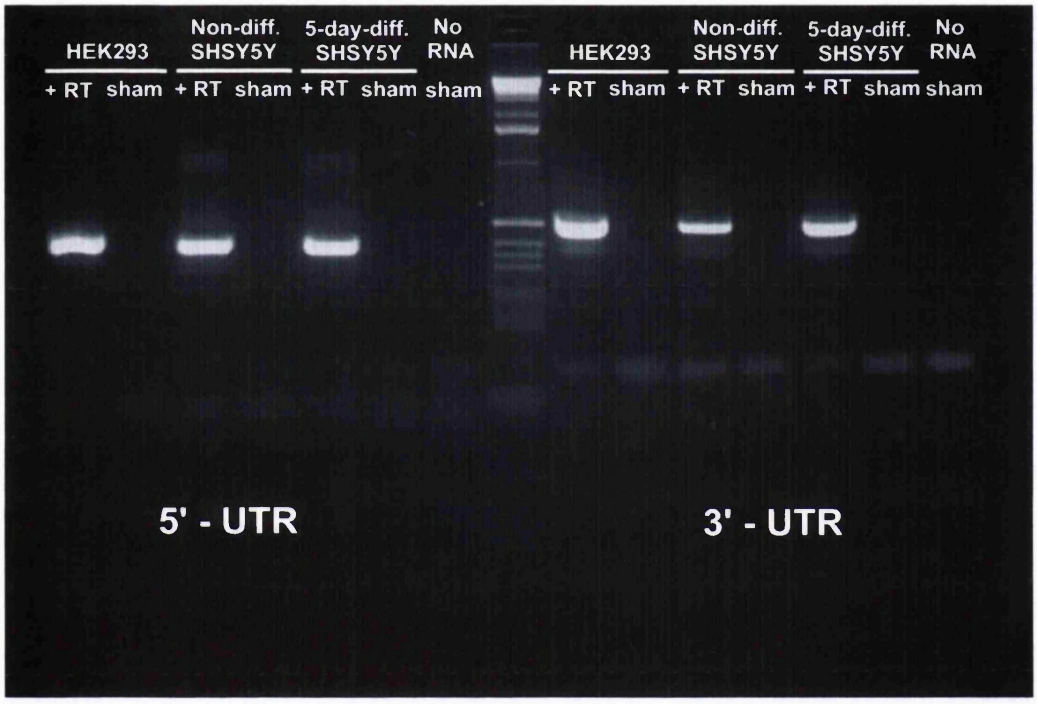

Figure 6.1: Endogenous LRRK2 expression is present at the transcriptional level in HEK293 cells and SH-SY5Y cells. The expression of LRRK2 in HEK293 cells, non-differentiated and 5-day-differentiated SH-SY5Y cells at the transcriptional level was confirmed by the presence of PCR product upon the amplification of the 5'- and 3'-UTRs of LRRK2 from cDNA, indicating the presence of LRRK2 mRNA in these cells. The stronger band in the HEK293 lane indicates a higher level of LRRK2 expression in the kidneys than in neurons. 'Sham' indicates the negative control where the extracted RNA from the cells was not treated with reverse transcriptase. 'RT' indicates reverse transcriptase.

In order to confirm the difference in LRRK2 expression level between HEK293 and SH-SY5Y cells, the expression level was quantified by employing the RQ-PCR

technique. The cDNA was subjected to PCR amplification, as detailed in section 2.5.3. The RQ-PCR results shown in figure 6.2 are expressed in terms of the percentage of the expression of the GAPDH housekeeping gene. It appeared that the expression level of LRRK2 was much lower than that of GAPDH in both HEK293 and SH-SY5Y cells. Furthermore, the RQ-PCR data (figure 6.2) provided quantitative evidence for a lower LRRK2 expression level in SH-SY5Y cells as shown in figure 6.1. Interestingly, LRRK2 expression level in differentiated SH-SY5Y cells appeared higher than that of non-differentiated ones. This suggests that the SH-SY5Y cells seemed to express slightly more LRRK2 during neuronal differentiation. Taken together, LRRK2 expression level was found to differ depending on cell line and stage of differentiation.

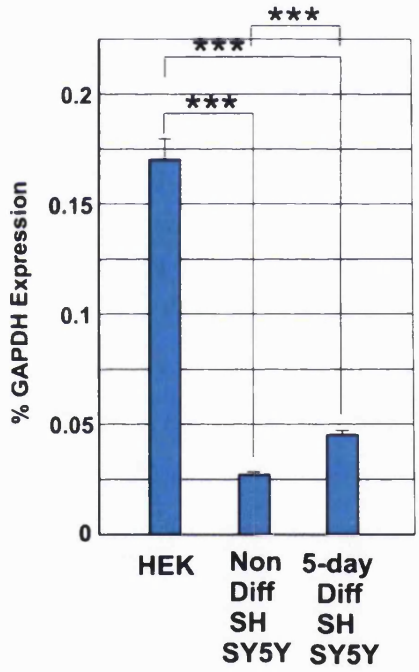

Figure 6.2: Quantitative comparison of endogenous LRRK2 expression in HEK293, non-differentiated and differentiated SH-SY5Y cells. The endogenous expression of LRRK2 in HEK293 and SH-SY5Y cells was quantitatively assessed by RQ-PCR. The level of expression is expressed in terms of the percentage of expression level of the housekeeping gene GAPDH in these cells. LRRK2 expression in HEK293 cells was considerably higher than that in SH-SY5Y cells. Furthermore, differentiated SH-SY5Y cells expressed significantly more LRRK2 than the non-differentiated SH-SY5Y cells. (*** $P < 0.001$, $n = 3$)

6.2 LRRK2 Protein Expression in Human Cell Lines

The presence of mRNA of LRRK2 in both HEK293 and SH-SY5Y cells could indicate the presence of expression of LRRK2, but LRRK2 expression at the translational level in these cells is yet to be confirmed. A western blot of the cell lysates from HEK293 cells, non-differentiated and differentiated SH-SY5Y cells was performed to assess the relative amount of LRRK2 protein present in the cells.

In order to better understand the changes of LRRK2 expression during SH-SY5Y differentiation, I decided to determine the changes of LRRK2 expression at the translational level through a time course of differentiation. Cell lysates of SH-SY5Y cells were obtained as described in section 2.5.4 after 3, 5 and 7 days of differentiation. The cell lysates were run in an SDS-PAGE gel. Western blotting was performed before probing the membrane with an anti-LRRK2 antibody (Everest Biotech Limited), recognising a region close to the C-terminus of LRRK2. The antibody was used at a dilution of 1:2500. In order to ensure that the antibody recognises LRRK2, an additional dish of HEK293 cells were transfected with the pRK5 myc full length LRRK2 construct (section 2.3.9). The lysate of these cells was run alongside the lysates of the non-transfected HEK293 and SH-SY5Y cells in the gel. If the antibody recognises LRRK2, the position of the protein bands of the non-transfected HEK293 and SH-SY5Y cells on the blot should appear the same as that of the transfected HEK293 cells.

The blot shown in figure 6.3 seemed to suggest a higher abundance of LRRK2 protein in the SH-SY5Y cells than in HEK293 cells, which was in contrast to the data showing LRRK2 expression at the transcriptional level. Furthermore, multiple bands appeared on the lane for the lysate taken from SH-SY5Y cells differentiated for 7 days. This could perhaps suggest a degradation of LRRK2 happening over the course of 7 days of differentiation, forming species that are smaller than the full length LRRK2. However, the position of the protein band for the transfected HEK293 cells appeared different from that of the other bands. There were two bands in the transfected HEK293 lane. The thicker one seemed to correspond to the full length LRRK2 protein, as it was present in abundance due to over-expression. This band was in a different position of the blot from the ones in the lanes for the lysates of the non-transfected cells. This suggests that the

anti-LRRK2 antibody from Everest Biotech Limited used in the experiment is unlikely to be recognising the endogenous LRRK2. Hence, the results were likely to be unreliable and a firm conclusion could not be made from these data.

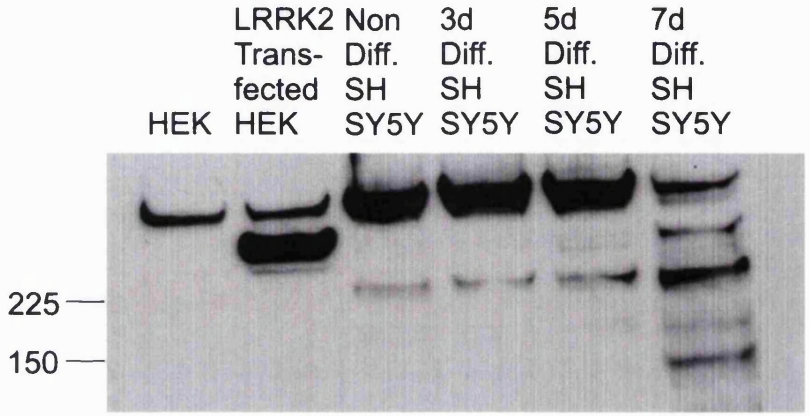

Figure 6.3: LRRK2 appears to be expressed in HEK293 and SH-SY5Y cells at the translational level. The lysates of the HEK293 and SH-SY5Y cells were subjected to western blotting for the detection of LRRK2 expression in these cells using an anti-LRRK2 antibody from Everest Biotech Limited at a 1:2500 dilution. The numbers shown on the left of the blot show the molecular weight in kDa. The band for the over-expressed LRRK2 appeared at a different position from those of the endogenous LRRK2 bands detected by the antibody, indicating that this antibody might not recognise endogenous LRRK2. (3d indicates 3 days, 5d indicates 5 days and 7d indicates 7 days after RA treatment to induce neuronal differentiation).

Recently, five monoclonal anti-LRRK2 antibodies produced by the Michael J Fox Foundation had become available, a generous gift from the Michael J Fox Foundation. These antibodies are referred to as MJFF antibodies hereafter. HEK293 and SH-SY5Y cell lysates were processed as above and probed with the MJFF antibodies at a 1:2000 dilution. However, no protein bands were detected, indicating that either the antibodies fail to detect endogenous LRRK2 or the protein extraction protocol was not compatible with the use of the MJFF antibodies. The protein extraction protocol was then modified to troubleshoot the problem. The amount of lysis buffer used was decreased to 500 µl,

as the failure of endogenous LRRK2 detection could be due to low LRRK2 expression levels in HEK293 and SH-SY5Y cells. However, the decrease in the volume of lysis buffer used had no effect on endogenous LRRK2 detection. Hence, another protocol of protein extraction was employed, which was adapted from Taymans *et al* (http://www.michaeljfox.org). They showed that LRRK2 appeared to be expressed endogenously in HEK293 and SH-SY5Y cells using the MJFF antibodies. The protocol involved lysing the cells using a buffer containing 0.1 % (v/v) SDS and 1x complete mini protease inhibitor. The cells were scraped and the lysate was transferred to a microcentrifuge tube. The contents were boiled at 95°C for 5 minutes. The boiled contents were homogenised by passing it through a 25G needle ten times. The homogenised lysate was boiled again for 3 minutes before running in a gel. The lysates were probed with the MJFF antibody at a 1:100 dilution. However, no protein bands were detected using this adapted protocol of protein extraction. The reason for the failure of LRRK2 detection is yet to be determined.

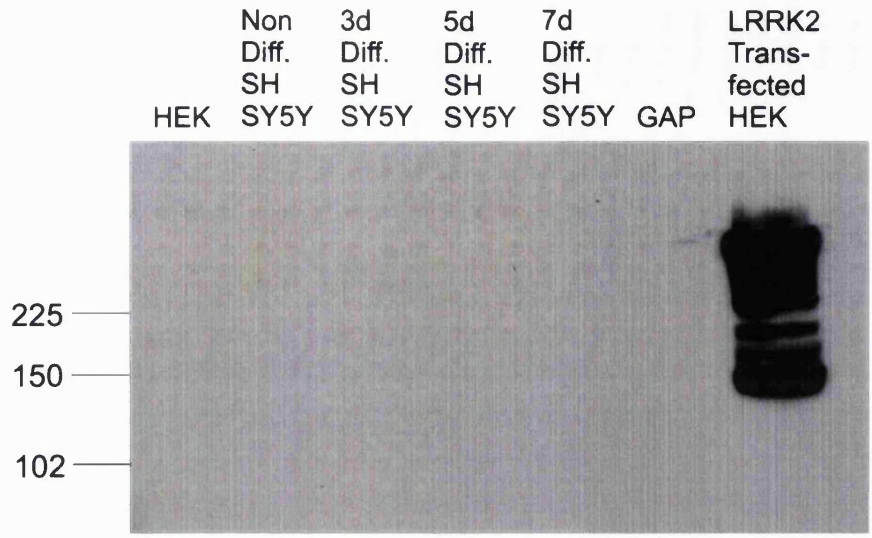

Figure 6.4: Endogenous LRRK2 protein expression was not detected using an anti-LRRK2 antibody from the Michael J Fox Foundation. The lysates of the HEK293 and SH-SY5Y cells obtained using the protein extraction protocol adopted from Taymans *et* al, (2010) were subjected to western blotting for the detection of LRRK2 expression in these cells using an anti-LRRK2 antibody from the Michael J Fox Foundation at a 1:100 dilution. The numbers shown on the left of the blot show the molecular weight in kDa. LRRK2 over-expression was detected by this antibody in HEK293 cell lysates, but endogenous LRRK2 was not detected in either HEK293 or SH-SY5Y cell lysates. (3d indicates 3 days, 5d indicates 5 days and 7d indicates 7 days after RA treatment to induce neuronal differentiation, GAP indicates the lane left unloaded).

6.3 The Association of LRRK2 with Neuronal Microtubules

The interaction between LRRK2 and tubulin in yeast and mammalian cell models were presented in previous chapters. In order to visualise the direct association of LRRK2 with microtubules, immunocytochemical experiments were performed on differentiated SH-SY5Y cells.

The first step was to visualise the association of over-expressed LRRK2 and microtubules in SH-SY5Y cells differentiated for 5 days by RA treatment. The cells

were transfected with the myc-tagged full length LRRK2 construct as shown in section 2.3.12 on the third day of differentiation. Cytoskeletal protein fixation was then employed in fixing the cells, so as to visualise only proteins associated with the cytoskeleton and extract all other proteins. The fixed cells were co-stained with the following two molecules. First, the anti-myc antibody (1:100 dilution) for the detection of over-expressed LRRK2. Second, the anti-acetylated tubulin antibody (1:200 dilution) for the detection of stable microtubules. In fact, acetylation was suggested to be one of the post-translational modifications of tubulin performed by an enzyme called α-tubulin acetyltransferase (Maruta *et al,* 1986), and this modification was shown to take place primarily on stable microtubules (Cambray-Deakin and Burgoyne, 1987). Furthermore, the co-stain would allow us to visualise the association of LRRK2 with stable microtubules.

Figure 6.5A – 6.5I shows the co-staining of over-expressed LRRK2 and endogenous acetylated tubulin. LRRK2 expression was seen in only a proportion of the cells. Interestingly, cells stained positively for LRRK2 often did not show processes containing acetylated tubulin. The limited co-localisation of over-expressed LRRK2 and acetylated tubulin suggests that the over-expression of LRRK2 could have a negative effect on the stability of microtubules. LRRK2 expression was present at a region that looked like a growth cone, which is indicated by a white arrow in figure 6.5D – 6.5F. In conclusion, over-expressed LRRK2 is associated with the cytoskeleton in differentiated SH-SY5Y cells but shows only limited co-localisation with stable microtubules.

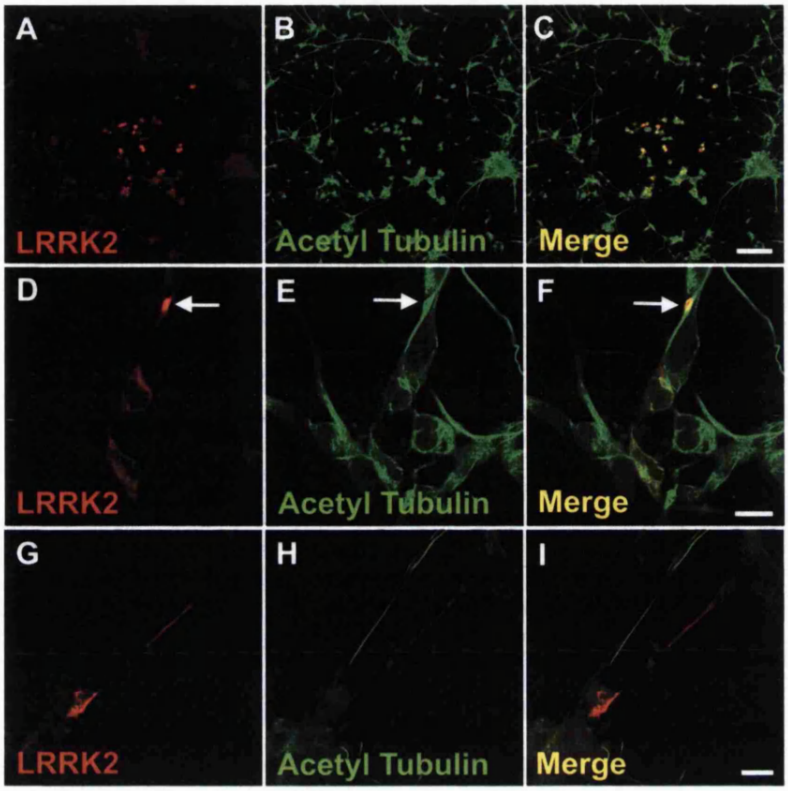

Figure 6.5: Over-expressed LRRK2 shows limited co-localisation with acetylated tubulin in differentiated SH-SY5Y cells. Immunocytochemical detection of over-expressed myc-LRRK2 and endogenous acetylated tubulin was performed using an anti-myc antibody and anti-acetylated tubulin antibody respectively on SH-SY5Y cells differentiated with RA for 5 days. (A-C) Cells over-expressing LRRK2 did not reveal acetylated-tubulin-positive processes. (D-F) Localisation of over-expressed LRRK2 in the growth cone of a differentiated SH-SY5Y cell. The white arrows indicate the position of the neuronal growth cone. (G-I) Over-expressed LRRK2 was found in neuronal processes that lacked immunoreactivity for acetylated tubulin almost completely, while acetylated tubulin was detected in processes without over-expressed LRRK2. (Scale bar: 100 μm (A-C), 10 μm (D-F), 20 μm (G-I))

After establishing the sub-cellular localisation of over-expressed LRRK2 in differentiated SH-SY5Y cells, I then used the same cytoskeletal fixation protocol to examine endogenous expression of LRRK2. Fixed, differentiated SH-SY5Y cells were stained for the presence of endogenous LRRK2 and stable microtubules using MJFF

antibodies (1:25 dilution) and anti-acetylated tubulin antibody (1:200 dilution) respectively in the first instance. As I observed very limited co-localisation of LRRK2 and acetylated tubulin as already shown for over-expressed LRRK2, I co-stained for F-actin and tyrosinated tubulin to see whether endogenous LRRK2 co-localises with the actin cytoskeleton and unstable microtubules respectively.

For the detection of F-actin, a molecule called phalloidin, a specific interactor of F-actin (Cooper, 1987), was used. The phalloidin molecule was conjugated with a fluorophore called Alexa 635, which emits blue fluorescence. The triple staining utilising an MJFF antibody (1:25 dilution), anti-acetylated tubulin antibody (1:200 dilution) and Alexa 635-conjugated phalloidin (1:40 dilution) showed preferred co-localisation of endogenous LRRK2 with F-actin especially in growth cones (Figure 6.6A – 6.6D). The acetylated tubulin staining in figure 6.6B, as indicated by the blue arrow, showed microtubules that appeared curved. This is indicative of a growth cone, as microtubules were shown to play a role in growth cone turning in response to extracellular guidance cues (Williamson *et al,* 1996). Turning of the growth cone could be mediated by the ability of microtubules to change shape and form curved structures. These data indicated the presence of abundant LRRK2 at the growth cones of neurons. Interestingly, endogenous LRRK2 was also distributed along the distal neurites. Furthermore, as shown in figure 6.6E – 6.6H, some LRRK2 – acetylated tubulin co-localisation was observed in the distal neurites but very little co-localisation in proximal neurites.

I then asked whether LRRK2 also co-localises, to a greater extent, with unstable microtubules. In unstable microtubules, the α-tubulin subunits are tyrosinated. In fact, α-tubulin was shown to possess a tyrosine residue at the C-terminus (Valenzuela *et al,* 1981). When it is incorporated into microtubules, the tyrosine would be removed by the action of tubulin specific carboxypeptidase (Argarana *et al,* 1978), forming detyrosinated tubulin. It was found that when microtubules become unstable due to dynamic instability, the tubulin molecule could be re-tyrosinated by the action of tubulin tyrosine ligase (Raybin and Flavin, 1977). Thus, tyrosinated tubulin could be a sign of microtubule instability. In order to show whether LRRK2 co-localises with unstable microtubules, a triple staining was performed using the MJFF antibody (1:25 dilution), anti-acetylated tubulin antibody (1:200 dilution) and anti-tyrosinated tubulin

antibody (1:50 dilution). Tyrosinated tubulin staining was present in the distal neurites, showing good co-localisation with endogenous LRRK2 (Figure 6.6E – 6.6H). This indicates a preferential co-localisation of LRRK2 with tyrosinated tubulin over acetylated tubulin.

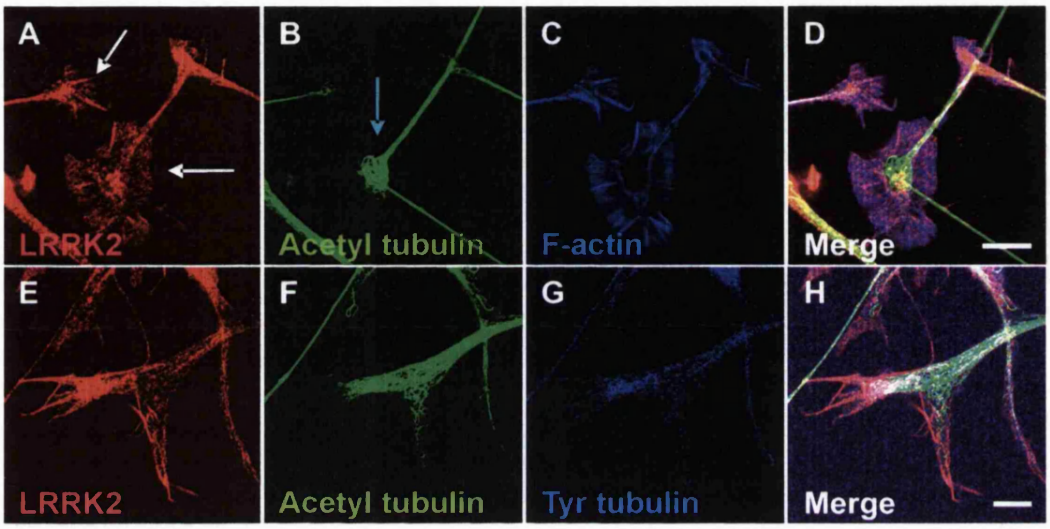

Figure 6.6: Endogenous LRRK2 shows a preferential co-localisation with tyrosinated tubulin and F-actin. Immunocytochemical staining for endogenous LRRK2 and tubulin using the MJFF anti-LRRK2 antibody, anti-acetylated tubulin or anti-tyrosinated tubulin antibodies, and Alexa 635-conjugated phalloidin on SH-SY5Y cells that were differentiated for 5 days. (A-D) Endogenous LRRK2 showed co-localisation with actin in the growth cone peripheral domain. The white arrows in (A) indicate the distal neurites in the growth cones. The blue arrow in (B) indicates the curved microtubules which are present at the growth cone. (E-H) Endogenous LRRK2 also showed co-localisation with tyrosinated tubulin, and to a lesser extent, acetylated tubulin. (A-H) Very little co-localisation of endogenous LRRK2 and acetylated tubulin was observed in proximal neurites, while some co-localisation was observed in the distal neurites. (Scale bar: 20 μm)

Taken together, endogenous LRRK2 appeared to be expressed at the actin and tubulin cytoskeleton in differentiated SH-SY5Y cells. Endogenous LRRK2 seemed to co-

localise preferentially with growing microtubules and F-actin in the distal neurites and the lamellipodial region of growth cones. The area where stable microtubules were present appeared to have little LRRK2 present. These data suggest a preferred localisation of LRRK2 to dynamic cytoskeletal components rather than stable microtubules, especially in proximal neurites.

6.4 Discussion

6.4.1 Endogenous Expression of LRRK2 in Human Cell Lines

Previous research into the characteristics of LRRK2 expression in humans revealed that LRRK2 is a ubiquitously expressed protein. Within the brain, LRRK2 expression was reported in many brain regions, including the SNpc and the caudate putamen (CP), the region innervated by the DA neurons from the SNpc. However, there were controversies over LRRK2 expression in these brain regions. Some groups reported that LRRK2 mRNA was present in the CP, but not in the SNpc (Galter *et al,* 2006; Melrose *et al,* 2006). Others revealed the presence of LRRK2 mRNA in DA neurons in the SNpc (Simón-Sánchez *et al,* 2006; Taymans *et al,* 2006; Han *et al*, 2008). The inconsistency in these findings could be explained, as suggested by Han *et al* (2008), by the low LRRK2 expression in neurons in these brain regions. My RQ-PCR data showed that the amount of LRRK2 mRNA in SH-SY5Y cells was considerably lower than that in HEK293 cells. This suggests that LRRK2 expression in neurons is likely to be lower than that in the kidneys. This is in agreement with the recent finding that LRRK2 expression in the kidney is much higher than that in the brain (Maekawa *et al,* 2010). My data provide further evidence that LRRK2 is expressed endogenously in neurons, albeit at low levels.

Furthermore, a higher amount of LRRK2 mRNA was observed in differentiated SH-SY5Y cells than non-differentiated ones. Since neurons become differentiated during development, my data hence suggested that LRRK2 expression increases during development. They also confirmed the previous findings by other research groups describing the presence of LRRK2 mRNA already during embryonic and early postnatal development (Westerlund *et al,* 2008; Zechel *et al,* 2010).

LRRK2 protein expression in human cell lines was then compared. Since some mRNAs, such as the c-myc mRNA, appear to have a short half-life (Herrick and Ross, 1994), the comparison would hence be more reliable if the amount of LRRK2 protein present in these cells was determined as well. The anti-LRRK2 antibody from Everest Biotech Limited was used to detect the endogenous proteins present in HEK293 and SH-SY5Y cells. However, the antibody appeared to recognise proteins that are of a higher molecular weight than the over-expressed LRRK2. It was reported that LRRK2 can form oligomers rather than dimers (Sen *et al,* 2009), but it is highly unlikely that the antibody recognised the oligomeric LRRK2, as the proteins were run in a denaturing gel, where the proteins were denatured before loading into the gel. It is hence likely that the anti-LRRK2 antibody from Everest Biotech Limited did not detect endogenous LRRK2. In light of this, another recently available MJFF antibody was used, which was shown by Taymans *et al* (http://www.michaeljfox.org) to recognise endogenous LRRK2. However, no protein bands were obtained on the western blot with the use of this antibody. It is unclear why this antibody yielded no protein bands on the blot, with the use of the modified protocol of protein extraction. This could be due to technical difficulties during the protein extraction procedures.

In conclusion, the RQ-PCR data revealed a significantly lower level of LRRK2 expression, at the transcriptional level, in SH-SY5Y cells, in comparison to the HEK293 cells. This suggests a lower LRRK2 expression in neurons than in kidneys. Differentiation of neurons also seemed to coincide with increased LRRK2 expression. This suggests that LRRK2 expression might increase during development.

6.4.2 LRRK2 Localisation at the Cytoskeleton in SH-SY5Y Cells

Previously, LRRK2 was found in dendrites and axons of the rat cortical neurons in immunocytochemical experiments (Biskup *et al,* 2006), implying a co-localisation of LRRK2 with microtubules due to the presence of microtubules in dendrites and axons. More recently, LRRK2 was suggested to be an interactor of microtubules as the Roc domain of LRRK2 was found to directly interact with heterodimers of α- and β-tubulin using co-IP experiments (Gandhi *et al,* 2008). LRRK2 was also reported to phosphorylate β-tubulin (Gillardon, 2009). Previously, Gandhi *et al* (2008) indicated a

co-localisation of LRRK2 with α- and β-tubulin in rat hippocampal neurons. Here, my data showed a preferential co-localisation of endogenous LRRK2 with unstable growing microtubules, especially in distal neurites and the peripheral domain of growth cones. There was however some co-localisation between endogenous LRRK2 and the stable, acetylated microtubules in distal neurites. Furthermore, over-expressed LRRK2 showed hardly any co-localisation with acetylated tubulin, suggesting that over-expressed LRRK2 might lead to microtubule destabilisation. This speculation, however, is in contrast to that made by Gillardon, who suggested that LRRK2 could be involved in the stabilisation of microtubules through phosphorylation of tubulin in the presence of MAPs (Gillardon, 2009). This discrepancy could be explained by the difference in the methods in determining the stability of microtubules. Gillardon utilised the rate of tubulin polymerisation as a parameter to indicate microtubule stability. I instead used the acetylation of tubulin in the microtubules as a parameter to do so. In fact, previous work had shown the ability of LRRK2 to affect neurites in primary rat cortical neurons. Knockdown of LRRK2 by siRNA interference in those neurons led to an increase in neurite length and branching (MacLeod *et al,* 2006). This indicates that LRRK2 could lead to a decrease in neurite length and branching, possibly by affecting the dynamic instability of microtubules. Furthermore, recent evidence had shown that hippocampal and midbrain neuronal cultures derived from LRRK2 knockout mice displayed more extensive neuronal arborisation than those derived from LRRK2 transgenic mice (Dächsel *et al,* 2010), suggesting that LRRK2 could possibly prevent the polymerisation of tubulin subunits into microtubules, subsequently leading to a decrease in the growth and branching of neurites. Hence, it seems more likely that LRRK2 plays a role in microtubule destabilisation.

My data also showed that endogenous LRRK2 was enriched in growth cones. Growth cones are regions in neurons where the distal ends of microtubules are located. Since growth cones might play a role in responding to extracellular guidance cues and trophic factors (Dickson, 2002), the microtubules in this region require dynamic instability for the growth cone to turn in response to these guidance cues. The more abundant presence of LRRK2 in the growth cones than in proximal neurites suggests that LRRK2 might lead to the instability of microtubules required for neurite growth or that LRRK2 preferentially co-localises with these structures to fulfill a role in growth cone

signalling. As co-localisation between LRRK2 and F-actin was also observed in growth cones, LRRK2 might influence the actin cytoskeleton as well.

The focus of the data presented in the previous result chapters is mainly on the molecular interactions, expression and distribution of LRRK2 in cells. In the final result chapter, the focus will shift from the molecular aspects of LRRK2 to the clinical aspects. This is another important avenue of LRRK2 research, which involves the search for new *PARK8* mutations present in PD patients. The discovery of new mutations might provide a platform in the search for the molecular mechanisms of how mutant LRRK2 contributes to PD pathogenesis.

7. Mutation Scanning of the *PARK8* Gene

Mutation scanning has been routinely used in the search for mutations or SNPs present within a gene. One of the applications is the scanning of DNA samples obtained from patients suffering from a disease for mutations present in a certain gene. The inheritance of mutations in some genes could be one of the causes of inheritable diseases such as PD. Previously, some genes were determined to be associated with PD pathogenesis. These are collectively known as '*PARK* genes'. *PARK8*, the gene encoding LRRK2, was discovered to be a '*PARK* gene' in 2004 (Paisán-Ruíz *et al*, 2004). Since then, a number of mutations have been found in *PARK8* that segregate with PD (section 1.3.5). Mutation scanning of *PARK8* in PD patients is currently underway in the hope to discover more PD-associated *PARK8* mutations. This search is one of the important branches of PD research, as further discovery of *PARK8* mutations could provide further information in the way that LRRK2 is involved in PD pathogenesis. The work presented in this chapter involves the use of mutation scanning and sequencing technology in the search for additional mutations present in the *PARK8* gene in the DNA samples of PD patients obtained from the Imperial Parkinson's Disease Society Brain Bank (Imperial Brain Bank).

7.1 Mutation Scanning of the Imperial Brain Bank DNA Samples

106 DNA samples obtained from the Imperial Brain Bank were subjected to mutation scanning of *PARK8* using the LightScanner instrument. Exons 31 and 35 were chosen for the scan as they house the triplet codes for the R1441 and Y1699 residues respectively. The procedures for the use of the instrument are detailed in section 2.6.1. DNA samples from four 'Coriell PD patients' (Coriell Institute of Medical Research, http://www.coriell.org) without mutations in exon 31 and 35 were used as control samples. In addition, eight of the samples from the Imperial Brain Bank were also sequenced in case all of the 'Coriell samples' contain amino acid differences in both exons.

Each sample was scanned in duplicates to ensure reproducibility of the scan results. Samples giving different melting profiles in the duplicate scans could possibly be

artefacts. These samples were sent for DNA sequencing, in order to ensure no mutations were present in the respective exon within these DNA samples.

7.1.1 Mutation Scanning in LRRK2 Exon 31

The DNA samples from the Imperial Brain Bank were first scanned for amino acid differences in exon 31 of *PARK8* (219 base pairs). Each sample was assigned a number for identification. Hereafter, the samples will be named as 'Im' followed by the assigned number. For example, Im 1 refers to sample number 1 from the Imperial Brain Bank. In addition to the 'Imperial samples', one 'Coriell sample' named Coriell ND01275 was included in the scan as a negative control due to the absence of mutations in exon 31 in this sample.

20 ng of the DNA samples were mixed in a black-body, white-well 96-well plate with 10 μM of the forward and reverse primers for exon 31 amplification and the LightScanner mastermix containing the LCGreen. The plate was loaded into a thermal cycler for PCR amplification as detailed in section 2.6.1. After PCR, the plate was loaded into the LightScanner instrument after a brief spin. A DNA melting profile was generated by the instrument, showing the denaturation of DNA as temperature increases. As shown in figure 7.1A, Im 1 was revealed to have a different melting behaviour from the other samples, including the negative control. Both of the duplicates of this sample showed the same outcome. This indicates that Im 1 probably contains a mutation or SNP in exon 31 of *PARK8*. This sample was hence used as a positive control in the next batches of sample analysis. In the second batch of DNA samples, Im 93 showed a different melting profile from that of the control, despite the fact that only one of the duplicates appeared to have a different profile (figure 7.1B). However, some of the samples in the last batch, including Im 125, Im 158 and Im 171, gave aberrant melting profiles showing great fluctuations (figure 7.1C). It is unclear as to how these fluctuations were generated, but they were likely to be artefacts. I also observed a slight variation in the melting profile of Im 207 from those of the negative control and the other samples. In order to ensure that the samples giving aberrant DNA melting profiles did not contain an amino acid difference, samples Im 1, Im 93, Im 125, Im 158, Im 171 and Im 207 were all sent for DNA sequencing of exon 31. The sequences were then

compared with the consensus sequence of LRRK2 exon 31 to ensure no amino acid differences are present within the exon.

7.1.2 Mutation Scanning in LRRK2 Exon 35

After the scan for mutations in exon 31 was performed, all 'Imperial samples' were subjected to a further scan for mutations in exon 35 (155 base pairs). The DNA samples were mixed with the LightScanner mastermix and the forward and reverse primers for the amplification of exon 35 before loading into the LightScanner instrument. For exon 35 scanning, Im 4 was used as a negative control. Figure 7.2A shows that all of the Imperial samples in the first batch gave similar DNA melting profiles. The second batch, however, contained two samples that gave aberrant profiles with great fluctuations, Im 99 and Im 125 (figure 7.2B). In the case of Im 125, both duplicates gave aberrant melting profiles. In the third batch (figure 7.2C), Im 145 and Im 222 gave different melting profiles compared to that of the negative control. However, only one of the duplicates of both samples gave this aberrant melting profile. In other words, with the exception of Im 125, none of the samples had both the duplicates giving a different melting profile compared to that of the control sample in the exon 35 scan. Hence, Im 99, Im 125, Im 145 and Im 222 were sent for DNA sequencing of exon 35.

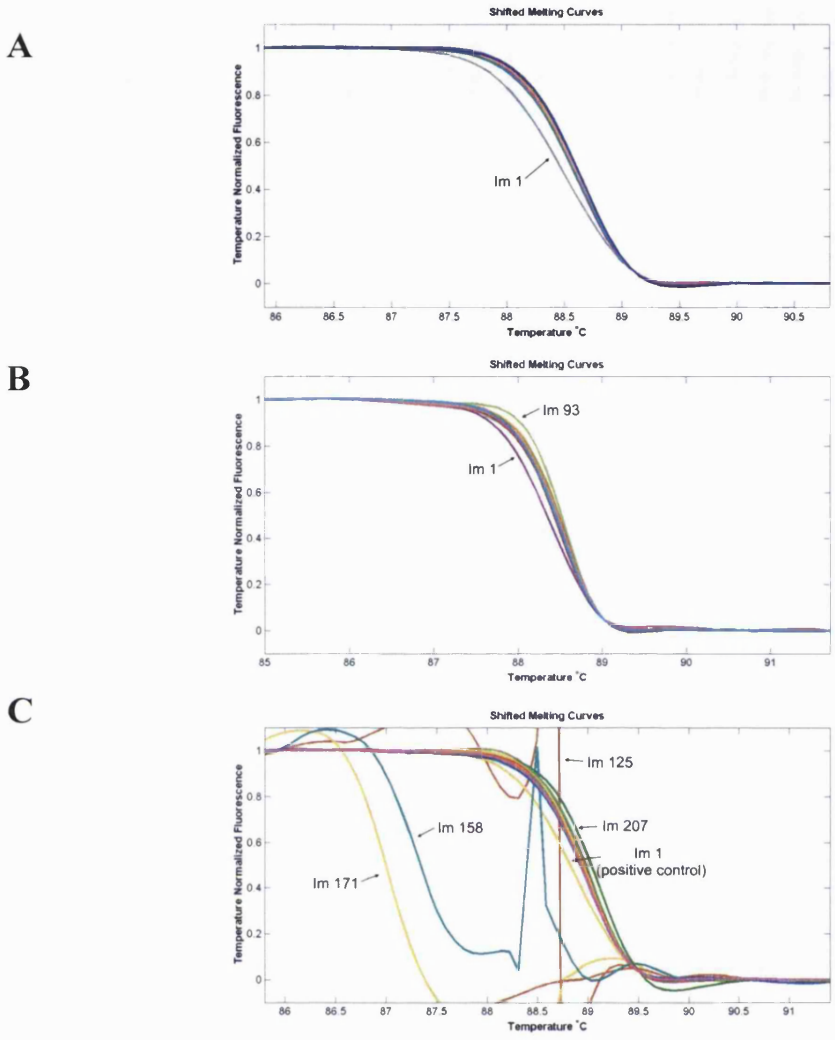

Figure 7.1: DNA melting profiles obtained from the LRRK2 Exon 31 scan of the DNA samples from the Imperial Brain Bank. The DNA samples were subjected to mutation scanning in the LightScanner and the results are presented in the form of DNA melting curves. (A) The first batch of the DNA samples (32 samples) was scanned. Im 1 appeared to have a mutation or SNP within exon 31 of LRRK2. The blue and grey curves represent the DNA melting curves for the duplicate experiments of Im 1. (B) The second batch of the DNA samples (35 samples) was scanned, and Im 1 was used as the positive control. One of the melting curves of Im 93, indicated by the light green curve, appeared different from the other melting curves, including that of the negative control. (C) The third batch of the DNA samples (39 samples) was scanned. Im 1 was used as a positive control. Aberrant DNA melting profiles were obtained for one of the duplicates of Im 125, Im 158 and Im 171. Im 207, whose melting curve is indicated in green, appeared to have a slightly different DNA melting profile from that of the negative control.

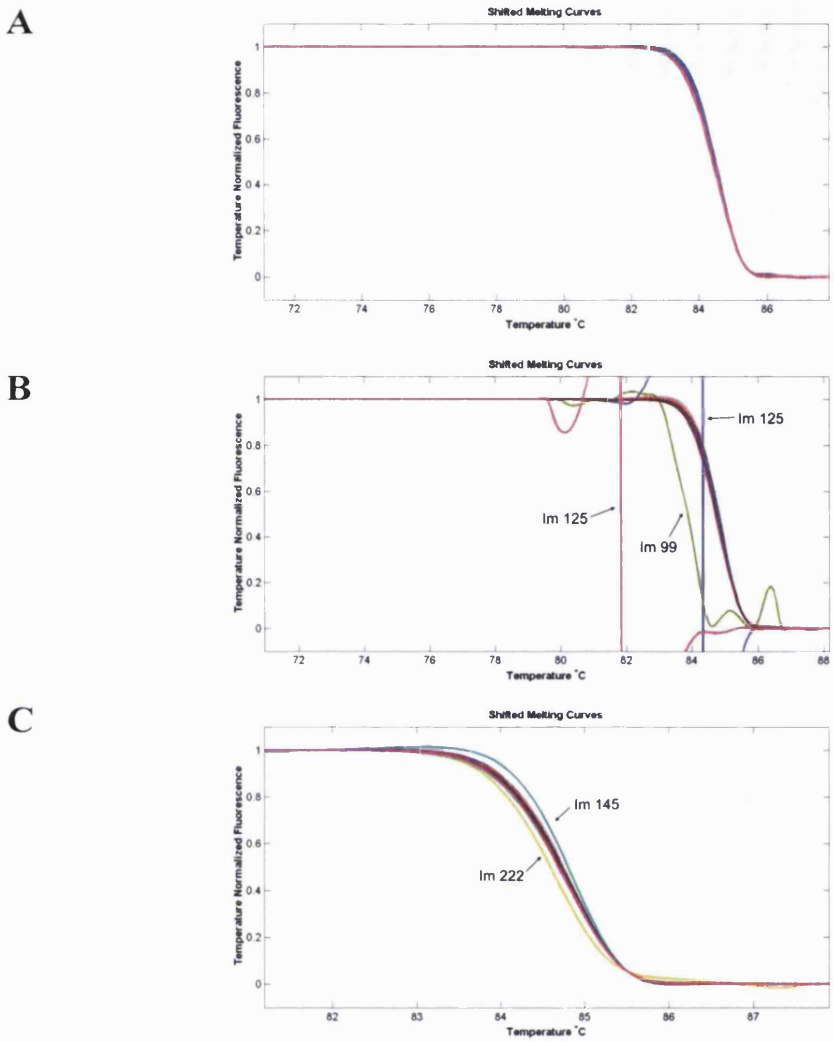

Figure 7.2: DNA melting profiles obtained from the LRRK2 exon 35 scan of the DNA samples from the Imperial Brain Bank. The DNA samples were subjected to mutation scanning in the LightScanner and the results are presented in the form of DNA melting curves. (A) The first batch of the DNA samples (32 samples) was scanned. No samples in this batch appeared to have a different DNA melting profile from that of the negative control. (B) The second batch of the DNA samples (35 samples) was scanned. One of the Im 99 duplicate samples and both of the Im 125 duplicate samples gave aberrant DNA melting profiles. (C) The third batch of the DNA samples (33 samples) was scanned. One of the duplicate samples of both Im 145 and Im 222 appeared to have an observable difference in the DNA melting profile from that of the negative control. (Note: The DNA of some samples in the first batch was directly sequenced for the purpose of finding the negative control for the mutation scanning and therefore these samples were not included in this mutation scanning experiment.)

7.2 DNA Sequencing of the TOPO-cloned Imperial Samples

DNA samples that gave either a different melting profile from that of the negative control or an aberrant melting profile in mutation scanning were sent for DNA sequencing of LRRK2 exon 31 or 35. Purified PCR products were sequenced initially, and the resultant sequences of each sample were compared to exon 31 and 35 of a LRRK2 consensus sequence (NM_198578). However, some of the sequences were of poor signal quality. To combat this problem, all samples were TOPO cloned (section 2.6.2), and re-sent for DNA sequencing. Only sample Im 1 showed a different DNA sequence in comparison to the consensus sequence (Figure 7.3 and 7.4). One mutation was present in the *PARK8* exon 31. A thymine to adenine mutation at position 4436 led to an amino acid change at position 1479 from a phenylalanine to a tyrosine. This mutation was not observed in any other samples, the consensus sequence or in SNP databases (http://www.ncbi.nlm.nih.gov/snp). Therefore, the newly identified amino acid change F1479Y is likely to segregate with PD. Nonetheless, further confirmation of the pathogenecity of this mutation is required. Table 7.1 shows a summary of the information of the patient whose DNA sample is referred to as Im 1.

Patient Im 1	
Sex	Female
Clinical cause of death	Not reported
Age of disease onset	76
Disease duration	12 years
Drugs used	Madopar, Sinemet, Selegiline
Clinical symptoms	• Confusion and dementia (but improved upon removal of drugs) • No tremor observed however • L-DOPA unresponsiveness
Family history	Unknown

Table 7.1: Summary of the information of patient Im 1. Family history refers to whether the family of the patient has also been suffering from PD.

A

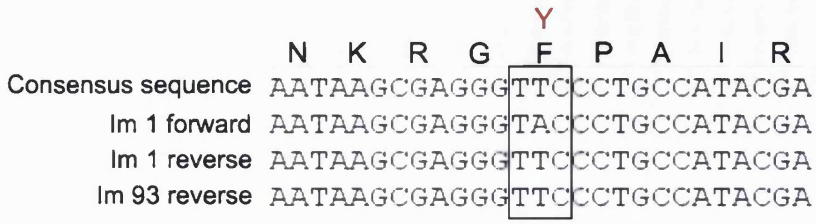

B

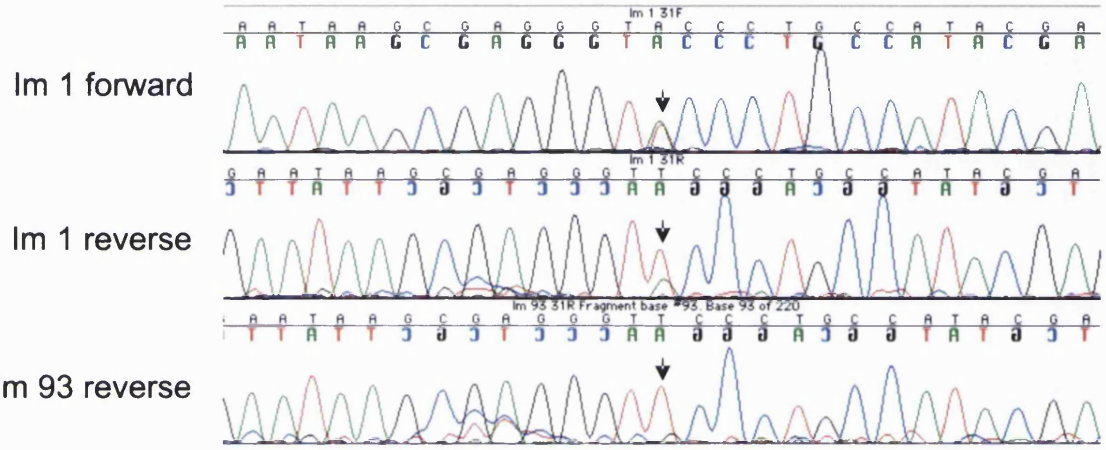

Figure 7.3: Identification of the F1479Y mutation. Im 1 DNA sample was sequenced using the forward and reverse primers of LRRK2 exon 31 (31F and 31R). (A) The nucleotide sequence of the stretch of DNA around the mutation site is shown, and the sequence is aligned to the consensus sequence of exon 31 of LRRK2. The letters above the nucleotide sequences show the amino acids that the DNA sequence codes for. The mutation site is indicated by a bracket around the bases. The thymine at position 4436 was found to be mutated to an adenine in Im 1, resulting in an alteration of one amino acid change from phenylalanine to tyrosine at position 1479, which is indicated in red. The triplet code at this position of Im 93 was not changed. (B) The chromatogram of the DNA sequencing result is shown. The mutation site is indicated by an arrow. Im 1, sequenced in the forward direction, appeared to have a thymine and an adenine present in equal proportions in the DNA sample, indicating the heterozygosity of the F1479Y mutation in *PARK8*. This mutation was not present in Im 93.

A

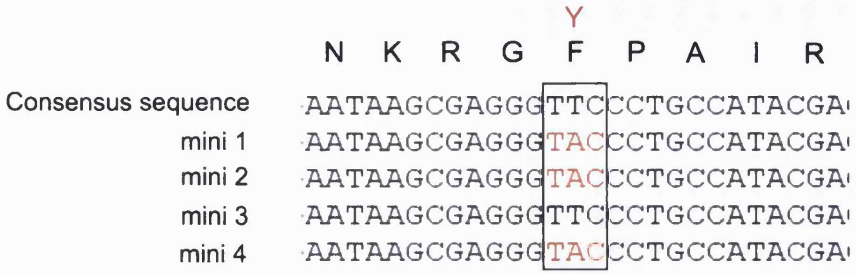

B

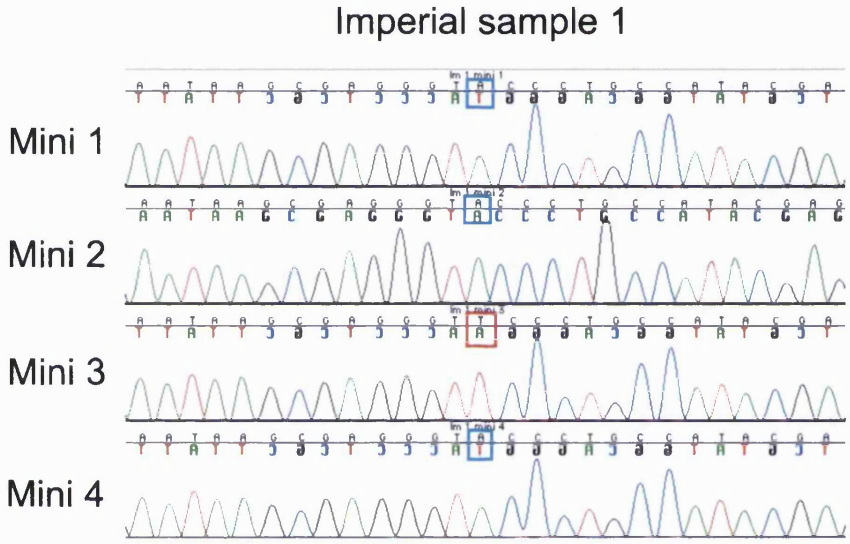

Figure 7.4: Confirmation of the F1479Y mutation in Im 1. The gel-purified genomic DNA of Im 1 was subjected to TOPO cloning, and the cloned DNA was sent for DNA sequencing. (A) The nucleotide sequence of the stretch of DNA around the mutation site is shown, and the sequence is aligned to the consensus sequence of exon 31 of LRRK2. The letters above the nucleotide sequences show the amino acids that the DNA sequence codes for. The F1479Y mutation was found in three of the minipreps (mini indicates the miniprep product). (B) The chromatogram of the DNA sequencing result is shown. The mutation site is indicated by a square around the mutated nucleotide. The blue square indicates the mutated base at the mutation site. The red square indicates the WT base in the second allele.

A

B

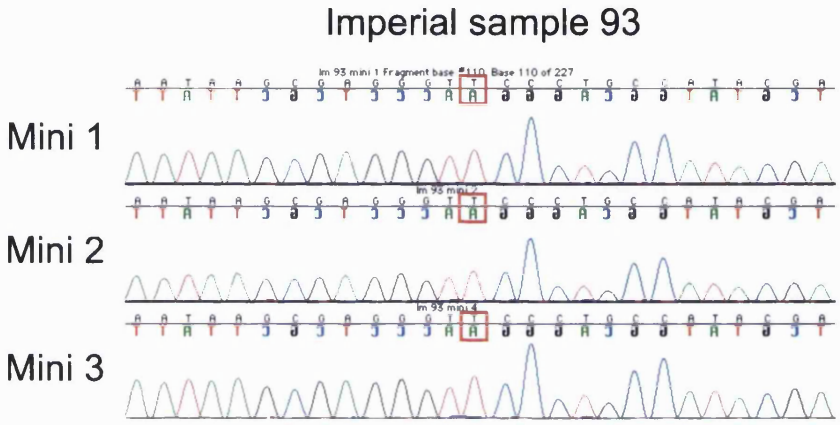

Figure 7.5: The F1479Y mutation was not present in any other TOPO-cloned DNA. The gel-purified genomic DNA of all samples showing an aberrant LightScanner profile were subjected to TOPO cloning, and the cloned DNA was sent for DNA sequencing. (A) The nucleotide sequence of the stretch of DNA around the mutation site is shown, and the sequence is aligned to the consensus sequence of exon 31 of LRRK2. The letters above the nucleotide sequences show the amino acids that the DNA sequence codes for. However, the F1479Y mutation was not found in any of the sequenced samples except for Im 1 (Figure 7.3 and 7.4). (B) Example chromatograms of the DNA sequencing result are shown for Im 93. The F1479Y mutation site is indicated by a red square. None of the miniprep samples showed a base change at that site. (mini indicates the miniprep product)

7.3 Discussion

The search for further PD-associated mutations in *PARK8* could offer a platform for unravelling the possible mechanism of how LRRK2 can contribute to PD pathogenesis, providing informative clues for the development of new therapeutic strategies for PD treatment. A number of pathogenic mutations were found in PD patients in previous years. A number of mutations and/or SNPs were also found in PD patients even though they do not seem to segregate with PD. Here, I report the discovery of the F1479Y mutation present in the DNA sample of one PD patient from the Imperial Brain Bank.

An interesting question regarding the F1479Y mutation is whether it could lead to a conformational change in LRRK2, large enough to modify the interaction with proteins involved in signalling pathways associated with neurodegeneration. Phenylalanine and tyrosine are structurally very similar to each other. The only difference is an extra hydroxyl group present in the side chain of tyrosine. It is unlikely that a missense mutation involving the two structurally similar amino acids can alter the protein structure significantly. However, one could argue that the oxygen in the hydroxyl group of tyrosine can provide an extra hydrogen bonding formed within the protein. Previously, Gotthardt *et al* (2008) suggested that the Y1699C mutation could weaken the LRRK2 dimeric structure due to the disruption of hydrogen bond between Y1699 and N1437 in the Roc domain. Indeed, my data showed that Roc-COR dimerisation was slightly but significantly affected by the Y1699C mutation (section 4.8). This suggests that a loss or addition of a hydrogen bond could have the potential to alter protein conformation and subsequently the dimerisation of LRRK2. Structural analysis in finding out where the F1479 is located could be useful. For example, if F1479 is located at the LRRK2 dimer interface, then the F1479Y mutation could have the potential to lead to an alteration in LRRK2 dimerisation, which potentially affects LRRK2 activities and functions.

It is noticeable that the majority of the samples from the Imperial Brain Bank did not possess a mutation, as shown by the identical DNA melting profiles between the samples and the negative controls. This observation might be rationalised by the fact that the majority of PD cases were found to be sporadic. Less than 10% of PD cases

appear to be familial (Thomas and Beal, 2007). The probability of a PD patient possessing a mutation in one of the *PARK8* exons would hence be relatively small.

Taken together, I have identified a new mutation in the LRRK2 Roc domain. This F1479Y mutation was present in one of the PD patients from the Imperial Brain Bank and was not found in any SNP databases, making it a mutation likely to segregate with PD. Further investigation is required to establish an effect of the F1479Y mutation on LRRK2 GTPase and kinase activities, cellular viability and protein interactions. If so, this mutation in the LRRK2 Roc domain could provide an additional avenue in the search for the molecular mechanism of how mutant LRRK2 leads to PD pathogenesis.

8. Final Discussion

PARK8 mutations are one of the major known causes of PD. As mutation carriers most often display symptoms and brain pathology typical for idiopathic PD, research into the function of LRRK2 in health and disease has become a major focus. LRRK2 harbours two functional domains that were shown to be deregulated in mutant LRRK2 and important to exert toxicity on cells in *in vitro* assays (West *et* al, 2005; Greggio *et al,* 2006; Li *et* al, 2007; Xiong *et al*, 2010). However, the molecular or signalling pathways that LRRK2 participates in remain elusive. Therefore, the identification of LRRK2 interactors is important to place LRRK2 into one or more signalling pathways. The determination of the effects of *PARK8* mutations segregating with PD on LRRK2 interaction with proteins, and in due course the effects on signalling, could provide clues on the identification of pathways that lead to neurodegeneration in PD and might open up new avenues for disease-modifying therapies. In a YTH screen in my laboratory, RTN3, S100A10, ApoE3 and β-tubulin (TUBB4) were identified as interactors of the LRRK2 Roc-COR tandem domain. My thesis focused on the interaction between LRRK2 and β-tubulin, with the prospect of providing further insight into the role of LRRK2 on the microtubule cytoskeleton with possible implications for PD pathogenesis.

8.1 LRRK2 Interacts with the Microtubule Cytoskeleton

In YTH experiments, LRRK2 was shown to interact specifically with two β-tubulin isoforms, TUBB and TUBB4. For this interaction, the Roc domain of LRRK2 and the C-terminus of β-tubulin were sufficient. This interaction was also confirmed in a mammalian cell model using co-IP. These data further refine previous findings (Biskup *et al,* 2006; Gandhi *et al,* 2008; Gillardon, 2009) indicating the ability of LRRK2 to interact with microtubules. The role of LRRK2 on microtubules requires further investigation but LRRK2 over-expression was shown to have a most likely indirect effect on tau phosphorylation and possibly direct effect on tubulin phosphorylation (Smith *et al,* 2005; MacLeod *et al,* 2006; Gillardon, 2009; Melrose *et al,* 2010). Both effects would have implications for microtubule stability and suggests a role for LRRK2 in the regulation of the dynamic instability of microtubules. This study also revealed that some *PARK8* mutations can modify the LRRK2 – β-tubulin interaction. The

R1441G/H mutants showed a decreased strength of this interaction, with R1441G having a clearer and more pronounced effect. This suggests a disruption of the LRRK2 – tubulin binding site caused by substitution of arginine at position 1441 with glycine or histidine that differs considerably in size and hydrophobicity. Interestingly, the R1441C mutation was shown to slightly enhance the LRRK2 – tubulin interaction. The reason why mutations on the same residue could have different outcomes in terms of protein-protein interactions is unclear, but a different protein folding pattern resulting from the R1441C and R1441G/H could be one of the reasons. The ability of cysteine to create disulphide bonds might also be considered.

The R1728H/L mutations also resulted in a significant increase in the level of the LRRK2 – β-tubulin interaction, possibly enabling LRRK2 to form a more stable complex with microtubules. Although the R1728H/L mutations are not proved to clearly segregate with PD, it is unlikely that two different mutations that are both found in PD patients would occur at the same residue, unless they are related to PD pathogenesis. Further work on investigating the effect of these two mutations on GTPase and kinase activities of LRRK2 might be of value.

In conclusion, the effect of *PARK8* mutations on the weakening as well as strengthening of the LRRK2 – tubulin interaction was observed. The strength of this interaction might well correlate with the time LRRK2 resides at microtubules containing different β-tubulin isoforms, and further suggests that a fine regulation of the LRRK2 function at microtubules is required for neuronal integrity, i.e. increased as well as decreased function might be detrimental.

Another interesting observation further confirmed the specificity of the LRRK2 – β-tubulin interaction and suggests the importance of post-translational modification in the regulation of this interaction. Alanine at position 364 of β-tubulin isoforms was shown to be crucial for the interaction with LRRK2. A substitution for serine at this position resulted in the loss of the LRRK2 – tubulin interaction. This amino acid change might influence the structure of tubulin but more interestingly introduces a phosphorylation site at this position. I therefore suggest that phosphorylation of S364 provides a likely reason for the abolition of the LRRK2 – β-tubulin interaction. Phosphorylation of tubulin would accordingly regulate LRRK2 – tubulin interaction, and might lead to the

dissociation of LRRK2 from the microtubule cytoskeleton. Previous data showed that phosphorylation of tubulin could lead to destabilisation of microtubules. For example, tubulin phosphorylation resulted in a loss of binding of MAP2 to microtubules, thereby abolishing the stabilising function of MAP2 at microtubules (Wandosell *et al,* 1986; Khan and Ludueña, 1996). Tubulin phosphorylation by LIM kinase I was also found to cause microtubule destabilisation (Gorovoy *et al,* 2005). Recently however, Gillardon suggested the phosphorylation of tubulin by LRRK2 has a stabilising effect on microtubules (Gillardon, 2009), and he also reported Thr107 as a LRRK2 phosphorylation site on tubulin.

Taken together, my data provide further evidence for the association of LRRK2 with the microtubule cytoskeleton, which might be regulated by the phosphorylation of tubulin. They also suggest a role of the LRRK2 – tubulin interaction in PD due to the observed alteration of the interaction strength caused by PD-associated mutations.

8.2 The Possible Role of the LRRK2 – tubulin Interaction in PD Pathogenesis

Mutant LRRK2 could exert toxic effects through an altered interaction with the microtubule cytoskeleton. Since the toxicity of LRRK2 was suggested to require kinase activity (Greggio *et al*, 2006), it is tempting to speculate that uncontrolled activation of the LRRK2 kinase activity is responsible for detrimental effects on cell viability. Therefore, I also looked at the effects of LRRK2 autophosphorylation on the LRRK2 – tubulin interaction.

LRRK2 autophosphorylation was shown to be the most reproducible effect of the LRRK2 kinase activity (Luzón-Toro *et al*, 2007; Greggio *et al*, 2008; Li *et al*, 2010). One of the major targets for autophosphorylation was found to be threonine residues in the Roc domain (Gloeckner *et al,* 2009; Greggio *et al,* 2009; Kamikawaji *et al,* 2009). Using the Q-YTH technique, I found that the introduction of the phosphomimetic mutants T1343D and T1491D at these Roc autophosphorylation sites reduced the strength of the LRRK2 – β-tubulin interaction. Mutation of these residues to alanine had

no significant or only a relatively small effect on the LRRK2 – β-tubulin interaction compared to the effect of the phosphomimetic mutants, indicating the likely specific effect of autophosphorylation on this interaction rather than an effect simply due to a conformational change. This observation raises the possibility that increased LRRK2 kinase activity as reported for the G2019S-LRRK2 mutant would lead to the dissociation of mutant LRRK2 from microtubules. Dissociation of LRRK2 from microtubules might render LRRK2 free to take up other functions in the cells or possibly be degraded. This possibility can only be speculative if dissociation of LRRK2 from microtubules is an event involved in the pathogenesis of PD possibly leading to a loss of microtubule stability important for axonal transport, or if dissociated LRRK2 causes detrimental effects at other sub-cellular locations. Even though an effect of LRRK2 on microtubule stability seems likely, at least through the observation of an influence of LRRK2 expression on neurite outgrowth (MacLeod *et al,* 2006; Plowey *et al,* 2008), effects on tau phosphorylation (MacLeod *et al,* 2006; Li *et* al, 2009b; Lin *et al,* 2010; Melrose *et al,* 2010) and possibly tubulin phosphorylation (Gillardon, 2009), no clear conclusions can be drawn if the end result of this interplay is microtubule stabilisation or destabilisation. My immunocytochemical studies showed the preferential co-localisation of endogenous LRRK2 with tyrosinated tubulin rather than acetylated tubulin, indicating a role for LRRK2 at highly dynamic, possibly growing, microtubules rather than stable microtubules. In addition, I observed less stable microtubules in cells over-expressing LRRK2 and previous work in my laboratory showed that LRRK2 was not able to stabilise microtubules in nocodazole-treated cells (Sancho *et al,* 2009). Therefore, my work indicates a role for LRRK2 at the microtubule cytoskeleton leading to a decrease in microtubule stability. Hence, I propose the following model to explain the role of LRRK2 in regulating microtubule stability. WT LRRK2 bound to GTP possesses kinase activity. The Roc domain is autophosphorylated. The phosphorylation state of the LRRK2 molecule affects the association to or dissociation from microtubules. This in due course affects the amount of LRRK2 available for additional LRRK2 functions at other sub-cellular locations. The suggested decreased GTP binding and kinase activities caused by Roc autophosphorylation (Kamikawaji *et al,* 2009) might provide a negative feedback mechanism to control LRRK2 kinase activity. This feedback mechanism possibly prevents a prolonged and/or increased activation of signalling pathways influenced by LRRK2 under physiological conditions. However, mutant LRRK2, for example the G2019S mutant with increased kinase activity, over-

rides this feedback mechanism, leading to increased LRRK2 activity in accordance with a gain-of-function effect of *PARK8* mutations.

It is likely that LRRK2 mutants in the Roc-COR GTPase domain, R1441C/G/H and Y1699C, can also cause a prolonged microtubule detachment of LRRK2 due to the inhibitory effect of these mutations on the Roc GTPase activity (Guo *et al,* 2007; Lewis *et al,* 2007; Li *et al,* 2007; Deng *et al,* 2008; Gotthardt *et al,* 2008; Daniëls *et al,* 2010; Xiong *et al,* 2010). The decreased GTPase activity would lead to prolonged kinase activation, keeping the Roc domain in a phosphorylated state and, in due course, LRRK2 detached from microtubules. The resultant increased kinase activation could also lead to the hyperphosphorylation of MAPs and possibly microtubule destabilisation in the process.

An interesting question one might ask is in what way could LRRK2 contribute to microtubule destabilisation, and which signalling pathways might be involved in this process. One possibility is through the activation of GSK3β. Previously, GSK3β activation was found to promote the phosphorylation of MAP1B concentrated in neuronal growth cones, with the result of microtubule destabilisation (Goold *et al,* 1999). The idea of an involvement of GSK3β in LRRK2-induced microtubule destabilisation is supported by the presence of hyperphosphorylated tau and AD-like symptoms in one PD patient possessing a G2019S mutation in *PARK8* (Gilks *et al,* 2005), and the increased phosphorylation of tau in dopaminergic neurons in G2019S-LRRK2 transgenic mice (Melrose *et al,* 2010). Recent work showing the increased phosphorylation of tau through the recruitment of autoactivated GSK3β by G2019S-LRRK2, and subsequent dendrite degeneration in *Drosophila*, further indicates the involvement of GSK3β in mutant LRRK2-induced neurodegeneration (Lin *et al,* 2010). GSK3β was shown to exhibit kinase activity on tau (Cho and Johnson, 2004). Hence, it is tempting to speculate that mutant LRRK2 could lead to microtubule destabilisation by tau or possibly MAP1B hyperphosphorylation via a pathway that involves GSK3β activation. Another possibility of how LRRK2 could lead to microtubule destabilisation is via the activation of the Erk/MAPK pathway, which was suggested to be involved in MAP2 phosphorylation (Rubinfeld and Seger, 2004). The observation that WT LRRK2 could attenuate stress-induced cell death via the Erk pathway (Liou *et al,* 2008) and the discovery of the MAPKKs in the Erk/MAPK pathway, MKK4/7, as LRRK2 interactors

(Gloeckner *et* al, 2009) suggest a possible involvement of this signalling pathway in LRRK2-induced microtubule destabilisation. The third possibility of how LRRK2 contributes to microtubule destabilisation would be a direct phosphorylation of MAPs, although evidence for a direct interaction between LRRK2 and MAPs is required. A hypothetical model of the involvement of LRRK2 in microtubule stability is depicted in figure 8.1.

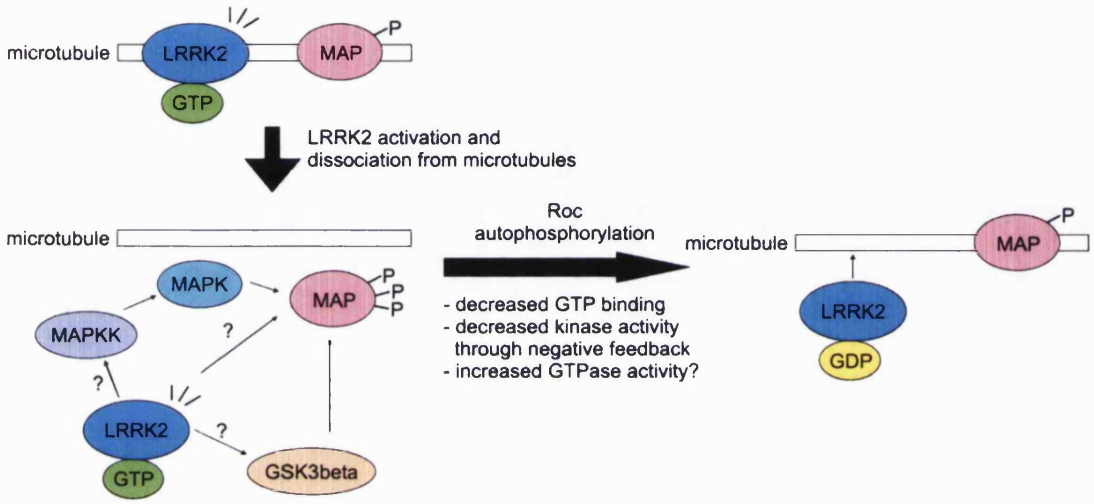

Figure 8.1: A proposed model for the effect of LRRK2 activation on microtubule stability. GTP binding to the LRRK2 Roc domain is necessary for kinase activity, leading to autophosphorylation of the activation loop of the kinase domain and the Roc domain. Roc autophosphorylation leads to the dissociation of LRRK2 from microtubules, due to the decreased interaction strength with tubulin. This renders LRRK2 free to localise to other sub-cellular locations and fulfill possible additional functions. The autophosphorylation of the activation loop might lead to phosphorylation of heterologous substrates, leading to the activation of certain signalling pathways involved in hyperphosphorylation of basally-phosphorylated MAPs and microtubule destabilisation. Negative feedback mechanisms on LRRK2 activities prevent WT LRRK2 from MAP hyperphosphorylation, while mutant LRRK2 over-ride these mechanisms which cause microtubule destabilisation. Here are three possible ways suggested on how LRRK2 might lead to MAP phosphorylation. First, through the activation of GSK3β, either by direct interaction or through additional proteins within a signalling pathway that activates GSK3β. Second, through the activation of the Erk/MAPK pathway. Third, through direct interaction between LRRK2 and MAPs.

8.3 Future Work

To further our understanding on the involvement of LRRK2 at the microtubule cytoskeleton and in neurodegeneration, additional experiments as suggested below may be helpful.

8.3.1 Are Any of the MAPs Substrates of LRRK2?

In section 8.2, three possible ways were suggested to explain how LRRK2 kinase activation could lead to microtubule instability. One of them was a direct interaction between LRRK2 and MAPs, including MAP1B and MAP2. Both of these MAPs can bind to and stabilise microtubules. Their microtubule binding is dependent on the phosphorylation state (Wandosell *et al*, 1986; Riederer, 2007). To date, there are no data that indicate a direct interaction between them and LRRK2. A possible LRRK2 – MAP interaction could be tested using the YTH system, co-IP and/or GST pull down assays. Furthermore, kinase assays could determine the ability of LRRK2 to phosphorylate MAPs. The establishment of the enzyme-substrate relationship between LRRK2 and MAPs may provide insight into the mechanism of microtubule destabilisation and subsequent neurodegeneration exhibited by mutant LRRK2.

8.3.2 The Effect of Roc Autophosphorylation on LRRK2 GTPase Activity

Recently, autophosphorylation of some threonine residues in the LRRK2 Roc domain were shown to lower both the GTP binding and kinase activities of LRRK2 (Kamikawaji *et al,* 2009). GTP binding is necessary for kinase activity. Once LRRK2 is bound to GTP, GTP hydrolysis occurs. GTP binding activity is hampered by Roc autophosphorylation with a possible effect on GTPase activity. In order to determine whether a negative feedback mechanism of LRRK2 activation exists, it would be of interest to investigate whether the phosphomimetic mutants, T1343D and T1491D, can affect not only GTP binding and kinase activities, but also the GTPase activity of LRRK2.

8.3.3 Further Characterisation of the Newly-discovered F1479Y Mutation

Using the mutation scanning technique, I have discovered a novel *PARK8* mutation in PD patients – the F1479Y mutation. However, further investigation of a clear segregation with PD is outstanding. Further characterisation of this mutation to shed light onto the functional consequence of this mutation is also required. For example, would this mutation lead to an alteration in β-tubulin binding, GTP binding, GTPase or kinase activities of LRRK2? Would the over-expression of the F1479Y-LRRK2 mutant lead to a decrease in cellular viability? The answers to these questions would indicate whether this mutation is likely to be involved in neurodegeneration.

8.4 Conclusions

The search for the molecular mechanisms mutant LRRK2 might employ to cause neurodegeneration is an important branch of PD research. This thesis contributes additional information to this research by providing data showing the direct interaction between LRRK2 and specific β-tubulin isoforms, and the association of LRRK2 with the microtubule cytoskeleton by a combination of techniques including YTH assays, co-IP and immunocytochemistry.

The specificity of the LRRK2 – β-tubulin interaction was shown to depend on the amino acid residue at position 364. An alanine at this position conferred an interaction between all investigated β-tubulin isoforms and LRRK2, and introduction of a serine abolished the interaction. This suggests that an interaction of LRRK2 and microtubules could be hindered by the phosphorylation state of β-tubulin. The β-tubulin isoforms that LRRK2 can interact with – TUBB4 and TUBB – were found to be predominantly expressed in the adult and foetal brain respectively by RQ-PCR experiments. This suggests a role of the LRRK2 – β-tubulin interaction during neuronal development and in neuronal maintenance. Assessment of the level of the LRRK2 – β-tubulin interaction by Q-YTH assays revealed that some PD-associated LRRK2 mutants can alter the level of this interaction, suggesting a possible role of the LRRK2 – β-tubulin interaction in PD. Further Q-YTH experiments to assess the level of the LRRK2 – β-tubulin

interaction using the phosphomimetic mutants revealed a decrease in the interaction level upon Roc autophosphorylation, an event during LRRK2 activation that is supposed to increase in the G2019S mutant. This suggests that LRRK2 could become detached from microtubules and perhaps localise to other sub-cellular locations upon activation and especially increased activation. In addition, the immunocytochemical co-staining of endogenous LRRK2 and tubulin in differentiated SH-SY5Y cells indicates a preferential localisation of LRRK2 to tyrosinated tubulin over acetylated tubulin, and hence growing microtubules over stable ones. This could indicate a role of LRRK2 at dynamic microtubules possibly affecting microtubule stability. It was hence speculated that LRRK2 activation could cause a temporary detachment of LRRK2 from microtubules, rendering a change in LRRK2 sub-cellular location. This might induce the activation of signalling pathways that affect microtubule stability, leading potentially to increased LRRK2 activity and neurodegeneration in *PARK8* mutation carriers.

In summary, the characterisation of the LRRK2 – β-tubulin interaction in the thesis provides further evidence for a role of the microtubule cytoskeleton in LRRK2-induced neurodegeneration and PD pathogenesis. Future PD research could be directed towards the search for the LRRK2-induced signalling pathways which involves the modification of the dynamics of the microtubule cytoskeleton, and the effects of the modulation of such pathways on neuronal viability.

9. Bibliography

Aasly, J.O., Vilarino-Guell, C., Dachsel, J.C., Webber, P.J., West, A.B., Haugarvoll, K., Johansen, K.K., Toft, M., Nutt, J.G., Payami, H., Kachergus, J.M., Lincoln, S.J., Felic, A., Wider, C., Soto-Ortolaza, A.I., Cobb, S.A., White, L.R., Ross, O.A., Farrer, M.J., (2010) Novel pathogenic LRRK2 p.Asn1437His substitution in familial Parkinson's disease. *Mov. Disord.* **25** 2156-2163.

Abbas, N., Lucking, C.B., Ricard, S., Durr, A., Bonifati, V., De Michele, G., Bouley, S., Vaughan, J.R., Gasser, T., Marconi, R., Broussolle, E., Brefel-Courbon, C., Harhangi, B.S., Oostra, B.A., Fabrizio, E., Bohme, G.A., Pradier, L., Wood, N.W., Filla, A., Meco, G., Denefle, P., Agid, Y., Brice, A., (1999) A wide variety of mutations in the parkin gene are responsible for autosomal recessive parkinsonism in Europe. French Parkinson's Disease Genetics Study Group and the European Consortium on Genetic Susceptibility in Parkinson's Disease. *Hum. Mol. Genet.* **8** 567-574.

Ahmadian, M.R., Kiel, C., Stege, P., Scheffzek, K., (2003) Structural fingerprints of the Ras-GTPase activating proteins neurofibromin and p120GAP. *J. Mol. Biol.* **329** 699-710.

Al-Bassam, J., Ozer, R.S., Safer, D., Halpain, S., Milligan, R.A., (2002) MAP2 and tau bind longitudinally along the outer ridges of microtubule protofilaments. *J. Cell. Biol.* **157** 1187-1196.

Alegre-Abarrategui, J., Christian, H., Lufino, M.M., Mutihac, R., Venda, L.L., Ansorge, O., Wade-Martins, R., (2009) LRRK2 regulates autophagic activity and localizes to specific membrane microdomains in a novel human genomic reporter cellular model. *Hum. Mol. Genet.* **18** 4022-4034.

Anderson, J.P., Walker, D.E., Goldstein, J.M., de Laat, R., Banducci, K., Caccavello, R.J., Barbour, R., Huang, J., Kling, K., Lee, M., Diep, L., Keim, P.S., Shen, X., Chataway, T., Schlossmacher, M.G., Seubert, P., Schenk, D., Sinha, S., Gai, W.P., Chilcote, T.J., (2006) Phosphorylation of Ser-129 is the dominant pathological modification of alpha-synuclein in familial and sporadic Lewy body disease. *J. Biol. Chem.* **281** 29739-29752.

Anderson, L.R., Betarbet, R., Gearing, M., Gulcher, J., Hicks, A.A., Stefansson, K., Lah, J.J., Levey, A.I., (2007) PARK10 candidate RNF11 is expressed by vulnerable neurons and localizes to Lewy bodies in Parkinson disease brain. *J. Neuropathol. Esp. Neurol.* **66** 955-964.

Argarana, C.E., Barra, H.S., Caputto, R., (1978) Release of [14C]tyrosine from tubulinyl-[14C]tyrosine by brain extract. Separation of a carboxypeptidase from tubulin-tyrosine ligase. *Mol. Cell. Biochem.* **19** 17-21.

Avruch, J., Khokhlatchev, A., Kyriakis, J.M., Luo, Z., Tzivion, G., Vawas, D., Zhang, X.F., (2001) Ras activation of the Raf kinase: tyrosine kinase recruitment of the MAP kinase cascade. *Recent. Prog. Horm. Res.* **56** 127-155.

Azmi, P., Seth, A., (2005) RNF11 is a multifunctional modulator of growth factor receptor signalling and transcriptional regulation. *Eur. J. Cancer.* **41** 2549-2560.

Bennett, M.J., Schlunegger, M.P., Eisenberg, D., (1995) 3D domain swapping: a mechanism for oligomer assembly. *Protein. Sci.* **4** 2455-2468.

Biskup, S., Moore, D.J., Celsi, F., Higashi, S., West, A.B., Andrabi, S.A., Kurkinen, K., Yu, S.W., Savitt, J.M., Waldvogel, H.J., Faull, R.L., Emson, P.C., Torp, R., Ottersen, O.P., Dawson, T.M., Dawson, V.L., (2006) Localization of LRRK2 to membranous and vesicular structures in mammalian brain. *Ann. Neurol.* **60** 557-569.

Bogaerts, V., Nuytemans, K., Reumers, J., Pals, P., Engelborghs, S., Pickut, B., Corsmit, E., Peeters, K., Schymkowitz, J., De Deyn, P.P., Cras, P., Rousseau, F., Theuns, J., Van Broeckhoven, C., (2008) Genetic variability in the mitochondrial serine protease HTRA2 contributes to risk for Parkinson disease. *Hum. Mutat.* **29** 832-840.

Bosgraaf, L., Van Haastert, P.J., (2003) Roc, a Ras/GTPase domain in complex proteins. *Biochim. Biophys. Acta.* **1643** 5-10.

Bradford, M.M., (1976) A rapid and sensitive method for the quantitation of microgram quantities of protein utilizing the principle of protein-dye binding. *Anal. Biochem.* **72** 248-54

Brugg, B., Matus, A., (1991) Phosphorylation determines the binding of microtubule-associated protein 2 (MAP2) to microtubules in living cells. *J. Cell. Biol.* **114** 735-743.

Cambray-Deakin, M.A., Burgoyne, R.D., (1987) Acetylated and detyrosinated alpha-tubulins are co-localized in stable microtubules in rat meningeal fibroblasts. *Cell. Motil. Cytoskeleton.* **8** 284-291.

Carlier, M.F., Pantaloni, D., (1981) Kinetic analysis of guanosine 5'-triphosphate hydrolysis associated with tubulin polymerization. *Biochemistry.* **20** 1918-1924.

Carney, D.S., Davies, B.A., Horazdovsky, B.F., (2006) Vps9 domain-containing proteins: activators of Rab5 GTPases from yeast to neurons. *Trends. Cell. Biol.* **16** 27-35.

Caruso, A., Motolese, M., Iacovelli, L., Caraci, F., Copani, A., Nicoletti, F., Terstappen, G.C., Gaviraghi, G., Caricasole, A., (2006) Inhibition of the canonical Wnt signaling pathway by apolipoprotein E4 in PC12 cells. *J. Neurochem.* **98** 364-371.

Chang, L., Jones, Y., Ellisman, M.H., Goldstein, L.S., Karin, M., (2003) JNK1 is required for maintenance of neuronal microtubules and controls phosphorylation of microtubule-associated proteins. *Dev. Cell.* **4** 521-533.

Chang, Y.F., Cheng, C.M., Chang, L.K., Jong, Y. J., Yuo, C.Y., (2006) The F-box protein Fbxo7 interacts with human inhibitor of apoptosis protein cIAP1 and promotes cIAP1 ubiquitination. *Biochem. Biophys. Res. Commun.* **342** 1022-1026.

Cherfils, J., Chardin, P., (1999) GEFs: structural basis for their activation of small GTP-binding proteins. *Trends. Biochem. Sci.* **24** 306-311.

Chinta, S.J., Andersen, J.K., (2006) Reversible inhibition of mitochondrial complex I activity following chronic dopaminergic glutathione depletion in vitro: implications for Parkinson's disease. *Free. Radic. Biol. Med.* **41** 1442-1448.

Chiueh, C.C., Andoh, T., Lai, A.R., Lai, E., Krishna, G., (2000) Neuroprotective strategies in Parkinson's disease: protection against progressive nigral damage induced by free radicals. *Neurotox. Res.* **2** 293-310.

Cho, J.H., Johnson, G.V., (2004) Primed phosphorylation of tau at Thr231 by glycogen synthase kinase 3beta (GSK3beta) plays a critical role in regulating tau's ability to bind and stabilize microtubules. *J. Neurochem.* **88** 349-358.

Chu, C.T., (2010) A pivotal role for PINK1 and autophagy in mitochondrial quality control: implications for Parkinson disease. *Hum. Mol. Genet.* **19** R28-R37.

Ciani, L., Salinas, P.C., (2007) c-Jun N-terminal kinase (JNK) cooperates with Gsk3beta to regulate Dishevelled-mediated microtubule stability. *BMC. Cell. Biol.* **8** 27

Clements, C.M., McNally, R.S., Conti, B.J., Mak, T.W., Ting, J.P., (2006) DJ-1, a cancer- and Parkinson's disease-associated protein, stabilizes the antioxidant transcriptional master regulator Nrf2. *Proc. Natl. Acad. Sci. USA.* **103** 15091-15096.

Conklin, D.S., Galaktionov, K., Beach, D., (1995) 14-3-3 proteins associate with cdc25 phosphatases. *Proc. Natl. Acad. Sci. USA.* **92** 7892-7896.

Cooper, J.A., (1987) Effects of cytochalasin and phalloidin on actin. *J. Cell. Biol.* **105** 1473-1478.

Dächsel, J.C., Behrouz, B., Yue, M., Beevers, J.E., Melrose, H.L., Farrer, M.J., (2010) A comparative study of Lrrk2 function in primary neuronal cultures. *Parkinsonism. Relat. Disord.* **16** 650-655.

Dale, T.C., (1998) Signal transduction by the Wnt family of ligands. *Biochem. J.* **329** 209-223.

Daniëls, V., Vancraenenbroeck, R., Law, B.M., Greggio, E., Lobbestael, E., Gao, F., De Maeyer, M., Cookson, M.R., Harvey, K., Baekelandt, V., Taymans, J.M., (2010) Insight into the mode of action of the LRRK2 Y1699C pathogenic mutant. *J. Neurochem.* doi: 10.1111/j.1471-4159.2010.07105.x.

Darios, F., Corti, O., Lücking, C.B., Hampe, C., Muriel, M.P., Abbas, N., Gu, W.J., Hirsch, E.C., Rooney, T., Ruberg, M., Brice, A., (2003) Parkin prevents mitochondrial swelling and cytochrome c release in mitochondria-dependent cell death. *Hum. Mol. Genet.* **12** 517-526.

de Hoop, M.J., Huber, L.A., Stenmark, H., Williamson, E., Zerial, M., Parton, R.G., Dotti, C.G., (1994) The involvement of the small GTP-binding protein Rab5a in neuronal endocytosis. *Neuron.* **13** 11-22.

de la Monte, S.M., Sohn, Y.K., Ganju, N., Wands, J.R., (1998) P53- and CD95-associated apoptosis in neurodegenerative diseases. *Lab. Invest.* **78** 401-411.

Deng, H., Jankovic, J., Guo, Y., Xie, W., Le, W., (2005) Small interfering RNA targeting the PINK1 induces apoptosis in dopaminergic cells SH-SY5Y. *Biochem. Biophys. Res. Commun.* **337** 1133-1138.

Deng, J., Lewis, P.A., Greggio, E., Sluch, E., Beilina, A., Cookson, M.R., (2008) Structure of the ROC domain from the Parkinson's disease-associated leucine-rich repeat kinase 2 reveals a dimeric GTPase. *Proc. Natl. Acad. Sci. USA.* **105** 1499-1504.

Derijard, B., Raingeaud, J., Barrett, T., Wu, I.H., Han, J., Ulevitch, R.J., Davis, R.J., (1995) Independent human MAP-kinase signal transduction pathways defined by MEK and MKK isoforms. *Science.* **267** 682-685.

Di Fonzo, A., Chien, H.F., Socal, M., Giraudo, S., Tassorelli, C., Iliceto, G., Fabbrini, G., Marconi, R., Fincati, E., Abbruzzese, G., Marini, P., Squitieri, F., Horstink, M.W., Montagna, P., Libera, A.D., Stocchi, F., Goldwurm, S., Ferreira, J.J., Meco, G., Martignoni, E., Lopiano, L., Jardim, L.B., Oostra, B.A., Barbosa, E.R., (2007) ATP13A2 missense mutations in juvenile parkinsonism and young onset Parkinson disease. *Neurology.* **68** 1557-1562.

Di Fonzo, A., Dekker, M.C., Montagna, P., Baruzzi, A., Yonova, E.H., Correia Guedes, L., Szczerbinska, A., Zhao, T., Dubbel-Hulsman, L.O., Wouters, C.H., de Graaff, E., Oyen, W.J., Simons, E.J., Breedveld, G.J., Oostra, B.A., Horstink, M.W., Bonifati, V., (2009) FBXO7 mutations cause autosomal recessive, early-onset parkinsonian-pyramidal syndrome. *Neurology* **72** 240-245.

Dickson, B.J., (2002) Molecular mechanisms of axon guidance. *Science.* **298** 1959-1964.

Drewes, G., Ebneth, A., Mandelkow, E.M., (1998) MAPs, MARKs and microtubule dynamics. *Trends. Biochem. Sci.* **23** 307-311.

Dzamko, N., Deak, M., Hentati, F., Reith, A.D., Prescott, A.R., Alessi, D.R., Nichols, R.J., (2010) Inhibition of LRRK2 kinase activity leads to dephosphorylation of Ser(910)/Ser(935), disruption of 14-3-3 binding and altered cytoplasmic localization. *Biochem. J.* **430** 405-413.

Eisenhofer, G., Kopin, I.J., Goldstein, D.S., (2004) Leaky catecholamine stores: undue waste or a stress response coping mechanism? *Ann. N. Y. Acad. Sci.* **1018** 224-230.

El-Agnaf, O.M., Jakes, R., Curran, M.D., Wallace, A., (1998) Effects of the mutations Ala30 to Pro and Ala53 to Thr on the physical and morphological properties of alpha-synuclein protein implicated in Parkinson's disease. *FEBS. Lett.* **440** 67-70.

Farrer, L.A., Cupples, L.A., Haines, J.L., Hyman, B., Kukull, W.A., Mayeux, R., Myers, R.H., Pericak-Vance, M.A., Risch, N., van Duijn, C.M., (1997) Effects of age, sex, and ethnicity on the association between apolipoprotein E genotype and Alzheimer disease. A meta-analysis. APOE and Alzheimer Disease Meta Analysis Consortium. *JAMA.* **278** 1349-1356.

Feany, M.B., Pallanck, C.J., (2003) Parkin: a multipurpose neuroprotective agent? *Neuron.* **38** 13-16.

Feng, J., (2006) Microtubule: a common target for parkin and Parkinson's disease toxins. *Neuroscientist.* **12** 469-476.

Funayama, M., Hasegawa, K., Kowa, H., Saito, M., Tsuji, S., Obata, F., (2002) A new locus for Parkinson's disease (PARK8) maps to chromosome 12p11.2-q13.1. *Ann.Neurol.* **51** 296-301.

Funayama, M., Hasegawa, K., Ohta, E., Kawashima, N., Komiyama, M., Kowa, H., Tsuji, S., Obata, F., (2005) An LRRK2 mutation as a cause for the parkinsonism in the original PARK8 family. *Ann. Neurol.* **57** 918-921.

Funayama, M., Li, Y., Tomiyama, H., Yoshino, H., Imamichi, Y., Yamamoto, M., Murata, M., Toda, T., Mizuno, Y., Hattori, N., (2007) Leucine-rich repeat kinase 2 G2385R variant is a risk factor for Parkinson disease in Asian population. *Neuroreport.* **18** 273-275.

Fung, H.C., Chen, C.M., Hardy, J., Hernandez, D., Singleton, A., Wu, Y.R., (2006) Lack of G2019S LRRK2 mutation in a cohort of Taiwanese with sporadic Parkinson's disease. *Mov. Disord.* **21** 880-881.

Galter, D., Westerlund, M., Carmine, A., Lindqvist, E., Sydow, O., Olson, L., (2006) LRRK2 expression linked to dopamine-innervated areas. *Ann. Neurol.* **59** 714-719.

Gandhi, P.N., Wang, X., Zhu, X., Chen S.G., Wilson-Delfosse, A.L., (2008) The Roc domain of leucine-rich repeat kinase 2 is sufficient for interaction with microtubules. *J. Neurosci. Res.* **86** 1711-1720.

Gandhi, P.N., Chen, S.G., Wilson-Delfosse, A.L., (2009) Leucine-rich repeat kinase 2 (LRRK2): a key player in the pathogenesis of Parkinson's disease. *J. Neurosci. Res.* **87** 1283-1295.

Gasser, T., (1998) Genetics of Parkinson's disease. *Clin. Genet.* **54** 259-265.

Gietz, R.D., Schiestl, R.H., Willems, A.R., Woods, R.A., (1995) Studies on the transformation of intact yeast cells by the LiAc/SS-DNA/PEG procedure. *Yeast.* **11** 355-360.

Gilks, W.P., Abou-Sleiman, P.M., Gandhi, S., Jain, S., Singleton, A., Lees, A.J., Shaw, K., Bhatia, K.P., Bonifati, V., Quinn, N.P., Lynch, J., Healy, D.G., Holton, J.L., Revesz, T., Wood, N.W., (2005) A common LRRK2 mutation in idiopathic Parkinson's disease. *Lancet.* **365** 415-416.

Gillardon, F., (2009) Leucine-rich repeat kinase 2 phosphorylates brain tubulin-beta isoforms and modulates microtubule stability--a point of convergence in parkinsonian neurodegeneration? *J. Neurochem.* **110** 1514-1522.

Gingras, A.C., Raught, B., Sonenberg, N., (1999) eIF4 initiation factors: effectors of mRNA recruitment to ribosomes and regulators of translation. *Annu. Rev. Biochem.* **68** 913-963.

Giovannone, B., Lee, E., Laviola, L., Giorgino, F., Cleveland, K.A., Smith, R.J., (2003) Two novel proteins that are linked to insulin-like growth factor (IGF-I) receptors by the Grb10 adapter and modulate IGF-I signaling. *J. Biol. Chem.* **278** 31564-31573.

Giovannone, B., Tsiaras, W.G., de la Monte, S., Klysik, J., Lautier, C., Karashchuk, G., Goldwurm, S., Smith, R.J., (2009) GIGYF2 gene disruption in mice results in neurodegeneration and altered insulin-like growth factor signaling. *Hum. Mol. Genet.* **18** 4629-4639.

Gloeckner, C.J., Kinkl, N., Schumacher, A., Braun, R.J., O'Neill, E., Meitinger, T., Kolch, W., Prokisch, H., Ueffing, M., (2006) The Parkinson disease causing LRRK2 mutation I2020T is associated with increased kinase activity. *Hum. Mol. Genet.* **15** 223-232.

Gloeckner, C.J., Schumacher, A., Boldt, K., Ueffing, M., (2009) The Parkinson disease-associated protein kinase LRRK2 exhibits MAPKKK activity and phosphorylates MKK3/6 and MKK4/7, in vitro. *J. Neurochem.* **109** 959-968.

Gloeckner, C.J., Boldt, K., von Zweydorf, F., Helm, S., Wiesent, L., Sarioglu, H., Ueffing, M., (2010) Phosphopeptide analysis reveals two discrete clusters of phosphorylation in the N-terminus and the Roc domain of the Parkinson-disease associated protein kinase LRRK2. *J. Proteome. Res.* **9** 1738-1745.

Gomez-Tortosa, E., Newell, K., Irizarry, M.C., Sanders, J.L., Hyman, B.T., (2000) alpha-Synuclein immunoreactivity in dementia with Lewy bodies: morphological staging and comparison with ubiquitin immunostaining. *Acta. Neuropathol.* **99** 352-357.

Gonzalez-Perez, A., Gayán, J., Marín, J., Galán, J.J., Sáez, M.E., Real, L.M., Antúnez, C., Ruiz, A., (2009) Whole-genome conditional two-locus analysis identifies novel candidate genes for late-onset Parkinson's disease. *Neurogenetics.* **10** 173-181.

Goold, R.G., Owen, R., Gordon-Weeks, P.R., (1999) Glycogen synthase kinase 3beta phosphorylation of microtubule-associated protein 1B regulates the stability of microtubules in growth cones. *J. Cell. Sci.* **112** 3373-3384.

Gorovoy, M., Niu, J., Bernard, O., Profirovic, J., Minshall, R., Neamu, R., Voyno-Yasenetskaya, T., (2005) LIM kinase 1 coordinates microtubule stability and actin polymerization in human endothelial cells. *J. Biol. Chem.* **280** 26533-26542.

Gotthardt, K., Weyand, M., Kortholt, A., Van haastert, P.J., Wittinghofer, A., (2008) Structure of the Roc-COR domain tandem of C. tepidum, a prokaryotic homologue of the human LRRK2 Parkinson kinase. *EMBO. J.* **27** 2239-2249.

Greggio, E., Jain, S., Kingsbury, A., Bandopadhyay, R., Lewis, P., Kaganovich, A., van der Brug, M.P., Beilina, A., Blackinton, J., Thomas, K.J., Ahmad, R., Miller, D.W., Kesavapany, S., Singleton, A., Lees, A., Harvey, R.J., Harvey, K., Cookson, M.R., (2006) Kinase activity is required for the toxic effects of mutant LRRK2/dardarin. *Neurobiol. Dis.* **23** 329-341.

Greggio, E., Zambrano, I., Kaganovich, A., Beilina, A., Taymans, J.M., Daniels, V., Lewis, P., Jain, S., Ding, J., Syed, A., Thomas, K.J., Baekelandt, V., Cookson, M.R., (2008) The Parkinson disease-associated leucine-rich repeat kinase 2 (LRRK2) is a dimer that undergoes intramolecular autophosphorylation. *J. Biol. Chem.* **283** 16906-16914.

Greggio, E., Taymans, J.M., Zhen, E.Y., Ryder, J., Vancraenenbroeck, R., Beilina, A., Sun, P., Deng, J., Jaffe, H., Baekelandt, V., Merchant, K., Cookson, M.R., (2009) The Parkinson's disease kinase LRRK2 autophosphorylates its GTPase domain at multiple sites. *Biochem. Biophys. Res. Commun.* **389** 449-454.

Guo, L., Wang, W., Chen, S.G., (2006) Leucine-rich repeat kinase 2: relevance to Parkinson's disease. *Int. J. Biochem. Cell. Biol.* **38** 1469-1475.

Guo, L., Gandhi, P.N., Wang, W., Petersen, R.B., Wilson-Delfosse, A.L., Chen, S.G., (2007) The Parkinson's disease-associated protein, leucine-rich repeat kinase 2 (LRRK2), is an authentic GTPase that stimulates kinase activity. *Exp. Cell. Res.* **313** 3658-3670.

Han, B.S., Iacovitti, L., Katano, T., Hattori, N., Seol, W., Kim, K.S., (2008) Expression of the LRRK2 gene in the midbrain dopaminergic neurons of the substantia nigra. *Neurosci. Lett.* **442** 190-194.

Harada, T., Harada, C., Wang, Y.L., Osaka, H., Amanai, K., Tanaka, K., Takizawa, S., Setsuie, R., Sakurai, M., Sato, Y., Noda, M., Wada, K., (2004) Role of ubiquitin carboxy terminal hydrolase-L1 in neural cell apoptosis induced by ischemic retinal injury in vivo. *Am. J. Pathol.* **164** 59-64.

Harhangi, B.S., de Rijk, M.C., van Duijn, C.M., van Broeckhoven, C., Hofman, A., Breteler, M.M., (2000) APOE and the risk of PD with or without dementia in a population-based study. *Neurology.* **54** 1272-1276.

Hartmann, A., Troadec. J.D., Hunot, S., Kikly, K., Faucheux, B.A., Mouatt-Prigent, A., Ruberg, M., Agid, Y., Hirsch, E.C., (2001) Caspase-8 is an effector in apoptotic death of dopaminergic neurons in Parkinson's disease, but pathway inhibition results in neuronal necrosis. *J. Neurosci.* **21** 2247-2255.

Hasegawa, M., Fujiwara, H., Nonaka, T., Wakabayashi, K., Takahashi, H., Lee, V.M., Trojanowski, J.Q., Mann, D., Iwatsubo, T., (2002) Phosphorylated alpha-synuclein is ubiquitinated in alpha-synucleinopathy lesions. *J. Biol. Chem.* **277** 49071-49076.

Hatano, T., Kubo, S., Imai, S., Maeda, M., Ishikawa, K., Mizuno, Y., Hattori, N., (2007) Leucine-rich repeat kinase 2 associates with lipid rafts. *Hum. Mol. Genet.* **16** 678-690.

Healy, D.G., Falchi, M., O'Sullivan, S.S., Bonifati, V., Durr, A., Bressman, S., Brice, A., Aasly, J., Zabetian, C.P., Goldwurm, S., Ferreira, J.J., Tolosa, E., Kay, D.M., Klein, C., Williams, D.R., Marras, C., Lang, A.E., Wszolek, Z.K., Berciano, J., Schapira, A.H., Lynch, T., Bhatia, K.P., Gasser, T., Lees, A.J., Wood, N.W., International LRRK2 Consortium. (2008) Phenotype, genotype, and worldwide genetic penetrance of LRRK2-associated Parkinson's Disease: A case control study. *Lancet. Neurol.* **7** 583-590.

Heath, J.E., Siedlak, S.L., Zhu, X., Lee, H. G., Thakur, A., Yan, R., Perry, G., Smith, M.A. and Castellani, R.J., (2010) Widespread distribution of reticulon-3 in various neurodegenerative diseases. *Neuropathology.* doi: 10.1111/j.1440-1789.2010.01107.x.

Hegde, R., Srinivasula, S.M., Zhang, Z., Wassell, R., Mukattash, R., Cilenti, L., Du Bois, G., Lazebnik, Y., Zervos, A.S., Fernandes-Alnemri, T., Alnemri, E.S., (2002) Identification of Omi/HtrA2 as a mitochondrial apoptotic serine protease that disrupts inhibitor of apoptosis protein-caspase interaction. *J. Biol. Chem.* **277** 432-438.

Henn, I.H., Bouman, L., Schlehe, J.S., Schlierf, A., Schramm, J.E., Wegener, E., Nakaso, K., Culmsee, C., Berninger, B., Krappmann, D., Tatzelt, J., Winklhofer, K.F., (2007) Parkin mediates neuroprotection through activation of IkappaB kinase/nuclear factor-kappaB signaling. *J. Neurosci.* **27** 1868-1878.

Herrick, D.J., Ross, J., (1994) The half-life of c-myc mRNA in growing and serum-stimulated cells: influence of the coding and 3' untranslated regions and role of ribosome translocation. *Mol. Cell. Biol.* **14** 2119-2128.

Hicks, A.A., Petursson, H., Jonsson, T., Stefansson, H., Johannsdottir, H.S., Sainz, J., Frigge, M.L., Kong, A., Gulcher, J.R., Stefansson, K., Sveinbjornsdottir, S., (2002) A susceptibility gene for late-onset idiopathic Parkinson's disease. *Ann. Neurol.* **52** 549-555.

Higashi, S., Biskup, S., West, A.B., Trinkaus, D., Dawson, V.L., Faull, R.L., Waldvogel, H.J., Arai, H., Dawson, T.M., Moore, D.J., Emson, P.C., (2007a) Localization of Parkinson's disease-associated LRRK2 in normal and pathological human brain. *Brain. Res.* **1155** 208-219.

Higashi, S., Moore, D.J., Colebrooke, R.E., Biskup, S., Dawson, V.L., Arai, H., Dawson, T.M., Emson, P.C., (2007b) Expression and localization of Parkinson's disease-associated leucine-rich repeat kinase 2 in the mouse brain. *J. Neurochem.* **100** 368-381.

Higashi, S., Iseki, E., Minegishi, M., Togo, T., Kabuta, T., Wada, K., (2010) GIGYF2 is present in endosomal compartments in the mammalian brains and enhances IGF-1-induced ERK1/2 activation. *J.Neurochem.* **115** 423-437.

Hirokawa, N., (1993) Mechanism of axonal transport. Identification of new molecular motors and regulations of transports. *Neurosci. Res.* **18** 1-9.

Ho, D.T., Bardwell, A.J., Grewal, S., Iverson, C., Bardwell, L., (2006) Interacting JNK-docking sites in MKK7 promote binding and activation of JNK mitogen-activated protein kinases. *J. Biol. Chem.* **281** 13169-13179.

Ho, C.C., Rideout, H.J., Ribe, E., Troy, C.M., Dauer, W.T., (2009) The Parkinson disease protein leucine-rich repeat kinase 2 transduces death signals via Fas-associated protein with death domain and caspase-8 in a cellular model of neurodegeneration. *J. Neurosci.* **29** 1011-1016.

Hoepken, H.H., Gispert, S., Morales, B., Wingerter, O., Del Turco, D., Mulsch, A., Nussbaum, R.L., Muller, K., Drose, S., Brandt, U., Deller, T., Wirth, B., Kudin, A.P., Kunz, W.S., Auburger, G., (2007) Mitochondrial dysfunction, peroxidation damage and changes in glutathione metabolism in PARK6. *Neurobiol. Dis.* **25** 401-411.

Horiuchi, D., Collins, C.A., Bhat, P., Barkus, R.V., Diantonio, A., Saxton, W.M., (2007) Control of a kinesin-cargo linkage mechanism by JNK pathway kinases. *Curr. Biol.* **17** 1313-1317.

Hsu, S.Y., Kaipia, A., Zhu, L., Hsueh, A.J., (1997) Interference of BAD (Bcl-xL/Bcl-2-associated death promoter)-induced apoptosis in mammalian cells by 14-3-3 isoforms and p11. *Mol. Endocrinol.* **11** 1858-1867.

Hsu, C.H., Chan, D., Wolozin, B., (2010) LRRK2 and the stress response: interaction with MKKs and JNK-interacting proteins. *Neurodegener. Dis.* **7** 68-75.

Illenberger, S., Drewes, G., Trinczek, B., Biernat, J., Meyer, H.E., Olmsted, J.B., Mandelkow, E.M., Mandelkow, E., (1996) Phosphorylation of microtubule-associated proteins MAP2 and MAP4 by the protein kinase p110mark. Phosphorylation sites and regulation of microtubule dynamics. *J. Biol. Chem.* **271** 10834-10843.

Imai, Y., Gehrke, S., Wang, H.Q., Takahashi, R., Hasegawa, K., Oota, E., Lu, B., (2008) Phosphorylation of 4E-BP by LRRK2 affects the maintenance of dopaminergic neurons in Drosophila. *EMBO. J.* **27** 2432-2443.

Ito, G., Okai, T., Fujino, G., Takeda, K., Ichijo, H., Katada, T., Iwatsubo, T., (2007) GTP binding is essential to the protein kinase activity of LRRK2, a causative gene product for familial Parkinson's disease. *Biochemistry.* **46** 1380-1388.

Jaleel, M., Nichols, R.J., Deak, M., Campbell, D.G., Gillardon, F., Knebel, A., Alessi, D.R., (2007) LRRK2 phosphorylates moesin at threonine-558: characterization of how Parkinson's disease mutants affect kinase activity. *Biochem. J.* **405** 307-317.

Johnson, L.N., Noble, M.E., Owen, D.J., (1996) Active and inactive protein kinases: structural basis for regulation. *Cell.* **85** 149-158.

Johnson, J., Hague, S.M., Hanson, M., Gibson, A., Wilson, K.E., Evans, E.W., Singleton, A.A., McInerney-Leo, A., Nussbaum, R.L., Hernandez, D.G., Gallardo, M., McKeith, I.G., Burn, D.J., Ryu, M., Hellstrom, O., Ravina, B., Eerola, J., Perry, R.H., Jaros, E., Tienari, P., Weiser, R., Gwinn-Hardy, K., Morris, C.M., Hardy, J., Singleton, A.B., (2004) SNCA multiplication is not a common cause of Parkinson disease or dementia with Lewy bodies. *Neurology.* **63** 554-556.

Jorgensen, N.D., Peng, Y., Ho, C.C., Rideout, H.J., Petrey, D., Liu, P., Dauer, W.T., (2009) The WD40 domain is required for LRRK2 neurotoxicity. *PLoS. One.* **24** e8463.

Kachergus, J., Mata, I.F., Hulihan, M., Taylor, J.P., Lincoln, S., Aasly, J., Gibson, J.M., Ross, O.A., Lynch, T., Wiley, J., Payami, H., Nutt, J., Maraganore, D.M., Czyzewski, K., Styczynska, M., Wszolek, Z.K., Farrer, M.J., Toft, M., (2005) Identification of a novel LRRK2 mutation linked to autosomal dominant parkinsonism: evidence of a common founder across European populations. *Am. J. Hum. Genet.* **76** 672-680.

Kamikawaji, S., Ito, G., Iwatsubo, T., (2009) Identification of the autophosphorylation sites of LRRK2. *Biochemistry.* **48** 10963-10975.

Khan, I.A., Ludueña, R.F., (1996) Phosphorylation of beta III-tubulin. *Biochemistry.* **35** 3704-3711.

Khan, N.L., Jain, S., Lynch, J.M., Pavese, N., Abou-Sleiman, P., Holton, J.L., Healy, D.G., Gilks, W.P., Sweeney, M.G., Ganguly, M., Gibbons, V., Gandhi, S., Vaughan, J., Eunson, L.H., Katzenschlager, R., Gayton, J., Lennox, G., Revesz, T., Nicholl, D., Bhatia, K.P., Quinn, N., Brooks, D., Lees, A.J., Davis, M.B., Piccini, P., Singleton, A.B., Wood, N.W., (2005) Mutations in the gene LRRK2 encoding dardarin (PARK8) cause familial Parkinson's disease: clinical, pathological, olfactory and functional imaging and genetic data. *Brain* **128** 2786-2796.

Kim, R.H., Smith, P.D., Aleyasin, H., Hayley, S., Mount, M.P., Pownall, S., Wakeham, A., You-Ten, A.J., Kalia, S.K., Horne, P., Westaway, D., Lozano, A.M., Anisman, H., Park, D.S., Mak, T.W., (2005) Hypersensitivity of DJ-1-deficient mice to 1-methyl-4-phenyl-1,2,3,6-tetrahydropyrindine (MPTP) and oxidative stress. *Proc. Natl. Acad. Sci. USA.* **102** 5215-5220.

Kitada, T., Asakawa, S., Hattori, N., Matsumine, H., Yamamura, Y., Minoshima, S., Yokochi, M., Mizuno, Y., Shimizu, N., (1998) Mutations in the parkin gene cause autosomal recessive juvenile parkinsonism. *Nature.* **392** 605-608.

Klein, C.L., Rovelli, G., Springer, W., Schall, C., Gasser, T., Kahle, P.J., (2009) Homo- and heterodimerization of ROCO kinases: LRRK2 kinase inhibition by the LRRK2 ROCO fragment. *J. Neurochem.* **111** 703-715.

Ko, H.S., Bailey, R., Smith, W.W., Liu, Z., Shin, J.H., Lee, Y.I., Zhang, Y.J., Jiang, H., Ross, C.A., Moore, D.J., Patterson, C., Petrucelli, L., Dawson, T.M., Dawson, V.L., (2009) CHIP regulates leucine-rich repeat kinase-2 ubiquitination, degradation, and toxicity. *Proc. Natl. Acad. Sci. USA.* **106** 2897-2902.

Kobe, B., Deisenhofer, J., (1995) Proteins with leucine-rich repeats. *Curr. Opin. Struct. Biol.* **5** 409-416.

Kumar, A., Greggio, E., Beilina, A., Kaganovich, A., Chan, D., Taymans, J.M., Wolozin, B., Cookson, M.R., (2010) The Parkinson's disease associated LRRK2 exhibits weaker in vitro phosphorylation of 4E-BP compared to autophosphorylation. *PLoS. One.* **5** e8730.

Kuzuhara, S., Mori, H., Izumiyama, N., Yoshimura, M., Ihara, Y., (1988) Lewy bodies are ubiquitinated. A light and electron microscopic immunocytochemical study. *Acta. Neuropathol.* **75** 345-353

Langston, J.W., Ballard, P., Tetrud, J.W., Irwin, I., (1983) Chronic Parkinsonism in humans due to a product of meperidine-analog synthesis. *Science.* **219** 979-980.

Leandro-García, L.J., Leskelä, S., Landa, I., Montero-Conde, C., López-Jiménez, E., Letón, R., Cascón, A., Robledo, M., Rodríguez-Antona, C., (2010) Tumoral and tissue-specific expression of the major human beta-tubulin isotypes. *Cytoskeleton.* **67** 214-223.

Lecine, P., Italiano, J.E. Jr, Kim, S.W., Villeval, J.L., Shivdasani, R.A., (2000) Hematopoietic-specific beta 1 tubulin participates in a pathway of platelet biogenesis dependent on the transcription factor NF-E2. *Blood.* **96** 1366-1373.

Lee, J.T., Lee, T.J., Kim, C.H., Kim, N.S., Kwon, T.K., (2009) Over-expression of Reticulon 3 (RTN3) enhances TRAIL-mediated apoptosis via up-regulation of death receptor 5 (DR5) and down-regulation of c-FLIP. *Cancer. Lett.* **279** 185-192.

Lennon, S.V., Martin, S.J., Cotter, T.G., (1991) Dose-dependent induction of apoptosis in human tumour cell lines by widely diverging stimuli. *Cell. Prolif.* **24** 203-214.

Leroy, E., Boyer, R., Auburger, G., Leube, B., Ulm, G., Mezey, E., Harta, G., Brownstein, M.J., Jonnalagada, S., Chernova, T., Dehejia, A., Lavedan, C., Gasser, T., Steinbach, P.J., Wilkinson, K.D., Polymeropoulos, M.H., (1998) The ubiquitin pathway in Parkinson's disease. *Nature.* **395** 451-452.

Lesage, S., Leutenegger, A.L., Ibanez, P., Janin, S., Lohmann, E., Brice, A., French Parkinson's Disease Genetics Study Group. (2005) LRRK2 haplotype analyses in European and North African families with Parkinson disease: a common founder for the G2019S mutation dating from the 13th century. *Am. J. Hum. Genet.* **77** 330-332.

Lesage, S., Durr, A., Tazir, M., Lohmann, E., Leutenegger, A.L., Janin, S., Pollak, P., Brice, A., French Parkinson's Disease Genetics Study Group. (2006) LRRK2 G2019S as a cause of Parkinson's disease in North African Arabs. *N. Engl. J. Med.* **354** 422-423.

Lewis, P.A., Greggio, E., Beilina, A., Jain, S., Baker, A., Cookson, M.R., (2007) The R1441C mutation of LRRK2 disrupts GTP hydrolysis. *Biochem. Biophys. Res. Commun.* **357** 668-671.

Li, D., Roberts, R., (2001) WD-repeat proteins: structure characteristics, biological function, and their involvement in human diseases. *Cell. Mol. Life. Sci.* **58** 2085-2097.

Li, X., Tan, Y.C., Poulose, S., Olanow, C.W., Huang, X.Y., Yue, Z., (2007) Leucine-rich repeat kinase 2 (LRRK2)/PARK8 possesses GTPase activity that is altered in familial Parkinson's disease R1441C/G mutants. *J. Neurochem.* **103** 238-247.

Li, Y., Dunn, L., Greggio, E., Krumm, B., Jackson, G.S., Cookson, M.R., Lewis, P.A., Deng, J., (2009a) The R1441C mutation alters the folding properties of the ROC domain of LRRK2. *Biochim. Biophys. Acta.* **1972** 1194-1197.

Li, Y., Liu, W., Oo, T.F., Wang, L., Tang, Y., Jackson-Lewis, V., Zhou, C., Geghman, K., Bogdanov, M., Przedborski, S., Beal, M.F., Burke, R.E., Li, C., (2009b) Mutant LRRK2(R1441G) BAC transgenic mice recapitulate cardinal features of Parkinson's disease. *Nat. Neurosci.* **12** 826-828.

Li, X., Moore, D.J., Xiong, Y., Dawson, T.M., Dawson, V.L., (2010) Reevaluation of phosphorylation sites in the Parkinson disease-associated leucine-rich repeat kinase 2. *J. Biol. Chem.* **285** 29569-29576.

Lim, M.Y., Dailey, D., Martin, G.S., Thorner, J., (1993) Yeast MCK1 protein kinase autophosphorylates at tyrosine and serine but phosphorylates exogenous substrates at serine and threonine. *J. Biol. Chem.* **268** 21155-21164.

Lin, C.H., Tan, E.K., Chen, M.L., Tan, L.C., Lim, H.Q., Chen, G.S., Wu, R.M., (2008) Novel ATP13A2 variant associated with Parkinson disease in Taiwan and Singapore. *Neurology.* **71** 1727-1732.

Lin, C.H., Tsai, P.I., Wu, R.M., Chien, C.T., (2010) LRRK2 G2019S mutation induces dendrite degeneration through mislocalization and phosphorylation of tau by recruiting autoactivated GSK3β. *J. Neurosci.* **30** 13138-13149.

Liou, A.K., Leak, R.K., Li, L., Zigmond, M.J., (2008) Wild-type LRRK2 but not its mutant attenuates stress-induced cell death via ERK pathway. *Neurobiol. Dis.* **32** 116-124.

Littauer, U.Z., Giveon, D., Thierauf, M., Ginzburg, I., Ponstingl, H., (1986) Common and distinct tubulin binding sites for microtubule-associated proteins. *Proc. Natl. Acad. Sci. USA.* **83** 7162-7166.

López-Carballo, G., Moreno, L., Masiá, S., Pérez, P., Barettino, D., (2002) Activation of the phosphatidylinositol 3-kinase/Akt signaling pathway by retinoic acid is required for neural differentiation of SH-SY5Y human neuroblastoma cells. *J. Biol. Chem.* **277** 25297-25304.

Lotharius, J., Brundin, P., (2002) Impaired dopamine storage resulting from alpha-synuclein mutations may contribute to the pathogenesis of Parkinson's disease. *Hum. Mol. Genet.* **11** 2395-2407.

Ludueña, R.F., (1998) Multiple forms of tubulin: different gene products and covalent modifications. *Int. Rev. Cytol.* **178** 207-275.

Luo, L.Z., Xu, Q., Guo, J.F., Wang, L., Shi, C.H., Wei, J.H., Long, Z.G., Pan, Q., Tang, B.S., Xia, K., Yan, X.X., (2010) FBXO7 gene mutations may be rare in Chinese early-onset Parkinsonism patients. *Neurosci. Lett.* **482** 86-89.

Luzón-Toro, B., Rubio de la Torre, E., Delgado, A., Pérez-Tur, J., Hilfiker, S., (2007) Mechanistic insight into the dominant mode of the Parkinson's disease-associated G2019S LRRK2 mutation. *Hum. Mol. Genet.* **16** 2031-2039.

MacLeod, D., Dowman, J., Hammond, R., Leete, T., Inoue, K., Abeliovich, A., (2006) The familial Parkinsonism gene LRRK2 regulates neurite process morphology. *Neuron.* **52** 587-593.

Maekawa, T., Kubo, M., Yokoyama, I., Ohta, E., Obata, F., (2010) Age-dependent and cell-population-restricted LRRK2 expression in normal mouse spleen. *Biochem. Biophys. Res. Commun.* **392** 431-435.

Marshall, L.E., Himes, R.H., (1978) Rotenone inhibition of tubulin self-assembly. *Biochim. Biophys. Acta.* **543** 590-594.

Maruta, H., Greer, K., Rosenbaum, J.L., (1986) The acetylation of alpha-tubulin and its relationship to the assembly and disassembly of microtubules. *J. Cell. Biol.* **103** 571-579.

Mata, I.F., Kachergus, J.M., Taylor, J.P., Lincoln, S., Aasly, J., Lynch, T., Hulihan, M.M., Cobb, S.A., Wu, R.M., Lu, C.S., Lahoz, C., Wszolek, Z.K., Farrer, M.J., (2005) Lrrk2 pathogenic substitutions in Parkinson's disease. *Neurogenetics.* **6** 171-177.

Mata, I.F., Wedemeyer, W.J., Farrer, M.J., Taylor, J.P., Gallo, K.A., (2006) LRRK2 in Parkinson's disease: protein domains and functional insights. *Trends. Neurosci.* **29** 286-293.

Melrose, H., Lincoln, S., Tyndall, G., Dickson, D., Farrer, M., (2006) Anatomical localization of leucine-rich repeat kinase 2 in mouse brain. *Neuroscience.* **139** 791-794.

Melrose, H.L., Dächsel, J.C., Behrouz, B., Lincoln, S.J., Yue, M., Hinkle, K.M., Kent, C.B., Korvatska, E., Taylor, J.P., Witten, L., Liang, Y.Q., Beevers, J.E., Boules, M., Dugger, B.N., Serna, V.A., Gaukhman, A., Yu, X., Castanedes-Casey, M., Braithwaite, A.T., Ogholikhan, S., Yu, N., Bass, D., Tyndall, G., Schellenberg, G.D., Dickson, D.W., Janus, C., Farrer, M.J., (2010) Impaired dopaminergic neurotransmission and microtubule-associated protein tau alterations in human LRRK2 transgenic mice. *Neurobiol. Dis.* **40** 503-517.

Miklossy, J., Arai, T., Guo, J.P., Klegeris, A., Yu, S., McGeer, E.G., McGeer, P.L., (2006) LRRK2 expression in normal and pathologic human brain and in human cell lines. *J. Neuropathol. Exp. Neurol.* **65** 953-963.

Mitchison, T., Kirschner, M., (1984) Dynamic instability of microtubule growth. *Nature.* **312** 237-242.

Nichols, W.C., Marek, D.K., Pauciulo, M.W., Pankratz, N., Halter, C.A., Rudolph, A., Shults, C.W., Wojcieszek, J., Foroud, T., Parkinson Study Group - PROGENI Investigators (2007) R1514Q substitution in Lrrk2 is not a pathogenic Parkinson's disease mutation. *Mov. Disord.* **22** 254-257.

Nichols, R.J., Dzamko, N., Hutti, J.,E., Cantley, L.C., Deak, M., Moran J., Bamborough, P., Reith, A.D., Alessi, D.R., (2009) Substrate specificity and inhibitors of LRRK2, a protein kinase mutated in Parkinson's disease. *Biochem. J.* **424** 47-60.

Nichols, R.J., Dzamko, N., Morrice, N.A., Campbell, D.G., Deak, M., Ordureau, A., Macartney, T., Tong, Y., Shen, J., Prescott, A.R., Alessi, D.R., (2010) 14-3-3 binding to LRRK2 is disrupted by multiple Parkinson's disease-associated mutations and regulates cytoplasmic localization. *Biochem. J.* **430** 393-404.

Nieto, M., Gil-Bea, F.J., Dalfo, E., Cuadrado, M., Cabodevilla, F., Sanchez, B., Catena, S., Sesma, T., Ribe, E., Ferrer, I., Ramirez, M.J., Gomez-Isla, T., (2006) Increased sensitivity to MPTP in human alpha-synuclein A30P transgenic mice. *Neurobiol. Aging.* **27** 848-856.

Nogales, E., Wolf, S.G., Downing, K, H., (1998) Structure of the alpha beta tubulin dimer by electron crystallography. *Nature.* **391** 199-203.

Nolen, B., Taylor, S., Ghosh, G., (2004) Regulation of protein kinases; controlling activity through activation segment conformation. *Mol. Cell.* **15** 661-675.

Oegema, K., Wiese, C., Martin, O.C., Milligan, R.A., Iwamatsu, A., Mitchison, T.J., Zheng, Y., (1999) Characterization of two related Drosophila gamma-tubulin complexes that differ in their ability to nucleate microtubules. *J. Cell. Sci.* **144** 721-733.

Oliveri, R.L., Nicoletti, G., Cittadella, R., Manna, I., Branca, D., Zappia, M., Gambardella, A., Caracciolo, M., Quattrone, A., (1999) Apolipoprotein E polymorphisms and Parkinson's disease. *Neurosci. Lett.* **277** 83-86.

Ostrerova, N., Petrucelli, L., Farrer, M., Mehta, N., Choi, P., Hardy, J., Wolozin, B., (1999) alpha-Synuclein shares physical and functional homology with 14-3-3 proteins. *J. Neurosci.* **19** 5782-5791.

Ozelius, L.J., Senthil, G., Saunders-Pullman, R., Ohmann, E., Deligtisch, A., Tagliati, M., Hunt, A.L., Klein, C., Henick, B., Hailpern, S.M., Lipton, R.B., Soto-Valencia, J., Risch, N., Bressman, S.B., (2006) LRRK2 G2019S as a cause of Parkinson's disease in Ashkenazi Jews. *N. Engl. J. Med.* **354** 424-425.

Paglini, G., Kunda, P., Quiroga, S., Kosik, K., Caceres, A., (1998) Suppression of radixin and moesin alters growth cone morphology, motility, and process formation in primary cultured neurons. *J. Cell. Biol.* **143** 443-455.

Paisán-Ruíz, C., Jain, S., Evans, E.W., Gilks, W.P., Simón, J., van der Brug, M., López de Munain, A., Aparicio, S., Gil, A.M., Khan, N., Johnson, J., Martinez, J.R., Nicholl, D., Carrera, I.M., Pena, A.S., de Silva, R., Lees, A., Martí-Massó, J.F., Pérez-Tur, J., Wood, N.W., Singleton, A.B., (2004) Cloning of the gene containing mutations that cause PARK8-linked Parkinson's disease. *Neuron.* **44** 595-600.

Pankratz, N., Nichols, W.C., Uniacke, S.K., Halter, C., Murrell, J., Rudolph, A., Shults, C.W., Conneally, P.M., Foroud, T., Parkinsons Study Group. (2003) Genome-wide linkage analysis and evidence of gene-by-gene interactions in a sample of 362 multiplex Parkinson disease families. *Hum. Mol. Genet.* **12** 2599-2608.

Pankratz, N., Uniacke, S.K., Halter, C.A., Rudolph, A., Shults, C.W., Conneally, P.M., Foroud, T., Nichols, W.C., Parkinsons Study Group. (2004) Genes influencing Parkinson disease onset: replication of PARK3 and identification of novel loci. *Neurology.* **62** 1616-1618.

Pankratz, N., Byder, L., Halter, C., Rudolph, A., Shults, C.W., Conneally, P.M., Foroud, T., Nichols, W.C., (2006a) Presence of an APOE4 allele results in significantly earlier onset of Parkinson's disease and a higher risk with dementia. *Mov. Disord.* **21** 45-49.

Pankratz, N., Pauciulo, M.W., Elsaesser, V.E., Marek, D.K., Halter, C.A., Rudolph, A., Shults, C.W., Foroud, T., Nichols, W.C., Parkinson Study Group-PROGENI Investigators (2006b) Mutations in LRRK2 other than G2019S are rare in a north American-based sample of familial Parkinson's disease. *Mov. Disord.* **21** 2257-2260.

Parisiadou, L., Xie, C., Cho, H.J., Lin, X., Gu, X.L., Long, C.X., Lobbestael, E., Baekelandt, V., Taymans, J.M., Sun, L., Cai, H., (2009) Phosphorylation of ezrin/radixin/moein proteins by LRRK2 promotes the rearrangement of actin cytoskeleton in neronal morphogenesis. *J. Neurosci.* **29** 13971-13980.

Pelech, S., (2006) Dimerization in protein kinase signaling. *J. Biol.* **5** 12

Petit, A., Kawarai, T., Paitel, E., Sanjo, N., Maj, M., Scheid, M., Chen, F., Gu, Y., Hasegawa, H., Salehi-Rad, S., Wang, L., Rogaeva, E., Fraser, P., Robinson, B., St George-Hyslop, P., Tandon, A., (2005) Wild-type PINK1 prevents basal and induced neuronal apoptosis, a protective effect abrogated by Parkinson disease-related mutations. *J. Biol. Chem.* **280** 34025-34032.

Pike, A.C., Rellos, P., Niesen, F.H., Turnbull, A., Oliver, A.W., Parker, S.A., Turk, B.E., Pearl, L.H., Knapp, S., (2008) Activation segment dimerization: a mechanism for kinase autophosphorylation of non-consensus sites. *EMBO. J.* **27** 704-714.

Plowey, E.D., Cherra, S.J. 3rd., Liu, Y.J., Chu, C.T., (2008) Role of autophagy in G2019S-LRRK2-associated neurite shortening in differentiated SH-SY5Y cells. *J. Neurochem.* **105** 1048-1056.

Plun-Favreau, H., Klupsch, K., Moisoi, N., Gandhi, S., Kjaer, S., Frith, D., Harvey, K., Deas, E., Harvey, R.J., McDonald, N., Wood, N.W., Martins, L.M., Downward, J., (2007) The mitochondrial protease HtrA2 is regulated by Parkinson's disease-associated kinase PINK1. *Nat. Cell. Biol.* **9** 1243-1252.

Polymeropoulos, M.H., Lavedan, C., Leroy, E., Ide, S.E., Dehejia, A., Dutra, A., Pike, B., Root, H., Rubenstein, J., Boyer, R., Stenroos, E.S., Chandrasekharappa, S., Athanassiadou, A., Papapetropoulos, T., Johnson, W.G., Lazzarini, A.M., Duvoisin, R.C., Di Iorio, G., Golbe, L.I., Nussbaum, R.L., (1997) Mutation in the alpha-synuclein gene identified in families with Parkinson's disease. *Science.* **276** 2045-2047.

Puig, B., Vinals, F., Ferrer, I., (2004) Active stress kinase p38 enhances and perpetuates abnormal tau phosphorylation and deposition in Pick's disease. *Acta. Neuropathol.* **107** 185-189.

Qu, X., Qi, Y., Lan, P., Li, Q., (2002) The novel endoplasmic reticulum (ER)-targeted protein HAP induces cell apoptosis by the depletion of the ER Ca(2+) stores. *FEBS. Lett.* **529** 325-331.

Rajput, A., Dickson, D.W., Robinson, C.A., Ross, O.A., Dächsel, S.C., Lincoln, S.J., Cobb, S.A., Rajput, M.L., Farrer, M.J., (2006) Parkinsonism, Lrrk2 G2019S, and tau neuropathology. *Neurology.* **67** 1506-1508.

Ramamoorthy, K., Wang, F., Chen, I.C., Norris, J.D., McDonnell, D.P., Leonard, L. S., Gaido, K.W., Bocchinfuso, W.P., Korach, K.S., Safe, S., (1997) Estrogenic activity of a dieldrin/toxaphene mixture in the mouse uterus, MCF-7 human breast cancer cells, and yeast-based estrogen receptor assays: no apparent synergism. *Endocrinology.* **138** 1520-1527

Ramirez, A., Heimbach, A., Gründemann, J., Stiller, B., Hampshire, D., Cid, L.P., Goebel, I., Mubaidin, A.F., Wriekat, A.L., Roeper, J., Al-Din, A., Hillmer, A.M., Karsak, M., Liss, B., Woods, C.G., Behrens, M.I., Kubisch, C., (2006) Hereditary parkinsonism with dementia is caused by mutations in ATP13A2, encoding a lysosomal type 5 P-type ATPase. *Nat. Genet.* **38** 1184-1191.

Raybin, D., Flavin, M., (1977) Enzyme which specifically adds tyrosine to the alpha chain of tubulin. *Biochemistry.* **16** 2189-2194.

Reiman, E.M., Chen, K., Alexander, G.E., Caselli, R.J., Bandy, D., Osborne, D., Saunders, A.M., Hardy, J., (2004) Functional brain abnormalities in young adults at genetic risk for late-onset Alzheimer's dementia. *Proc. Natl. Acad. Sci. USA.* **101** 284-289.

Ren, Y., Zhao, J., Feng, J., (2003) Parkin binds to alpha/beta tubulin and increases their ubiquitination and degradation. *J. Neurosci.* **23** 3316-3324.

Ren, Y., Liu, W., Jiang, H., Jiang, Q., Feng, J., (2005) Selective vulnerability of dopaminergic neurons to microtubule depolymerization. *J. Biol. Chem.* **280** 34105-34112.

Ren, Y., Jiang, H., Yang, F., Nakaso, K., Feng, J., (2009) Parkin protects dopaminergic neurons against microtubule-depolymerizing toxins by attenuating microtubule-associated protein kinase activation. *J. Biol. Chem.* **284** 4009-4017.

Richter, J.D., Sonenberg, N., (2005) Regulation of cap-dependent translation by eIF4E inhibitory proteins. *Nature.* **433** 477-480.

Riederer, B.M., (2007) Microtubule-associated protein 1B, a growth-associated and phosphorylated scaffold protein. *Brain. Res. Bull.* **71** 541-558.

Rubinfeld, H., Seger, R., (2004) The ERK cascade as a prototype of MAPK signaling pathways. *Methods. Mol. Biol.* **250** 1-28.

Sancho, R.M., Law, B.M., Harvey, K., (2009) Mutations in the LRRK2 Roc-COR tandem domain link Parkinson's disease to Wnt signalling pathways. *Hum. Mol. Genet.* **18** 3955-3968.

Sato, S., Chiba, T., Sakata, E., Kato, K., Mizuno, Y., Hattori, N., Tanaka, K., (2006) 14-3-3eta is a novel regulator of parkin ubiquitin ligase. *EMBO. J.* **25** 211-221.

Savitt, J.M., Dawson, V.L., Dawson, T.M., (2006) Diagnosis and treatment of Parkinson disease: molecules to medicine. *J. Clin. Invest.* **116** 1744-1754.

Schapira, A.H., (2006) The importance of LRRK2 mutations in Parkinson disease. *Arch. Neurol.* **63** 1225-1228.

Schlossmacher, M.G., Frosch, M.P., Gai, W.P., Medina, M., Sharma, N., Forno, L., Ochiishi, T., Shimura, H., Sharon, R., Hattori, N., Langston, J.W., Mizuno, Y., Hyman, B.T., Selkoe, D.J., Kosik, K.S., (2002) Parkin localizes to the Lewy bodies of Parkinson disease and dementia with Lewy bodies. *Am. J. Pathol.* **160** 1655-1667.

Schnapp, B.J., Reese, T.S., (1989) Dynein is the motor for retrograde axonal transport of organelles. *Proc. Natl. Acad. Sci. USA.* **86** 1548-1552.

Schnitzer, M.J., Block, S.M., (1997) Kinesin hydrolyses one ATP per 8-nm step. *Nature.* **388** 386-390.

Sen, S., Webber, P.J., West, A.B., (2009) Dependence of leucine-rich repeat kinase 2 (LRRK2) kinase activity on dimerization. *J. Biol. Chem.* **284** 36346-36356.

Shendelman, S., Jonason, A., Martinat, C., Leete, T., Abeliovich, A., (2004) DJ-1 is a redox-dependent molecular chaperone that inhibits alpha-synuclein aggregate formation. *PLoS. Biol.* **2** e362.

Sheng, D., Qu, D., Kwok, K.H., Ng, S.S., Lim, A.Y., Aw, S.S., Lee, C.W., Sung, W.K., Tan, E.K., Lufkin, T., Jesuthasan, S., Sinnakaruppan, M., Liu, J., (2010) Deletion of the WD40 domain of LRRK2 in Zebrafish causes Parkinsonism-like loss of neurons and locomotive defect. *PLoS. Genet.* **22** e1000914.

Shimizu, F., Katagiri, T., Suzuki, M., Watanabe, T.K., Okuno, S., Kuga, Y., Nagata, M., Fujiwara, T., Nakamura, Y., Takahashi, E., (1997) Cloning and chromosome assignment to 1q32 of a human cDNA (RAB7L1) encoding a small GTP-binding protein, a member of the RAS superfamily. *Cytogenet. Cell. Genet.* **77** 261-263.

Shin, N., Jeong, H., Kwon, J., Heo, H.Y., Kwon, J.J., Yun, H.J., Kim, C.H., Han, B,S., Tong, Y., Shen, J., Hatano, T., Hattori, N., Kim, K.S., Chang, S., Seol, W., (2008) LRRK2 regulates synaptic vesicle endocytosis. *Exp. Cell. Res.* **314** 2055-2065.

Shinoda, S., Schindler, C.K., Quan-Lan, J., Saugstad, J.A., Taki, W., Simon, R.P., Henshall, D.C., (2003) Interaction of 14-3-3 with Bid during seizure-induced neuronal death. *J. Neurochem.* **86** 460-469.

Simón-Sánchez, J., Herranz-Pérez, V., Olucha-Bordonau, F., Pérez-Tur, J., (2006) LRRK2 is expressed in areas affected by Parkinson's disease in the adult mouse brain. *Eur. J. Neurosci.* **23** 659-666.

Simón-Sánchez, J., Singleton, A.B., (2008) Sequencing analysis of OMI/HTRA2 shows previously reported pathogenic mutations in neurologically normal controls. *Hum. Mol. Genet.* **17** 1988-1993.

Singleton, A.B., Farrer, M., Johnson, J., Singleton, A., Hague, S., Kachergus, J., Hulihan, M., Peuralinna, T., Dutra, A., Nussbaum, R., Lincoln, S., Crawley, A., Hanson, M., Maraganore, D., Adler, C., Cookson, M.R., Muenter, M., Baptista, M., Miller, D., Blancato, J., Hardy, J., Gwinn-Hardy, K., (2003) alpha-Synuclein locus triplication causes Parkinson's disease. *Science.* **302** 841.

Smith, W.W., Pei, Z., Jiang, H., Moore, D.J., Liang, Y., West, A.B., Dawson, V.L., Dawson, T.M., Ross, C.A., (2005) Leucine-rich repeat kinase 2 (LRRK2) interacts with parkin, and mutant LRRK2 induces neuronal degeneration. *Proc. Natl. Acad. Sci. USA.* **102** 18676-18681.

Smith, W.W., Pei, Z., Jiang, H., Dawson, V.L., Dawson, T.M., Ross, C.A., (2006) Kinase activity of mutant LRRK2 mediates neuronal toxicity. *Nat. Neurosci.* **9** 1231-1233.

Spillantini, M.G., Crowther, R.A., Jakes, R., Hasegawa, M., Goedert, M., (1998) alpha-Synuclein in filamentous inclusions of Lewy bodies from Parkinson's disease and dementia with lewy bodies. *Proc. Natl. Acad. Sci. USA.* **95** 6469-6473.

Strauss, K.M., Martins, L.M., Plun-Favreau, H., Marx, F.P., Kautzmann, S., Berg, D., Gasser, T., Wszolek, Z., Müller, T., Bornemann, A., Wolburg, H., Downward, J., Riess, O., Schulz, J.B., Krüger, R., (2005) Loss of function mutations in the gene encoding Omi/HtrA2 in Parkinson's disease. *Hum. Mol. Genet.* **14** 2099-2111.

Strittmatter, W.J., Saunders, A.M., Goedert, M., Weisgraber, K.H., Dong, L.M., Jakes, R., Huang, D.Y., Pericak-Vance, M., Schmechel, D., Roses, A.D., (1994) Isoform-specific interactions of apolipoprotein E with microtubule-associated protein tau: implications for Alzheimer disease. *Proc. Natl. Acad. Sci. USA.* **91** 11183-11186.

Strittmatter, W.J., Bova Hill, C., (2002) Molecular biology of apolipoprotein E. *Curr. Opin. Lipidol.* **13** 119-123.

Sunkel, C.E., Gomes, R., Sampaio, P., Perdigao, J., Gonzalez, C., (1995) Gamma-tubulin is required for the structure and function of the microtubule organizing centre in Drosophila neuroblasts. *EMBO. J.* **14** 28-36.

Svenningsson, P., Chergui, K., Rachleff, I., Flajolet, M., Zhang, X., El Yacoubi, M., Vaugeois, J.M., Nomikos, G.G., Greengard, P., (2006) Alterations in 5-HT1B receptor function by p11 in depression-like states. *Science.* **311** 77-80.

Taira, T., Saito, Y., Niki, T., Iguchi-Ariga, S.M., Takahashi, K., Ariga, H., (2004) DJ-1 has a role in antioxidative stress to prevent cell death. *EMBO. Rep.* **5** 213-218.

Tan, E.K., Kwok, H.H., Tan, L.C., Zhao, W.T., Prakash, K.M., Au, W.L., Pavanni, R., Ng, Y.Y., Satake, W., Zhao, Y., Toda, T., Liu, J.J., (2010) Analysis of GWAS-linked loci in Parkinson disease reaffirms PARK16 as a susceptibility locus. *Neurology.* **75** 508-512.

Taymans, J.M., Van den Haute, C., Baekelandt, V., (2006) Distribution of PINK1 and LRRK2 in rat and mouse brain. *J. Neurochem.* **98** 951-961.

Tesseur, I., Van Dorpe, J., Spittaels, K., Van den Haute, C., Moechars, D., Van Leuven, F., (2000) Expression of human apolipoprotein E4 in neurons causes hyperphosphorylation of protein tau in the brains of transgenic mice. *Am. J. Pathol.* **156** 951-964.

Thomas, B., Beal, M.F., (2007) Parkinson's Disease. *Hum. Mol. Genet.* **16** R183-R194.

Ubl, A., Berg, D., Holzmann, C., Kruger, R., Berger, K., Arzberger, T., Bornemann, A., Riess, O., (2002) 14-3-3 protein is a component of Lewy bodies in Parkinson's disease-mutation analysis and association studies of 14-3-3 eta. *Brain. Res. Mol. Brain. Res.* **108** 33-39.

Valenzuela, P., Quiroga, M., Zaldivar, J., Rutter, W.J., Kirschner, M.W., Cleveland, D.W., (1981) Nucleotide and corresponding amino acid sequences encoded by alpha and beta tubulin mRNAs. *Nature.* **289** 650-655.

Vitte, J., Traver, S., Maues De Paula, A., Lesage, S., Rovelli, G., Corti, O., Duyckaerts, C., Brice, A., (2010) Leucine-rich repeat kinase 2 is associated with the endoplasmic reticulum in dopaminergic neurons and accumulates in the core of Lewy bodies in Parkinson disease. *J. Neuropathol. Exp. Neurol.* **69** 959-972.

Wagner, U., Utton, M., Gallo, J.M., Miller, C.C., (1996) Cellular phosphorylation of tau by GSK-3 beta influences tau binding to microtubules and microtubule organization. *J. Cell. Sci.* **109** 1537-1543.

Wan, Q., Kuang, E., Dong, W., Zhou, S., Xu, H., Qi, Y., Liu, Y., (2007) Reticulon 3 mediates Bcl-2 accumulation in mitochondria in response to endoplasmic reticulum stress. *Apoptosis.* **12** 319-328.

Wandosell, F., Serrano, L., Hernandez, M.A., Avila, J., (1986) Phosphorylation of tubulin by a calmodulin-dependent protein kinase. *J. Biol. Chem.* **261** 10332-10339.

Wang, D., Qian, L., Xiong, H., Liu, J., Neckameyer, W.S., Oldham, S., Xia, K., Wang, J., Bodmer, R., Zhang, Z., (2006) Antioxidants protect PINK1-dependent dopaminergic neurons in Drosophila. *Proc. Natl. Acad. Sci. USA.* **103** 13520-13525.

Wang, L., Xie, C., Greggio, E., Parisiadou, L., Shim, H., Sun, L., Chandran, J., Lin, X., Lai, C., Yang, W.J., Moore, D.J., Dawson, T.M., Dawson, V.L., Chiosis, G., Cookson, M.R., Cai, H., (2008) The chaperone activity of heat shock protein 90 is critical for maintaining the stability of leucine-rich repeat kinase 2. *J. Neurosci.* **28** 3384-3391.

Wang, X., She, H., Mao, Z., (2009) Phosphorylation of neuronal survival factor MEF2D by glycogen synthase kinase 3beta in neuronal apoptosis. *J. Biol. Chem.* **284** 32619-32626.

Webber, P.J., West, A.B., (2009) LRRK2 in Parkinson's disease: function in cells and neurodegeneration. *FEBS. J.* **276** 6436-6444.

West, A.B., Moore, D.J., Biskup, S., Bugayenko, A., Smith, W.W., Ross, C.A., Dawson, V.L., Dawson, T.M., (2005) Parkinson's disease-associated mutations in leucine-rich repeat kinase 2 augment kinase activity. *Proc. Natl. Acad. Sci. USA.* **102** 16842-16847.

West, A.B., Moore, D.J., Choi, C., Andrabi, S.A., Li, X., Dikeman, D., Biskup, S., Zhang, Z., Lim, K.L., Dawson, V.L., Dawson, T.M., (2007) Parkinson's disease-associated mutations in LRRK2 link enhanced GTP-binding and kinase activities to neuronal toxicity. *Hum. Mol. Genet.* **16** 223-232.

Westerlund, M., Belin, A.C., Anvret, A., Bickford, P., Olson, L., Galter, D., (2008) Developmental regulation of leucine-rich repeat kinase 1 and 2 expression in the brain and other rodent and human organs: Implications for Parkinson's disease. *Neuroscience.* **152** 429-436.

Whitmarsh, A.J., Kuan, C.Y., Kennedy, N.J., Kelkar, N., Haydar, T.F., Mordes, J.P., Appel, M., Rossini, A.A., Jones, S.N., Flavell, R.A., Rakic, P., Davis, R.J., (2001) Requirement of the JIP1 scaffold protein for stress-induced JNK activation. *Genes. Dev.* **15** 2421-2432.

Williams, N.G., Roberts, T.M., Li, P., (1992) Both p21ras and pp60v-src are required, but neither alone is sufficient, to activate the Raf-1 kinase. *Proc. Natl. Acad. Sci. USA.* **89** 2922-2926.

Williams, D.R., Hadeed, A., al-Din, A.S., Wreikat, A.L., Lees, A.J., (2005) Kufor Rakeb disease: autosomal recessive, levodopa-responsive parkinsonism with pyramidal degeneration, supranuclear gaze palsy, and dementia. *Mov. Disord.* **20** 1264-1271.

Williamson, T., Gordon-Weeks, P.R., Schachner, M., Taylor, J., (1996) Microtubule reorganization is obligatory for growth cone turning. *Proc. Natl. Acad. Sci. USA.* **93** 15221-15226.

Wu, T., Angus, C.W., Yao, X.L., Logun, C., Shelhamer, J.H., (1997) P11, a unique member of the S100 family of calcium-binding proteins, interacts with and inhibits the activity of the 85-kDa cytosolic phospholipase A2. *J. Biol. Chem.* **272** 17145-17153.

Xiang, R., Liu, Y., Zhu, L., Dong, W., Qi, Y., (2006) Adaptor FADD is recruited by RTN3/HAP in ER-bound signaling complexes. *Apoptosis.* **11** 1923-1932.

Xiong, Y., Coombes, C.E., Kilaru, A., Li, X., Gitler, A.D., Bowers, W.J., Dawson, V.L., Dawson, T.M., Moore, D.J., (2010) GTPase activity plays a key role in the pathobiology of LRRK2. *PLoS. Genet.* **6** e1000902.

Yaffe, M.B., Smerdon, S.J., (2004) The use of in vitro peptide-library screens in the analysis of phosphoserine/threonine-binding domain structure and function. *Annu. Rev. Biophys. Biomol. Struct.* **33** 225-244.

Yang, F., Jiang, Q., Zhao, J., Ren, Y., Sutton, M.D., Feng, J., (2005) Parkin stabilizes microtubules through strong binding mediated by three independent domains. *J. Biol. Chem.* **280** 17154-17162.

Yang, Y., Gehrke, S., Imai, Y., Huang, Z., Ouyang, Y., Wang, J.W., Yang, L., Beal, M.F., Vogel, H., Lu, B., (2006) Mitochondrial pathology and muscle and dopaminergic neuron degeneration caused by inactivation of Drosophila Pink1 is rescued by Parkin. *Proc. Natl. Acad. Sci. USA.* **103** 10793-10798.

Yao, C., El-Khoury, R., Wang, W., Byrd, T.A., Pehek, E.A., Thacker, C., Zhu, X., Smith, M.A., Wilson-Delfosse, A.L., Chen, S.G., (2010) LRRK2-mediated neurodegeneration and dysfunction of dopaminergic neurons in a Caenorhabditis elegans model of Parkinson's disease. *Neurobiol. Dis.* **40** 73-81.

Yavich, L., Tanila, H., Vepsäläinen S, Jäkälä P., (2004) Role of alpha-synuclein in presynaptic dopamine recruitment. *J. Neurosci.* **24** 11165-11170.

Yokota, T., Sugawara, K., Ito, K., Takahashi, R., Ariga, H., Mizusawa, H., (2003) Down regulation of DJ-1 enhances cell death by oxidative stress, ER stress, and proteasome inhibition. *Biochem. Biophys. Res. Commun.* **312** 1342-1348.

Yoshino, H., Tomiyama, H., Tachibana, N., Ogaki, K., Li, Y., Funayama, M., Hashimoto, T., Takashima, S., Hattori, N., (2010) Phenotypic spectrum of patients with PLA2G6 mutation and PARK14-linked parkinsonism. *Neurology.* **75** 1356-1361.

Yun, J., Cao, J.H., Dodson, M.W., Clark, I, E., Kapahi, P., Chowdhury, R.B., Guo, M., (2008) Loss-of-function analysis suggests that Omi/HtrA2 is not an essential component of the PINK1/PARKIN pathway in vivo. *J. Neurosci.* **28** 14500-14510.

Zechel, S., Meinhardt, A., Unsicker, K., von Bohlen Und Halbach, O., (2010) Expression of leucine-rich-repeat-kinase 2 (LRRK2) during embryonic development. *Int. J. Dev. Neurosci.* **28** 391-399.

Zhou, W., Freed, C.R., (2005) DJ-1 up-regulates glutathione synthesis during oxidative stress and inhibits A53T alpha-synuclein toxicity. *J. Biol. Chem.* **280** 43150-43158.

Zhu, L., Xiang, R., Dong, W., Liu, Y., Qi, Y., (2007) Anti-apoptotic activity of Bcl-2 is enhanced by its interaction with RTN3. *Cell. Biol. Int.* **31** 825-830.

Zimprich, A., Biskup, S., Leitner, P., Lichtner, P., Farrer, M., Lincoln, S., Kachergus, J., Hulihan, M., Uitti, R.J., Calne, D.B., Stoessl, A.J., Pfeiffer, R.F., Patenge, N., Carbajal, I.C., Vieregge, P., Asmus, F., Muller-Myhsok, B., Dickson, D.W., Meitinger, T., Strom, T.M., Wszolek, Z.K., Gasser, T., (2004) Mutations in LRRK2 cause autosomal-dominant parkinsonism with pleomorphic pathology. *Neuron.* **44** 601-607.